

J A E R I - M
90-129

COLD LEG INJECTION REFLOOD TEST RESULTS IN THE
SCTF CORE-I UNDER CONSTANT SYSTEM PRESSURE

August 1990

Hiromichi ADACHI*, Takamichi IWAMURA
Makoto SOBAJIMA, Masahiro OSAKABE**
Akira OHNUKI, Yutaka ABE and Yoshio MURAO

日本原子力研究所
Japan Atomic Energy Research Institute

JAERI-Mレポートは、日本原子力研究所が不定期に公刊している研究報告書です。
入手の問合せは、日本原子力研究所技術情報部情報資料課（〒319-11 茨城県那珂郡東海村）あて、
お申しこみください。なお、このほかに財団法人原子力弘済会資料センター（〒319-11 茨城県那珂郡
東海村日本原子力研究所内）で複写による実費領布をおこなっております。

JAERI-M reports are issued irregularly.
Inquiries about availability of the reports should be addressed to Information Division Department
of Technical Information, Japan Atomic Energy Research Institute, Tokaimura, Naka-gun, Ibaraki-
ken 319-11, Japan.

© Japan Atomic Energy Research Institute, 1990

編集兼発行 日本原子力研究所
印 刷 ニッセイエプロ株式会社

Cold Leg Injection Reflood Test Results in the
SCTF Core-I under Constant System Pressure

Hiromichi ADACHI*, Takamichi IWAMURA

Makoto SOBAJIMA†, Masahiro OSAKABE**

Akira OHNUKI, Yutaka ABE and Yoshio MURAO

Department of Reactor Engineering
Tokai Research Establishment
Japan Atomic Energy Research Institute
Tokai-mura, Naka-gun, Ibaraki-ken

(Received July 12, 1990)

The Slab Core Test Facility (SCTF) was constructed to investigate two-dimensional thermal-hydrodynamics in the core and the interaction in fluid behavior between the core and the upper plenum during the last part of blowdown, refill and reflood phases of a postulated loss-of-coolant accident (LOCA) of a pressurized water reactor (PWR).

The present report describes the analytical results on the system behavior observed in the SCTF Core-I cold leg injection tests, S1-14 (Run 520), S1-15 (521), S1-16 (522), S1-17 (523), S1-20 (530), S1-21 (531), S1-23 (536) and S1-24 (537), performed under constant system pressure condition during transient. Major discussion items are: (1) steam binding, (2) U-tube oscillations, (3) bypass of ECC water (4) core cooling behavior, (5) effect of vent valve and (6) other parameter effects. These results give us very useful information and suggestion on reflood behavior.

Keywords: Reactor Safety, LOCA, PWR, Reflood, Core Cooling, ECCS, Cold Leg Injection, Steam Binding, U-tube oscillation, SCTF

* Department of Fuel Safety Research

† Yamagata University

** Tokyo Marine University

平板炉心第1次模擬炉心再冠水試験における
一定系圧力コールドレグ注入試験の結果

日本原子力研究所東海研究所原子炉工学部
安達 公道・岩村 公道・傍島 真⁺・刑部 真弘^{**}
大貫 晃・阿部 豊・村尾 良夫

(1990年7月12日受理)

平板炉心試験装置（SCTF）は、加圧水型原子炉（PWR）の冷却材喪失事故（LOCA）過程のうち、ブローダウン過程末期から、リフィル、再冠水過程にかけての、炉心内二次元熱水力挙動や、炉心と上部プレナムとの間の流動的相互干渉等を解明することを目的として建設された。

本報告書では、一定系圧力条件下で行われたSCTF第1次炉心コールドレグ注入再冠水試験 S1-14 (Run 520), S1-15 (521), S1-16 (522), S1-17 (523), S1-20 (530), S1-21 (531), S1-23 (536), S1-24 (537)において観察されたシステム挙動について紹介する。主な検討項目は、(1)蒸気バインディング、(2)U字管振動、(3)ECC水のバイパス、(4)炉心冷却挙動、(5)ベント弁の効果および(6)試験パラメータの影響である。ここに紹介する結果は、再冠水挙動について極めて有用な情報や示唆を与えるものである。

東海研究所：〒319-11 茨城県那珂郡東海村白方字白根2-4

+ 燃料安全工学部

* 山形大学

** 東京商船大学

Contents

1.	Introduction	1
2.	Test Conditions	3
3.	Test Results and Discussions	9
3.1	Steam Binding	9
3.2	U-Tube Oscillations	10
3.3	Bypass of ECC Water	11
3.4	Core Cooling Behavior	12
3.5	Effect of Vent Valve	13
3.6	Parameter Effects	14
4.	Recommendation for Cold Leg Injection Test Procedure	45
5.	Conclusions	47
	Acknowledgment	48
	References	48
Appendix A	Slab Core Test Facility (SCTF) Core-I	49
Appendix B	Selected Data for Test S1-14 (Run 520)	92
Appendix C	Selected Data for Test S1-15 (Run 521)	103
Appendix D	Selected Data for Test S1-16 (Run 522)	114
Appendix E	Selected Data for Test S1-17 (Run 523)	125
Appendix F	Selected Data for Test S1-20 (Run 530)	136
Appendix G	Selected Data for Test S1-21 (Run 531)	147
Appendix H	Selected Data for Test S1-23 (Run 536)	158
Appendix I	Selected Data for Test S1-24 (Run 537)	169

目 次

1. 緒 言	1
2. 試験条件	3
3. 試験結果及び討論	9
3.1 蒸気バインディング	9
3.2 U字管振動	10
3.3 ECC水のバイパス	11
3.4 炉心冷却挙動	12
3.5 ベント弁の効果	13
3.6 試験パラメータの影響	14
4. コールドレグ注入試験方法への提言	45
5. 結 論	47
謝 辞	48
文 献	48
付録 A 平板炉心試験装置 (SCTF) 第1次模擬炉心	49
付録 B 試験S1-14 (Run 520) のデータ	92
付録 C 試験S1-15 (Run 521) のデータ	103
付録 D 試験S1-16 (Run 522) のデータ	114
付録 E 試験S1-17 (Run 523) のデータ	125
付録 F 試験S1-20 (Run 530) のデータ	136
付録 G 試験S1-21 (Run 531) のデータ	147
付録 H 試験S1-23 (Run 536) のデータ	158
付録 I 試験S1-24 (Run 537) のデータ	169

1. Introduction

The Slab Core Test Facility (SCTF) Test Program is a part of the Large Scale Reflood Test (LSRT) Program⁽¹⁾ of the Japan Atomic Energy Research Institute (JAERI) as well as the Cylindrical Core Test Facility (CCTF) Test Program. The purposes of the LSRT Program are to clarify the thermal-hydraulic Behavior in the core and the primary cooling system of a pressurized water reactor (PWR) during the last part of blowdown, refill and reflood phases of a postulated loss-of-coolant accident (LOCA) and to demonstrate the effectiveness of the emergency core cooling system (ECCS) experimentally. In the CCTF Test Program, overall simulation of the system behavior is the primary concern. On the other hand, in the SCTF Test Program, the major objectives are to clarify the following items:

- (1) Two-dimensional thermal-hydraulics in a wide core (chimney effect, blockage effect sputtering-induced fluid behavior, etc.),
- (2) Flow interaction between core and upper plenum (fall-back, core entrainment, etc.), and
- (3) Hot leg carryover characteristics (upper plenum entrainment/deentrainment, counter-current flow in hot leg, etc.).

The SCTF Test Program is a part of the coordinated research program called the 2D/3D Program among the United States (US), the Federal Republic of Germany (FRG) and Japan. Coupling tests with the Upper Plenum Test Facility (UPTF) test of the FRG are planned to perform in the SCTF Core-III test series to investigate the core and upper plenum fluid behavior and the resultant core cooling behavior under the proper interfacial two-phase flow conditions between the core and the upper plenum.

To meet these objectives, the SCTF pressure vessel is designed and fabricated to simulate a radial slab with full height, full radius and one bundle width extracted from a 1,100 MWe PWR core. The relation between the SCTF pressure vessel and the PWR Pressure vessel is illustrated in Fig. 1.1.

In the present report, important experimental information obtained from Tests S1-14 (Run 520), S1-15 (521), S1-16 (522), S1-17 (523), S1-20 (530), S1-21 (531), S1-23 (536) and S1-24 (537) of the SCTF Core-1 test series shall be introduced. These tests are cold leg injection tests at almost constant system pressure during transient. Major test parameters are water injection rates from accumulator injection system (Acc) and low pressure coolant injection system (LPCI), Acc water temperature, Acc water injection time and the valve open/close for the vent valve line connecting the upper plenum to the top of the downcomer.

Steam binding effect during transient, U-tube oscillations between the core and the downcomer in the initial period of the test, ECC water bypassing, core heat transfer behavior, effect of the vent valve line and effect of some other test parameters on reflood phenomena shall be discussed in detail.

A brief description on the design⁽²⁾ of the SCTF is given in Appendix A for reference. Selected test data from the eight cold leg injection tests are also given in Appendixes B through I.

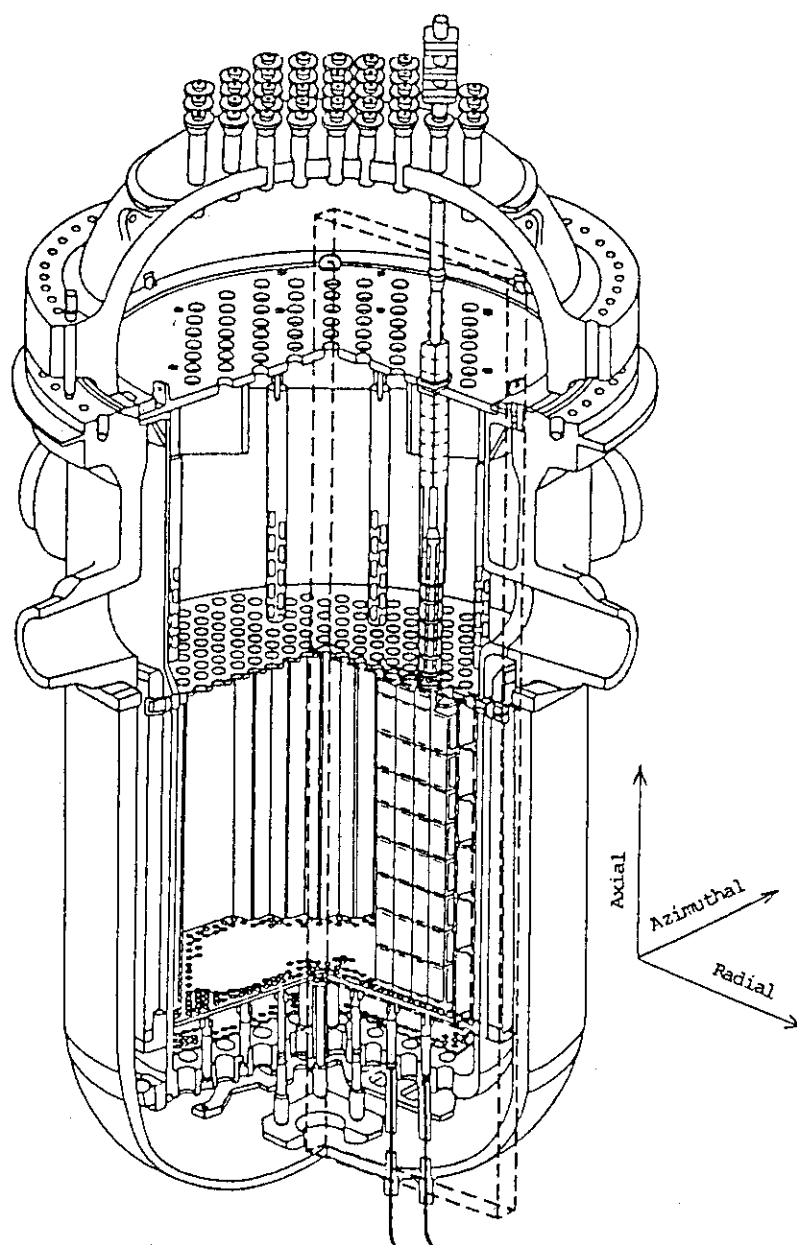


Fig. 1.1 Simulated Part of PWR Pressure Vessel with SCTF

2. Test Conditions

Tables 2.1 and 2.2 give the measured test conditions and chronologies of important events for the eight tests. Major objectives of each test are as follow:

(1) Test S1-14

This test was performed to examine the differences in system behavior between the SCTF and the CCTF by comparing the data from the CCTF Core-I base case test, Test C1-05⁽³⁾. Some test conditions are, however, different from those for Test C1-05 because of differences in facility design and special requirement of the test to compare with the forced-feed reflooding tests of the SCTF Core-I test series. Major differences in test conditions from Test C1-05 are (1) the lower total core heating power of 7.09 MW (9.41 MW in Test C1-05), (2) the lower maximum heat flux of 43.1 kW/m² (73.0 kW/m²) resulted from the lower core heating power and the smaller peaking factor, (3) the higher initial maximum rod temperature of 1,087 K (873 K) and (4) existence of steam flow through the open vent line valve (closed vent line valve). ECC water injection rate and temperature are also different from Test C1-05, but they are intended to be equivalent to the corresponding values for Test C1-05 with the following corrections.

Injection rate and temperature of Acc water in Test S1-14 were 86.8 kg/s and 340 K, respectively. On the other hand, they were 77.3 kg/s and 308 K, respectively, for Test C1-05. The difference in injection rate came from difference in flow area ratio of the core and the downcomer. In SCTF, properly simulated core baffle region is attached to the core, and in addition, some additional fluid volumes such as the gap between the core barrel and the vessel wall and many large instrumentation penetration holes are attached to the core. On the other hand, in CCTF, core baffle region is included in the downcomer.

In Test S1-14, therefore, Acc water injection rate was estimated assuming that water accumulation rates in the core baffle region and the other additional fluid volumes were the same as the core inlet water velocity and the ratio of the core inlet water velocity and the downcomer water accumulation rate was equal to that for Test C1-05.

Acc water temperature for Test S1-14 was estimated with the following two corrections. One was for the weak downcomer heat slab effect and constant 25 K was added to Acc water temperature in CCTF between Test C1-03⁽⁴⁾ and C1-02⁽⁵⁾ in which the downcomer wall temperatures were the saturated temperature and the superheated temperature by 79 K, respectively. Another

correction was for the different Acc injection rate. Necessary enthalpy to heat up the increased part of Acc water from the injection temperature to the saturated temperature was added to the original injection temperature in advance. The elevated temperature was 7.3 K.

In order to prevent from sudden system depressurization due to condensation, Acc water was at first injected into the lower-plenum and then at 5 s after the estimated beginning of reflood the injection location was switched from the lower plenum to the intact cold leg.

On the other hand, injection rate and temperature of LPCI water were estimated as 8.49 kg/s and 336 K, respectively, based on the corresponding values for Test C1-05 of 8.28 kg/s and 308 K, respectively. Correction method applied to the injection rate was that the LPCI injection rate was determined so as to be proportional to the core flow area excluded the core baffle region and the other additional fluid volumes. Because, the effect of water accumulation in these additional volumes to the effective core inlet water flow rate was considered to be insignificant for LPCI injection period. It must be noted that difference in ECC water bypass characteristics between the two facilities was implicitly taken into account in this estimation.

For LPCI water temperature, two kinds of correction were made. One was for the weaker downcomer heat slab effect and constant 10 K was added to the original temperature value based on the data from the CCTF tests. The other correction was for the smaller steam flow rate in the intact cold leg due to the lack of active steam generators and 18.3 K was added as the latent heat of lacking steam flow rate which was estimated as 10 % of the total steam flow rate of the three intact cold legs in Test C1-05.

(2) Test S1-15

In this test, Acc water temperature was raised from that for Test S1-14 up to 389 K in order to reduce the condensation induced oscillations during Acc injection period. The other conditions were almost the same as Test S1-14.

(3) Test S1-16

In this test, Acc water injection rate was much reduced from that for Test S1-15. The value of 27 kg/s was almost the same as the value to realize the same core inlet water flow rate as the base case, Test S1-01, for the SCTF Core-I forced-feed reflooding test series if there was no steam binding effect. The other test conditions were almost the same as Test S1-

15.

The purpose of this reduced Acc water injection rate is to suppress the oscillations which occurred in the previous tests during Acc injection and just after the switching from Acc injection to LPCI injection.

(4) Test S1-17

In this test, LPCI injection rate was reduced to about 60 % that for Test S1-16. To obtain experimental information on core reflooding behavior under low reflooding velocity condition is the main purpose of this test.

(5) Test S1-20

In the previous cold leg injection tests, valve in the vent line simulator connecting the upper plenum to the top of downcomer was fully opened during the transient. To examine the effect of the vent line on reflooding behavior by closing the valve was the main purpose of this test. In addition, small modifications were made on Acc injection conditions as follows.

In this test, water accumulation rate in the core baffle region and the other additional fluid volumes were assumed to be equal to the water accumulation rate in the core instead of the core inlet water velocity. As the result, Acc injection rate was slightly reduced from Test S1-14. Due to the change in Acc injection rate, estimated Acc water temperature was also slightly changed. The other test conditions were almost the same as Test S1-14, as shown in Table 2.1.

(6) Test S1-21

Test conditions for Test S1-20 were intended to be almost equivalent to those for Test C1-05. However, total core heating power and initial core stored energy were different between the two tests. In addition, through the experiences of previous five cold leg injection tests, it was found that the core inlet water flow rate in the SCTF test was almost the same as the ECC water injection rate especially in the LPCI injection period. Consequently, the core inlet water velocities in this period in the previous cold leg injection tests have been much higher than that for Test C1-05 except for Test S1-17. Therefore, we needed to make clear whether the SCTF test shows the similar core cooling behavior as observed in the CCTF test under the same core inlet boundary conditions or not.

In Test S1-21, a counterpart test for the high initial core temperature test of the CCTF, Test C1-14⁽⁶⁾, was performed, i.e. the total core heating power and the initial maximum core temperature were chosen to be

the same as Test C1-14 and the LPCI injection rate was determined so as to realize the same core inlet water velocity as Test C1-14. Acc injection rate was chosen to be almost equal to that for Test C1-20 because the value was considered to be almost equivalent to that for Test C1-14. However, Acc water was kept to be injected into the lower plenum instead of the intact cold leg except the last 2 s of the injection period for preventing from condensation-induced oscillations. The other test conditions were almost equal to those for Test S1-20.

(7) Test S1-23

This test was performed to compare mainly the water accumulation characteristics in the core and the resultant core cooling behavior with Test C1-14 under eliminated condition of initial system oscillations which were still observed in Test S1-21.

For this purpose, Acc injection rate was reduced to 31.5 kg/s and the injection time after the beginning of reflood was extended to 26 s (18.5 in Test S1-21). Core water level at the switching time from Acc injection to LPCI injection was intended to be the same as Test S1-21.

This test was terminated at 97 s after the beginning of reflood because the maximum core temperature exceeded the initial set value for protection of core and then the core heating power was tripped.

(8) Test S1-24

This test was the repeated test for Test S1-23. However, Acc injection rate was decreased slowly in the last about 8 s and the total injection time of Acc water after the beginning of reflood was extended up to 40 s to more correctly equalize the core water level at the switching time to LPCI injection to Test S1-21.

Table 2.1 Measured Test Conditions

Parameter	SI-14	SI-15	SI-16	SI-17	SI-20	SI-21	SI-23	SI-24
Initial P at Core Center (MPa)	0.2	0.2	0.2	0.2	0.20	0.20	0.20	0.20
Maximum P at Cont-II (MPa)	0.24	0.23	0.25	0.24	0.23	0.29	0.26	0.28
Maximum Core T at BOCREC (K)	1090	1099	1081	1140	1140	1073	1054	1067
Initial Power (MW)	(7.09)	(7.09)	(7.09)	(7.09)	(7.09)	(9.41)	(9.41)	9.38
Power Holding Time after Acc Initiation (s)	2	2	3	3	3	2.5	1	2
Decay Curve	(ANS+Act. +DN(Voided Core))							
Acc Inj. Location	LP → ICL	LP *	LP	LP				
Inj. Rate (KG/s)	86.5	85.9	27	35.3	80.0	78.0	31.5	31.5
Temp. (K)	333	389	393	370	335	333	337	333
LPCI Inj. Location	ICL							
Inj. Rate (KG/s)	7.8	8.34	8.1	4.72	8.2	5	5.3	4.9
Temp. (K)	338	338	337	338	338	337	338	336
Vent Line Valve	Open	Open	Open	Open	Close	Close	Close	Close

Note: () is the estimated value.

* Except last 2 s of ICL injection for smooth switching.

Table 2.2 Chronologies of Events

Event	S1-14	S1-15	S1-16	S1-17	S1-20	S1-21	S1-23	S1-24
Core Power "ON"	-137 s	-138 s	-135 s	-148 s	-134 s	-99 s	-101 s	-100 s
Acc Inj. Initiation	- 1	- 2	- 2	- 2	- 1	- 1.5	- 1	- 2
BOCREC	0	0	0	0	0	0	0	0
Core Power Decay Initiation	1	0	3	1	2	1	0	- 2
Max. Acc Inj. Rate	1	13	2.5	0	3	7.5	0	0
Max. Core Temp.	2	2	74.5	125	10	103.5	99	134.5
Max. Cont-II Press.	8	25	1.3	12	31	14.5	25	27
Switch Acc → LPCT	19	19	17	19	19	18.5	26	40
Max. Core Press.	22	17	29	25	24	14	27	40
Whole Core Quench	315	329	378.5	475	316	464.5	421	508.5

3. Test Results and Discussions

3.1 Steam Binding

Generated steam in the core during reflood flows out through the upper plenum to the primary loops. In the case of actual PWRs, entrained water by the steam flow evaporates in the steam generators and consequently the loop steam flow rates increase. Resultant high pressure drop across the loops causes the high upper plenum pressure and the core water is pushed back by the pressure toward the lower plenum. Therefore, the core cooling is degraded. Such kind of influence of loop resistances to the core cooling is called the steam binding effect.

In the case of SCTF, since there was no enhancement of the steam binding effect due to evaporation of entrained water because of the lack of active steam generators, stronger loop resistances were applied in the loop design in order to cancel the weaker steam binding effect. That is, 90 % of hot leg steam quality was assumed in the loop orifice K-factor estimation. In other words, stronger orifice resistance was chosen so as to realize the higher loop differential pressure corresponding to the 10 % higher steam flow rate.

Figure 3.1 shows an example of measured hot leg steam quality. In this example, the hot leg steam quality was higher than 90 % until about 110 s after the beginning of reflood and thus the steam binding effect in SCTF was supposed to be stronger than the actual one in this period. On the other hand, the hot leg steam quality was lower than 90 % after 110 s, suggesting the weaker steam binding effect in the SCTF. Such unrealistic steam binding characteristics of SCTF can generally be seen in the other tests under cold leg injection.

Figure 3.2 shows the comparison of differential pressure data between the top of upper plenum and the top of downcomer among the two SCTF cold leg injection tests and one CCTF test. Test S1-21 is the counterpart test for Test C1-14. Test S1-21 gives a larger differential pressure across the primary loop than Test C1-14 until about 50 s after the beginning of reflood and the relation in the differential pressure between the two tests reverses after that.

Figures 3.3 and 3.4 show the comparisons of core differential pressure and downcomer water head, respectively, among the tests. The core water head in Test S1-21 was equal to or slightly lower than in Test C1-14 until about 140 s and the downcomer water head was oppositely higher

until about 50 s. After these times, the relations become opposite, respectively. These three kinds of comparison suggest that the steam binding effect in Test S1-21 was initially stronger than in Test C1-14 and then it becomes weaker than Test C1-14.

The differential pressure data between the upper plenum and the containment tank-II also show the consistent characteristics to the above mentioned fact as seen in Fig. 3.5. However, the cross point of the curves for Tests S1-21 and C1-14 is at about 75 s in this case.

The most important effect of the weaker steam binding in the later portion of the test is the change of governing mechanism of core inlet water flow rate. If the steam binding is so sufficiently strong that the downcomer water level reaches the overflow level, the core inlet water flow rate is governed by the magnitude of the steam binding effect. However, when the downcomer water level does not reach the overflow level, the core inlet water flow rate is basically governed by the ECC water injection rate. Because, since the bypass rate of ECC water in this case is not so high and, in addition, increase in downcomer water penetration rate due to the condensation effect induced by ECC water injection and water accumulation rate in the downcomer are both much less than the ECC water injection rate itself, the core inlet water flow rate is in this case approximately equal to the ECC water injection rate.

For the initial period of test, the loop resistance can relatively easily be simulated because the amount of entrained water through the hot leg is small. However, the downcomer water level at the switching time from Acc injection to LPCI injection is quite important for the correct simulation of the core inlet flow rate transient. If the water level is higher than that for the following portion of the test, the core inlet water flow rate increases temporarily as shown in Fig. 3.6.

3.2 U-Tube Oscillations

In the SCTF cold leg injection tests, U-tube oscillations occurred generally between the core and the downcomer, especially in the early period of the tests. The effect was extended to the entire primary system: inside and outside of the pressure vessel.

Unique features of the oscillations are in the phase relationship. As shown in Fig. 3.7, the oscillations of the core differential pressure and the downcomer differential pressure are almost the in-phase. On the other hand, velocity oscillations measured with the drag disk flo meter at the interface between the downcomer and the lower plenum are not in-phase to the lower downcomer differential pressure oscillations as shown in Fig.

3.8.

Observation just below the end box tie-plate indicated strong upward two-phase flow when the downcomer differential pressure was at the maximum and downcomer two-phase flow when the downcomer differential pressure was at the minimum, as shown in Fig. 3.9.

Similar U-tube oscillations can be seen in some of the CCTF tests, PKL tests and so on. This suggests that the causes of the U-tube oscillations observed in the SCTF tests are general ones. However, the amplitude seems to be much larger in SCTF than in CCTF. The reasons of the difference in oscillatory characteristics between the two facilities are unknown yet. The followings are the possible candidates.

- (1) Difference in flow area ratio of the core side and the downcomer side (larger in SCTF)
- (2) Difference between the pipe type downcomer (SCTF) and the annulus downcomer (CCTF)
- (3) Difference in initial core temperature (higher in SCTF)
- (4) Difference between the downcomer water level below the overflow level (SCTF) and that the overflow level (CCTF)
- (5) Difference in lower plenum structure (more open in SCTF)
- (6) Difference in downcomer heat slab effect (less-significant in SCTF).

Major trigger of the oscillations seems to be the boiling disturbance in the core. Especially, when the core water level is rapidly rising the oscillations seem to be more significant. For example, the temporary increase in the core inlet water flow rate just after the switching from Acc injection to LPCI injection seems to have magnified the oscillations remarkably. Therefore, lower Acc injection rate and smaller downcomer water level overshoot just before the switching to LPCI injection are considered to be very effective measures to reduce the oscillations. Test S1-24 was performed under such conditions and thus the oscillations were much less-significant than Test S1-21 as shown in Fig. 3.10.

On the other hand, unstable condensation in the intact cold leg induced by Acc injection also seems to be a strong trigger for the oscillations. Therefore, to inject Acc water into the lower plenum instead of the cold leg is considered to be another effective measure to reduce the oscillations.

3.3 Bypass of ECC Water

In SCTF, ECC water bypassing was less-significant than CCTF as shown in Fig. 3-11. The causes are unclear at present but the followings can be

raised as candidates.

- (1) The pipe type downcomer instead of annulus downcomer
- (2) Geometrical configuration of the top part of the downcomer, especially its steam-water separator effect
- (3) Weak heat slab effect of the downcomer
- (4) Low steam flow rate in the intact cold leg
- (5) Low downcomer water level below the overflow level

3.4 Core Cooling Behavior

Core cooling during reflood is affected by various factors but the most important factor seems to be the transient of core inlet water flow rate.

In Test S1-14, S1-15 and S1-20, almost no significant core temperature overshoot was observed because of the high water flow rate of Acc injection. On the other hand, in Tests S1-16, S1-17, S1-21, S1-23 and S1-24, significant core temperature overshoot was seen at the several points due to the low core water flow rate of Acc and/or LPCI injection and/or high core heating power. This is clearly recognized in Figs. 3.12 through 3.19, respectively.

Figures 3.20 through 3.22 show the comparison of core temperature transients between the SCTF and the CCTF. Test conditions were very close between Tests S1-21 and C1-14, however initial total core stored energy was larger in Test S1-21 than Test C1-14 because of the smaller axial peaking factor and the higher core temperature just before the initiation of core heating up. In addition, elevation of thermo-couples and the corresponding local power density are not exactly equal to each other between the tests. However, we can find the following general trends for SCTF in comparison with CCTF.

- (1) In the SCTF test, remarkable core cooling can be seen in the initial portion of the test, i.e., clear suppression of temperature rise or temporary decrease in temperature can be observed.
- (2) After that, core cooling in the SCTF test was kept also better than the CCTF test, thus the turnaround temperature was not so high in spite of the much higher initial temperature and thus the quench was earlier.
- (3) In Test S1-24, because of the lower Acc injection rate, initial temperature rise was much larger than Test S1-21. This resulted in the higher turnaround temperature and the later quench. However, the temperature transient curves seem to be quite similar to Test S1-21,

suggesting the similar transient of the cooling effect during LPCI injection period.

Causes of the better core cooling in the initial portion of the test than the rest are unclear at present. It is roughly corresponding to the temporary increase in core inlet water flow rate just after the switching from Acc injection to LPCI injection. However, the temporary enhancement of core cooling can be seen even in the test without the temporary increase in core inlet water flow rate.

Since U-tube oscillations are more significant in SCTF than CCTF, they may be one of the possible candidates for the remarkable temporary decrease in rod temperature in SCTF. However, since there is a large uncertainty in core flooding rate during Acc injection and just after switching from Acc injection to LPCI injection, it is impossible to strictly compare the SCTF and CCTF data.

The difference in long term core cooling between SCTF and CCTF is more difficult to explain. As compared in Fig. 3.3, the core water head in the SCTF test is usually higher than the CCTF test except the initial portion of the test. However, the difference is seen only in the lower part of the core (maybe in the quenched part of the core) and void fraction in the upper part of the core is higher in SCTF in comparison with CCTF, as shown in Fig. 3.23. In spite of this fact, core cooling before the quench was usually better in the SCTF than the CCTF. Of course there are some possible reasons to enhance the core cooling. For example, two-dimensional fluid behavior in the core and fall back water flow from the upper plenum may improve the core cooling.

3.5 Effect of Vent Valve

Test conditions for Tests S1-14 and S1-20 were almost the same except for the vent valve line connecting the upper plenum to the top of the downcomer, i.e., this valve was fully open in Test S1-14, on the other hand, completely closed in Test S1-20.

The most significant effect of the vent valve can be seen in the downcomer water head transient as shown in Fig. 3.24. That is, in the case of closed vent valve, the downcomer water head increased significantly. On the other hand, the figure also shows only a small decrease in core water head until about 130 s after the beginning of reflood and almost no effect after that. As known from Figs. 3.12 and 3.16, only a small change in core cooling behavior caused by the vent valve. These results suggest that the core inlet water flow rate was not so much affected by the vent valve.

This is probably due to the fact that the downcomer water level in

the SCTF test was lower than the overflow level even in the case of the closed vent valve. In such case, stronger steam bindind effect due to the closed vent valve does not reduce the core inlet water flow rate but only pushes up the downcomer water level. Since the effect of downcomer water accumulation on the core inlet water flow rate is small, the core inlet water flow rate is almost the same between the two tests. Therefore, it can be reasonably concluded that the vent valves between the upper plenum and the top of downcomer in some current designs of PWRs are expected to be effective for the enhancement of core cooling and the reduction of the peak clad temperature (PCT) only when the downcomer water level during reflood cannot be kept below the overflow level without opening the vent valves.

3.6 Parameter Effects

In this section, parameter effect observed in the cold leg injection tests shall be briefly described.

(1) Effect of Acc water temperature

Major difference in test condition of Test S1-15 from Test S1-14 is the higher Acc water temperature. Although it did not eliminate the initial system oscillations as expected, core reflooding behavior was significantly changed.

As known by comparing Figs. 3.25 and 3.26, core inlet water subcooling was significantly reduced due to the higher Acc water temperature. This resulted in the smaller core water accumulation as known from Figs. 3.27 and 3.28 and consequently the slightly poorer core cooling as known from Figs. 3.12 and 3.13.

(2) Effect of Acc injection flow rate

Major difference in test condition of Test S1-16 from Test S1-15 is the lower Acc injection flow rate. As known by comparing Figs. 3.26 and 3.29, core inlet water subcooling was slightly smaller in the early period and slightly larger in the later period. However, the difference was small. Most remarkable difference in reflood phenomena was the smaller core water mass as known from Figs. 3.28 and 3.30. This is due to the smaller initial water accumulation and resulted in much poorer core cooling as known from comparison between Figs. 3.13 and 3.14. Reduced U-tube oscillations in Test S1-16 is considered also to have degraded the core cooling.

(3) Effect of LPCI injection flow rate

In Test S1-17, much smaller LPCI injection flow rate was applied than Test S1-16. As shown in Fig. 3.31, almost no change was seen for core inlet water subcooling due to the reduction of LPCI injection flow rate because downcomer penetration water temperature in LPCI injection period was the saturated one. However, core water mass was much smaller as shown in Fig. 3.32 and thus the core cooling was much degraded from Test S1-16 as known from Figs. 3.14 and 3.15.

(4) Coupled effect of Acc injection flow rate and time

In Test S1-24, Acc injection flow rate was much reduced from Test S1-21 and the injection time was extended by 21.5 s.

The smaller Acc injection flow rate resulted in the lower core inlet subcooling in the initial portion of test period as shown in Figs. 3.33 and 3.34. This may be mainly caused by more complete mixing of downcomer penetration water with lower plenum water. In addition, the initial core water accumulation rate was significantly lower than Test S1-21 as known from Figs. 3.35 and 3.36. These resulted in much poorer initial core cooling as shown in Figs. 3.17 and 3.19.

However, if we shift the horizontal axis by 21.5 s, we can know that the core water mass at the switching time from Acc injection to LPCI injection was almost the same between the two tests as intended, and in addition, core inlet water subcooling was also almost the same. These facts resulted in the almost similar core cooling behavior in the later portion of test period as known from Figs. 3.17 and 3.19. These experimental information suggests that especially the transient of core water mass is very sensitive to the core cooling behavior.

One of the important results of Test S1-24 is that core differential pressure increased gradually during LPCI injection similarly as in Test S1-21 even if the U-tube oscillations were much reduced. This gradual increase in core differential pressure is one of the quite different behaviors from CCTF tests in which core differential pressure increases very slowly or is kept at an almost constant value as shown in Fig. 3.3.

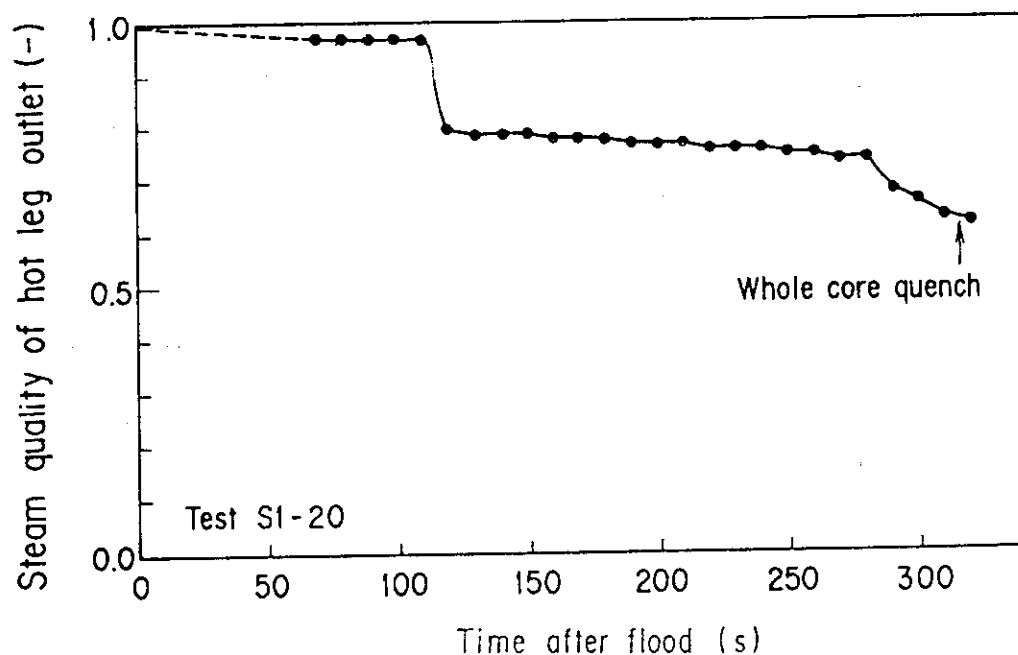


Fig. 3.1 Hot Leg Outlet Steam Quality for Test S1-20

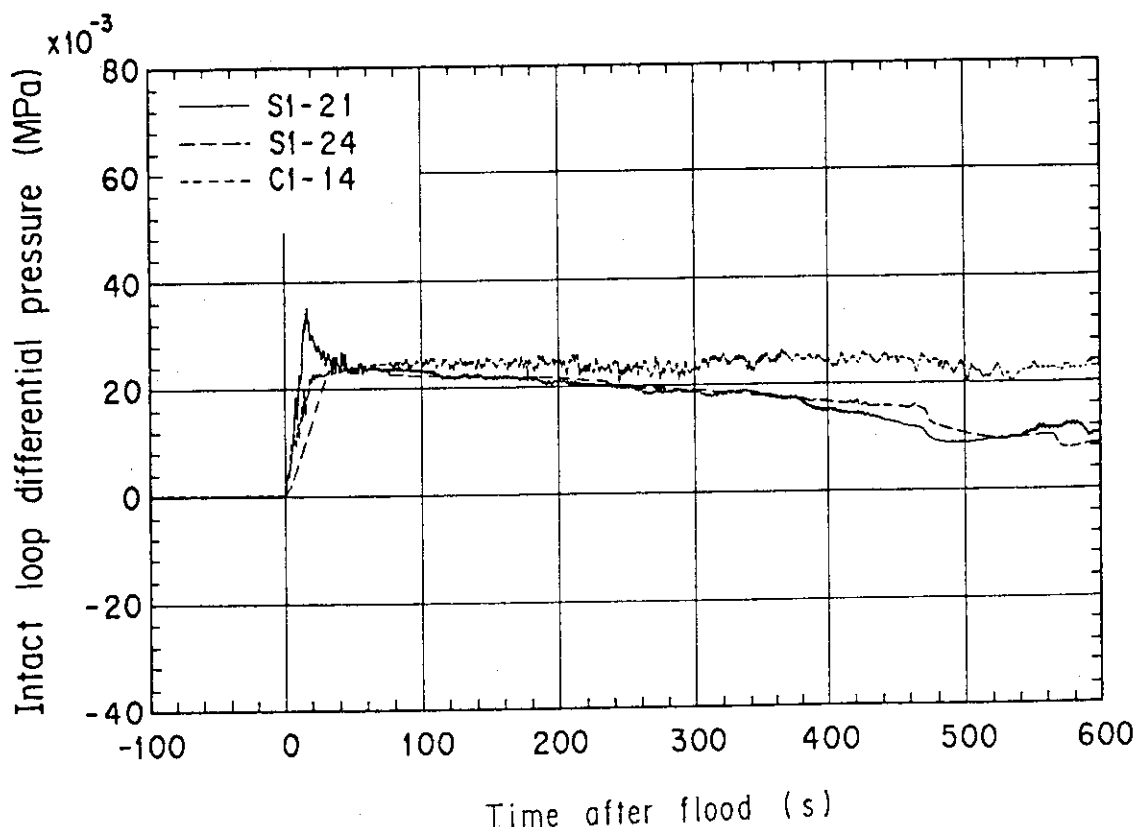


Fig. 3.2 Comparison in Intact Loop Differential Pressure between
SCTF and CCTF Tests

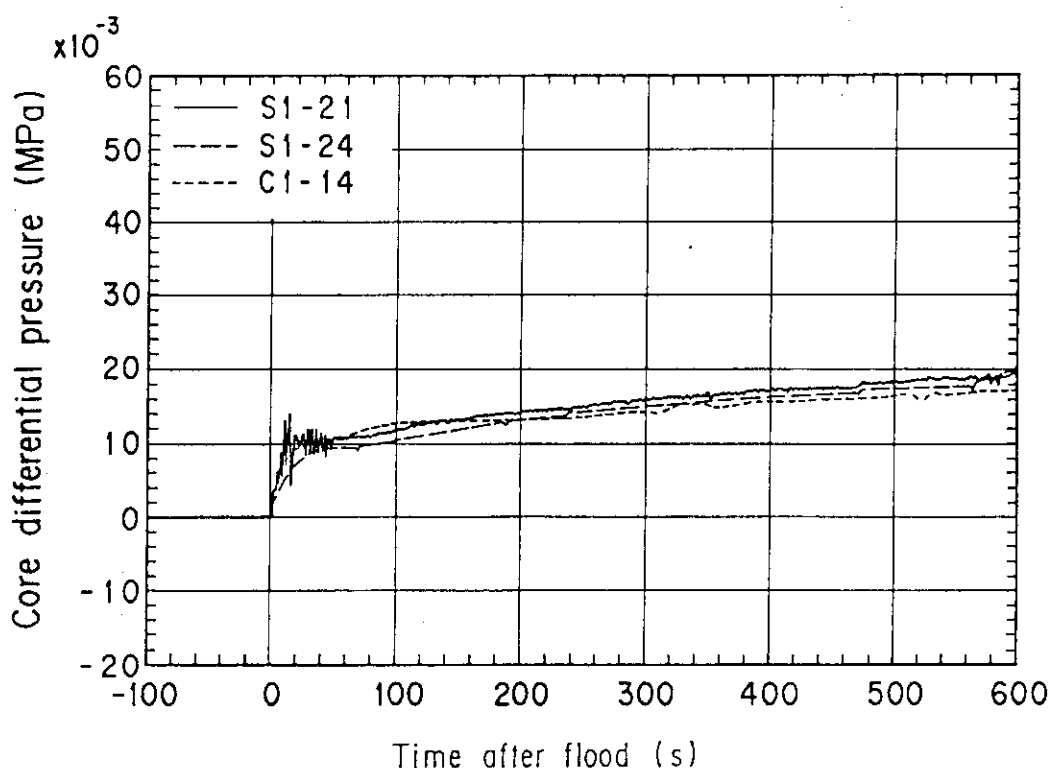


Fig. 3.3 Comparison in Core Differential Pressure between SCTF and CCTF Tests

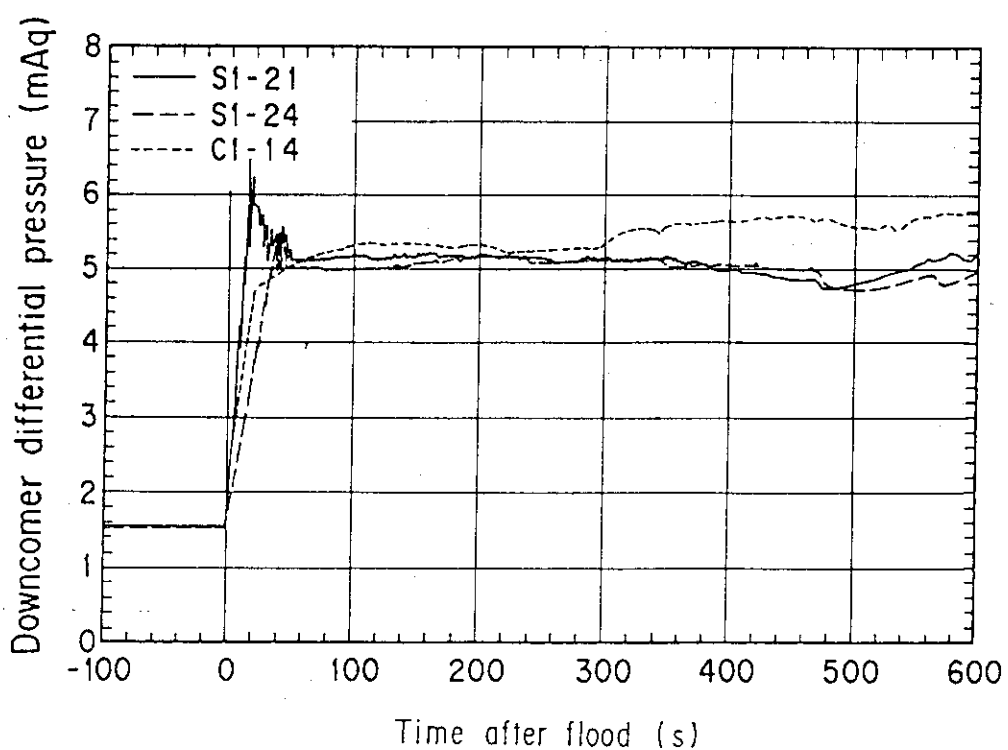


Fig. 3.4 Comparison in Downcomer Water Head between SCTF and CCTF Tests

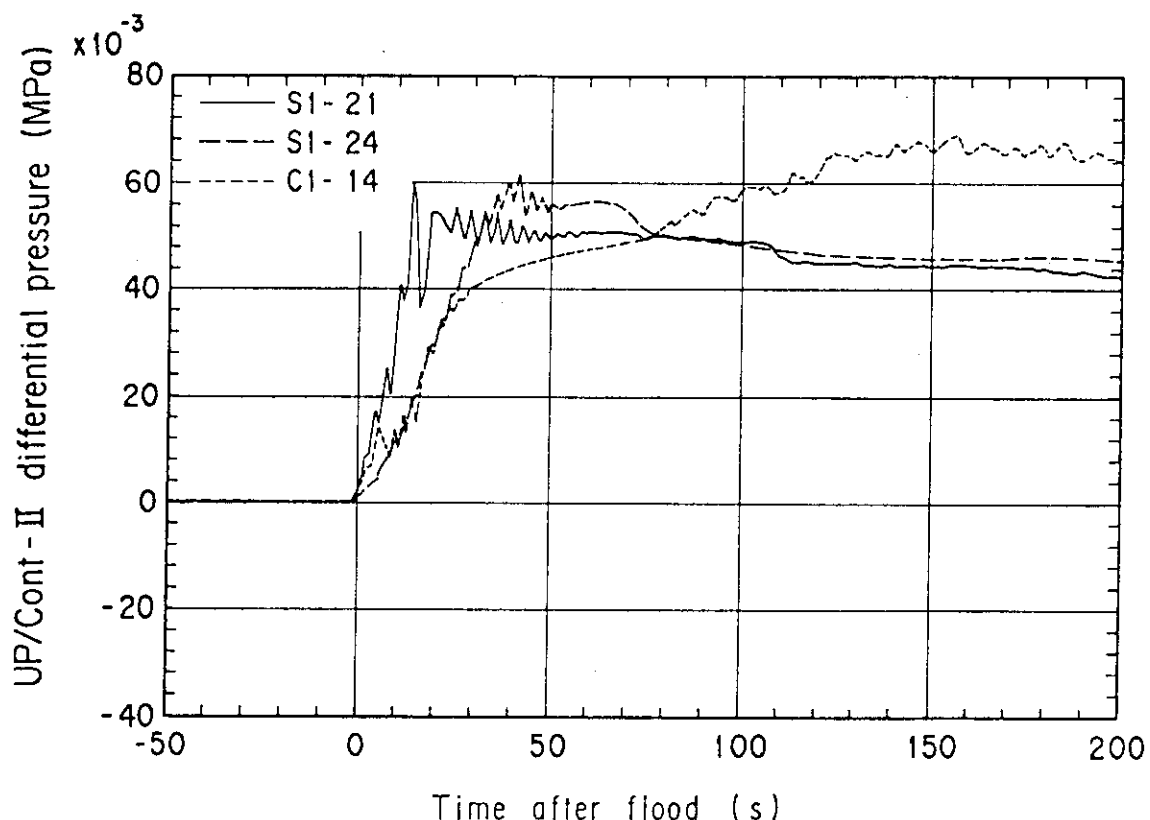


Fig. 3.5 Comparison in Differential Pressure between Upper Plenum and Containment Tank-II between SCTF and CCTF Tests

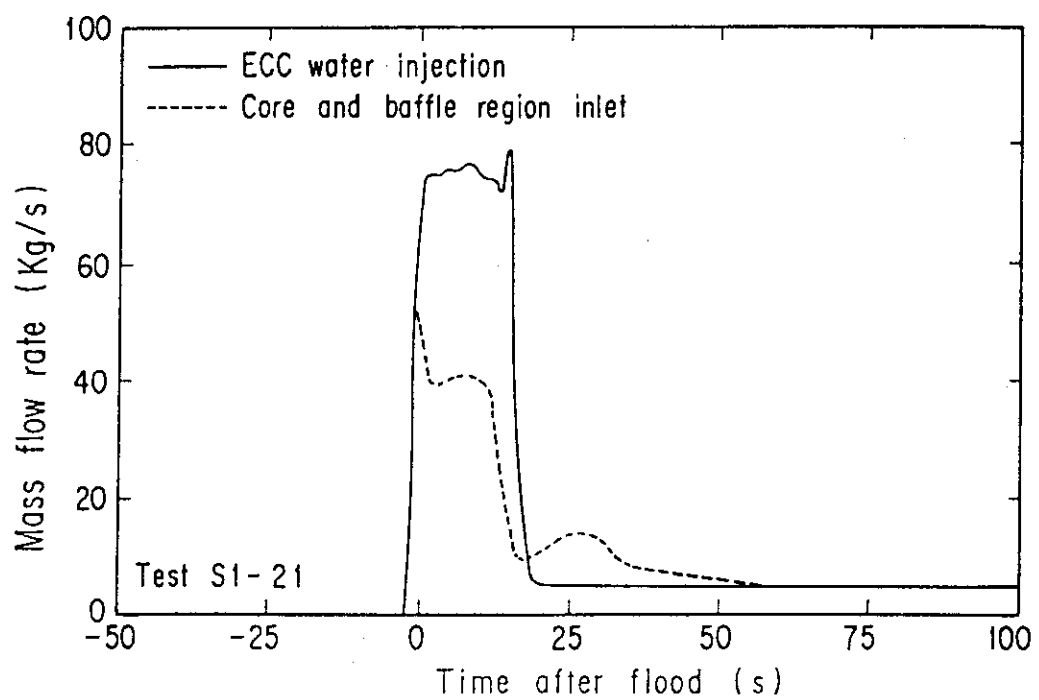


Fig. 3.6 Transient of Core Inlet Water Flow Rate

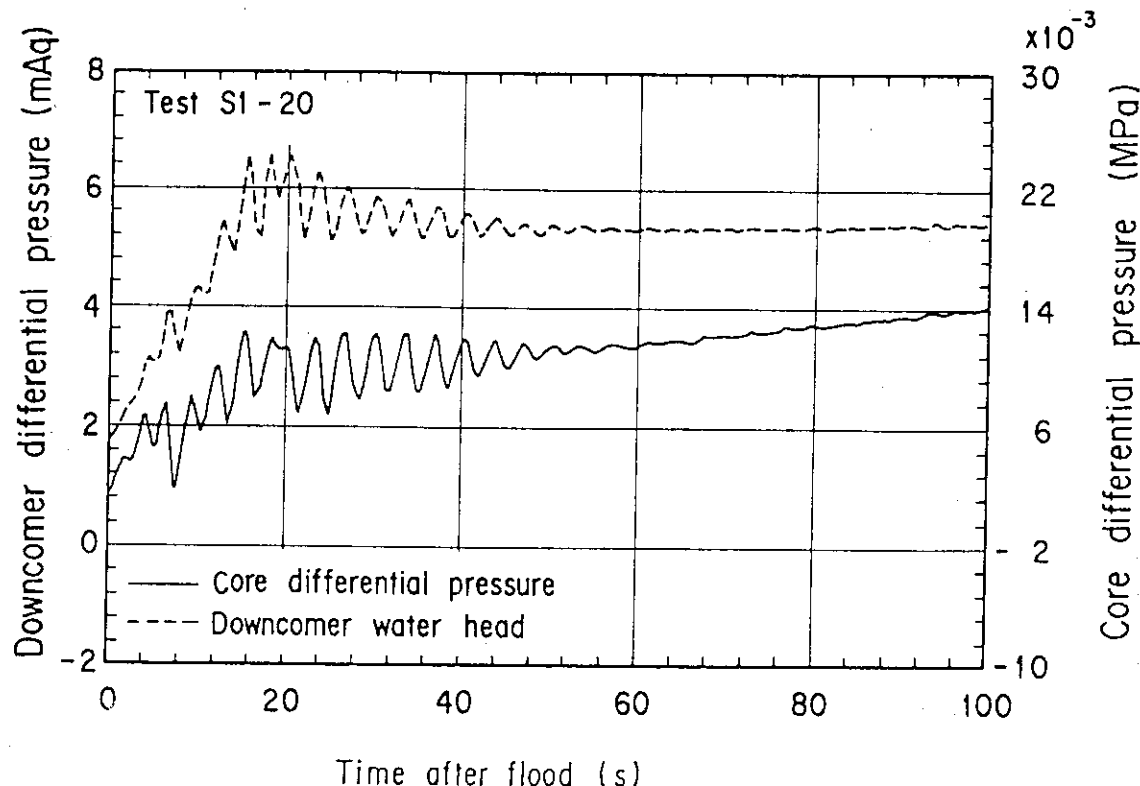


Fig. 3.7 Comparison in Oscillation Phase between Core Differential Pressure and Downcomer Water Head for Test S1-20

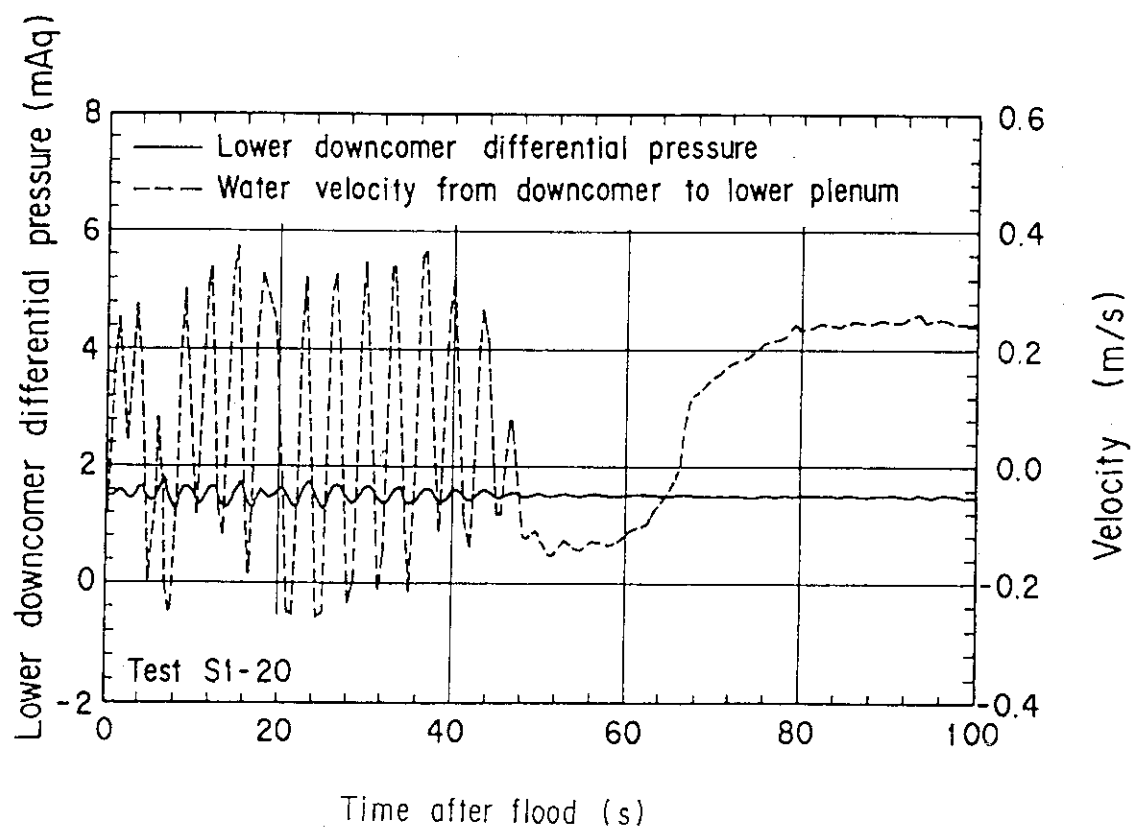


Fig. 3.8 Comparison in Oscillation Phase between Lower Downcomer Differential Pressure and Water Velocity at Lower Plenum Inlet

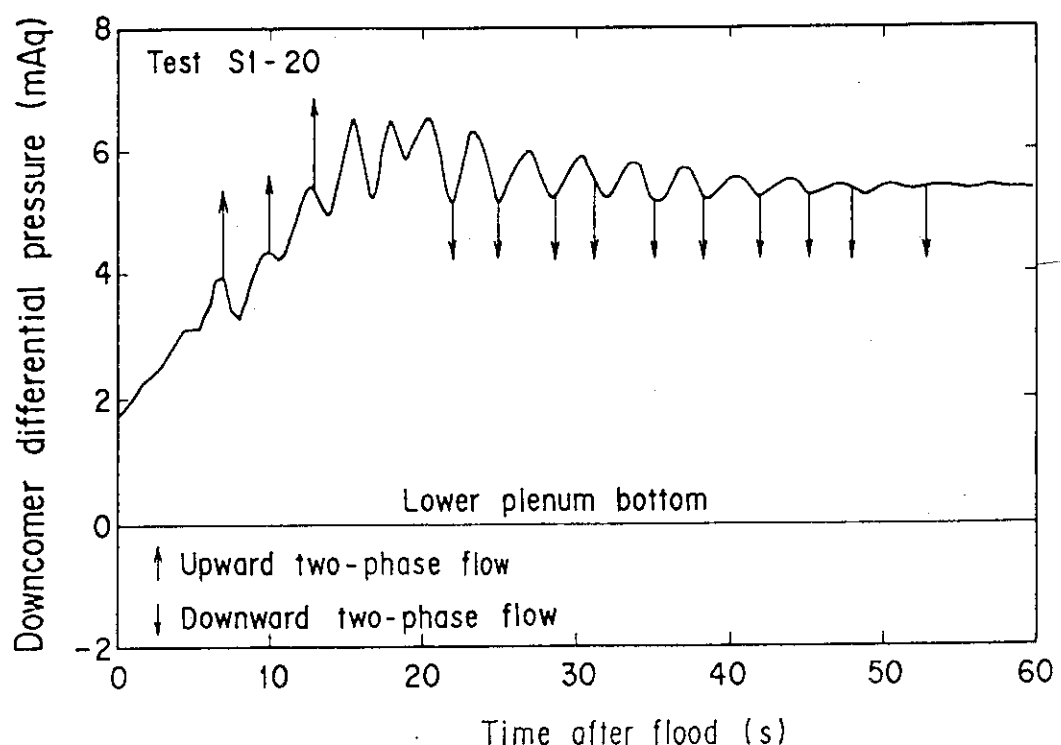


Fig. 3.9 Comparison in Oscillation Phase between Downcomer Differential Pressure and Flow Regime just below End Box Tie Plate

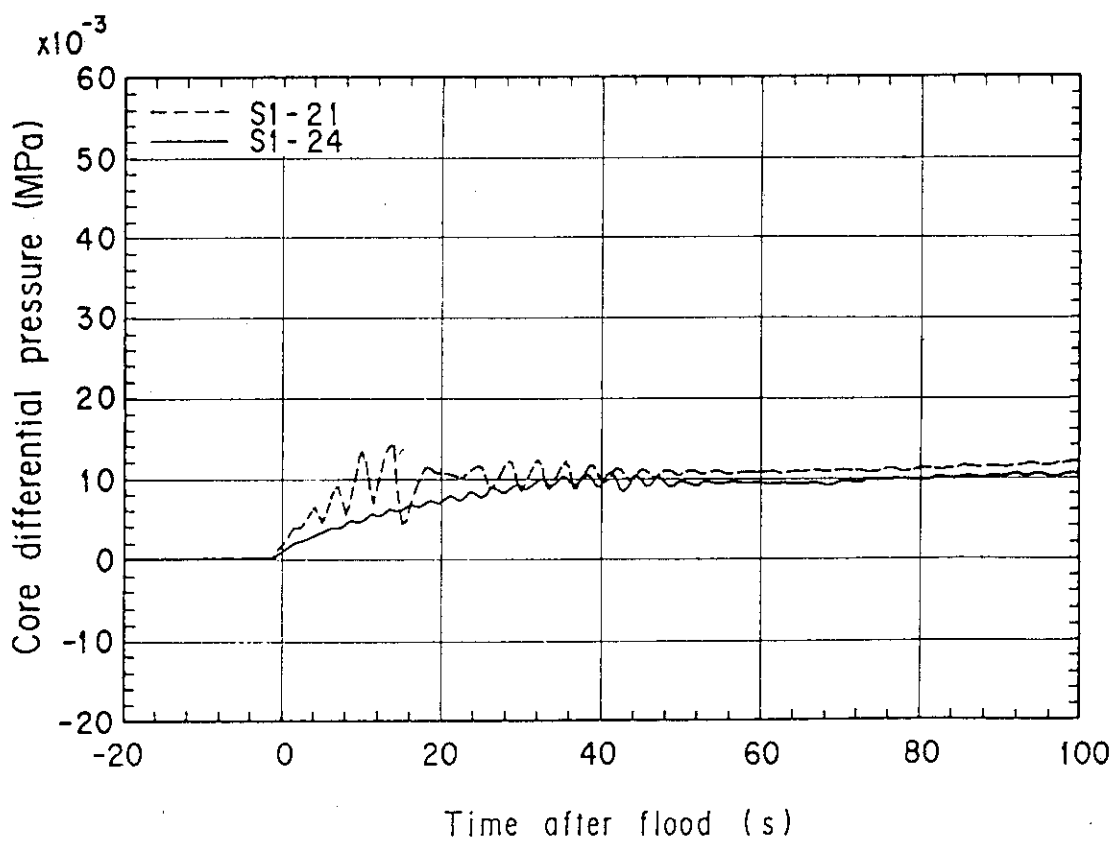


Fig. 3.10 Comparison in Core Differential Pressure Oscillations between Tests S1-21 and S1-24

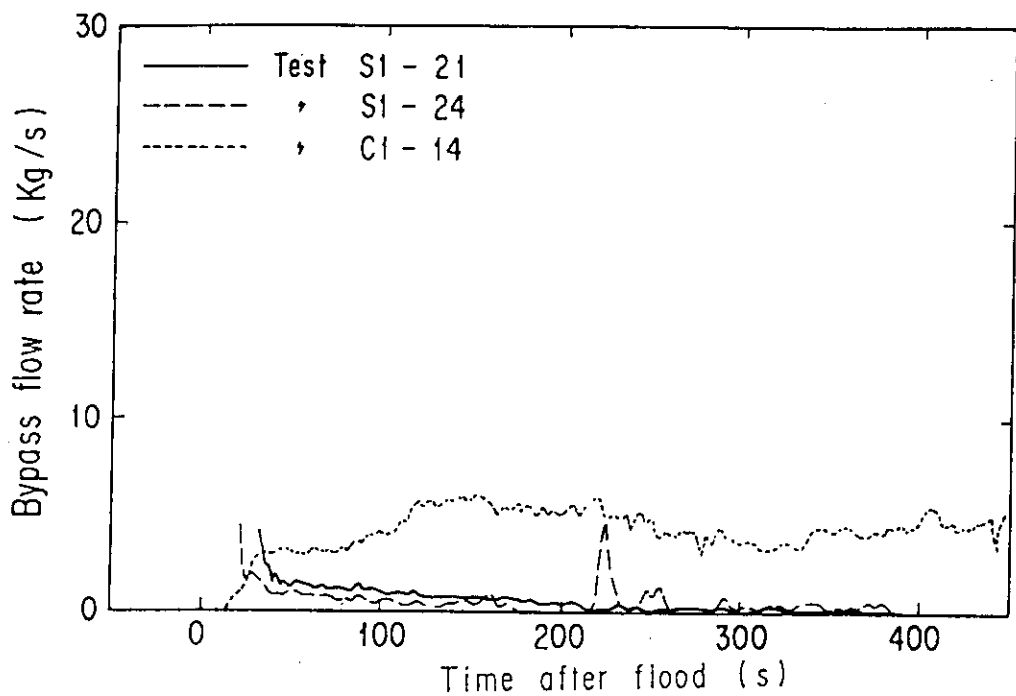


Fig. 3.11 Comparison in Bypass Flow Rate between SCTF and CCTF Tests

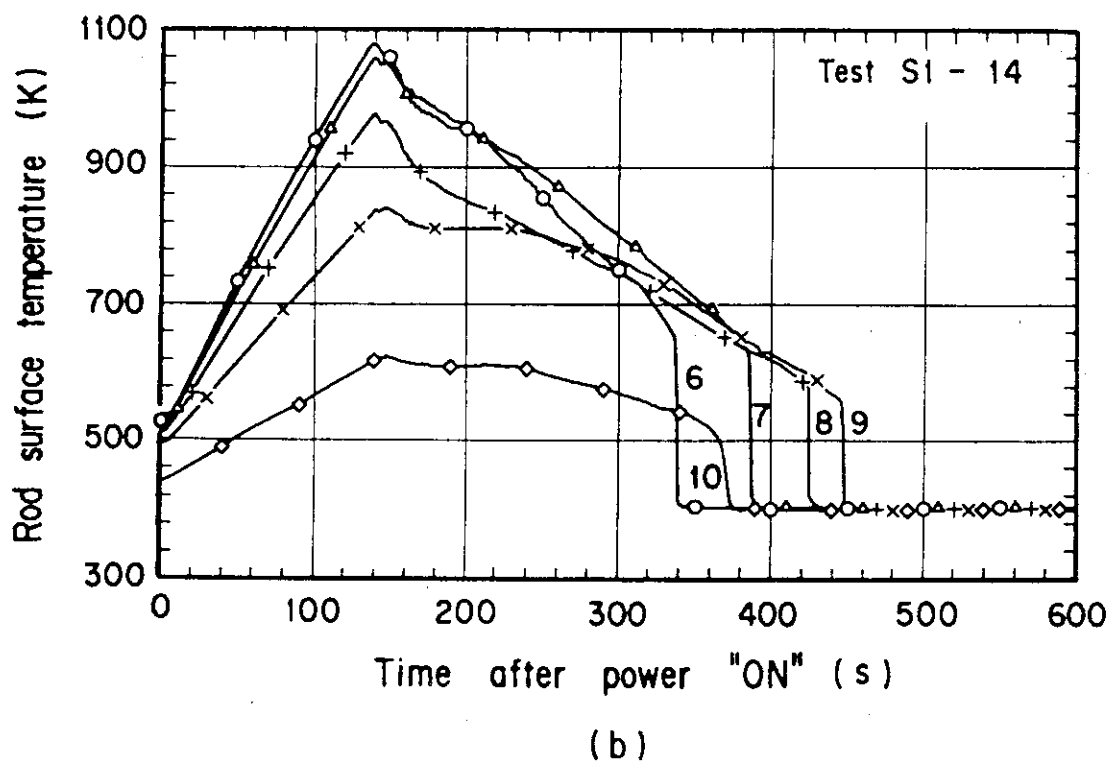
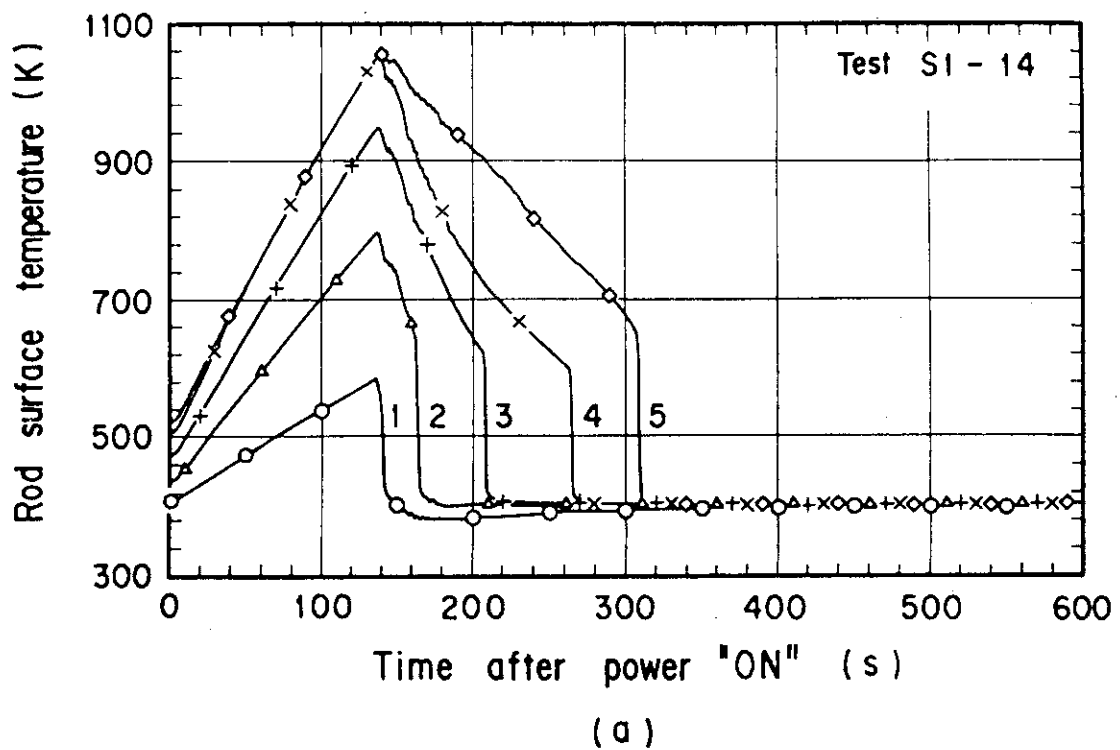


Fig. 3.12 Rod Surface Temperature at the Center of Bundle 4 for Test S1-14

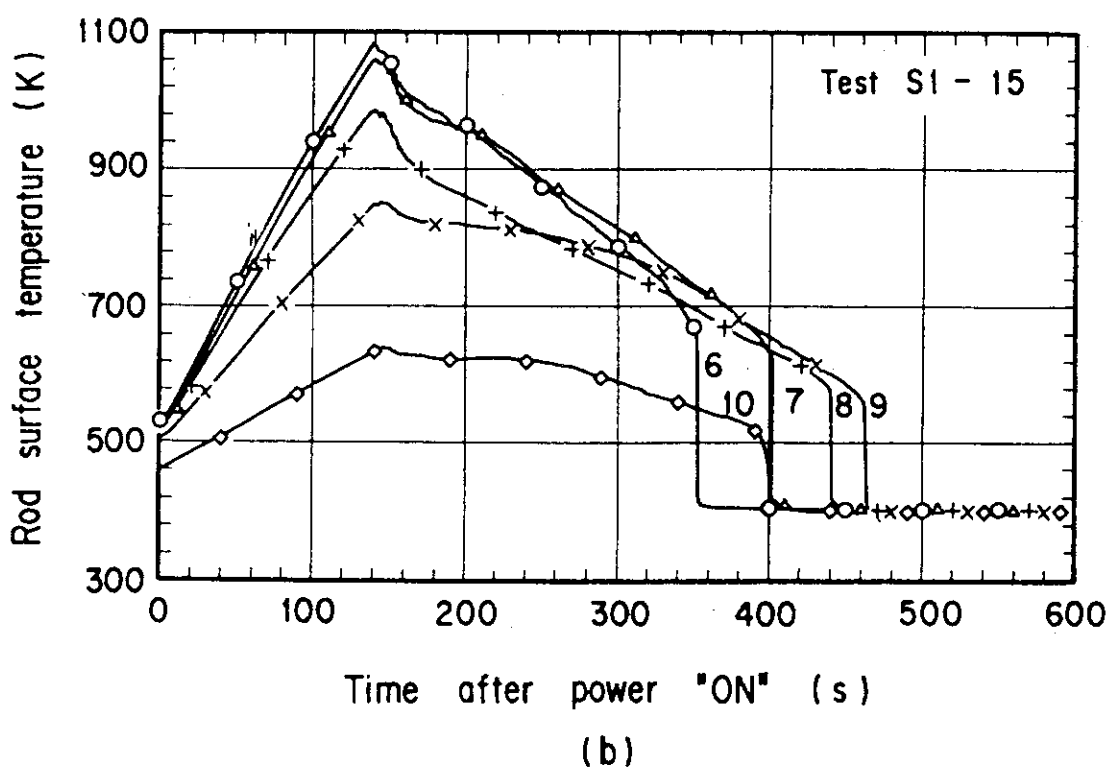
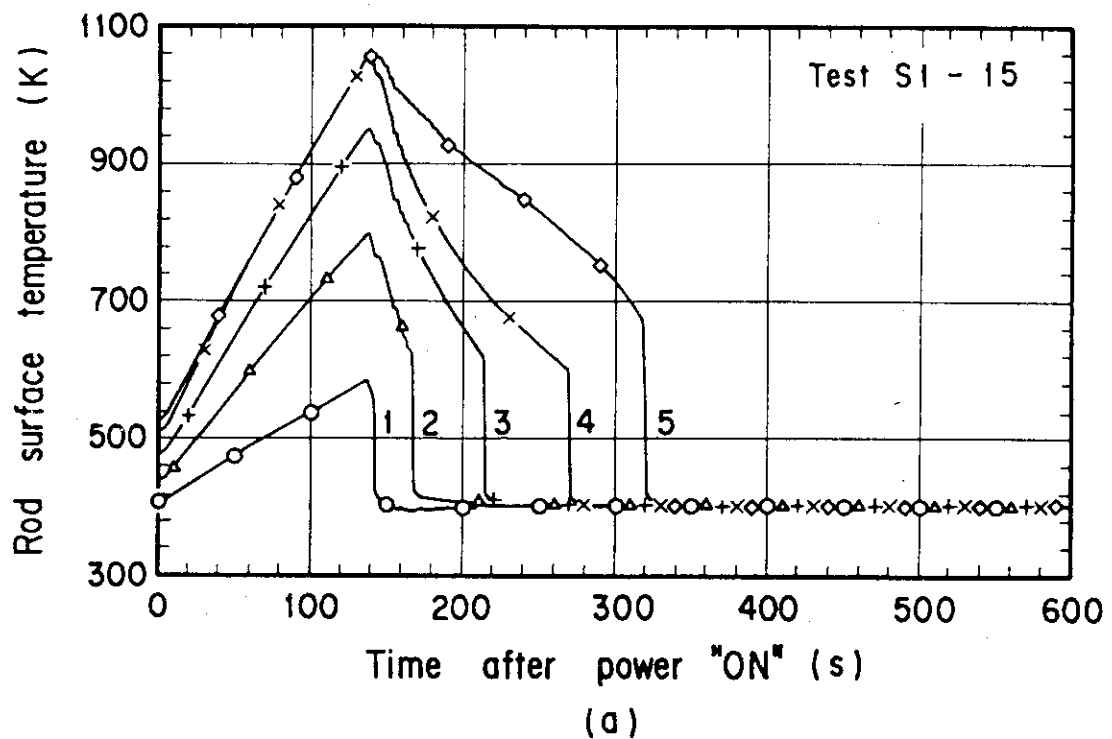


Fig. 3.13 Rod Surface Temperature at the Center of Bundle 4 for Test S1-15

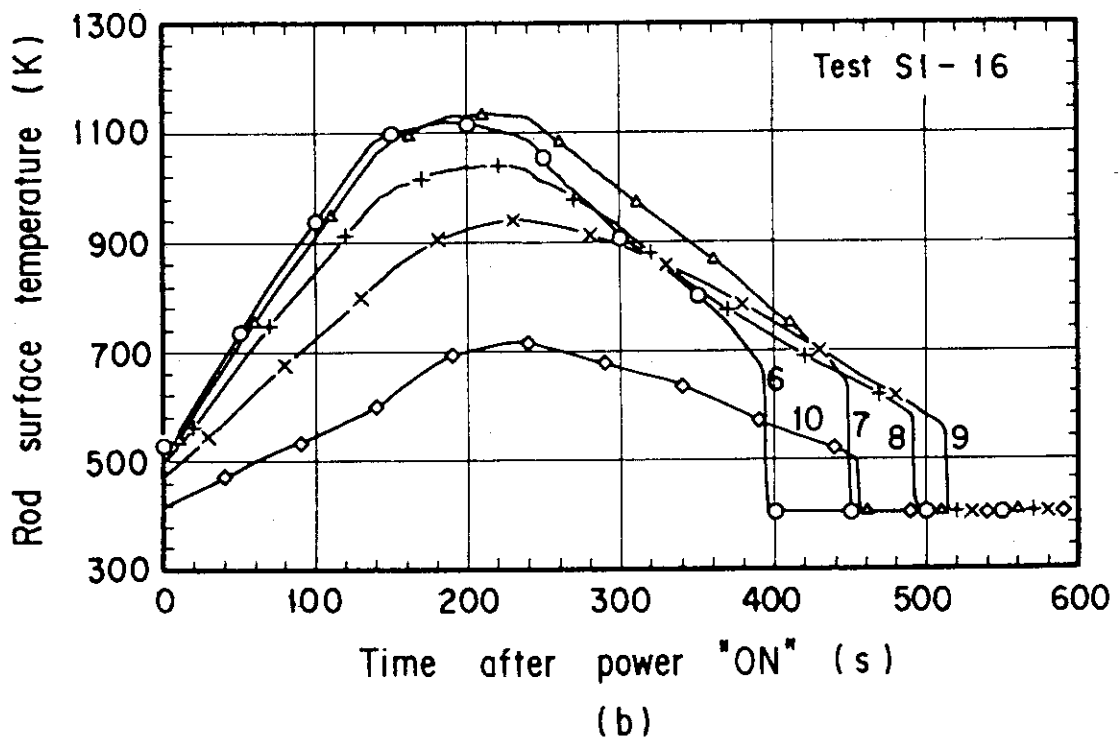
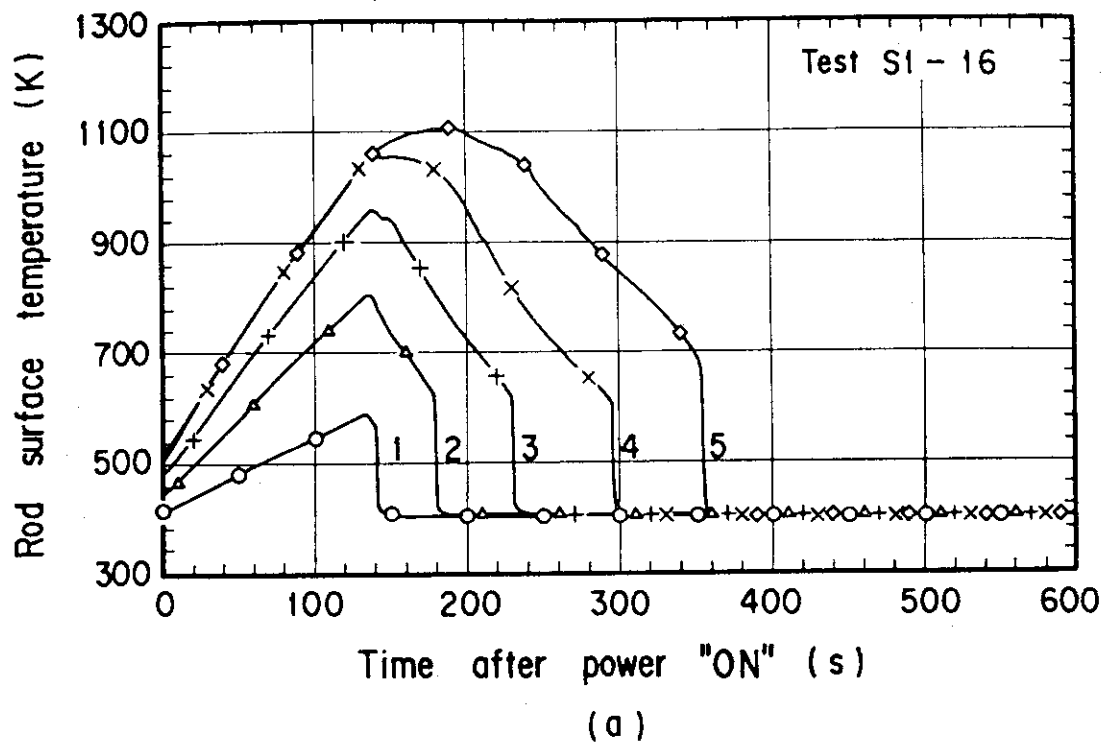


Fig. 3.14 Rod Surface Temperature at the Center of Bundle 4 for Test S1-16

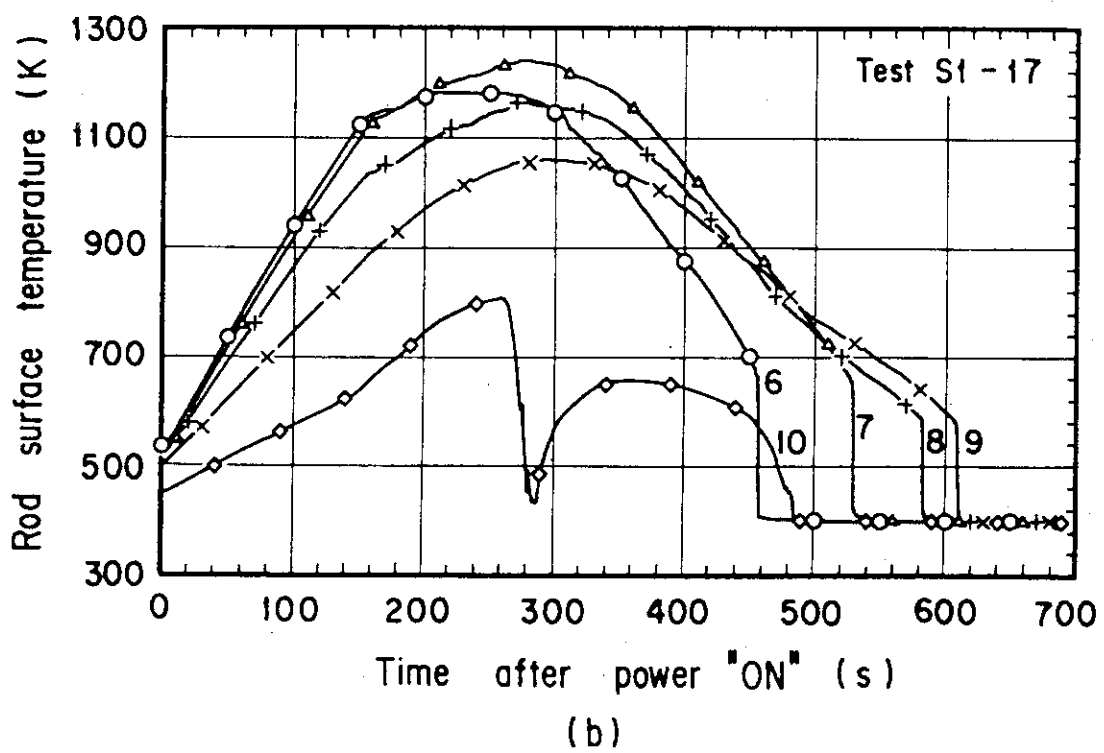
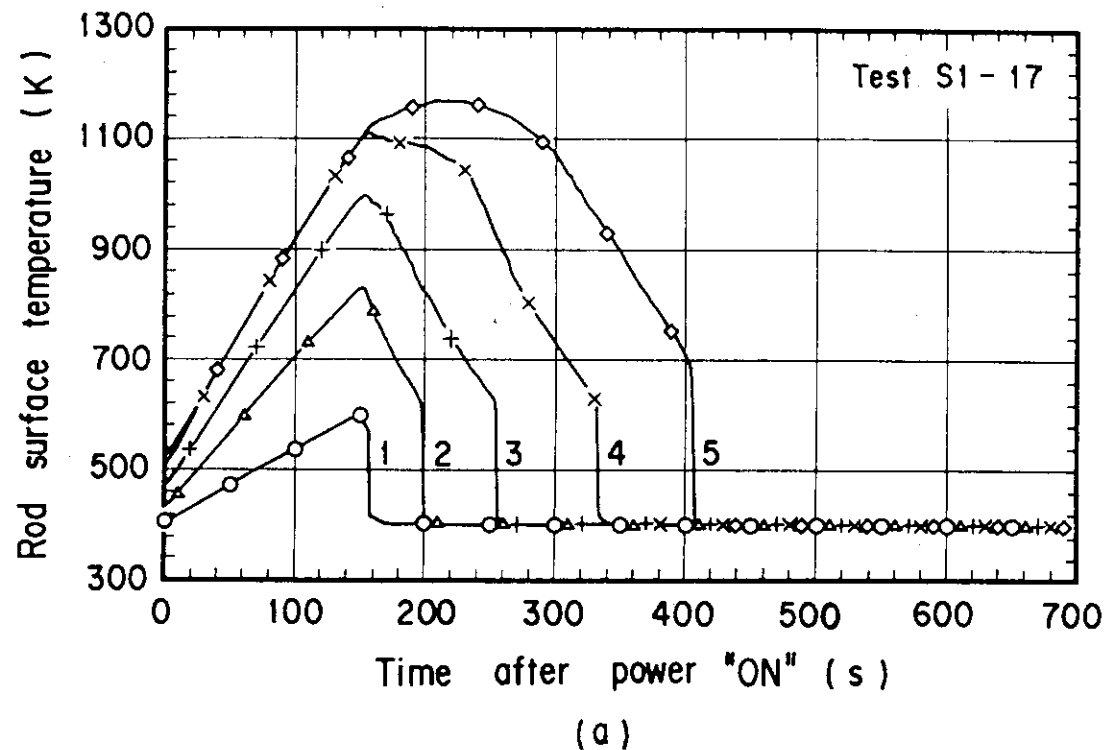


Fig. 3.15 Rod Surface Temperature at the Center of Bundle 4 for Test S1-17

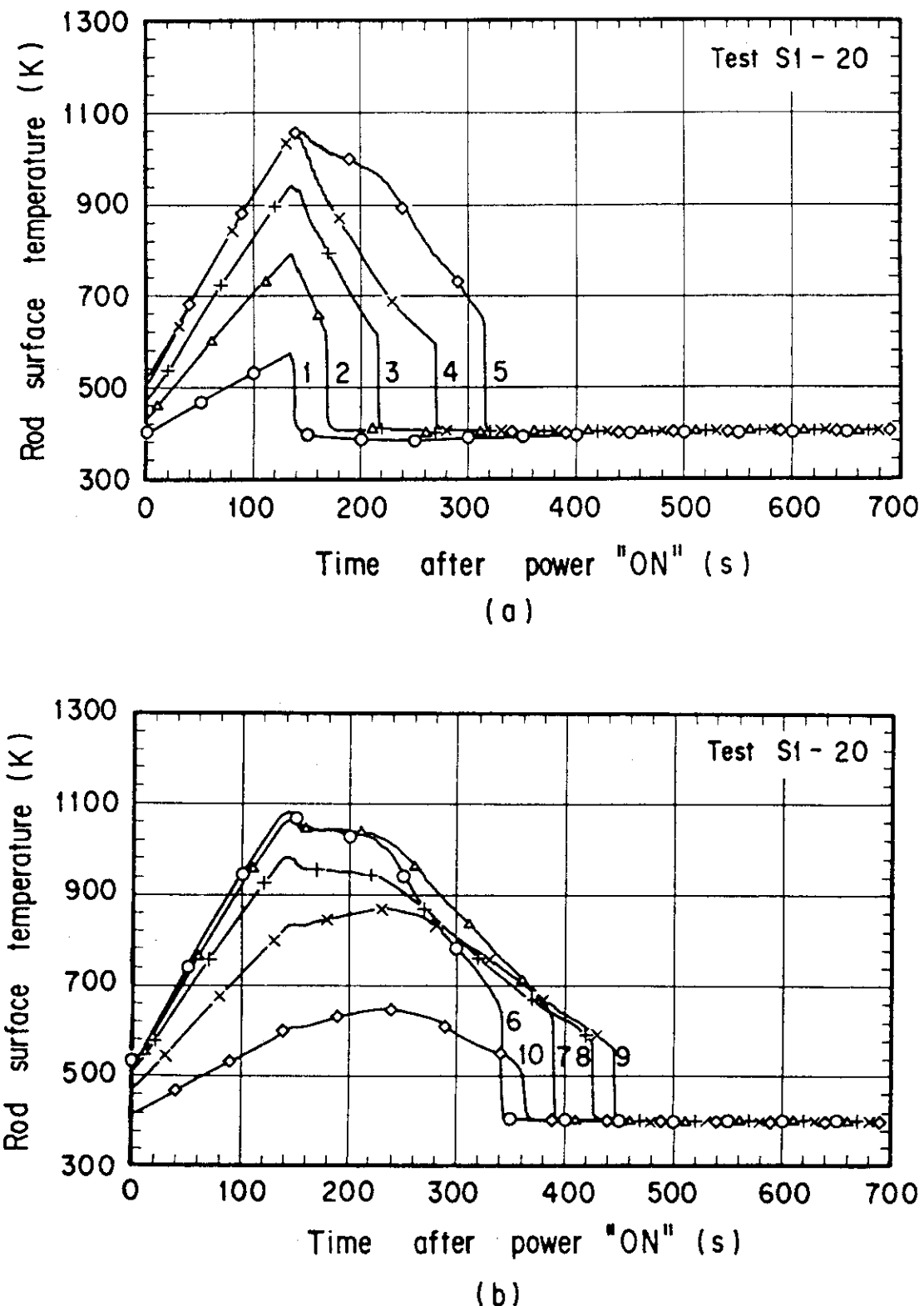


Fig. 3.16 Rod Surface Temperature at the Center of Bundle 4 for Test S1-20

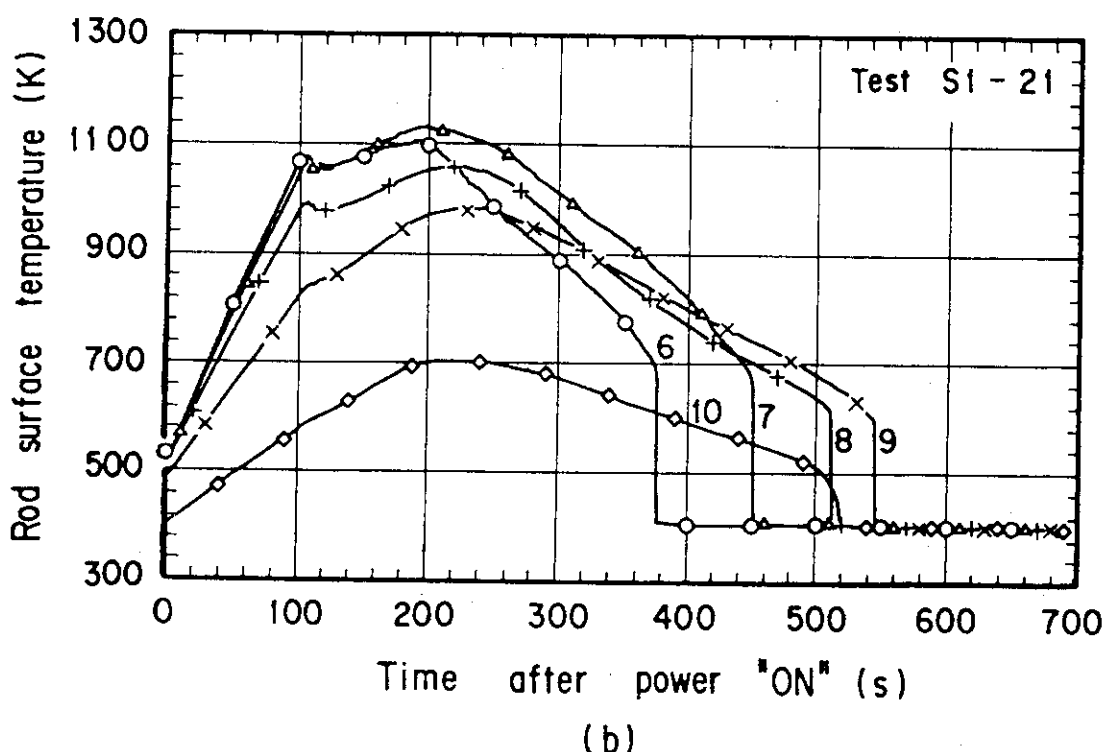
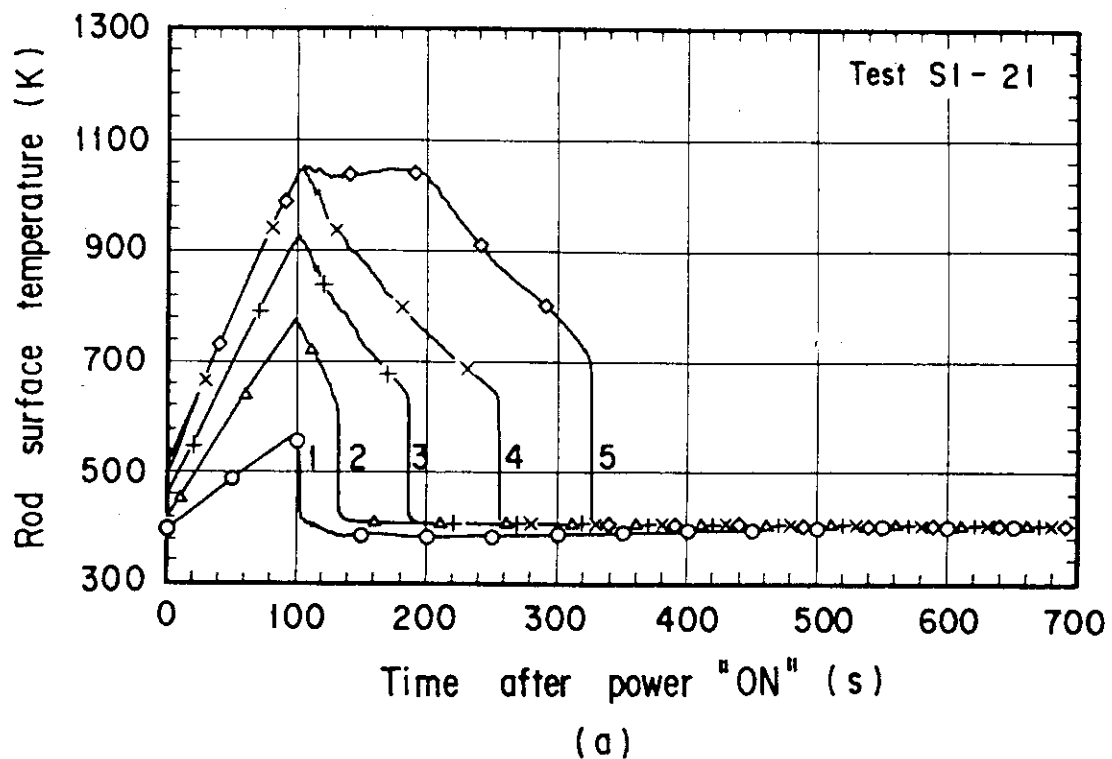


Fig. 3.17 Rod Surface Temperature at the Center of Bundle 4 for Test S1-21

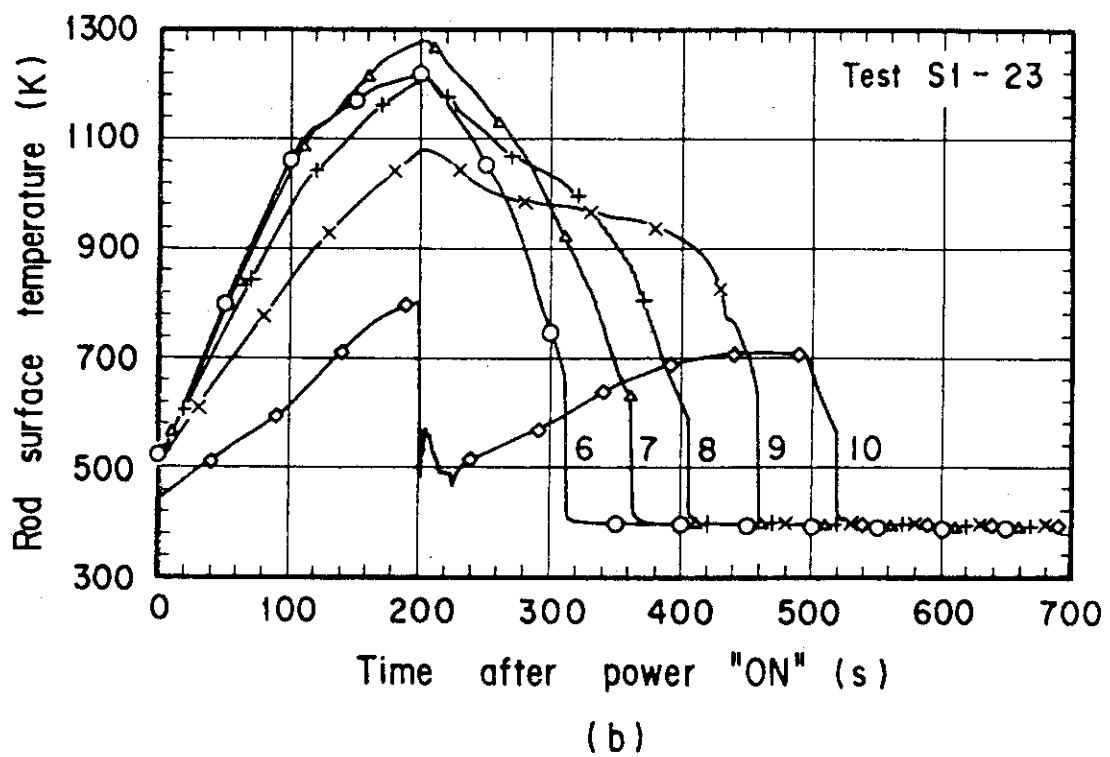
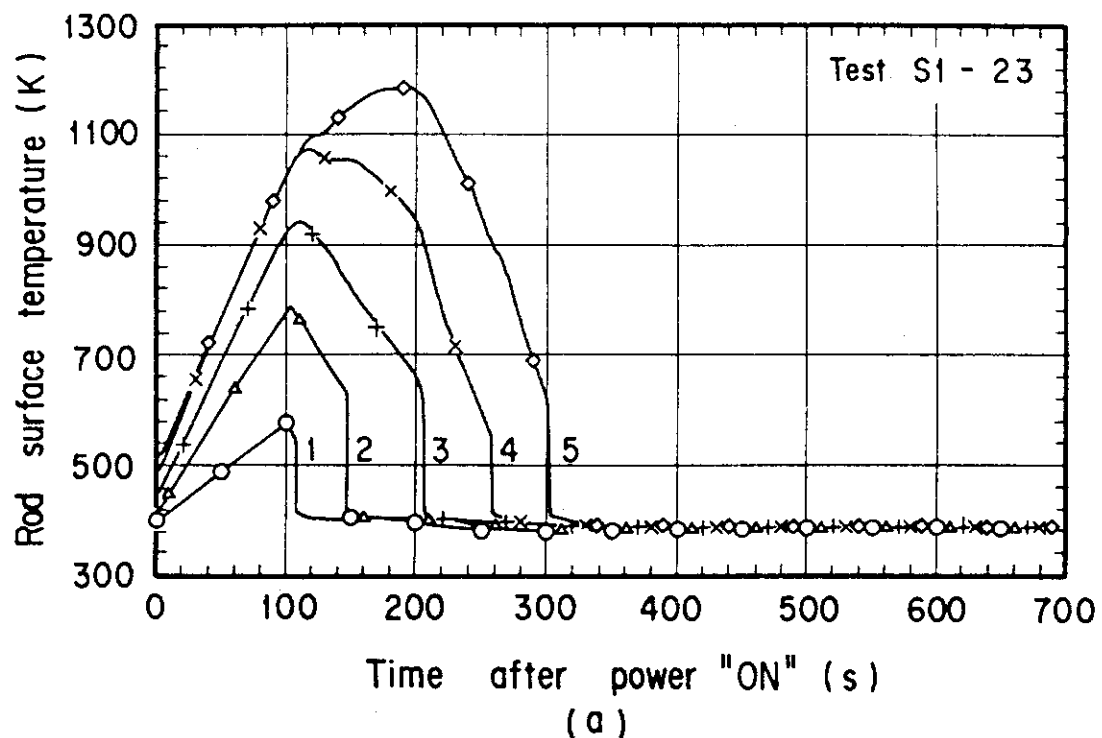


Fig. 3.18 Rod Surface Temperature at the Center of Bundle 4 for Test S1-23

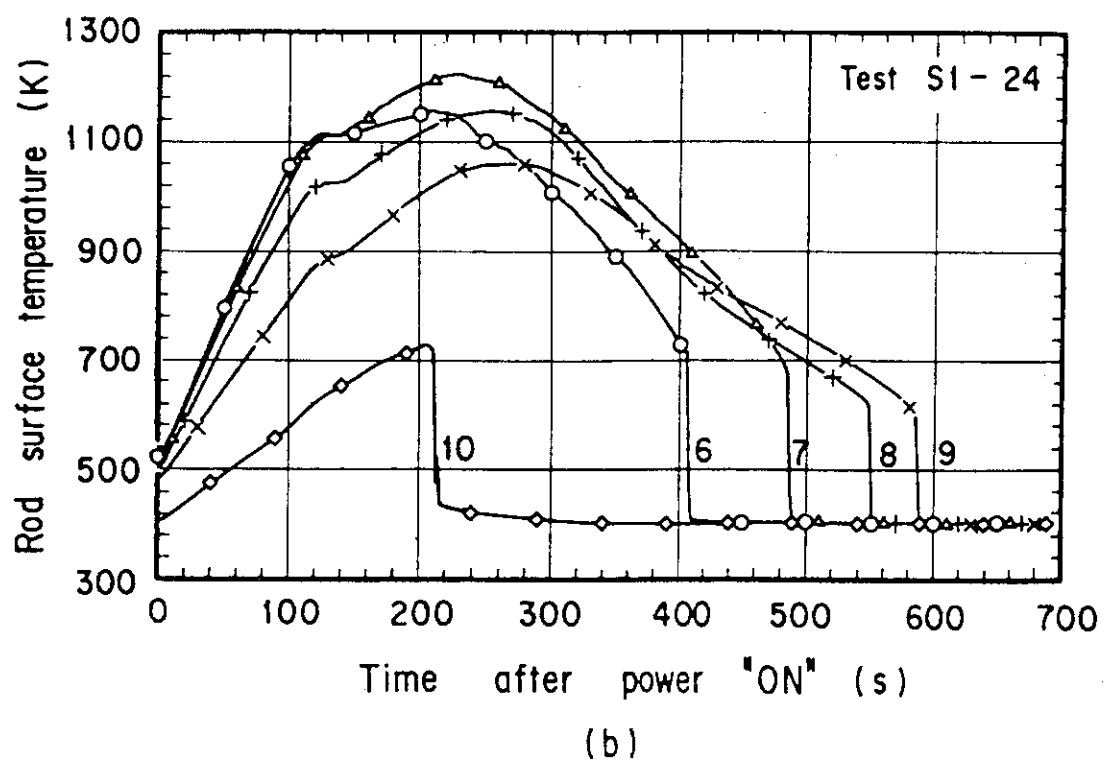
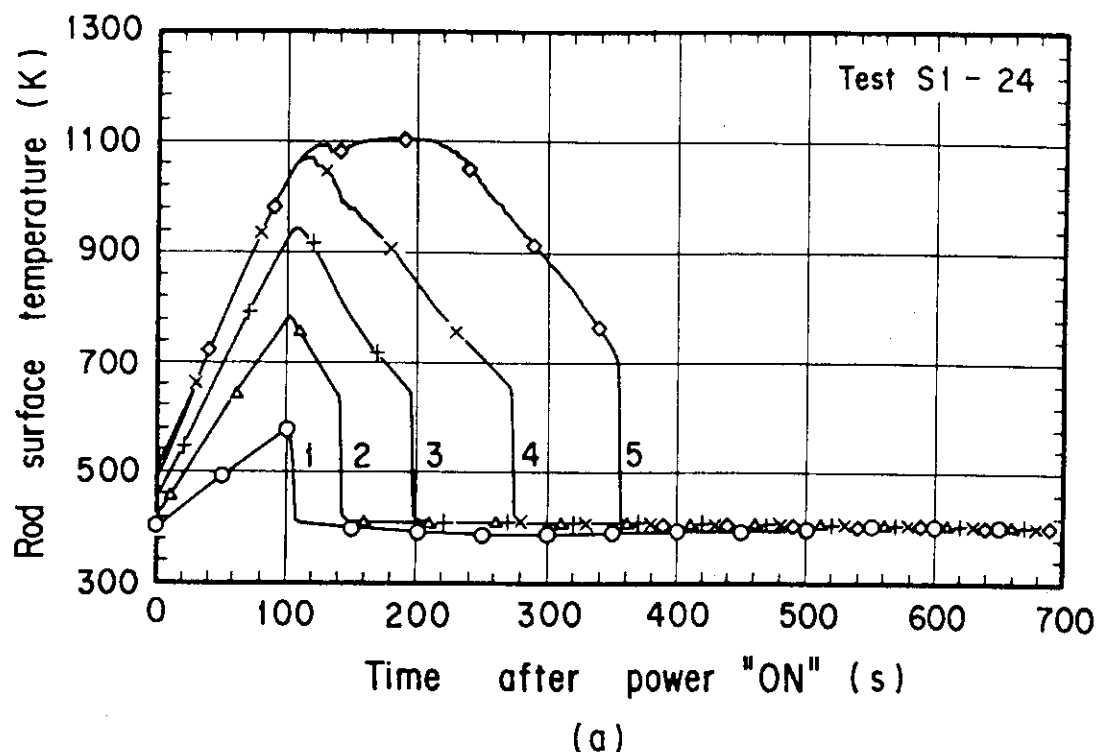


Fig. 3.19 Rod Surface Temperature at the Center of Bundle 4 for Test S1-24

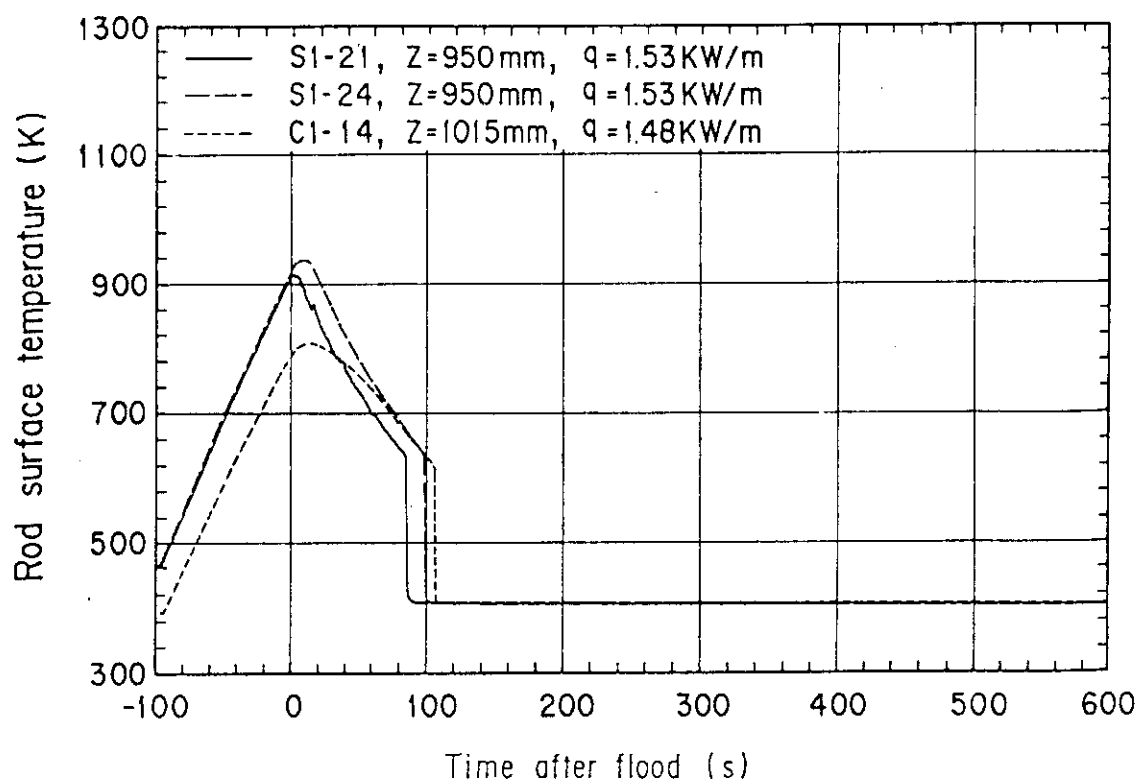


Fig. 3.20 Comparison in Rod Surface Temperature at the Lower Part of Core between SCTF and CCTF Tests

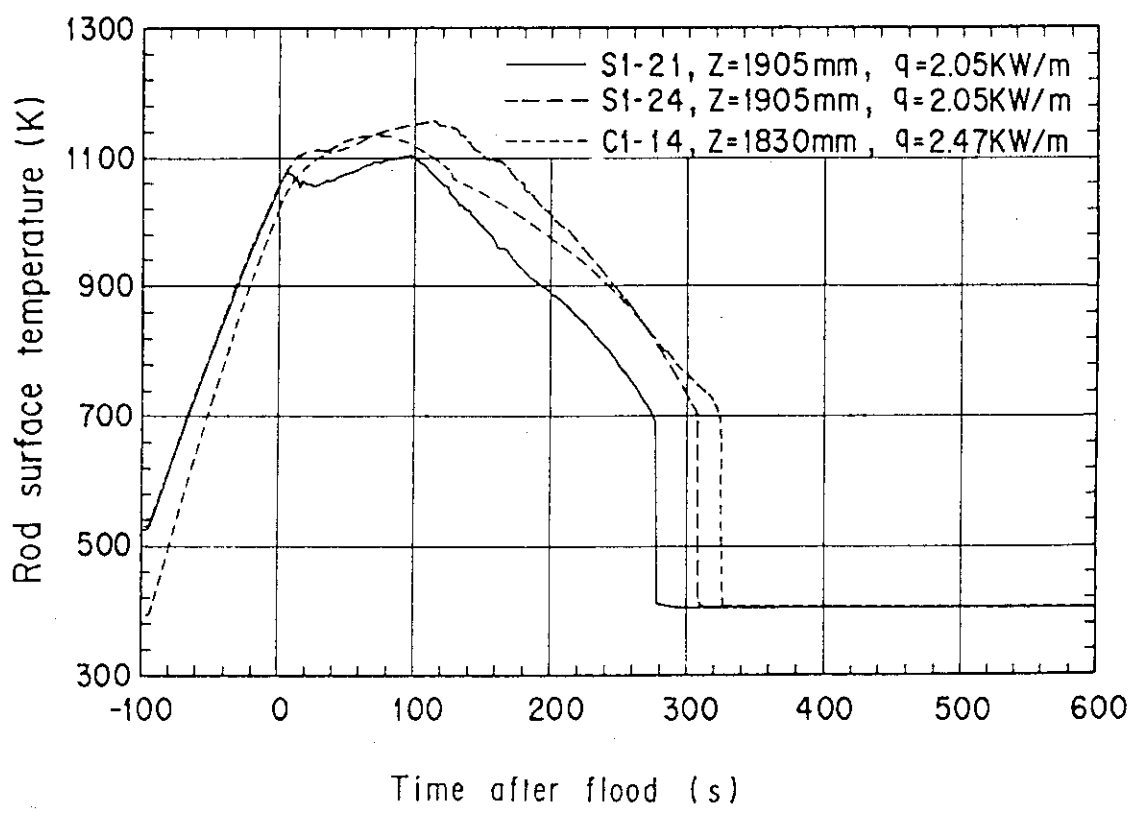


Fig. 3.21 Comparison in Rod Surface Temperature at the Mid-Elevation of Core between SCTF and CCTF Tests

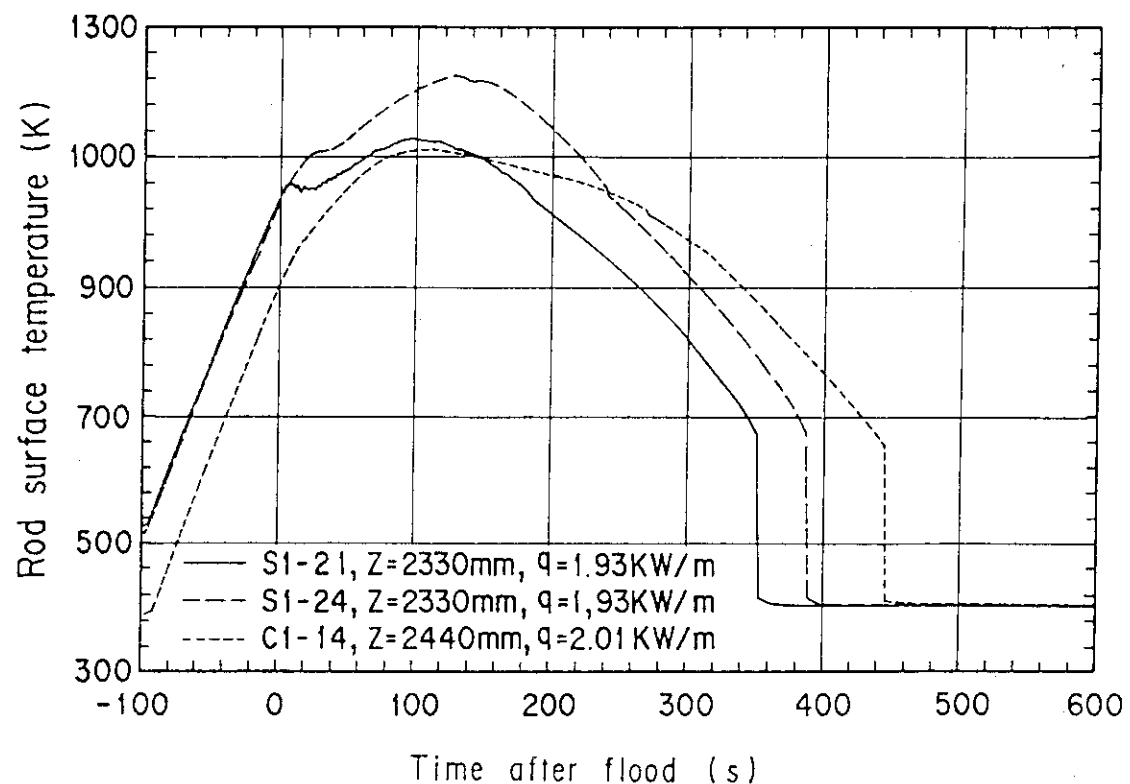


Fig. 3.22 Comparison in Rod Surface Temperature at the Upper Part of Core between SCTF and CCTF Tests

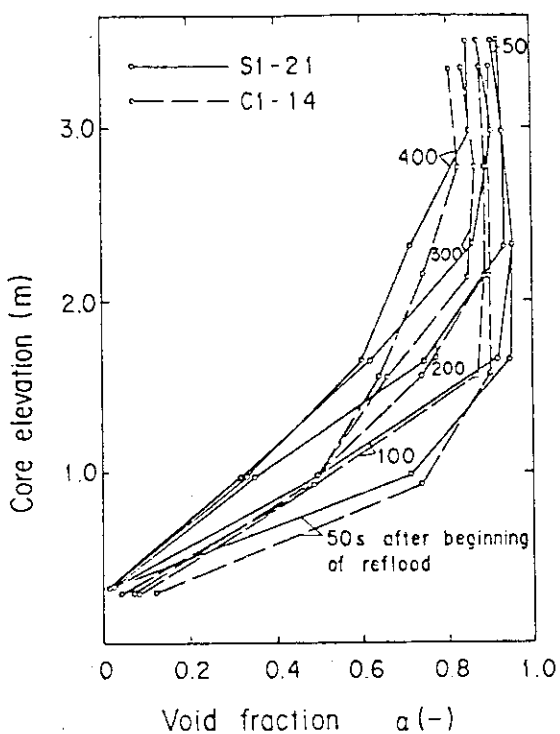


Fig. 3.23 Comparison in Void Fraction Distribution between SCTF and CCTF Tests

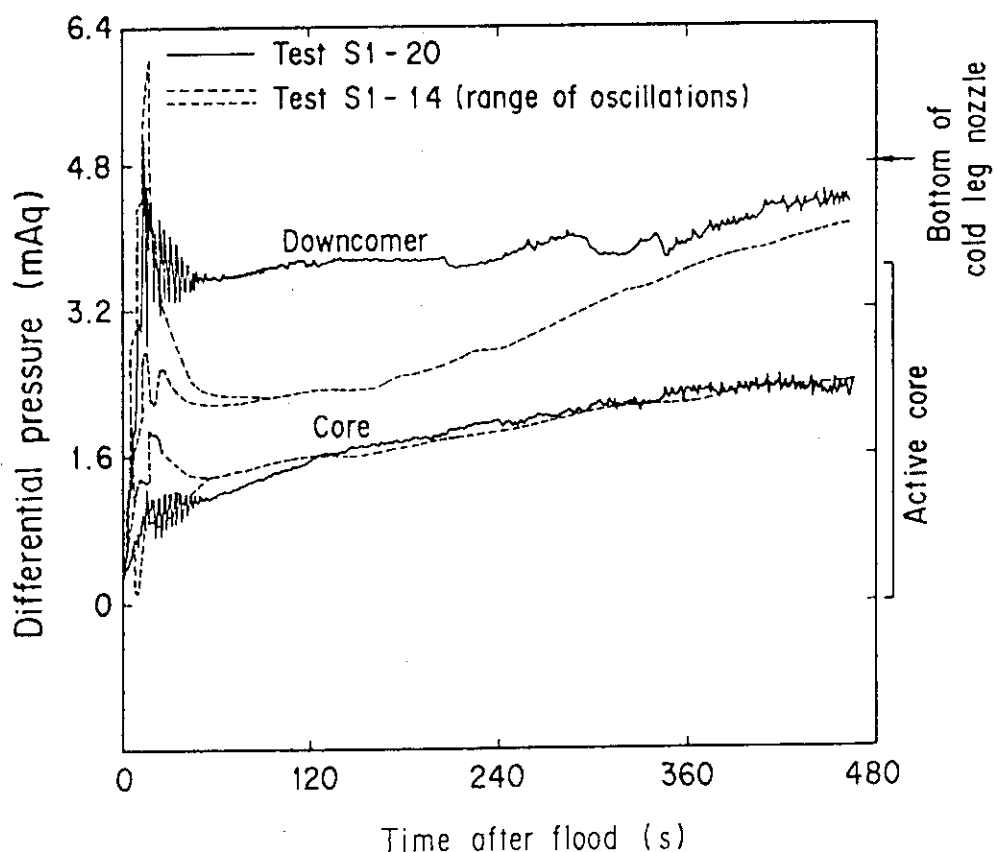


Fig. 3.24 Comparison in Downcomer Differential Pressure and Core Differential Pressure between Tests S1-14 and S1-20

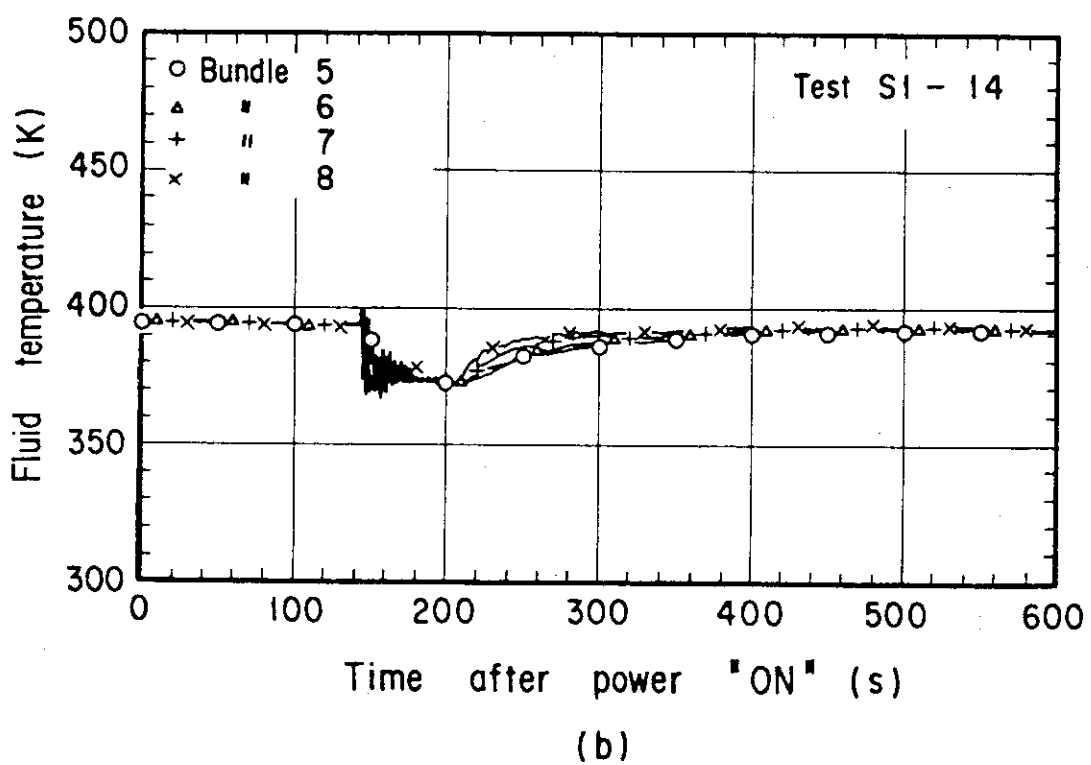
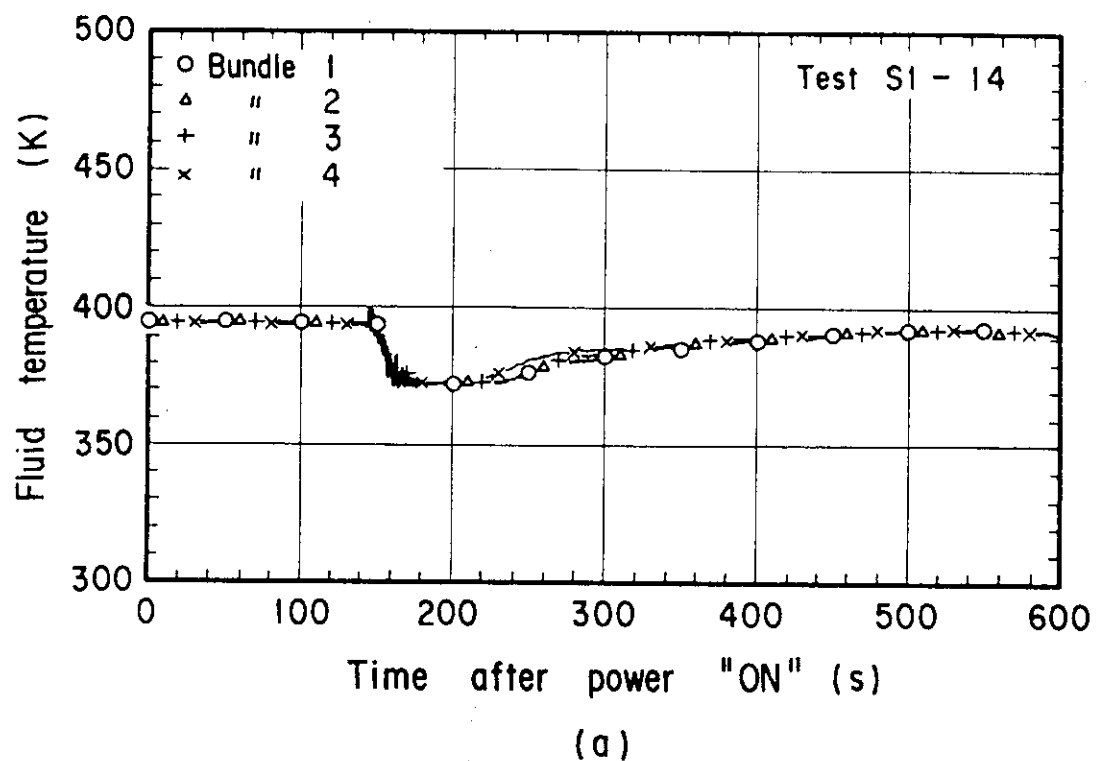


Fig. 3.25 Core Inlet Water Temperature for Test S1-14

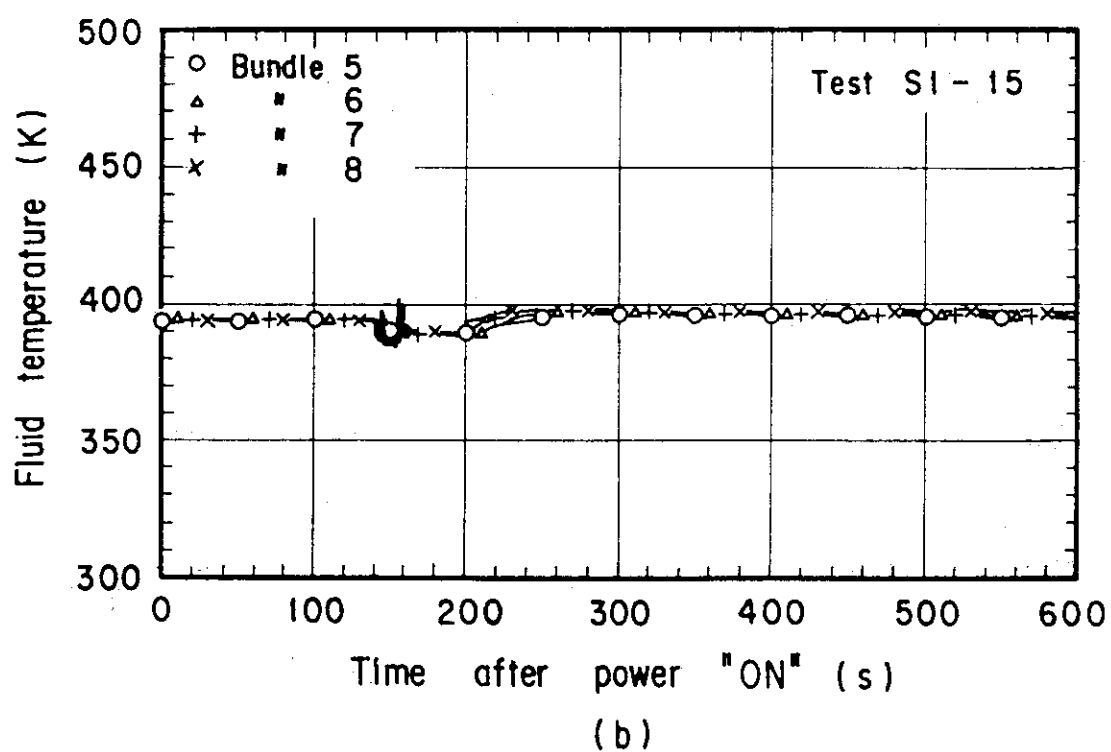
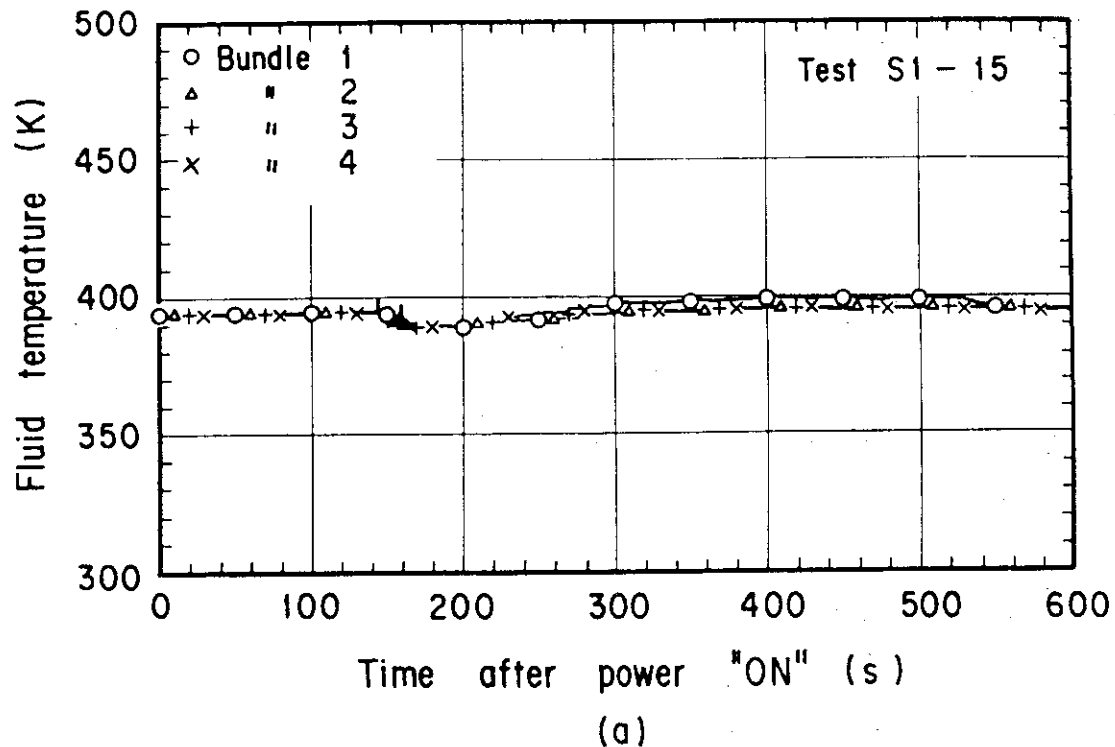


Fig. 3.26 Core Inlet Water Temperature for Test S1-15

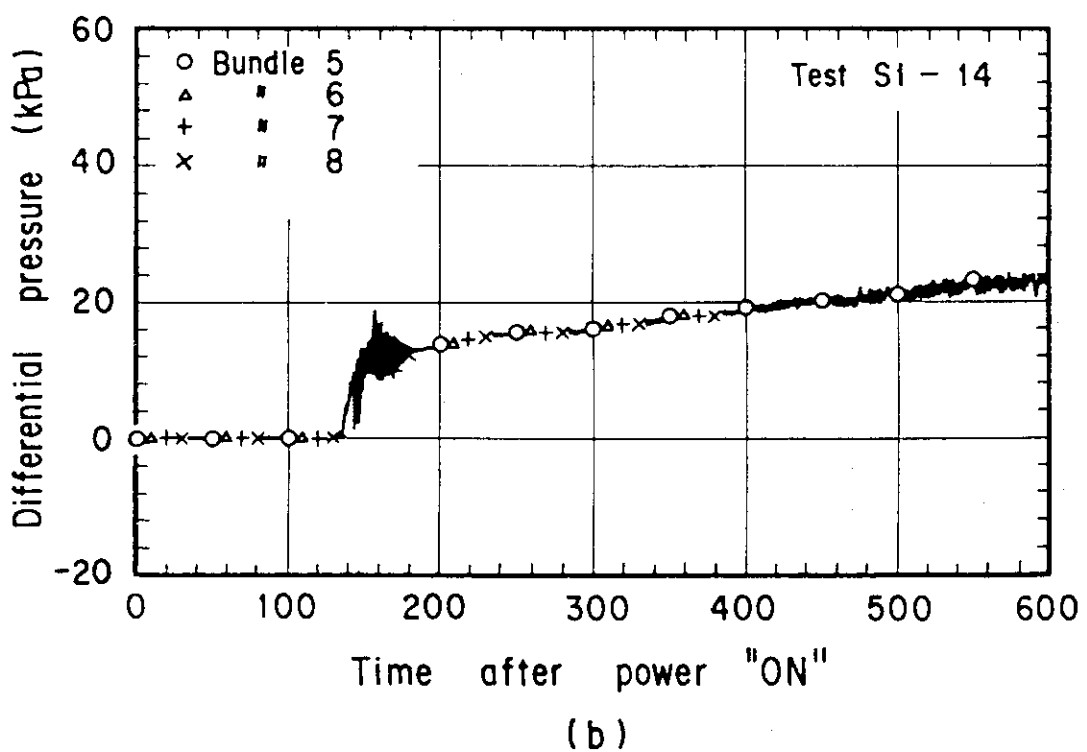
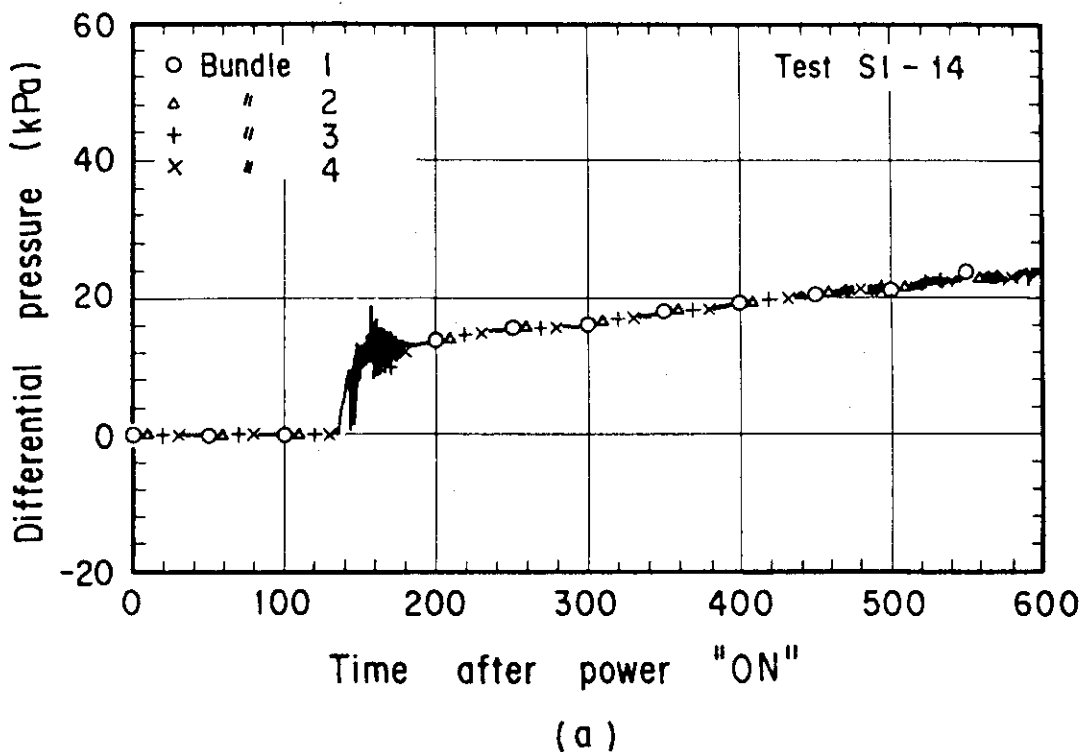


Fig. 3.27 Core Differential Pressure for Test SI-14

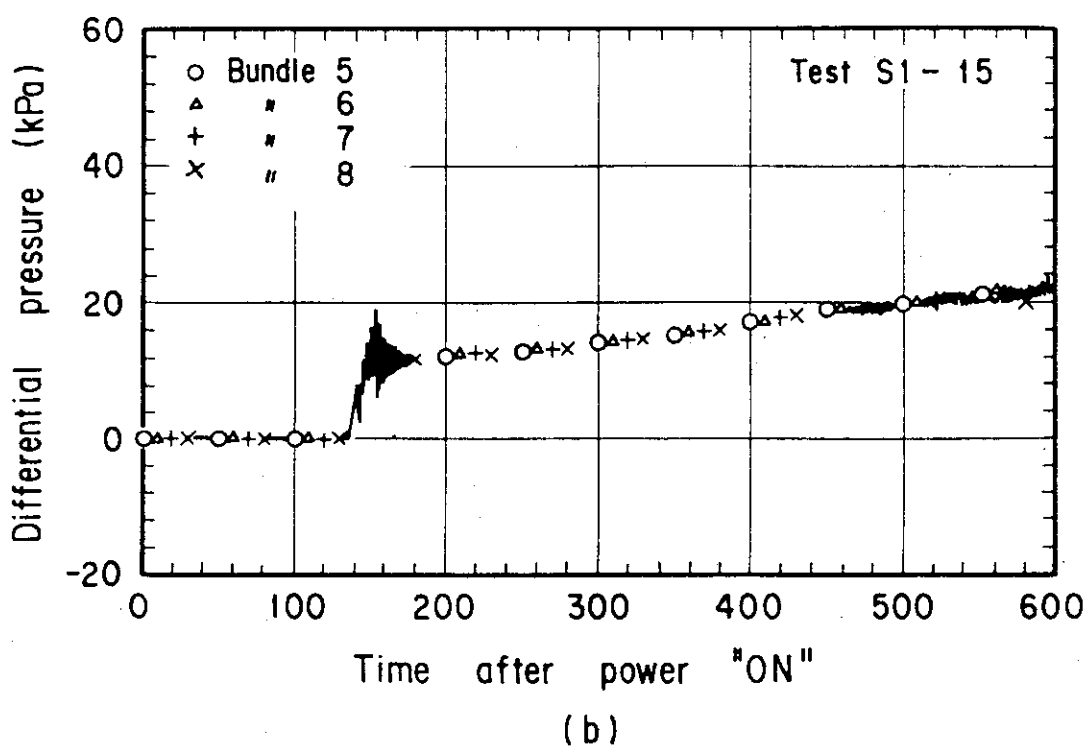
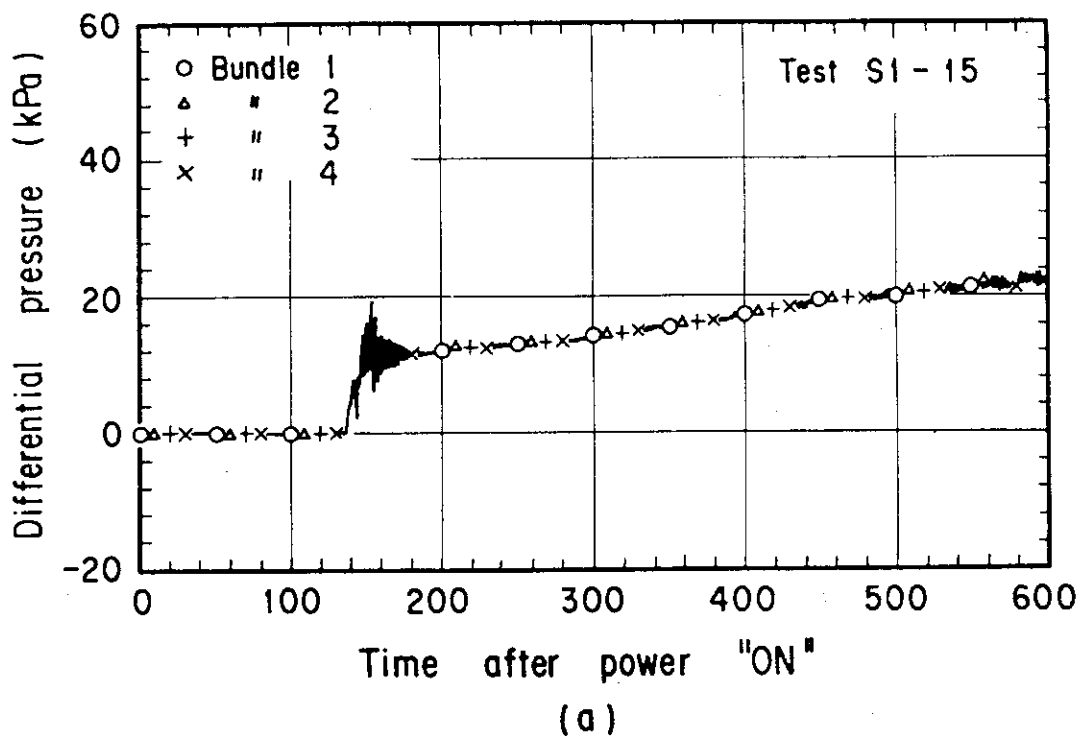


Fig. 3.28 Core Differential Pressure for Test S1-15

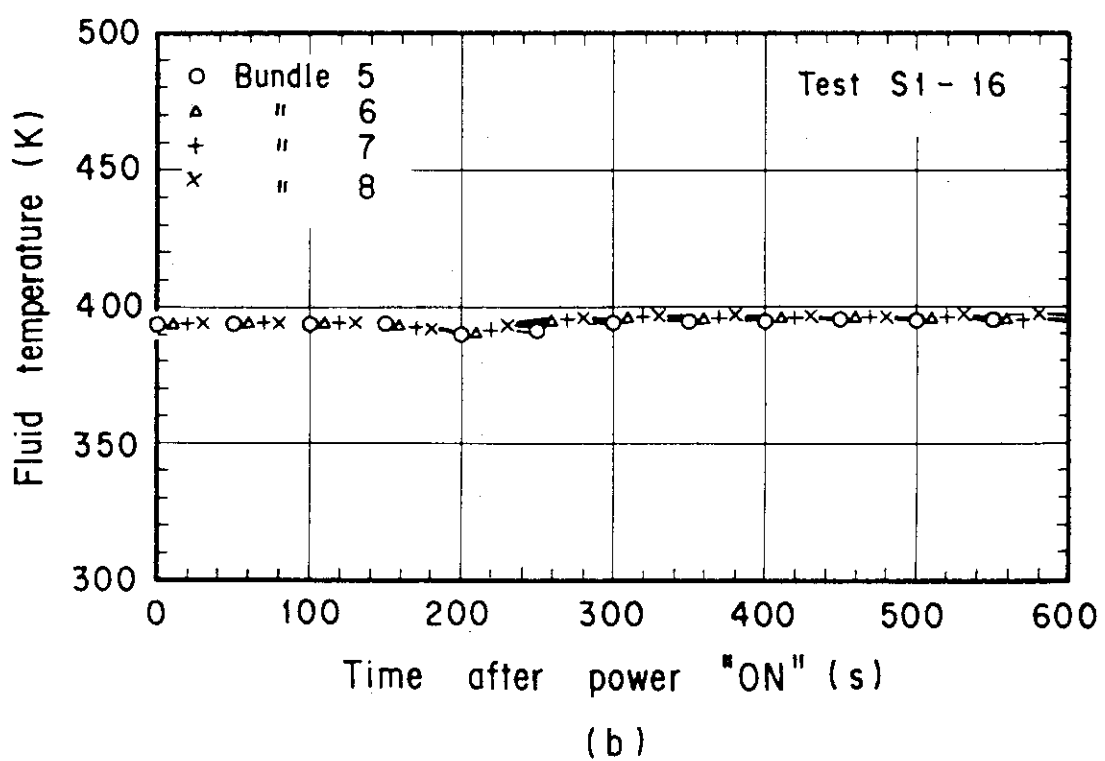
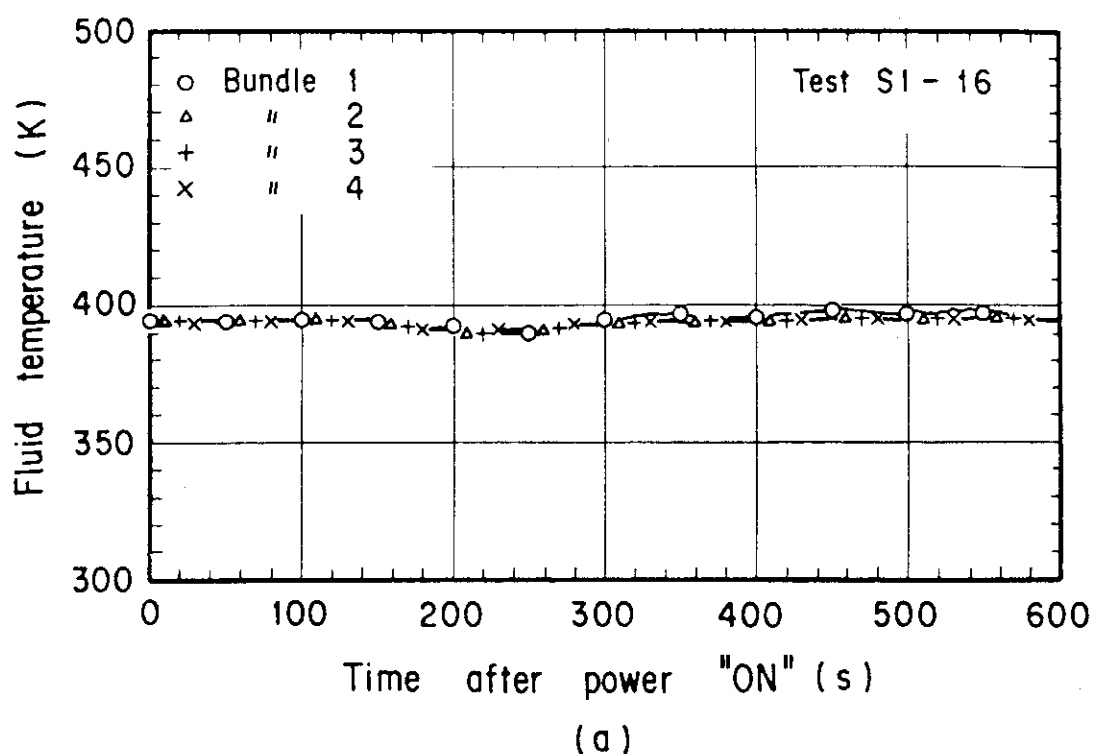


Fig. 3.29 Core Inlet Water Temperature for Test S1-16

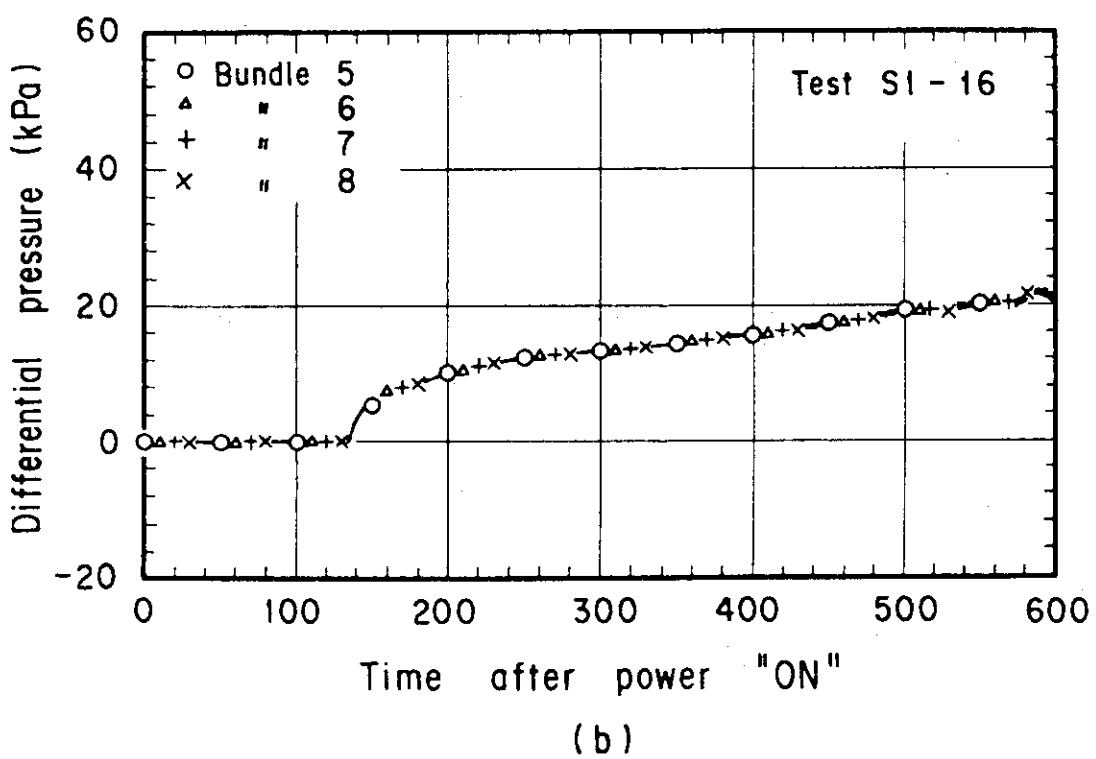
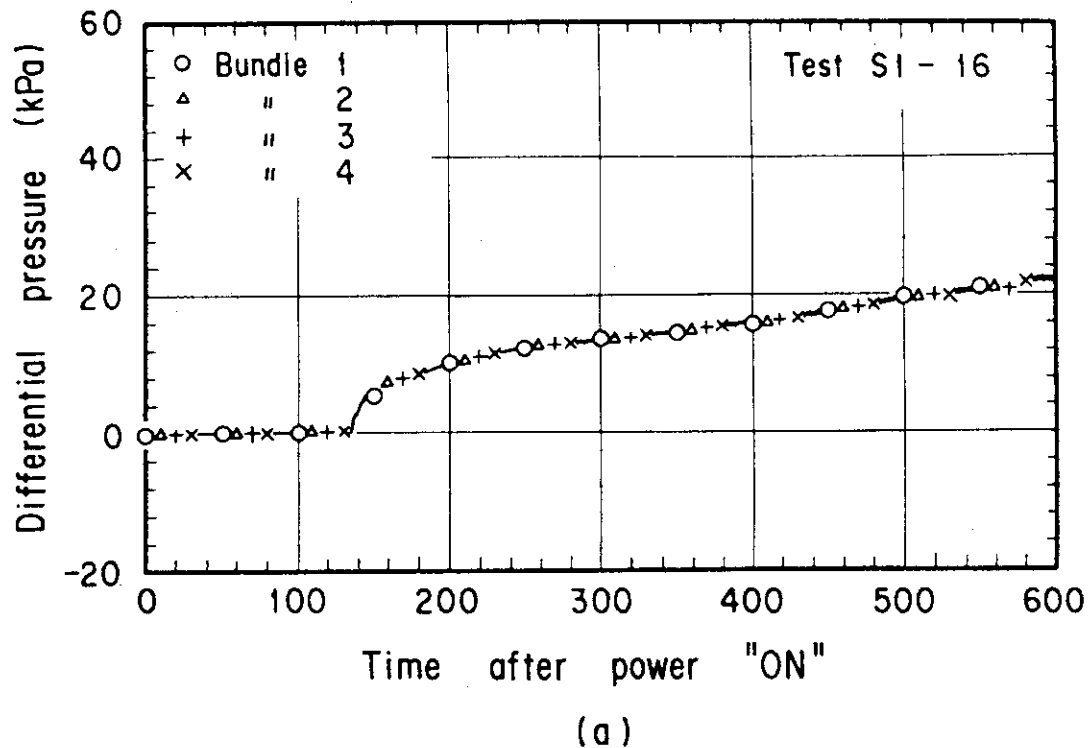


Fig. 3.30 Core Differential Pressure for Test S1-16

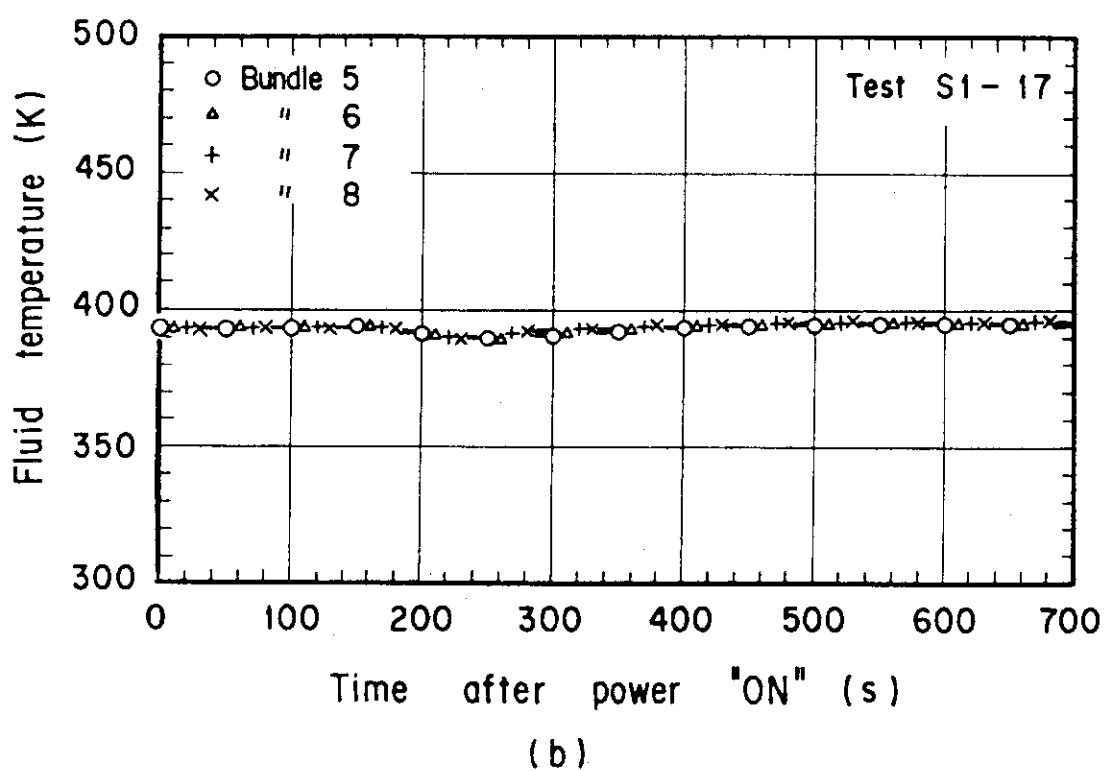
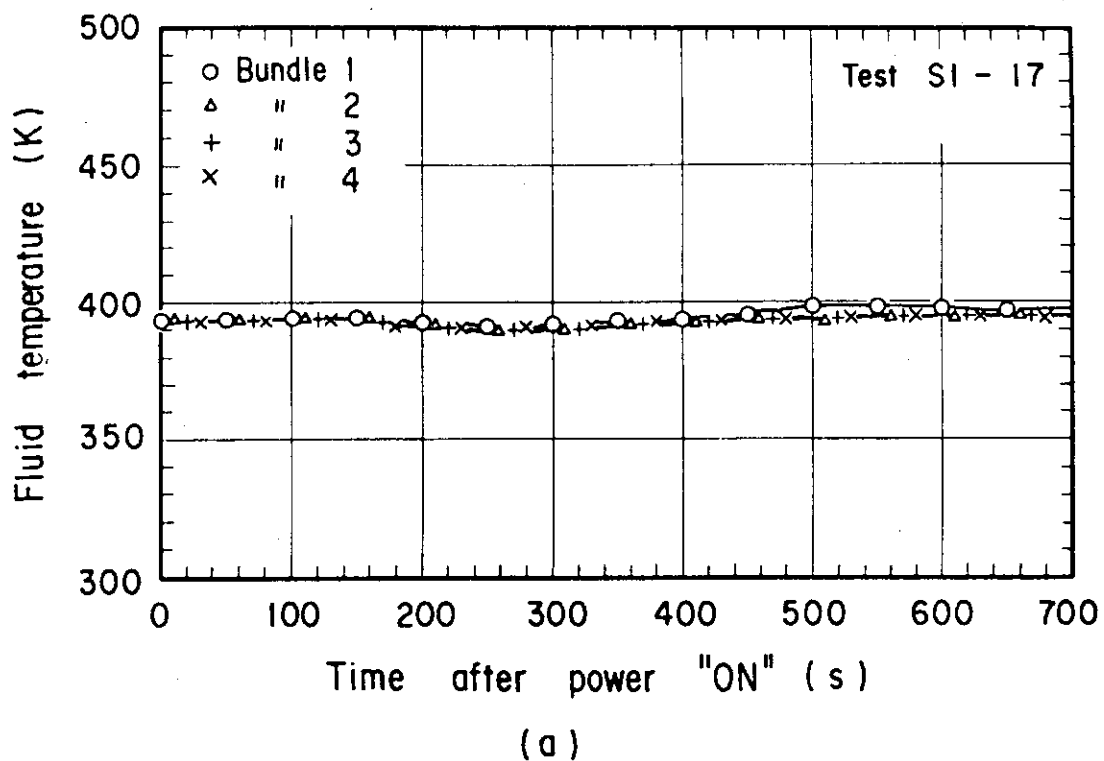


Fig. 3.31 Core Inlet Water Temperature for Test S1-17

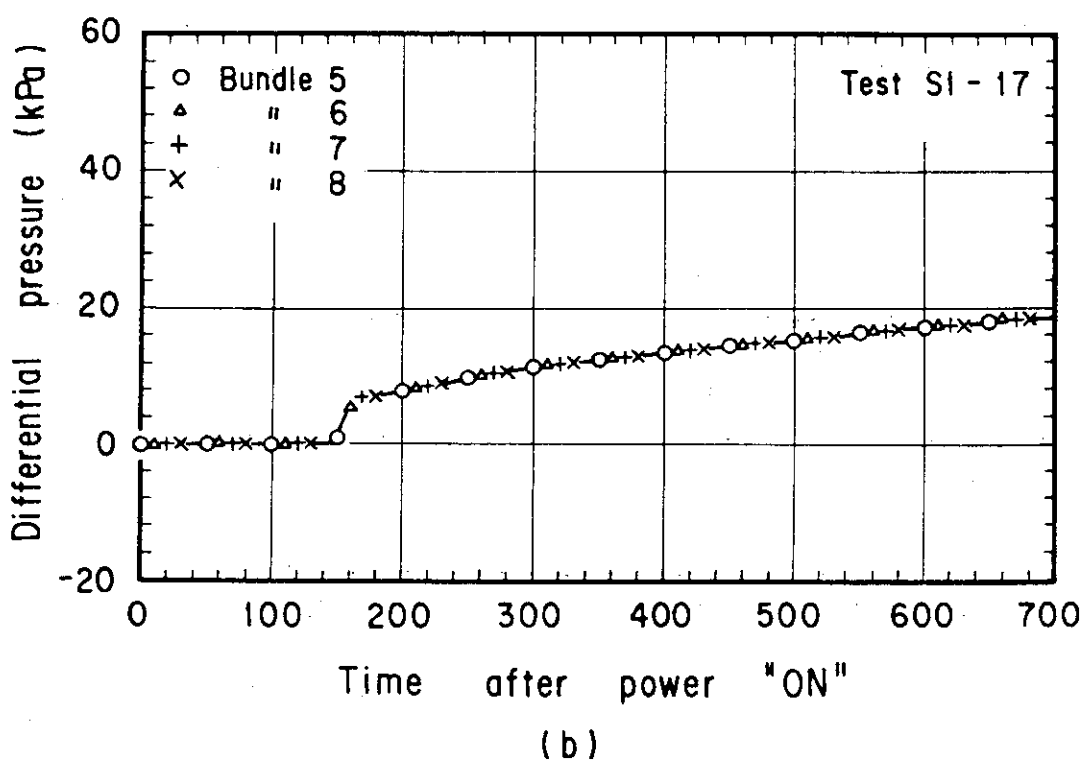
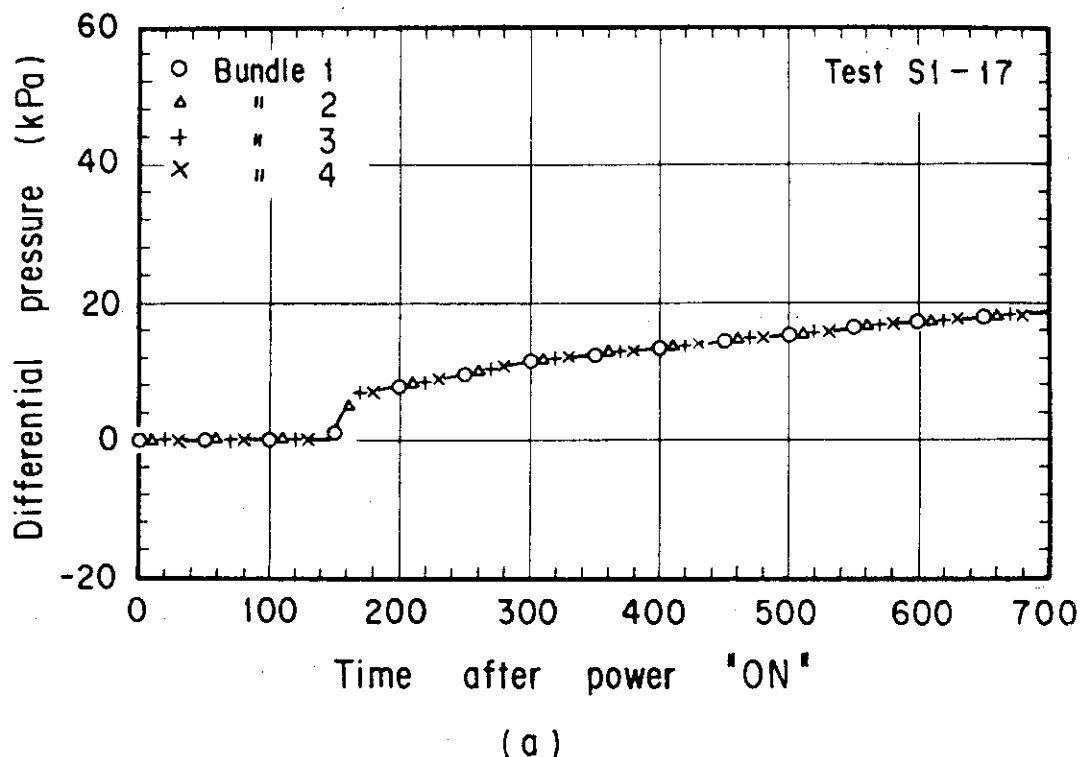


Fig. 3.32 Core Differential Pressure for Test S1-17

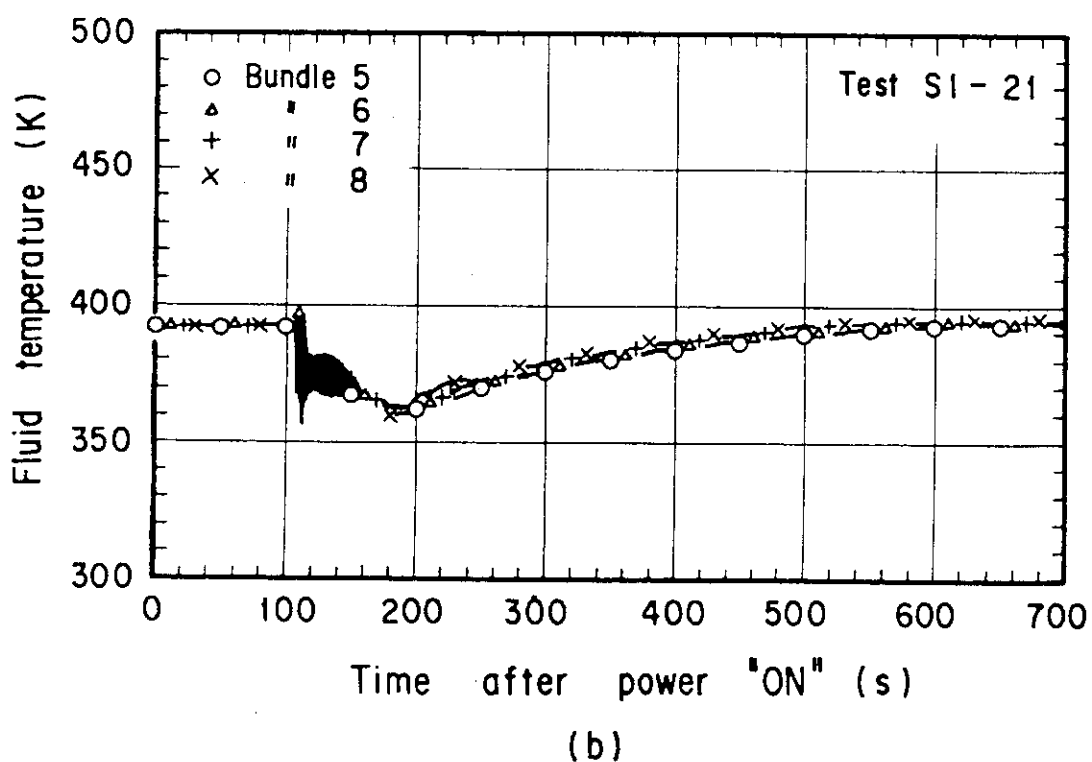
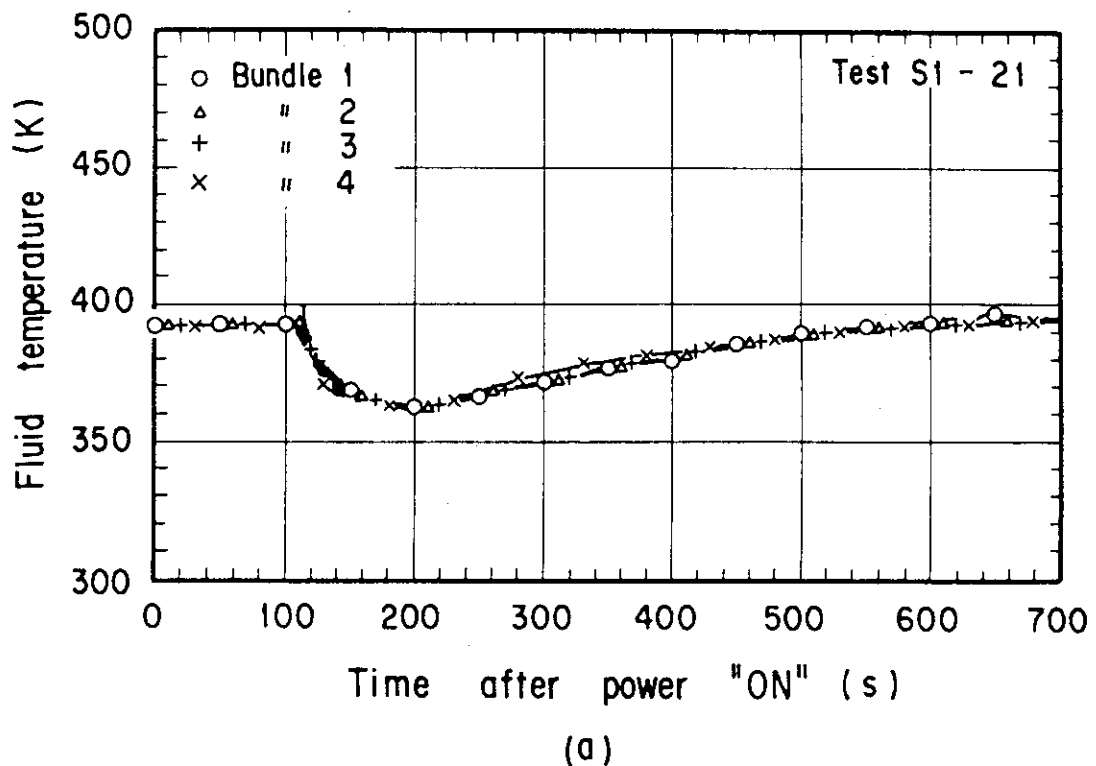


Fig. 3.33 Core Inlet Water Temperature for Test S1-21

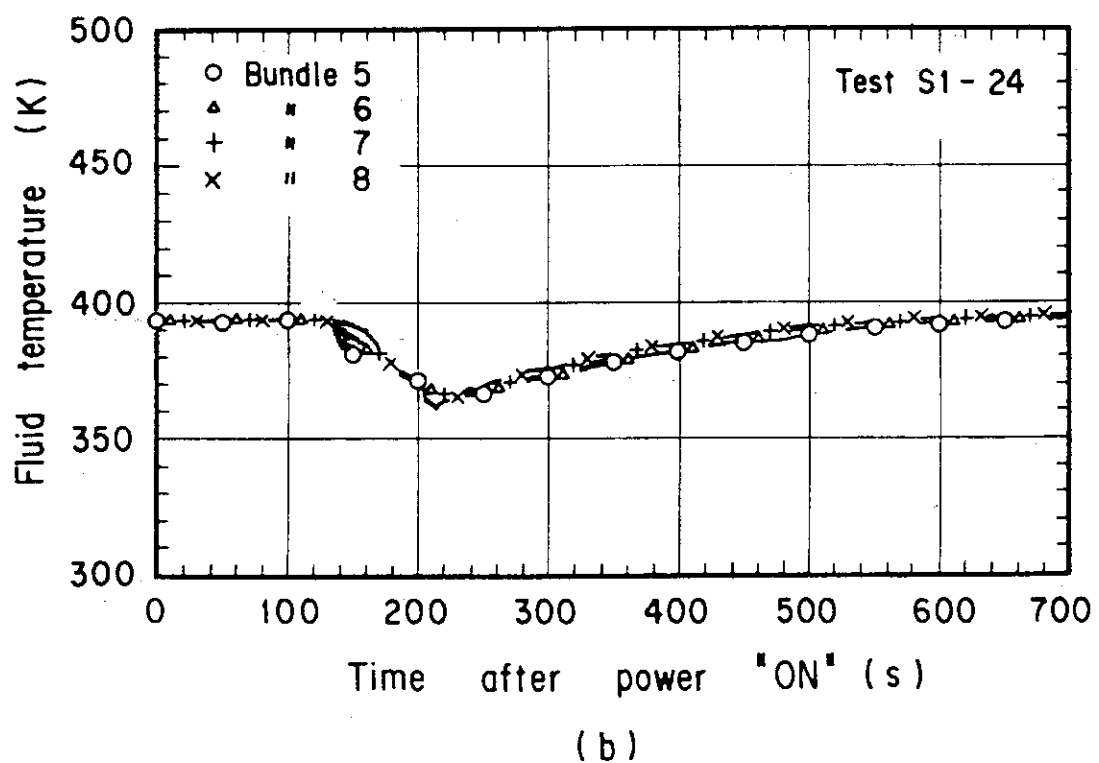
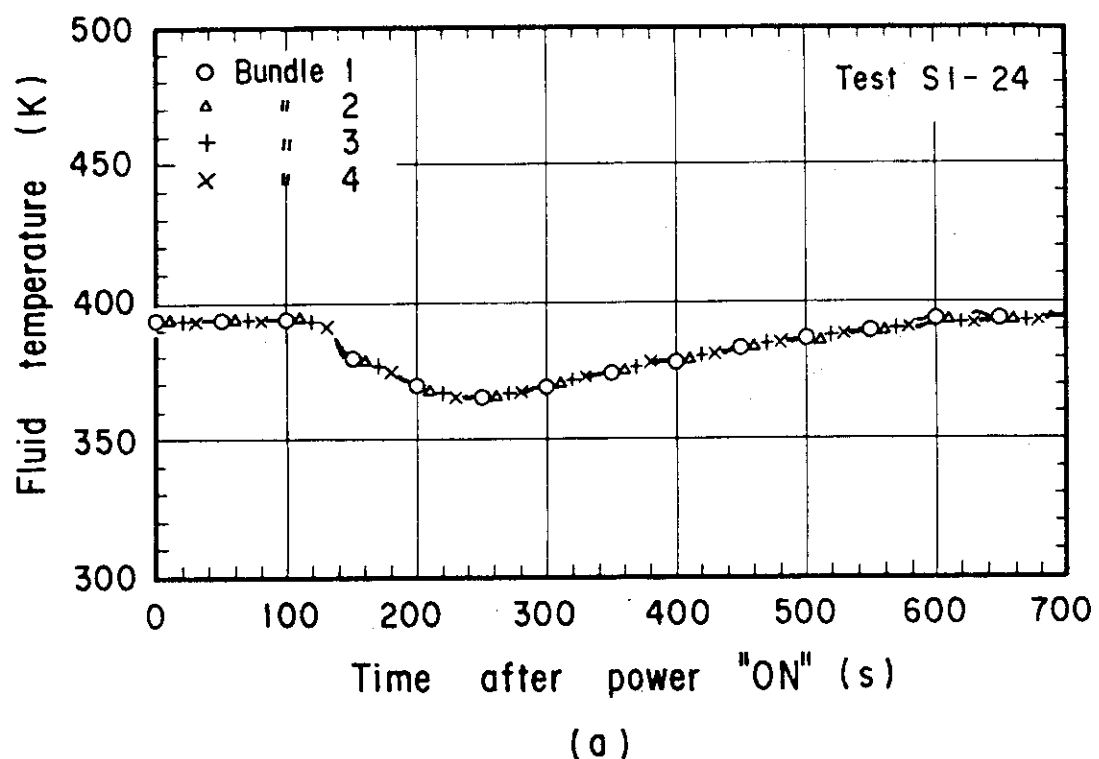


Fig. 3.34 Core Inlet Water Temperature for Test S1-24

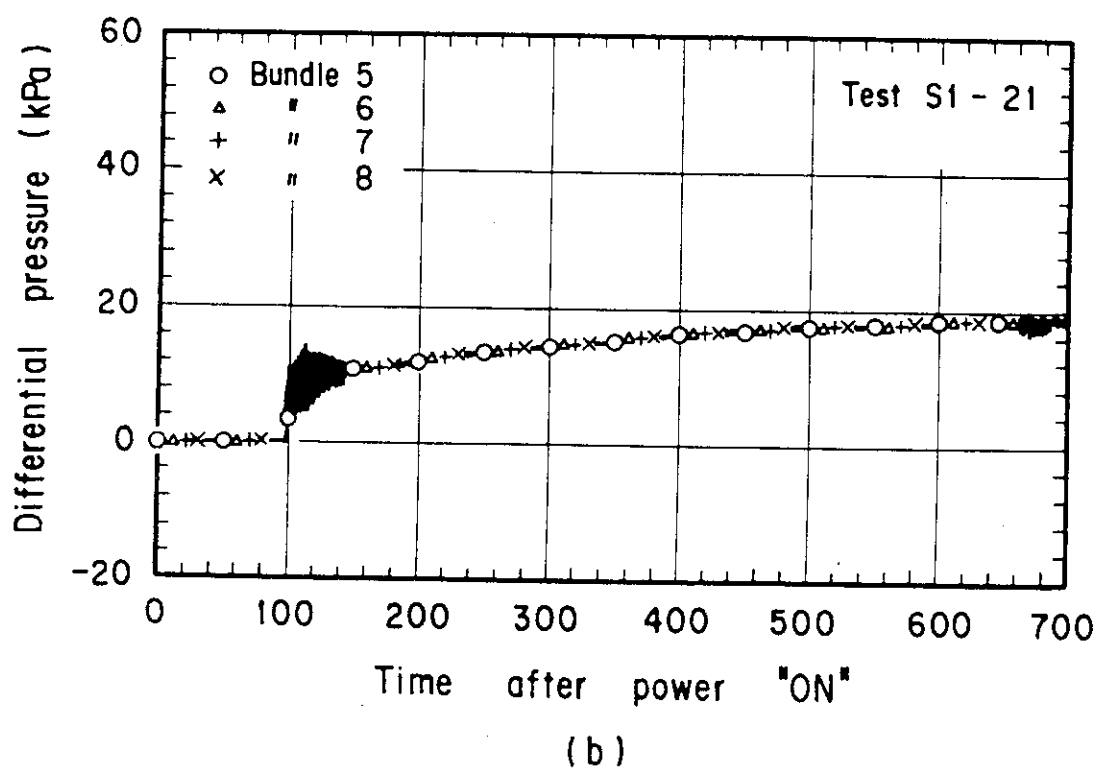
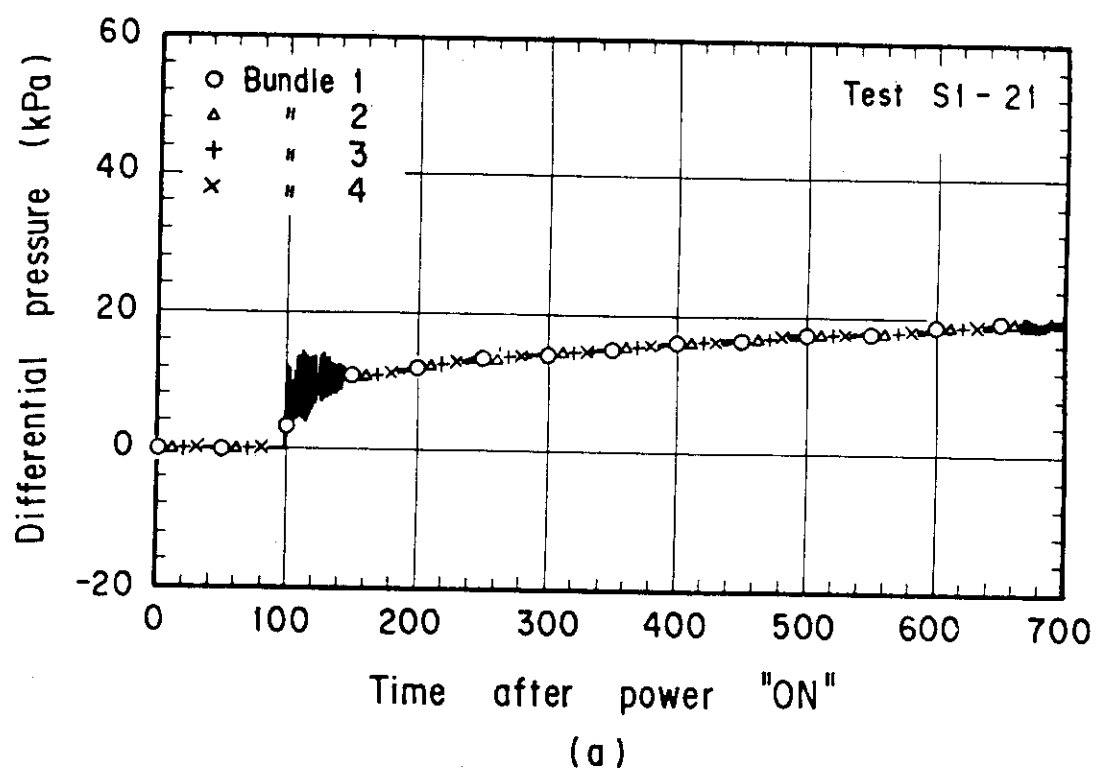


Fig. 3.35 Core Differential Pressure for Test S1-21

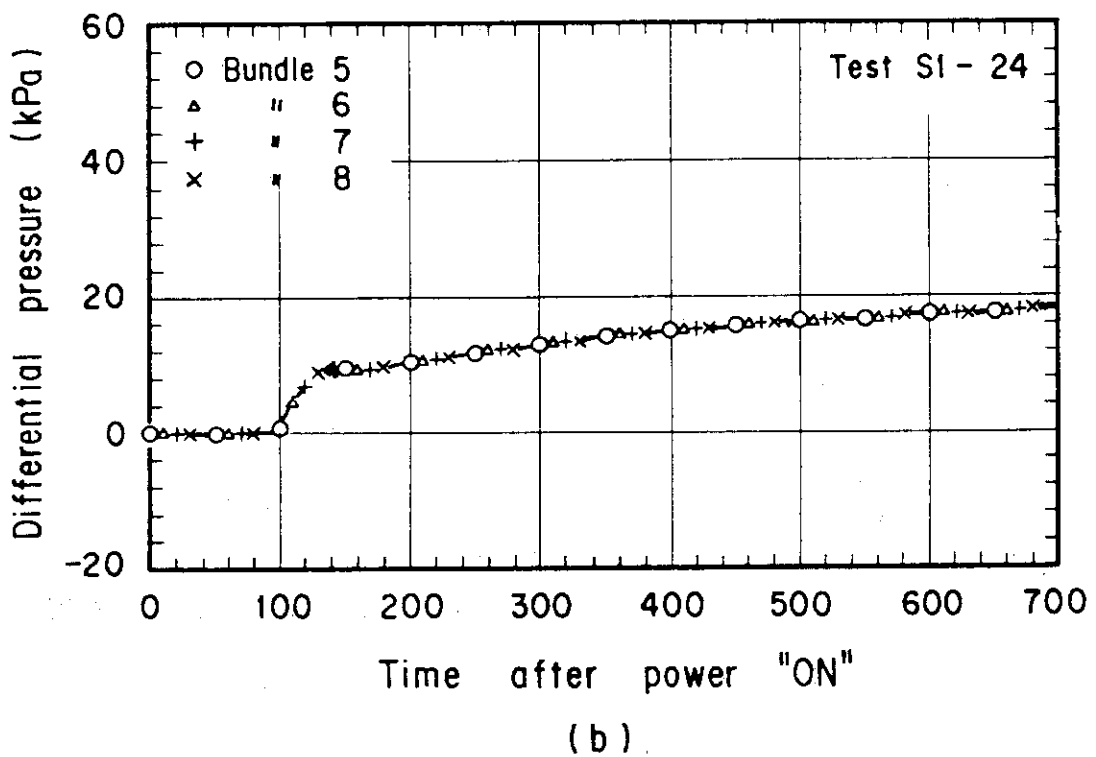
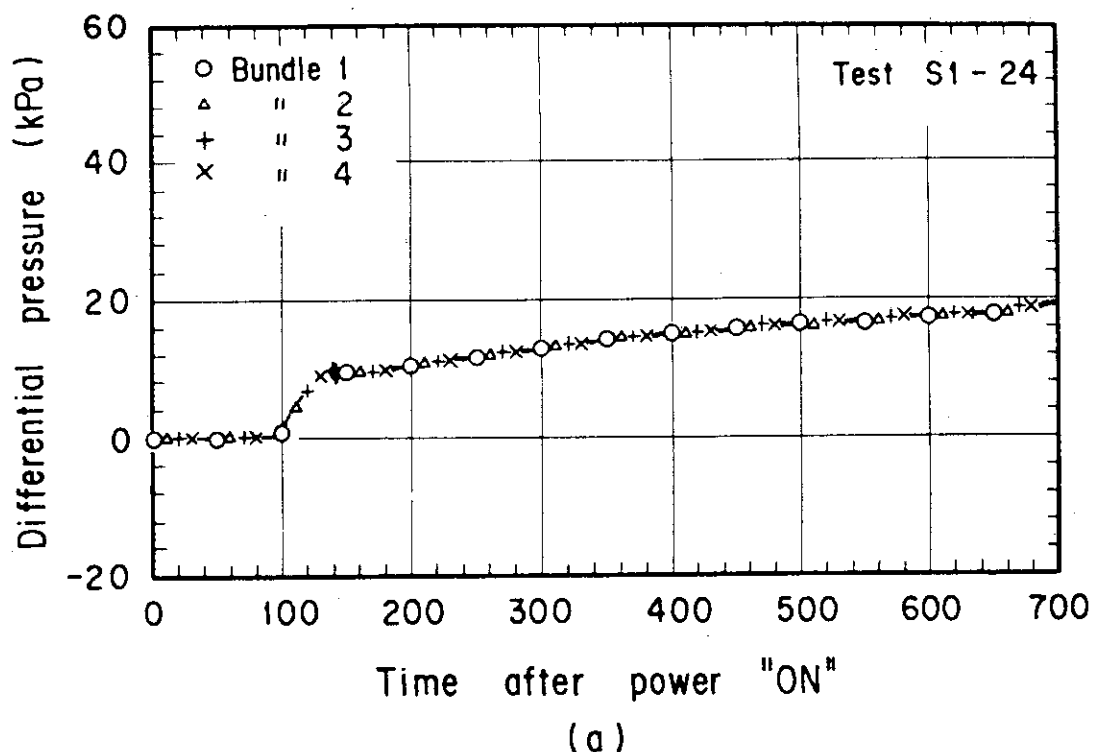


Fig. 3.36 Core Differential Pressure for Test S1-24

4. Recommendation for Cold Leg Injection Test Procedure

As described in the previous chapter, SCTF has the following differences from CCTF in system characteristics which might result in the different core cooling behavior from the actual PWR situation, i.e.:

- (1) Different transient in steam binding effect, especially weak steam binding in the later portion of reflooding process.
- (2) More significant oscillatory behavior which is seen especially during the early stage of reflooding process.
- (3) Smaller ECC water bypassing during reflooding process.

Since the main purpose of the SCTF test is not to simulate the system behavior but to obtain useful experimental information on two-dimensional core thermal-hydraulics, these problems in system simulation are thought not fatal. However, to perform tests at a reasonable core inlet water flow rate transient is of course one of the most important points for the SCTF test. From this point of view, the following recommendations are made for cold leg injection test procedure at SCTF.

- (1) For Acc injection period, simulation of steam binding effect is not so difficult because enhancement of steam binding due to evaporation of carryover water in steam generators is supposed not so strong in an actual PWR also. Furthermore, important of the steam binding simulation is not so large for this period because during the most of the period the downcomer water level is at lower than the overflow level and under such condition different steam binding effect does not result in so much different core inlet flow rate but different downcomer water level only as described in section 3.5. Therefore, only required thing for this period is to roughly simulate the loop flow resistance.
- (2) However, too high downcomer water level at the switching time from Acc injection to LPCI injection can result in a temporary increase in core inlet water flow rate and significant U-tube oscillations just after the switching. Therefore, excess Acc water injection should not be done.
- (3) For LPCI injection, reduction of the injection rate is importance to realize proper transient of core inlet water flow rate because when the downcomer water level does not reach the overflow level the core inlet water flow rate is not strongly governed by steam binding effect but governed basically by LPCI water injection flow rate.
- (4) Intact cold leg seems to be suitable for the LPCI injection location. Uncertainty in core inlet water flow rate due to condensation in the

intact cold leg and the LPCI water bypassing is not so large because the effects of these phenomena are not so significant in comparison with ECC water injection rate itself and in addition almost cancel with each other.

- (5) However, if we inject LPCI water into the lower plenum instead of the intact cold leg, we can measure core inlet water flow rate more accurately. On the other hand, condensation effect in the intact cold leg especially to the system oscillations is ignored in the case.
- (6) If injection location and injection water flow rate from ECCSs are changed, the injection water temperature should also be corrected because enthalpy balance for each part of the test facility and for the entire test facility will be shifted.
- (7) Also some corrections should be made for ECC water temperature to compensate the weak downcomer heat slab effect.

5. Conclusions

Based on the data from Tests S1-14, S1-15, S1-16, S1-17, S1-20, S1-21, S1-23 and S1-24 of the SCTF Core-I cold leg injection test series under constant system pressure, the following experimental information was obtained.

(1) Steam Binding

i) In SCTF, the steam binding effect during the most part of transient was weaker than CCTF, though it was stronger in the initial period of test. This is caused by the lack of active steam generator and the relatively high loop resistance.

ii) If downcomer water level does not reach the overflow level, core inlet water flow rate is not strongly governed by the steam binding effect but mainly by the ECC water injection rate especially in the LPCI injection period.

(2) U-Tube Oscillations

i) In the SCTF cold leg injection tests U-tube oscillations occurred generally between the core and the downcomer, especially in the early period of the transient. The larger amplitude of oscillations than CCTF may be caused by the difference in system characteristics. However, the mechanism of U-tube oscillations seems to be general.

ii) Measured differential pressure oscillations are almost in-phase between the core and the downcomer.

(3) Bypass of ECC Water

Bypass fraction was much smaller in the SCTF tests than in the CCTF tests

(4) Core Cooling Behavior

i) Core inlet water flow rate is much sensitive to the turnaround behavior of rod temperature.

ii) In spite of the lower water fraction in the upper portion of the core, better core cooling above the quench front than CCTF was observed.

(5) Parameter Effects

i) High temperature of Acc water resulted in the low core inlet water subcooling, small core water mass and poor core cooling.

ii) Low Acc injection flow rate resulted in the small core ater

mass, insignificant U-tube oscillation and poor core cooling.

iii) Low LPCI injection flow rate resulted in the smaller core water mass and poor core cooling. On the other hand, the effect of the LPCI injection flow rate on the core inlet water subcooling was almost negligible.

iv) Even if U-tube oscillations are eliminated, core water mass increases gradually during the LPCI injection period in SCTF. This characteristics of core water accumulation is different from CCTF.

Acknowledgment

The authors are much indebted to Dr. M. Hirata and Dr. K. Hirano for their guidance and encouragement for this program.

They would like to express their appreciation to Dr. Y. Sudo, Mr. T. Iguchi, Mr. T. Sudoh, Dr. J. Sugimoto, Dr. H. Akimoto and Dr. K. Okabe for their useful discussions.

They also would like to express thanks to the 2D/3D project members of the USA and the FRG for their valuable discussions.

References

- (1) K. Hirano and Y. Murao: "Large Scale Reflood Test", J. At. Energy Soc. Japan, Vol. 22, No. 10, pp. 681~686 (1980).
- (2) H. Adachi, et al.: "Design of Slab Core Test Facility (SCTF) in Large Scale Reflood Test Program, Part I: Core-I", JAERI-M 83-080 (1983).
- (3) Y. Murao, et al.: "Evaluation Report on CCTF Core-I Reflood Test C1-S (Run 14)", JAERI-M 83-027 (1983).
- (4) H. Akimoto, et al.: "Evaluation Report on CCTF Core-I Reflood Test C1-3 (Run 12)", JAERI-M 83-090 (1983).
- (5) H. Akimoto, et al.: "Evaluation Report on CCTF Core-I Reflood Test C1-2 (Run 11)", JAERI-M 83-094 (1983).
- (6) J. Sugimoto, et al.: "Evaluation Report on CCTF Core-I Reflood Test C1-14 (Run 23)", JAERI-M 83-026 (1983).

mass, insignificant U-tube oscillation and poor core cooling.

iii) Low LPCI injection flow rate resulted in the smaller core water mass and poor core cooling. On the other hand, the effect of the LPCI injection flow rate on the core inlet water subcooling was almost negligible.

iv) Even if U-tube oscillations are eliminated, core water mass increases gradually during the LPCI injection period in SCTF. This characteristics of core water accumulation is different from CCTF.

Acknowledgment

The authors are much indebted to Dr. M. Hirata and Dr. K. Hirano for their guidance and encouragement for this program.

They would like to express their appreciation to Dr. Y. Sudo, Mr. T. Iguchi, Mr. T. Sudoh, Dr. J. Sugimoto, Dr. H. Akimoto and Dr. K. Okabe for their useful discussions.

They also would like to express thanks to the 2D/3D project members of the USA and the FRG for their valuable discussions.

References

- (1) K. Hirano and Y. Murao: "Large Scale Reflood Test", J. At. Energy Soc. Japan, Vol. 22, No. 10, pp. 681~686 (1980).
- (2) H. Adachi, et al.: "Design of Slab Core Test Facility (SCTF) in Large Scale Reflood Test Program, Part I: Core-I", JAERI-M 83-080 (1983).
- (3) Y. Murao, et al.: "Evaluation Report on CCTF Core-I Reflood Test C1-S (Run 14)", JAERI-M 83-027 (1983).
- (4) H. Akimoto, et al.: "Evaluation Report on CCTF Core-I Reflood Test C1-3 (Run 12)", JAERI-M 83-090 (1983).
- (5) H. Akimoto, et al.: "Evaluation Report on CCTF Core-I Reflood Test C1-2 (Run 11)", JAERI-M 83-094 (1983).
- (6) J. Sugimoto, et al.: "Evaluation Report on CCTF Core-I Reflood Test C1-14 (Run 23)", JAERI-M 83-026 (1983).

mass, insignificant U-tube oscillation and poor core cooling.

iii) Low LPCI injection flow rate resulted in the smaller core water mass and poor core cooling. On the other hand, the effect of the LPCI injection flow rate on the core inlet water subcooling was almost negligible.

iv) Even if U-tube oscillations are eliminated, core water mass increases gradually during the LPCI injection period in SCTF. This characteristics of core water accumulation is different from CCTF.

Acknowledgment

The authors are much indebted to Dr. M. Hirata and Dr. K. Hirano for their guidance and encouragement for this program.

They would like to express their appreciation to Dr. Y. Sudo, Mr. T. Iguchi, Mr. T. Sudoh, Dr. J. Sugimoto, Dr. H. Akimoto and Dr. K. Okabe for their useful discussions.

They also would like to express thanks to the 2D/3D project members of the USA and the FRG for their valuable discussions.

References

- (1) K. Hirano and Y. Murao: "Large Scale Reflood Test", J. At. Energy Soc. Japan, Vol. 22, No. 10, pp. 681~686 (1980).
- (2) H. Adachi, et al.: "Design of Slab Core Test Facility (SCTF) in Large Scale Reflood Test Program, Part I: Core-I", JAERI-M 83-080 (1983).
- (3) Y. Murao, et al.: "Evaluation Report on CCTF Core-I Reflood Test C1-S (Run 14)", JAERI-M 83-027 (1983).
- (4) H. Akimoto, et al.: "Evaluation Report on CCTF Core-I Reflood Test C1-3 (Run 12)", JAERI-M 83-090 (1983).
- (5) H. Akimoto, et al.: "Evaluation Report on CCTF Core-I Reflood Test C1-2 (Run 11)", JAERI-M 83-094 (1983).
- (6) J. Sugimoto, et al.: "Evaluation Report on CCTF Core-I Reflood Test C1-14 (Run 23)", JAERI-M 83-026 (1983).

Appendix A Slab Core Test Facility (SCTF) Core-I

A.1 Test Facility

The Slab Core Test Facility was designed under the following design philosophy and design criteria:

(1) Design Philosophy

- 1) The facility should provide the capability to study the two-dimensional, thermohydraulic behavior and core flow within the reactor vessel especially due to the radial power distribution during the end of blowdown, refill and reflood phases of a simulated LOCA for a pressurized water reactor.
- 2) To properly simulate the core heat transfer and hydrodynamics, a special emphasis is put on the proper simulation of the components in the pressure vessel. As the components in the pressure vessels are provided a simulated core, downcomer, core baffle region, lower plenum, upper plenum and upper head. On the other hand, simplified primary coolant loops are provided. As the primary coolant loops are provided a hot leg, an intact cold leg, broken cold legs and a steam water separator. The object of the steam/water separator is to measure the flow rate of carryover water coming out of the upper plenum.

(2) Design Criteria

- 1) The reference reactor for simulation to the SCTF is the Trojan reactor in the United States which is a four loop 3300 MWe PWR. The Ooi reactor in Japan is also referred which is of the similar type to the Trojan reactor.
- 2) A full scale radial and axial section of a pressurized water reactor is provided as a simulated core of the SCTF with single bundle width.
- 3) The simulated core consists of 8 bundles arranged in a row. Each bundle has electrically heated rods simulating fuel rods and non-heated rod with 16X16 array.
- 4) The flow area and fluid volume of components are scaled down based on the core flow area scaling.

- 5) To properly simulate the flow behavior of carryover water and entrainment, the elevations of hot leg and cold legs are designed to be the same as the PWRs as much as possible.
- 6) The honeycomb structure is used as the side walls which accommodate the slab core, upper plenum and the upper part of lower plenum, so as to minimize the effect of walls on the disturbance of the core heat transfer and hydrodynamics.
- 7) To investigate the effect of flow resistance in the primary loops are provided the orifices of which dimension is changeable.
- 8) The maximum allowable temperature of the simulated fuel rods is 1900 °C and the maximum allowable pressure of the facility is 6 kg/cm² absolute.
- 9) The facility is equipped with a hot leg equivalent to four actual hot legs connecting the upper plenum and the steam water separator, an intact cold leg equivalent to three actual intact cold legs connecting the steam water separator and the downcomer and two broken cold legs, one is for the steam water separator side and the other for the pressure vessel side.
- 10) The ECCS consists of an Acc., a LPCI and a combined injection systems.
- 11) ECC water injection ports are the cold leg, hot leg, upper plenum, downcomer, lower plenum and above the upper core support plate. These portions are to be chosen according to the object of the test.
- 12) For better simulation of lower plenum flow resistance, simulated fuel rods do not penetrate through the bottom plate of the lower plenum but terminate below the bottom of the core.
- 13) For measurements in the pressure vessel including core measurements, the feature of the slab geometry of the pressure vessel is utilized as much as possible. Design and arrangement of the instruments are done so as to be able to carry out installation, calibration and removal of the instruments.
- 14) View windows are provided where flow pattern recognition is important. The locations are, the interface between the core and the upper plenum, the hot leg, the pressure vessel side broken cold leg and the downcomer.
- 15) The blocked bundle test is carried out in Core-I in order to investigate the effect of the ballooned fuel rods and the unblocked normal bundle test for the Core-II and -III.

- 16) Simulated types of break are cold leg break and hot leg break.
- 17) The components and systems such as the containment tanks and ECC water supply system in the CCTF are shared with the SCTF to the maximum extent.

The overall schematic diagram of the SCTF is shown in Fig. A-1. The principal dimensions of the facility is shown in Table A-1, and the comparison of dimensions between the SCTF and the referred PWR is shown in Fig. A-2.

A.1.1 Pressure Vessel and Internals

The pressure vessel is of slab geometry as shown in Fig. A-3. The height of the components in the pressure vessel is almost the same as the reference reactor's, and the flow area and the fluid volume of each component are scaled down based on the nominal core flow area scaling.

The core consists of 8 bundles in a row and each bundle includes simulated fuel rods and non-heated rods with 16×16 array. The core arrangement for the SCTF Core-I is shown in Fig. A-4, which includes 6 normal bundles and 2 blocked bundles. The core is enveloped by the honeycomb thermal insulator which is attached on the barrel.

The downcomer is located at one end of the pressure vessel which corresponds to the periphery of the actual reactor. The core baffle region is, on the other hand, located between the core and the downcomer. For better understanding, the cross section of the pressure vessel at the elevation of midplane of the core is shown in Fig. A-5.

The design of upper plenum internals is based on that of the new Westinghouse 17×17 array fuel assemblies. The internals consist of control rod guide tubes, support columns, orifice plates and open holes and those arrangements is shown in Fig. A-6. The radius of each internal is scaled down by factor $8/15$ from that of an actual reactor. Flow resistance baffles are inserted into the guide tubes. The elevation and the configuration of baffles plates are shown in Figs. A-7 and A-8.

The height of the hot leg and cold legs are designed as close to the actual PWR as possible. However, in order to avoid the interference of the nozzles in the downcomer, the height of nozzles for the broken cold leg and the intact cold leg are shifted down compared to that of the hot leg as shown in Fig. A-3.

A.1.2 Heater Rod Assembly

The heater rod assembly for the SCTF Core-I consists of 8 bundles arranged in a row. These bundles are composed of 6 normal unblocked bundles which are located at the 1st, 2nd and 5th to 8th bundles and 2 blocked bundles which are 3rd and 4th bundles as shown in Fig. A-4. Each bundle has 234 electrically heated rods and 22 non-heated rods. The dimensions of the heater rods are based on a 15×15 fuel rod bundle, and the heated length and the outer diameter of each heater rod are 3.66 mm and 10.7 mm, respectively. A heater rod consists of a nichrome heater element, magnesium oxide (MgO) and Nichrofer-7216 sheath (equivalent to Inconel 600). The sheath wall thickness is about 1.0 mm and is thicker than the actual fuel cladding because of the requirements for thermocouple installation. The heating element is a helical coil and has a 17 step chopped cosine axial power profile as shown in Fig. A-9. The peaking factor is 1.4.

Non-heated rods are either stainless steel pipes or solid rods of 13.8 mm O.D. The heater rods and non-heated rods are fixed at the top of the core allowing the rods to move downward when the thermal expansion occurs. In Fig. A-10 the axial position where blockage sleeves for simulating the ballooned fuel rod are equipped is shown. The blockage sleeves consist of three types of sleeve, one is used for the rods at the corner adjacent to the next blocked bundle, another for the rods adjacent to the side walls and the third for the rods except for the periphery of the blocked bundle. These are named A, B and C respectively in the Fig. A-11 and these configurations for these are shown in Fig. A-12.

For better simulation for flow resistance in the lower plenum the simulated rods do not penetrate through the bottom plate of the lower plenum as shown in Fig. A-10.

A.1.3 Primary Loops and ECCS

Primary loops consist of a hot leg equivalent to the four actual hot legs, a steam/water separator for measuring the flow rate of carry over water, an intact cold leg equivalent to the three actual intact loops, a broken cold leg on the pressure vessel side and a broken cold leg on the steam water separator side. These two broken cold legs are connected to two containment tanks through break valves, respectively. The arrangement of the primary loops is shown in Fig. A-13. The flow area of each loop is scaled down based on the core flow area scaling. It should be

emphasized that the cross section of the hot leg is an elongated circle to realize the proper flow pattern in the hot leg. The steam/water separator has a steam generator inlet plenum simulator to realize the flow characteristics of carryover water. The cross section of the hot leg and the configuration of the steam generator inlet plenum simulator are shown in Fig. A-14.

A pump simulator and a loop seal part are provided for the intact cold leg. The arrangement of the intact cold leg is shown in Fig. A-15. The pump simulator consists of the casing and duct simulators and an orifice plate as shown in Fig. A-16. The loop resistance is adjusted with the orifice plate.

In principle, ECCS consists of an accumulator and a low pressure injection system. The injection port is located as already described in the design criteria. Besides, the UCSP extraction system is provided and the UCSP water injection and extraction systems will be used for combined injection tests.

A.1.4 Containment Tanks and Auxiliary System

Two containment tanks are provided to the SCTF. The containment tank-I is connected with the downcomer through the pressure vessel side broken cold leg and the containment tank-II is connected with the steam/water separator through the steam/water separator side broken cold leg. Especially in the containment tank-I, carryover water from the downcomer is measured by phase separation. These containment tanks and auxiliary system such as a pressurizer for injecting water from the Acc. tank, etc. are shared with the CCTF.

A.2 Instrumentation

The instrumentation in the SCTF has been provided both by JAERI and USNRC. The JAERI-provided instrumentation includes the measurement of temperatures, pressures, differential pressures, liquid levels, flow velocities, and heating powers. USNRC has provided film probes, impedance probes, string probes, liquid level detectors (LLDs), fluid distribution grids (FDGs), turbine meters, drag disks, γ -densitometers, spool pieces and video optical probes. The measurement items of the JAERI- and USNRC-provided instruments are listed in Table A-2 and A-3,

respectively. Location of each instrument is shown in Figs. A-17 through A-30.

Table A-1 Principal Dimensions of Test Facility

1. Core Dimension

(1) Quantity of Bundle	8 Bundles
(2) Bundle Array	1×8
(3) Bundle Pitch	230 mm
(4) Rod Array in a Bundle	16×16
(5) Rod Pitch in a Bundle	14.3 mm
(6) Quantity of Heater Rod in a Bundle	234 rods
(7) Quantity of Non-Heated Rod in a Bundle	22 rods
(8) Total Quantity of Heater Rods	$234 \times 8 = 1872$ rods
(9) Total Quantity of Non-Heated Rods	$22 \times 8 = 176$ rods
(10) Effective Heated Length of Heater Rod	3660 mm
(11) Diameter of Heater Rod	10.7 mm
(12) Diameter of Non-Heated Rod	13.8 mm

2. Flow Area & Fluid Volume

(1) Core Flow Area* (nominal)	0.227 m^2
(2) Core Fluid Volume	0.92 m^3
(3) Baffle Region Flow Area	0.10 m^2
(4) Baffle Region Fluid Volume	0.36 m^3
(5) Downcomer Flow Area	0.121 m^2
(6) Upper Annulus Flow Area	0.158 m^2
(7) Upper Plenum Horizontal Flow Area	0.525 m^2
(8) Upper Plenum Fluid Volume	1.16 m^3
(9) Upper Head Fluid Volume	0.86 m^3
(10) Lower Plenum Fluid Volume	1.38 m^3
(11) Steam Generator Inlet Plenum Simulator Flow Area	0.626 m^2
(12) Steam Generator Inlet Plenum Simulator Fluid Volume	0.931 m^3
(13) Steam Water Separator Fluid Volume	5.3 m^3
(14) Flow Area at the Top Plate of Steam Generator Inlet Plenum Simulator	0.195 m^2
(15) Hot Leg Flow Area	0.0826 m^2
(16) Intact Cold Leg Flow Area (Diameter = 297.9 mm)	0.0697 m^2
(17) Broken Cold Leg Flow Area (Diameter = 151.0 mm)	0.0179 m^2

* Flow area in the core is 0.35 m^2 , including the excess flow area of gaps between the bundle and the surface of thermal insulator and between the core barrel and the pressure vessel wall.

Table A-1 Principal Dimensions of Test Facility

(18) Containment Tank I Fluid Volume	30 m ³
(19) Containment Tank II Fluid Volume	50 m ³
3. Elevation & Height	
(1) Top Surface of Upper Core Support Plate (UCSP)	0 mm
(2) Bottom Surface of UCSP	-76 mm
(3) Top of the Effective Heated Length of Heater Rod	-393 mm
(4) Bottom of the Skirt in the Lower Plenum	-5270 mm
(5) Bottom of Intact Cold Leg	+724 mm
(6) Bottom of Hot Leg	+1050 mm
(7) Top of Upper Plenum	+2200 mm
(8) Bottom of Steam Generator Inlet Plenum Simulator	+1933 mm
(9) Centerline of Loop Seal Bottom	-2281 mm
(10) Bottom Surface of End Box	- 185.1 mm
(11) Top of the Upper Annulus	+2234 mm
(12) Height of Steam Generator Inlet Plenum Simulator	1595 mm
(13) Height of Loop Seal	3140 mm
(14) Inner Height of Hot Leg Pipe	737 mm
(15) Bottom of Lower Plenum	-5770 mm
(16) Top of Upper Head	+2887 mm

Table A-2 Measurement Items of SCTF
(JAERI-provided instruments)

LOCATION	ITEM	PROBE	QUANTITY
1. CORE			
center	pressure	DP cell	1
short range of core	diff. press.	DP cell	22
half length of core	diff. press.	DP cell	16
full length of core	diff. press.	DP cell	8
across spacers	diff. press.	DP cell	7
across end box	diff. press.	DP cell	8
across 4 assemblies	diff. press.	DP cell	3
across 8 assemblies	diff. press.	DP cell	3
below and above end box	steam velocity	Pitot-tube	3
sub channel	steam velocity	Pitot-tube	13
below end box hole	fluid temp.	T/C	16
above end box hole	fluid temp.	T/C	16
core baffle	fluid temp.	T/C	6
non-heating rods	fluid temp.	T/C	96
	steam temp.	SSP	16
	clad temp.	T/C	108
heater rods	clad temp.	T/C	640
side walls	wall temp.	T/C	36
core baffle	wall temp.	T/C	6
core baffle	liquid level	DP cell	1
short range of core baffle	liquid level	DP cell	6
heated rod	power		8
			sum(1039)
2. UPPER PLENUM			
centre	pressure	DP cell	1
across end box tie plate	diff. press.	DP cell	8
core outlet-hot leg inlet	diff. press.	DP cell	4
periphery of UCSP hole	fluid temp.	T/C	8
centre of UCSP hole	fluid temp.	T/C	8
250mm & 1000mm above UCSP	fluid temp.	T/C	8
surface of UCSP	fluid temp.	T/C	8
above UCSP hole	steam temp.	SSP	8

Table A-2 Measurement Items of SCTF (JAERI-provided instruments)

(Continued)

LOCATION	ITEM	PROBE	QUANTITY
surface of structure	wall temp.	T/C	15
side walls	wall temp.	T/C	8
above end box tie plate	liquid level	DP cell	8
above UCSP	liquid level	DP cell	9
above UCSP (v.)	steam velocity	Pitot-tube	2
inter-structures (h.)	steam velocity	Pitot-tube	2
			sum(97)
3. LOWER PLENUM			
below bottom spacer	pressure	DP cell	1
lower plenum - upper plenum	diff. press.	DP cell	1
core inlet	fluid temp.	T/C	8
inlet from downcomer	fluid temp.	T/C	2
side & bottom walls	wall temp.	T/C	4
below bottom spacer	liquid level	DP cell	1
			sum(17)
4. DOWNCOMER			
upper position	pressure	DP cell	1
horizontal direction	diff. press.	DP cell	1
four levels	fluid temp.	T/C	8
side wall	wall temp.	T/C	2
inner wall	wall temp.	T/C	2
below cold leg level	liquid level	DP cell	1
above cold leg level	liquid level	DP cell	1
below core inlet level	liquid level	DP cell	1
bottom	momentum flux	Drag disk	2
			sum(19)
5. HOT LEG			
full length	diff. press.	DP cell	1
multiple points	fluid temp.	T/C	3
	steam temp.	SSP	3
	wall temp.	T/C	1
	liquid level	DP cell	2
			sum(10)

Table A-2 Measurement Items of SCTF (JAERI-provided instruments)

(Continued)

LOCATION	ITEM	PROBE	QUANTITY
6. S/W SEPARATOR SIDE BROKEN COLD LEG			
across resistance simulator	diff. press.	DP cell	1
S/W separator to contain- ment tank II	flow rate	venturi	1
multiple points	fluid temp.	T/C	1
	steam temp.	SSP	1
	wall temp.	T/C	1
		sum(5)	
7. INTACT COLD LEG			
full length	diff. press.	DP cell	1
across resistance simulator	diff. press.	DP cell	1
across pump simulator	diff. press.	DP cell	1
	flow rate	venturi	1
near resistance simulator	fluid temp.	T/C	1
pump simulator	fluid temp.	T/C	3
	wall temp.	T/C	1
		sum(9)	
8. PV SIDE BROKEN COLD- LEG			
full length	pressure	DP cell	1
across resistance simulator	diff. press.	DP cell	1
multiple points	diff. press.	DP cell	1
	fluid temp.	T/C	4
	wall temp.	T/C	2
	liquid level	DP cell	2
		sum(11)	
9. VENT LINE			
across the length	diff. pres.	DP cell	1
		sum(1)	

Table A-2 Measurement Items of SCTF (JAERI-provided instruments)
(Continued)

LOCATION	ITEM	PROBE	QUANTITY
10. S/W SEPARATOR			
between inlet and outlet	pressure	DP cell	1
SG plenum simulator	diff. press.	DP cell	1
SG plenum simulator	diff. press.	DP cell	1
top and bottom	fluid temp.	T/C	2
wall	fluid temp.	T/C	2
full height	wall temp.	T/C	2
liquid extraction	liquid level	DP cell	1
	flow rate	DP cell	1
			sum(11)
11. CONTAINMENT TANK-I			
downcomer-CT-I	pressure	DP cell	1
CT-I - CT-II	diff. press.	DP cell	1
	diff. press.	DP cell	1
	flow rate	DP cell	1
full height	liquid level	DP cell	1
	float		1
top, middle & bottom	fluid temp.	T/C	3
wall	wall temp.	T/C	1
			sum(10)
12. CONTAINMENT TANK-II			
upper plenum - CT-II	pressure	DP cell	1
separator - CT-II	diff. press.	DP cell	1
steam blow line	diff. press.	DP cell	1
full height	flow rate	DP cell	1
top, middle & bottom	liquid level	DP cell	1
	fluid temp.	T/C	3
			sum(8)
13. ECC INJECTION SYSTEM			
ACC tank	pressure	DP cell	1
total and LPCI	flow rate	E-M flow meter	2
			1
ACC tank	fluid temp.	T/C	1

Table A-2 Measurement Items of SCTF (JAERI-provided instruments)
(Continued)

LOCATION	ITEM	PROBE	QUANTITY
13. ECC INJECTION SYSTEM header	fluid temp.	T/C	2
ACC tank	liquid level	DP cell	1
			sum(8)
14. UCSP WATER EXTRACTION SYSTEM extraction line	flow rate	E-M flow meter	4
steam line	flow rate	DP cell	4
extraction line	fluid temp.	T/C	5
steam line	fluid temp.	T/C	1
extraction line	liquid level	DP cell	4
			sum(18)
15. SATURATED WATER TANK	fluid temp	T/C	1
	liquid level	DP cell	1
			sum(2)
16. NITROGEN GAS SYSTEM injection port	flow rate	DP cell	1
	fluid temp.	T/C	1
			sum(2)

Total 1267

**Table A-3 Measurement Items of SCTF
(USNRC-provided instruments)**

LOCATION	ITEM	PROBE	QUANTITY
1. CORE			
non-heated rods	liquid level	LLD	$20 \times 4 = 80$
non-heated rods	film thickness and velocity	film probe	6
non-heated rods	void fraction and droplet velocity	flag probe	8
side walls	film thickness and velocity	film probe	8
sub-channel	fluid density	γ -densitometer	10
end box	fluid density	γ -densitometer	5
end box	flow pattern	video optical probe	1
2. UPPER PLENUM			
full height	liquid level	FDG	$8 \times 8 = 64$
structure surface	film thickness and velocity	film probe	6
side walls	film thickness and velocity	film probe	6
inter structure	void fraction	prong probe	8
above UCSP hole	velocity	turbine	8
inter structure	velocity	turbine	4
inter structure	fluid density	γ -densitometer	4
hot leg inlet	flow pattern	video optical probe	1
3. LOWER PLENUM			
core inlet	velocity	turbine	4
bottom	reference conductivity	reference probe	1
4. DOWNCOMER			
full height	liquid level	FDG	$2 \times 3 \times 7 = 42$
two levels	velocity	drag disk	3
two levels	void fraction	string probe	3

Table A-3 Measurement Items of SCTF
 (USNRC-provided instruments)
 (Continued)

LOCATION	ITEM	PROBE	QUANTITY
5. HOT LEG	mass flow rate fluid density void fraction	spool piece	1
6. PV SIDE BROKEN COLD-LEG	mass flow rate fluid density void fraction	spool piece	1
7. VENT LINE	mass flow rate void fraction	spool piece	1

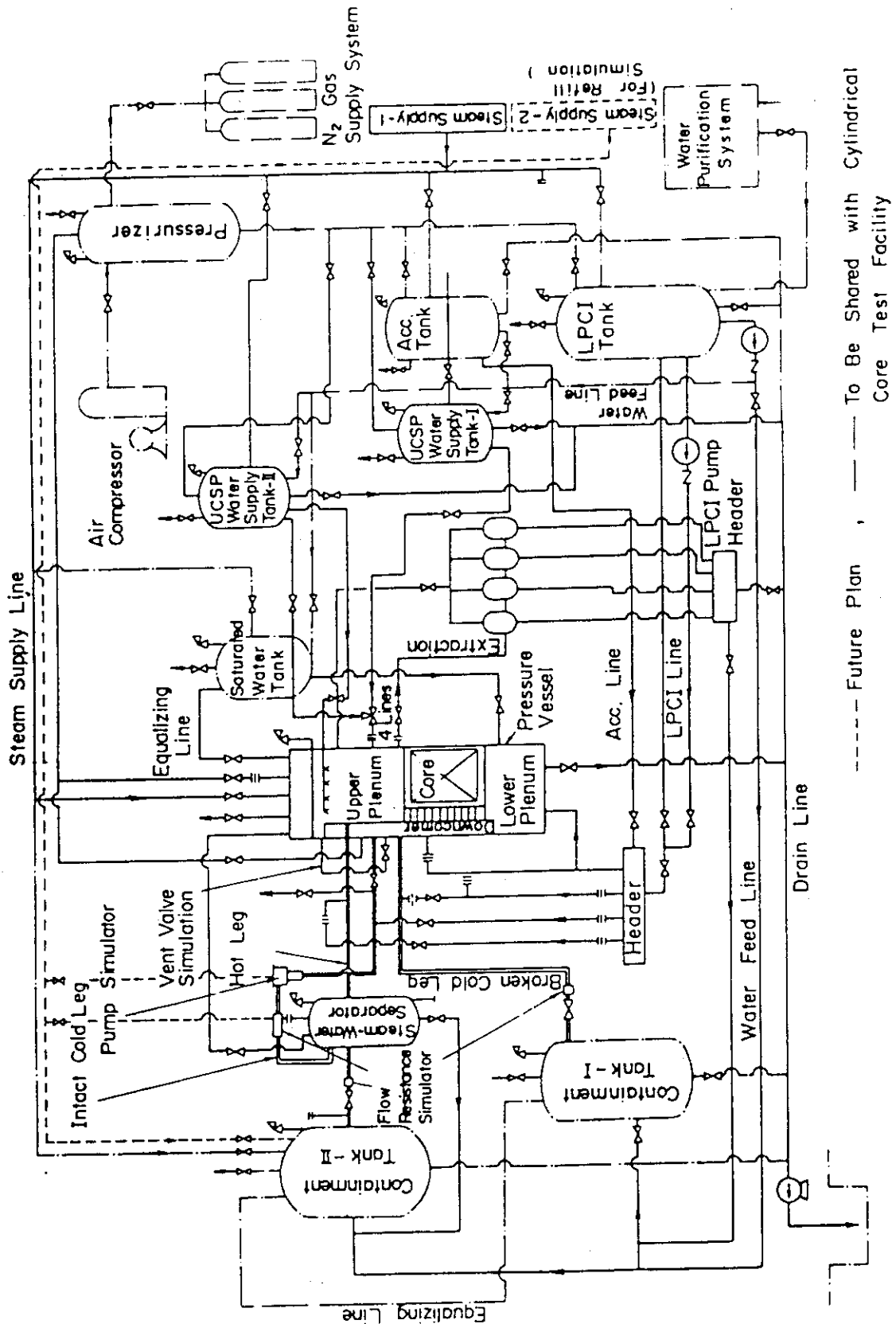


Fig. A-1 Schematic Diagram of Slab Core Test Facility

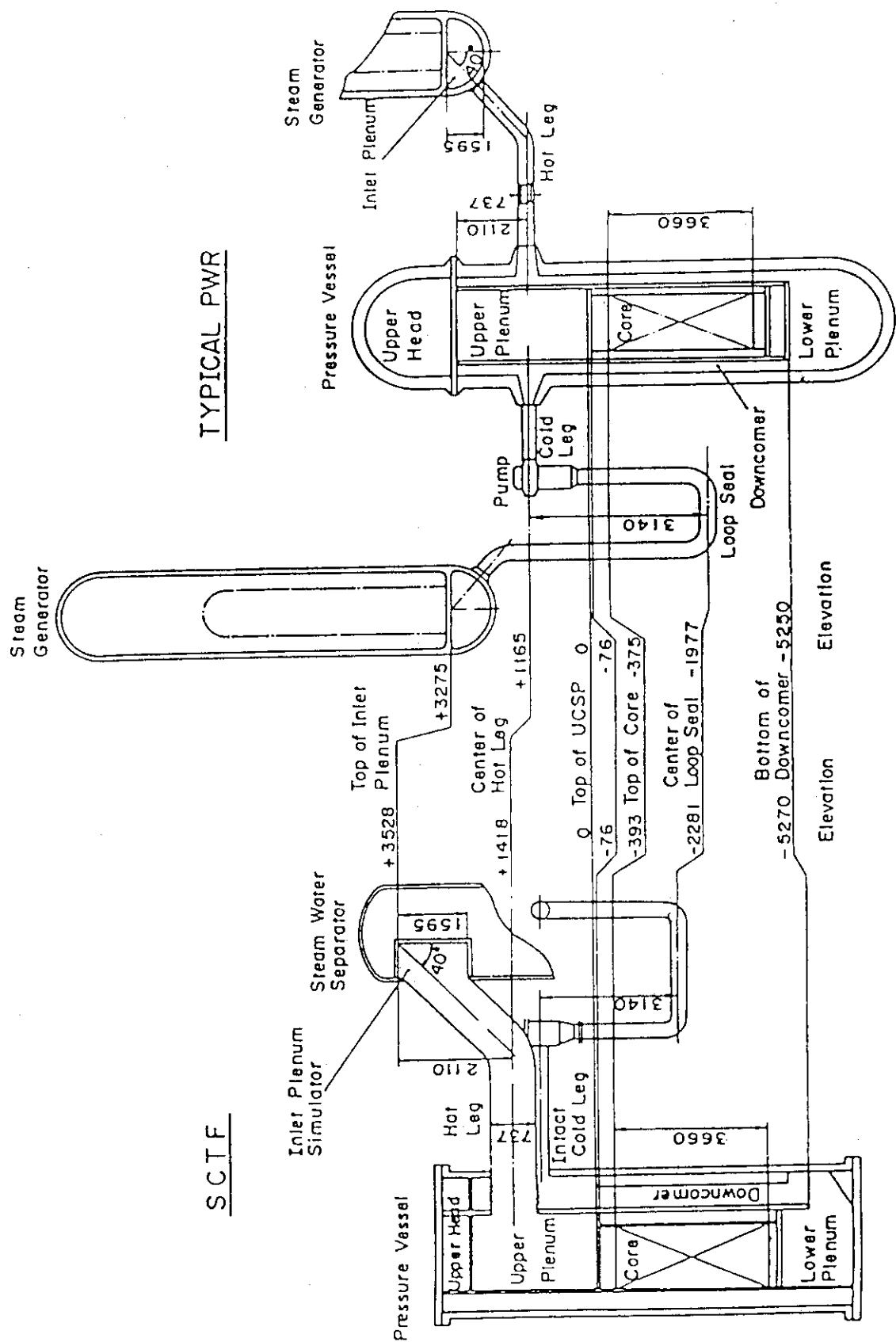


Fig. A-2 Comparison of Dimensions between SCTF and a Reference PWR

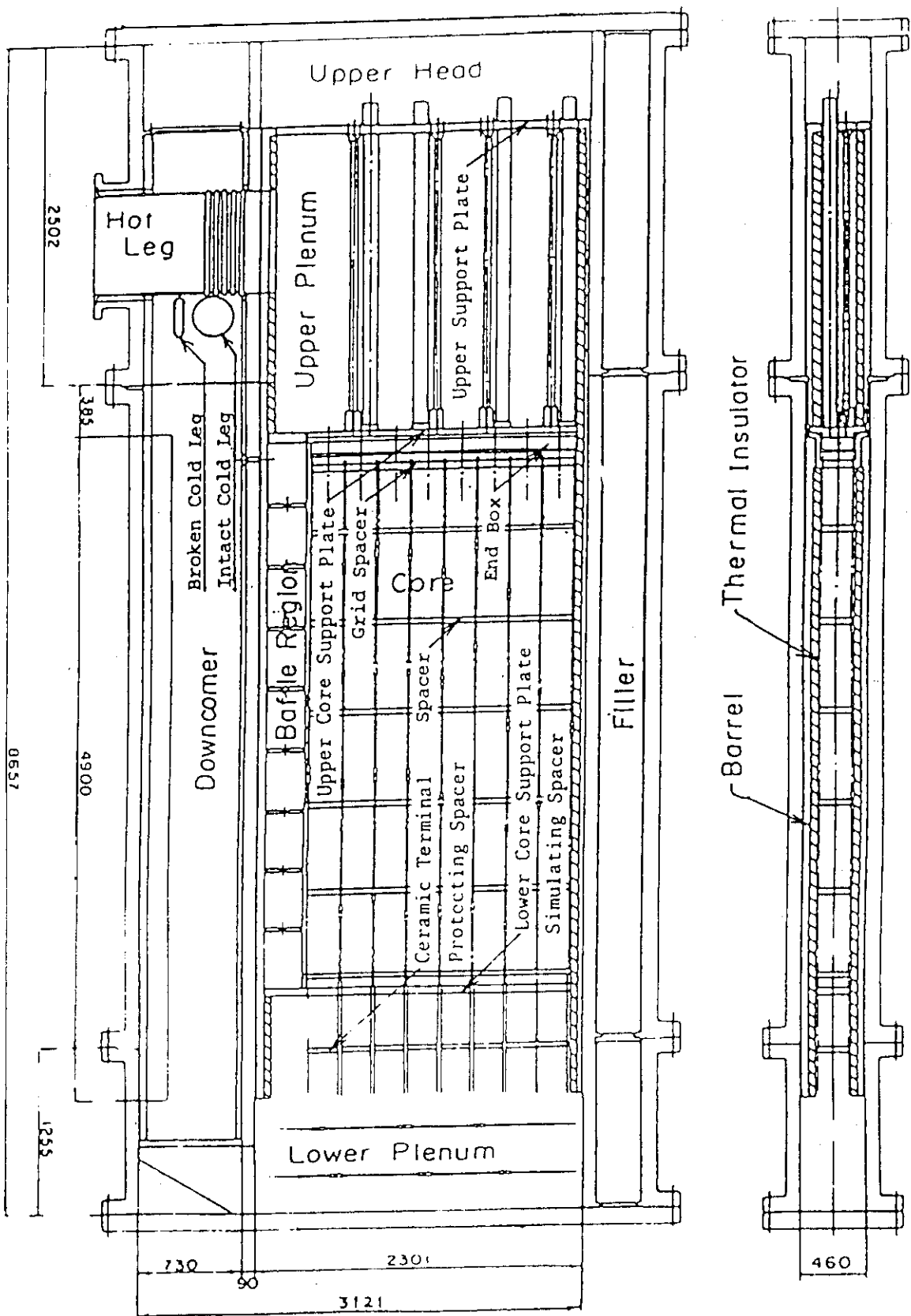


Fig. A-3 Vertical Cross Section of the Pressure Vessel

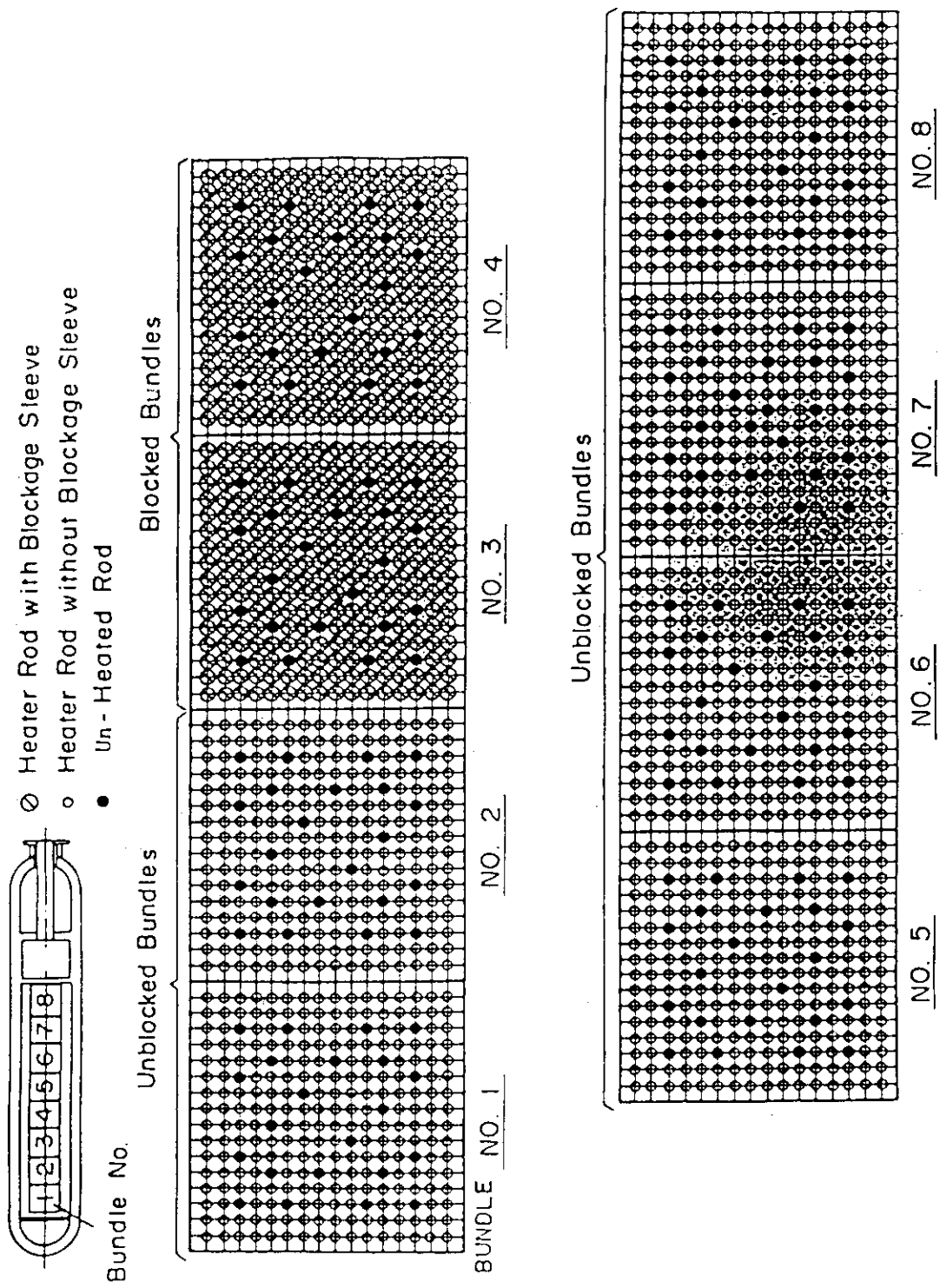


Fig. A-4 Arrangement of Heater Bundles

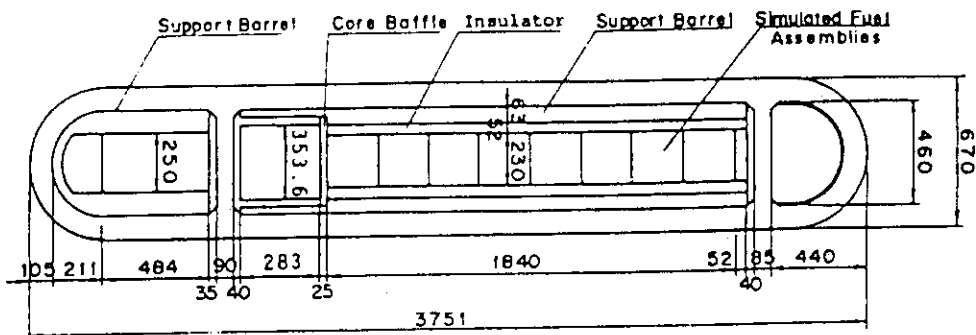


Fig. A-5 Horizontal Cross Section of the Pressure Vessel (1)

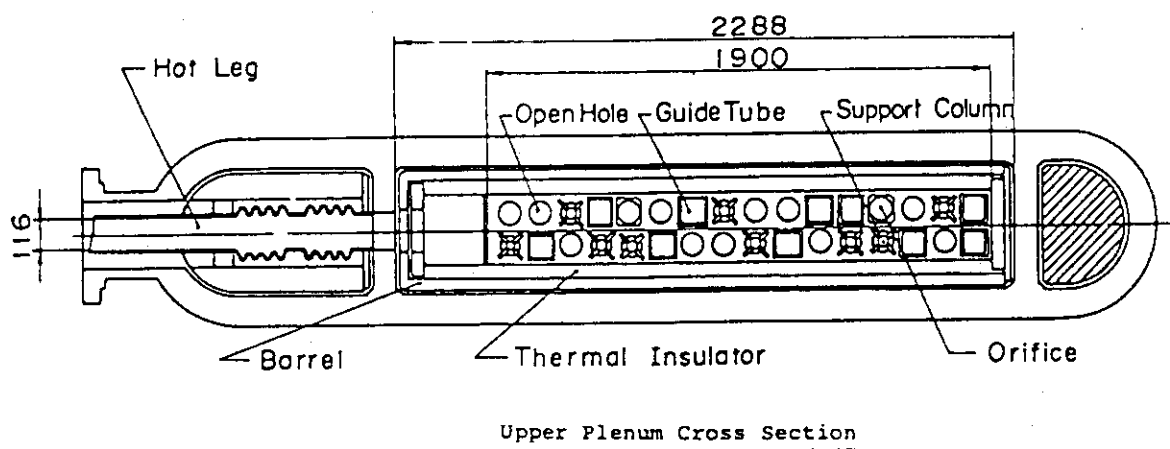


Fig. A-6 Horizontal Cross Section of the Pressure Vessel (2)

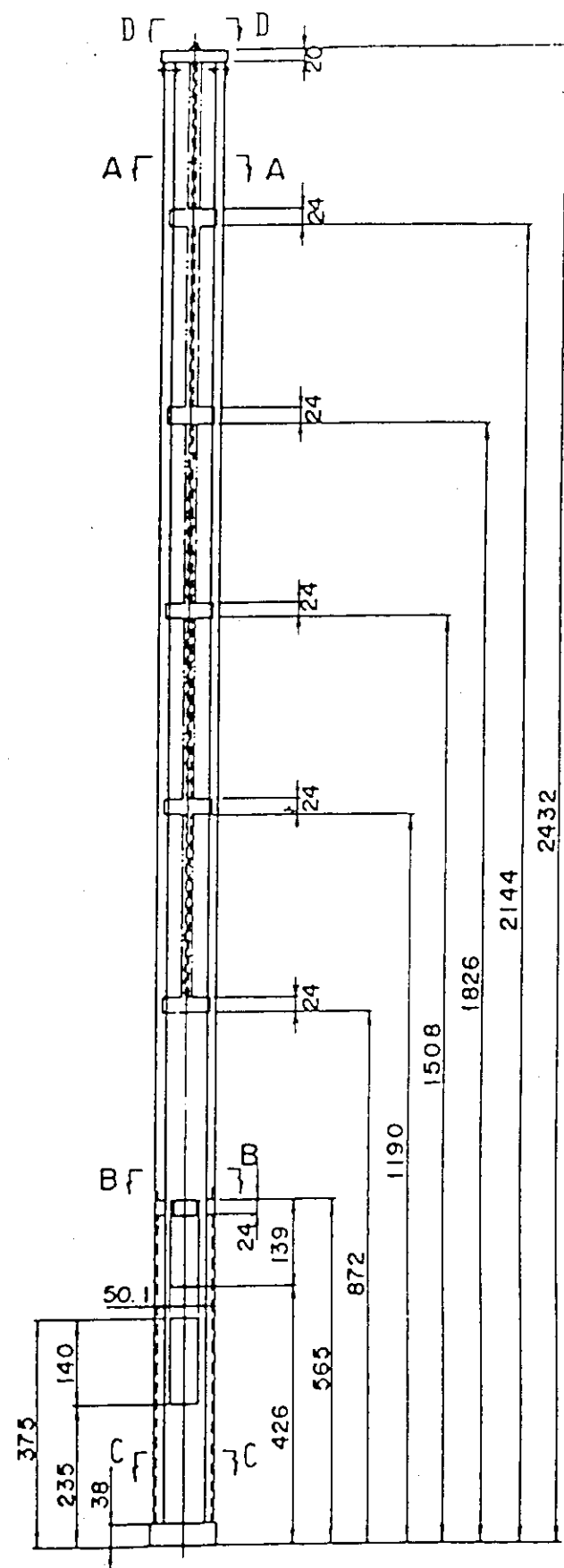


Fig. A-7 Dimension of Guide Tube (1)

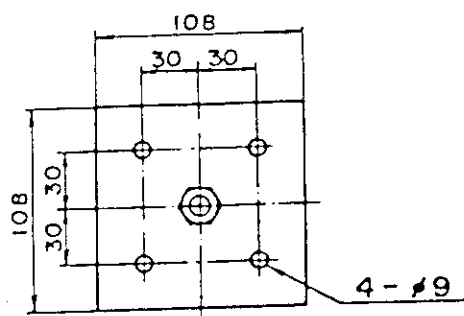
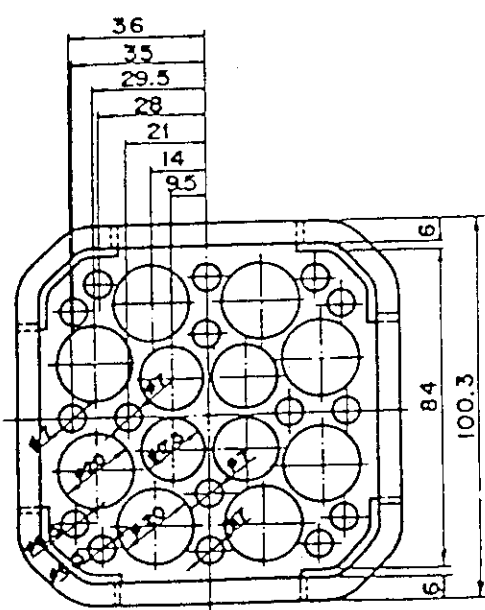
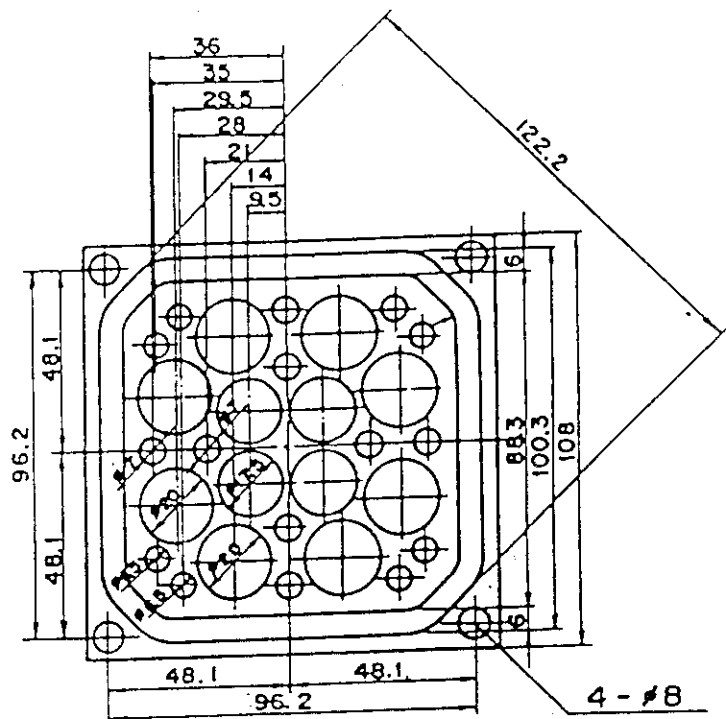
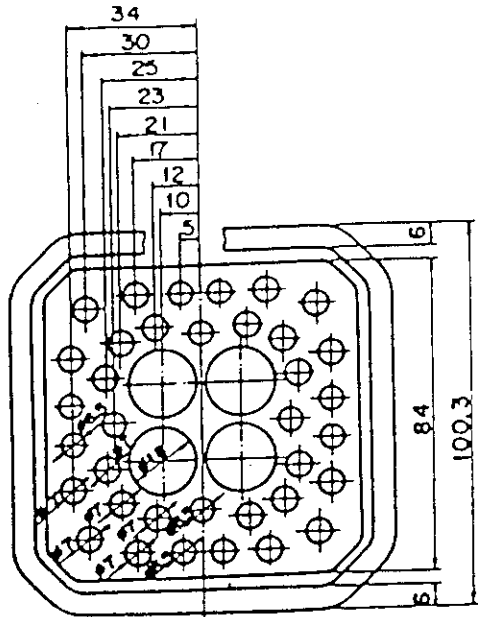


Fig. A-8 Dimension of Guide Tube (2)

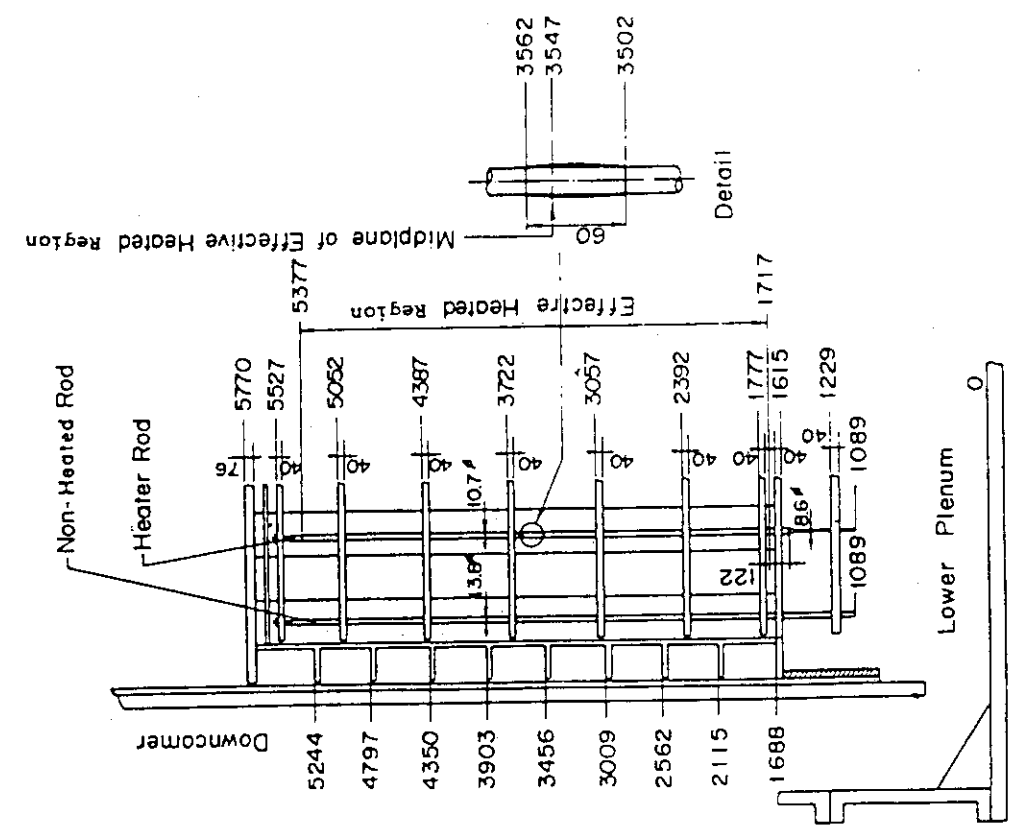


Fig. A-9 Axial Power Distribution of Heater Rod

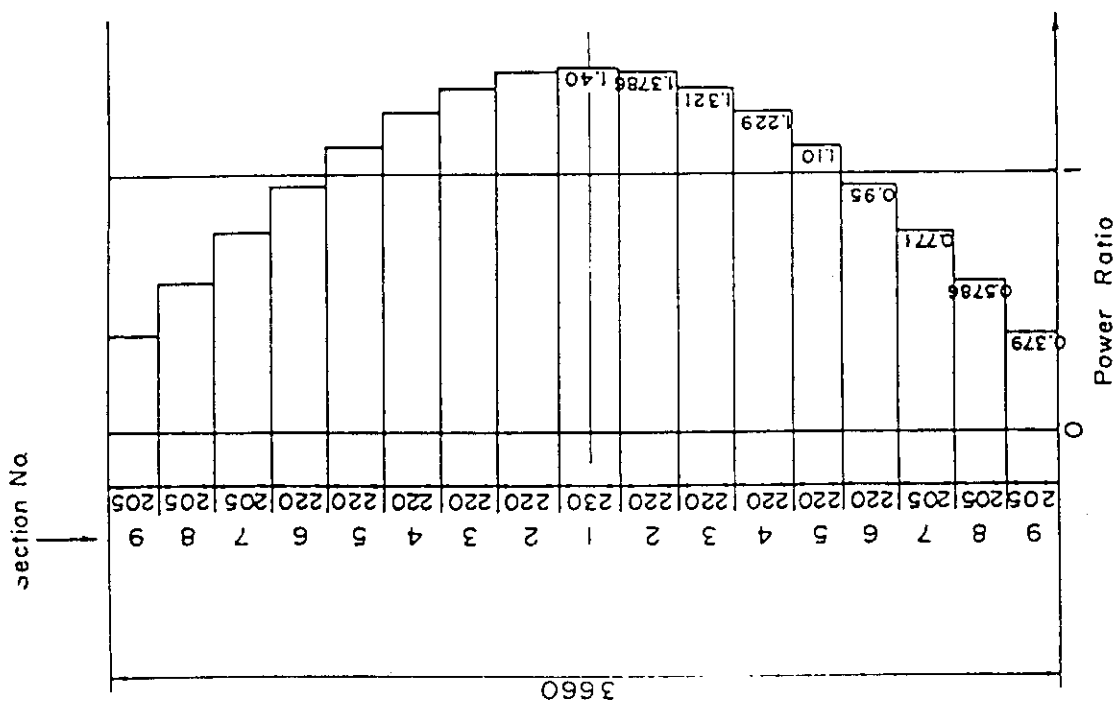


Fig. A-10 Relative Elevation and Dimension of the Core in SCTF

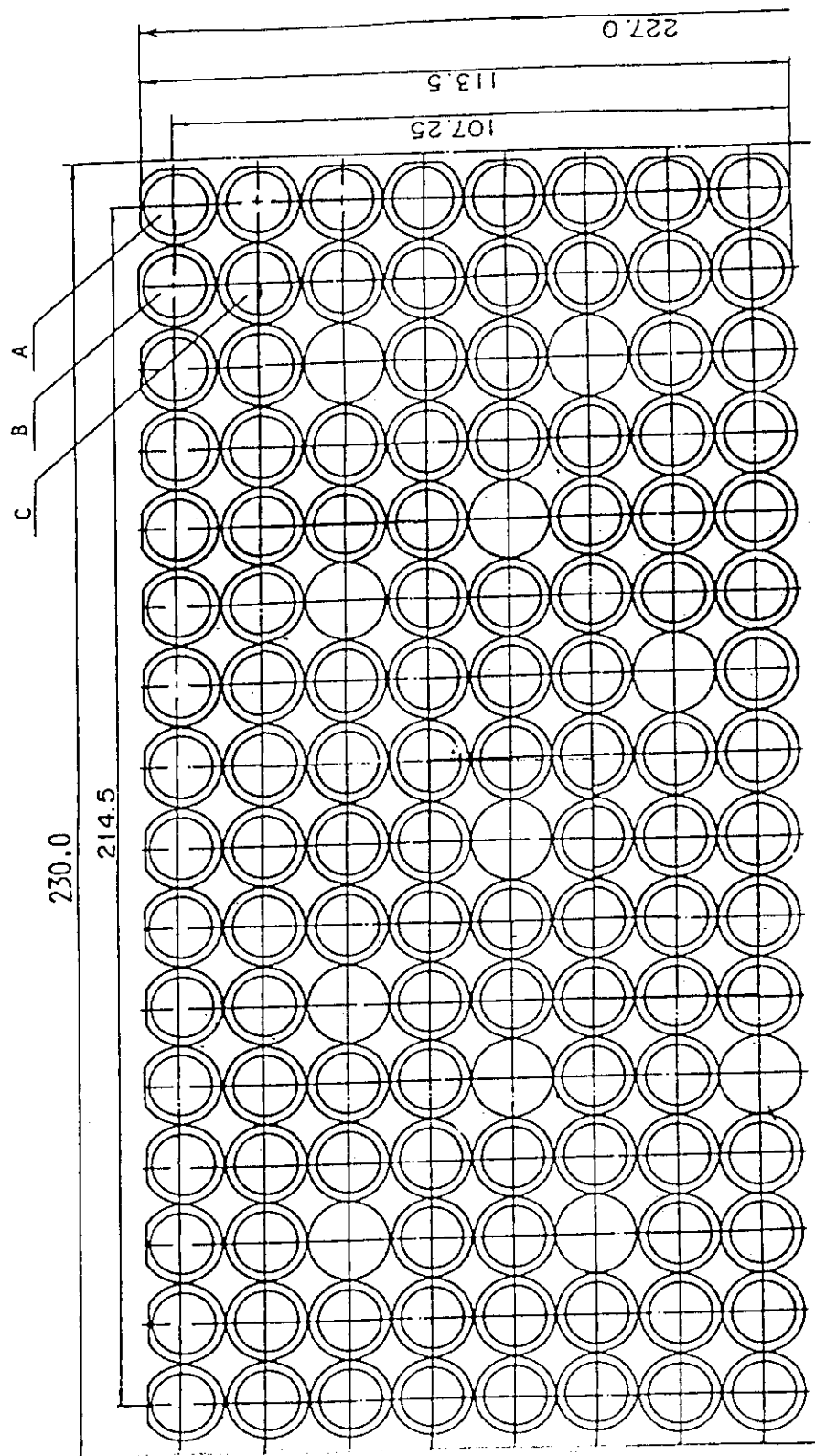


Fig. A-11 Arrangement of the Heater Rods with Three Kinds of Blockage
Sleeve

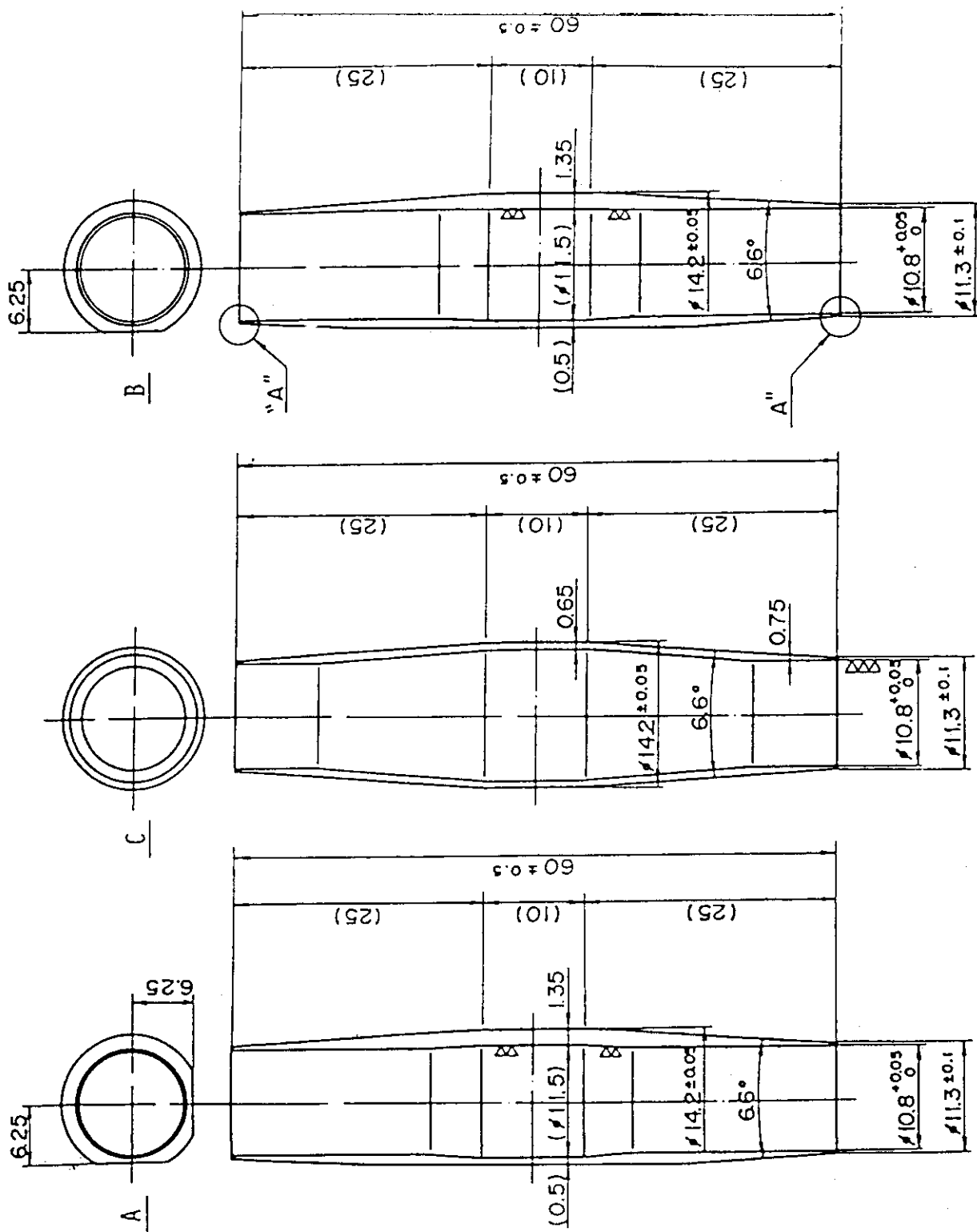


Fig. A-12 Configuration and Dimension of the Thre Blockage Sleeves

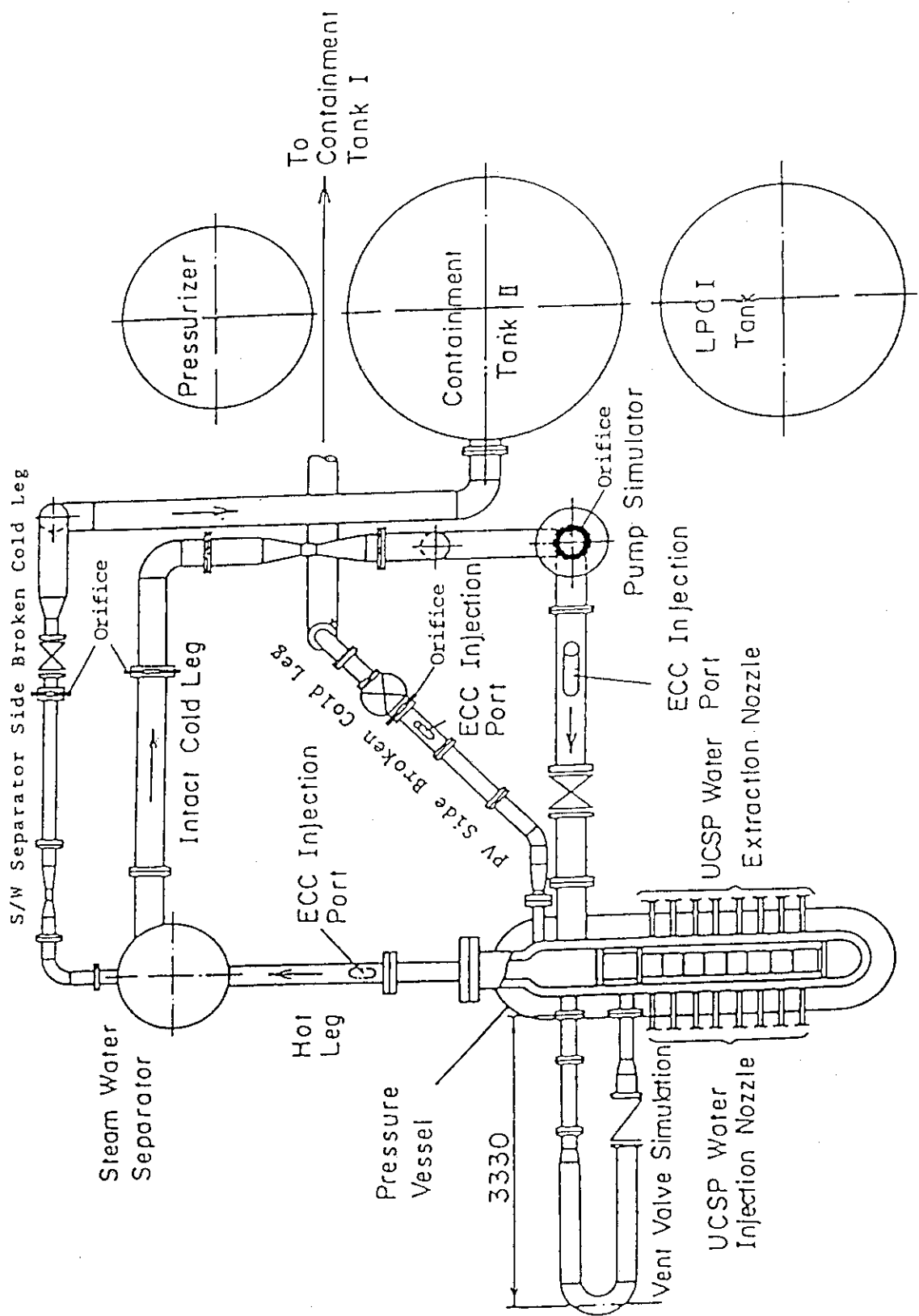


Fig. A-13 Overview of the Arrangements of the SCTF

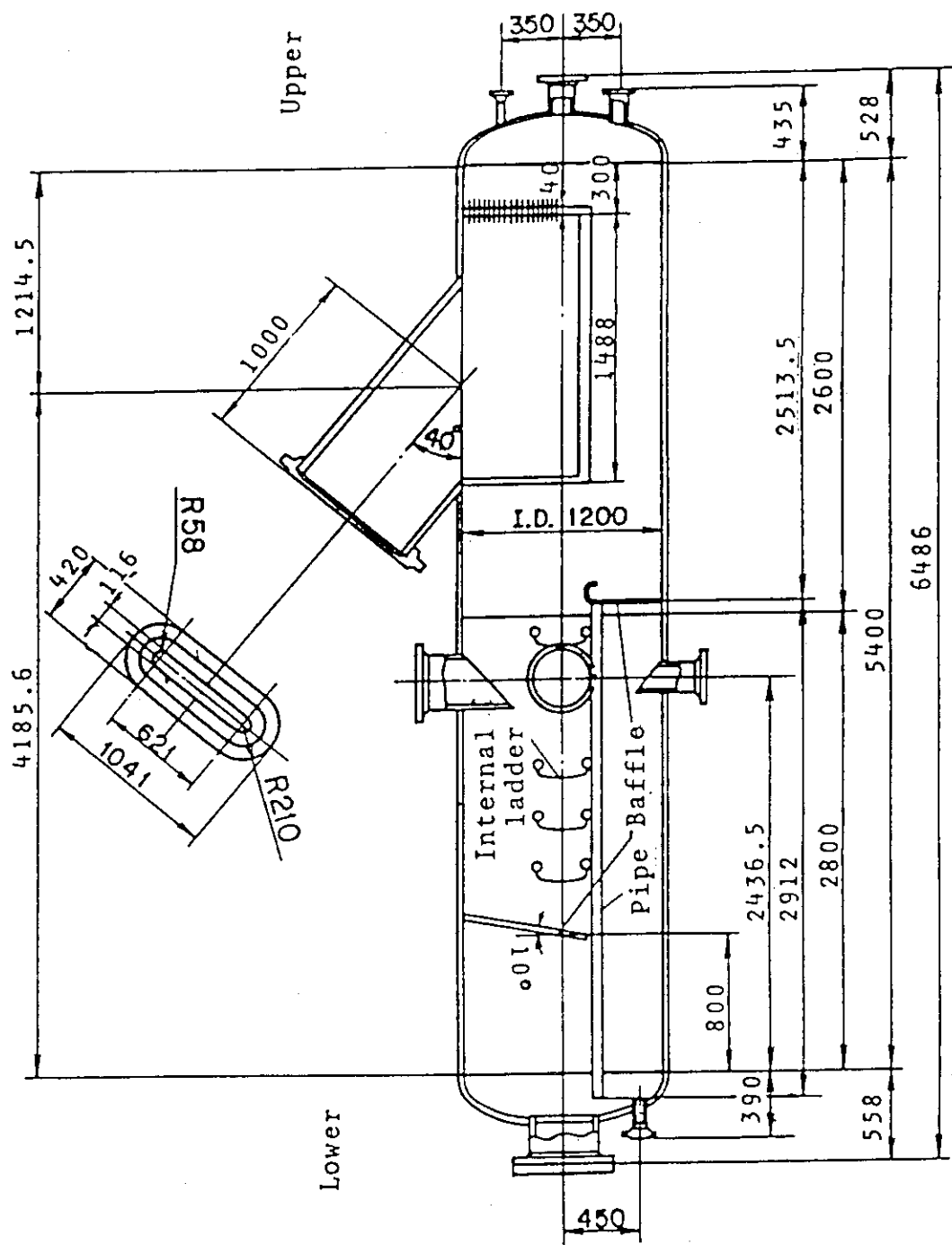


Fig. A-14 Steam-Water Separator

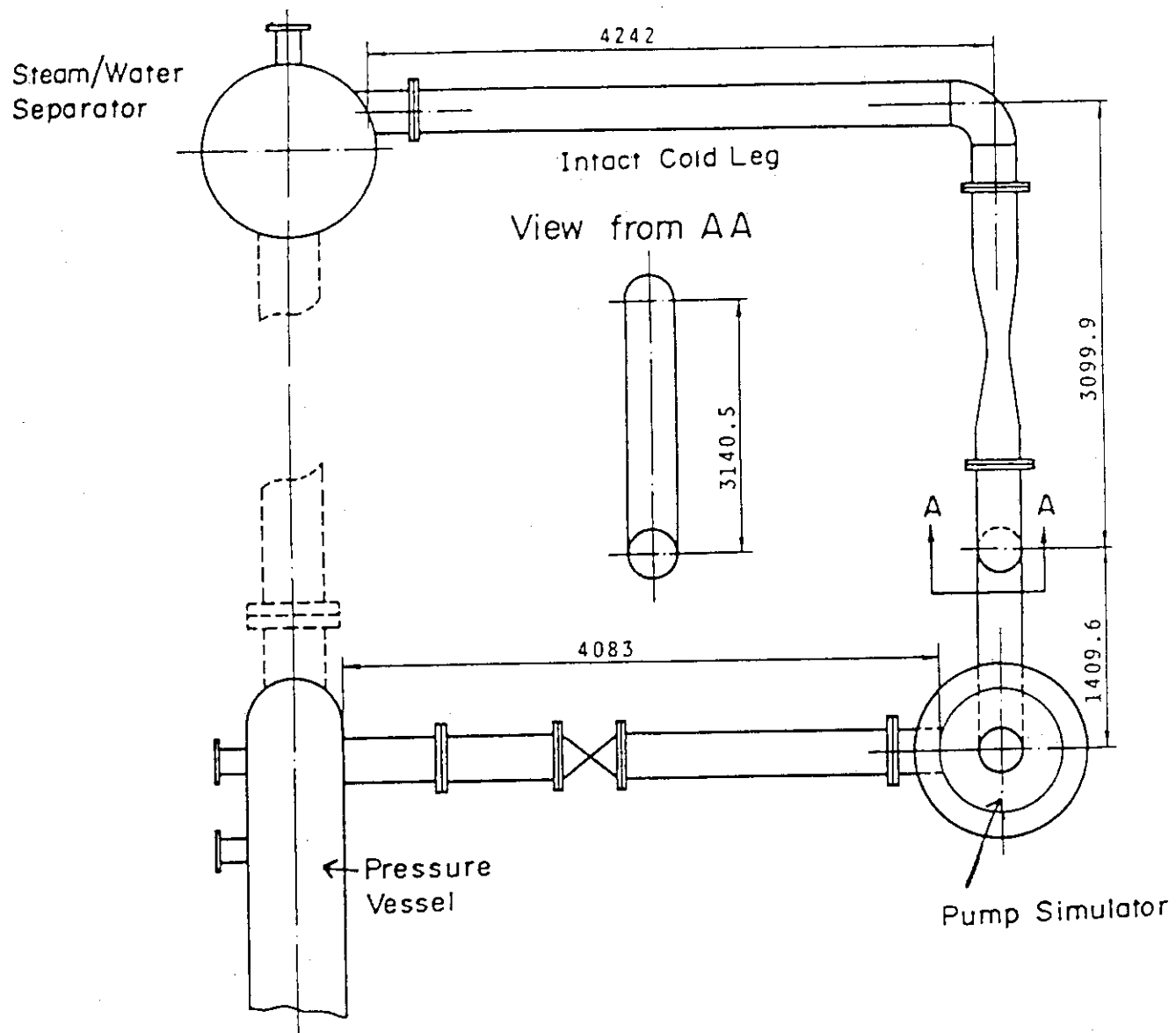


Fig. A-15 Arrangement of Intact Cold Leg

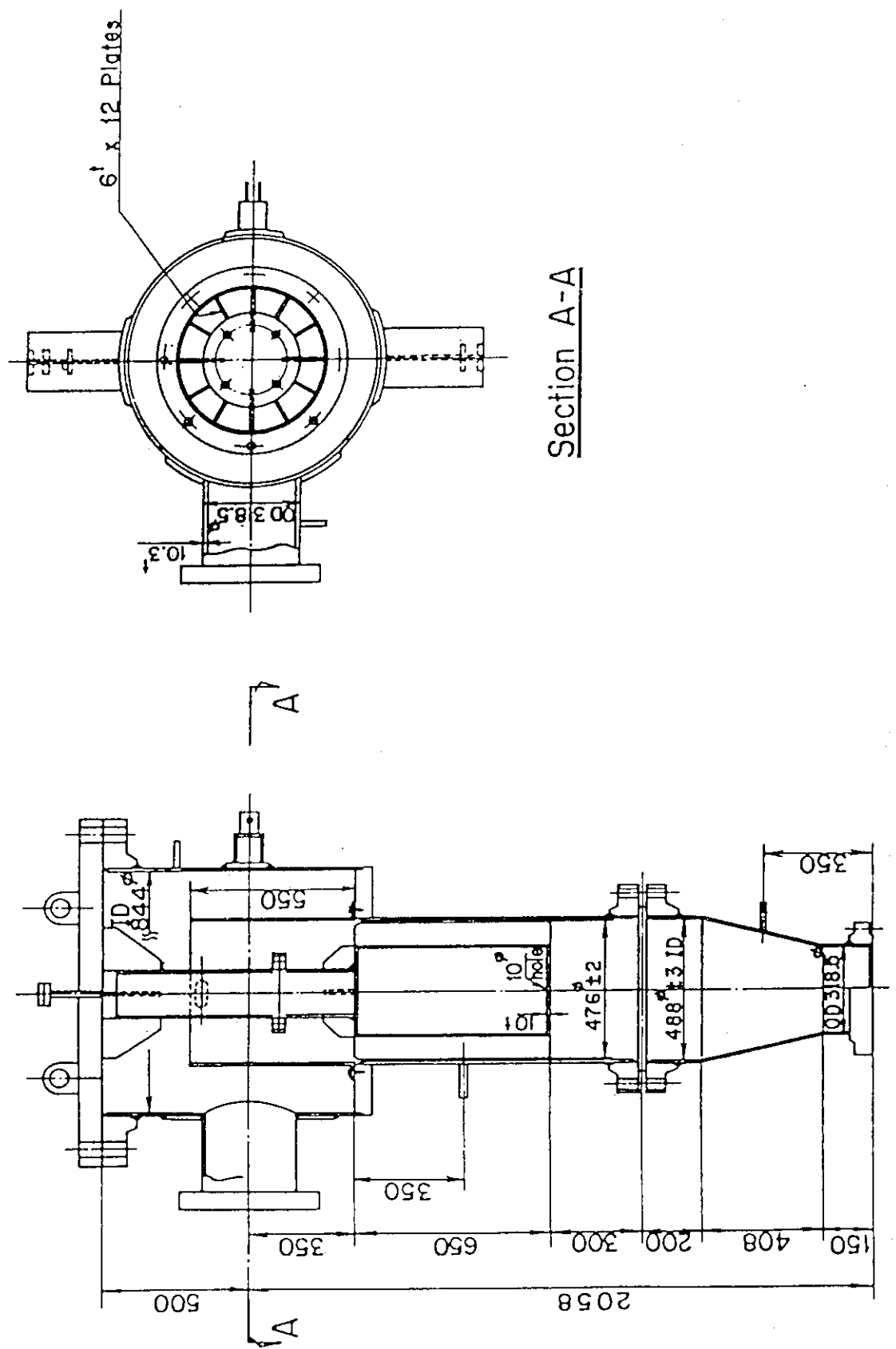


Fig. A-16 Configuration and Dimension of Pump Simulator

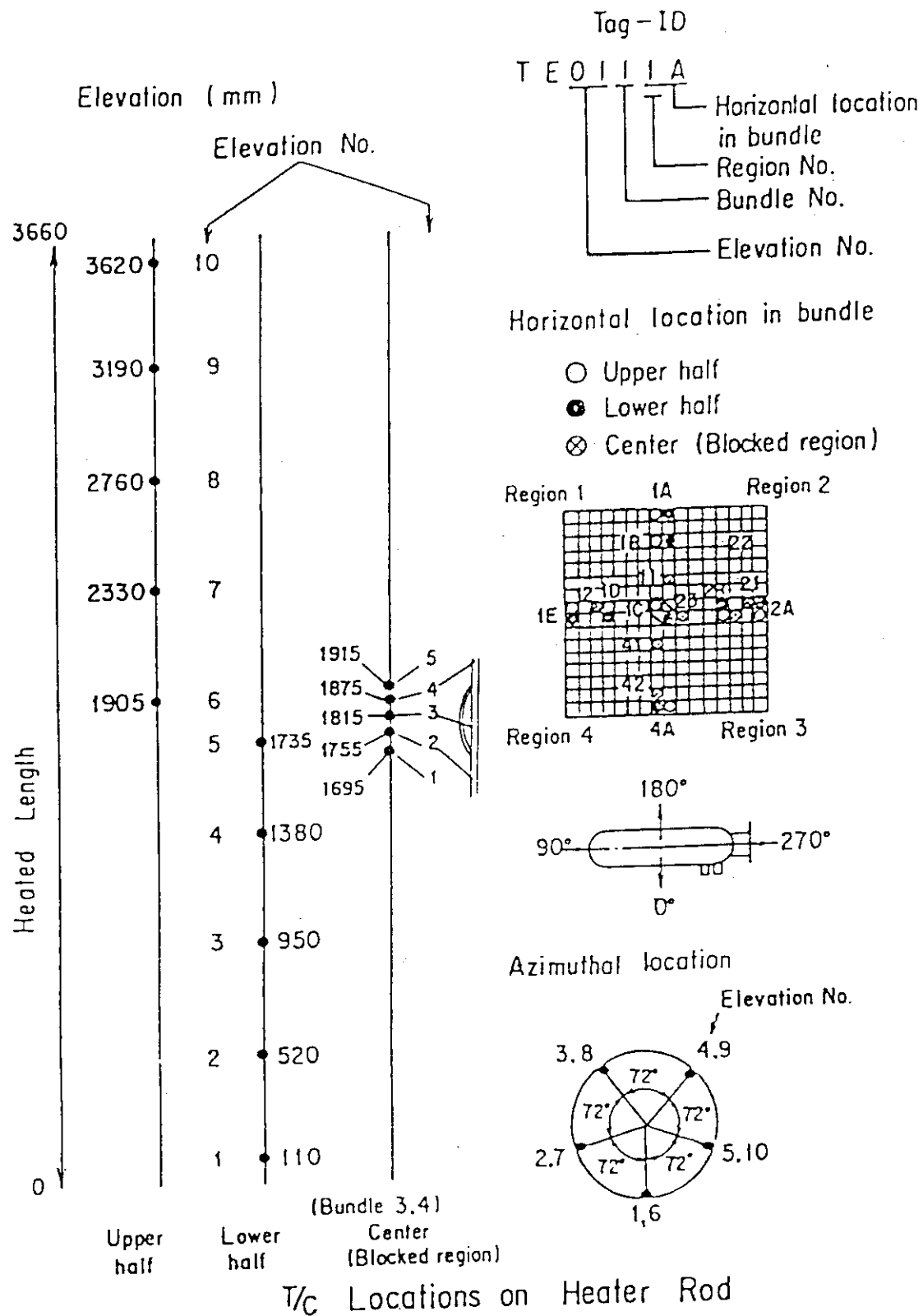


Fig. A-17 Thermocouple Locations of Heater Rod Surface Temperature Measurements

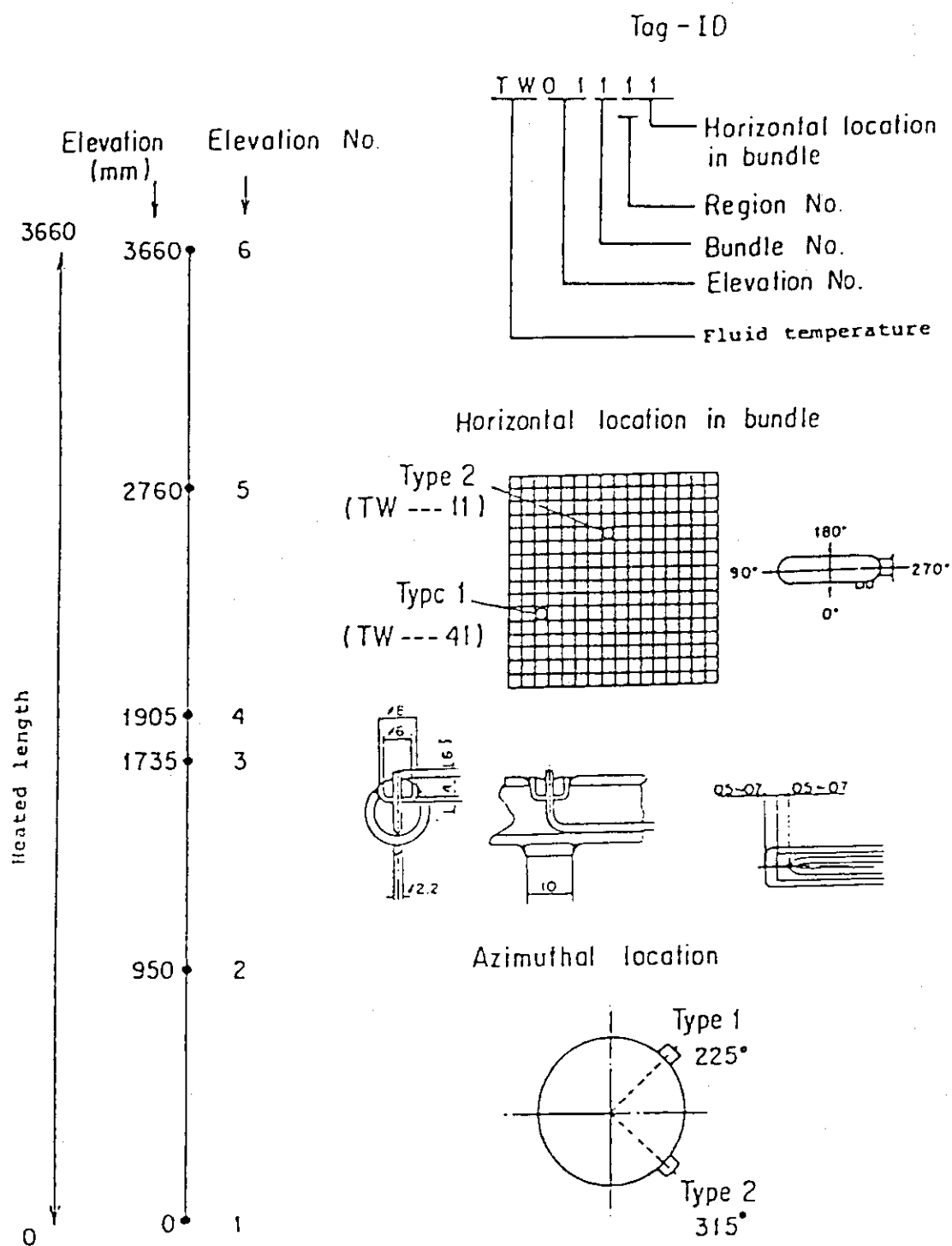


Fig. A-18 Thermocouple Locations of Fluid Temperature Measurements in Core

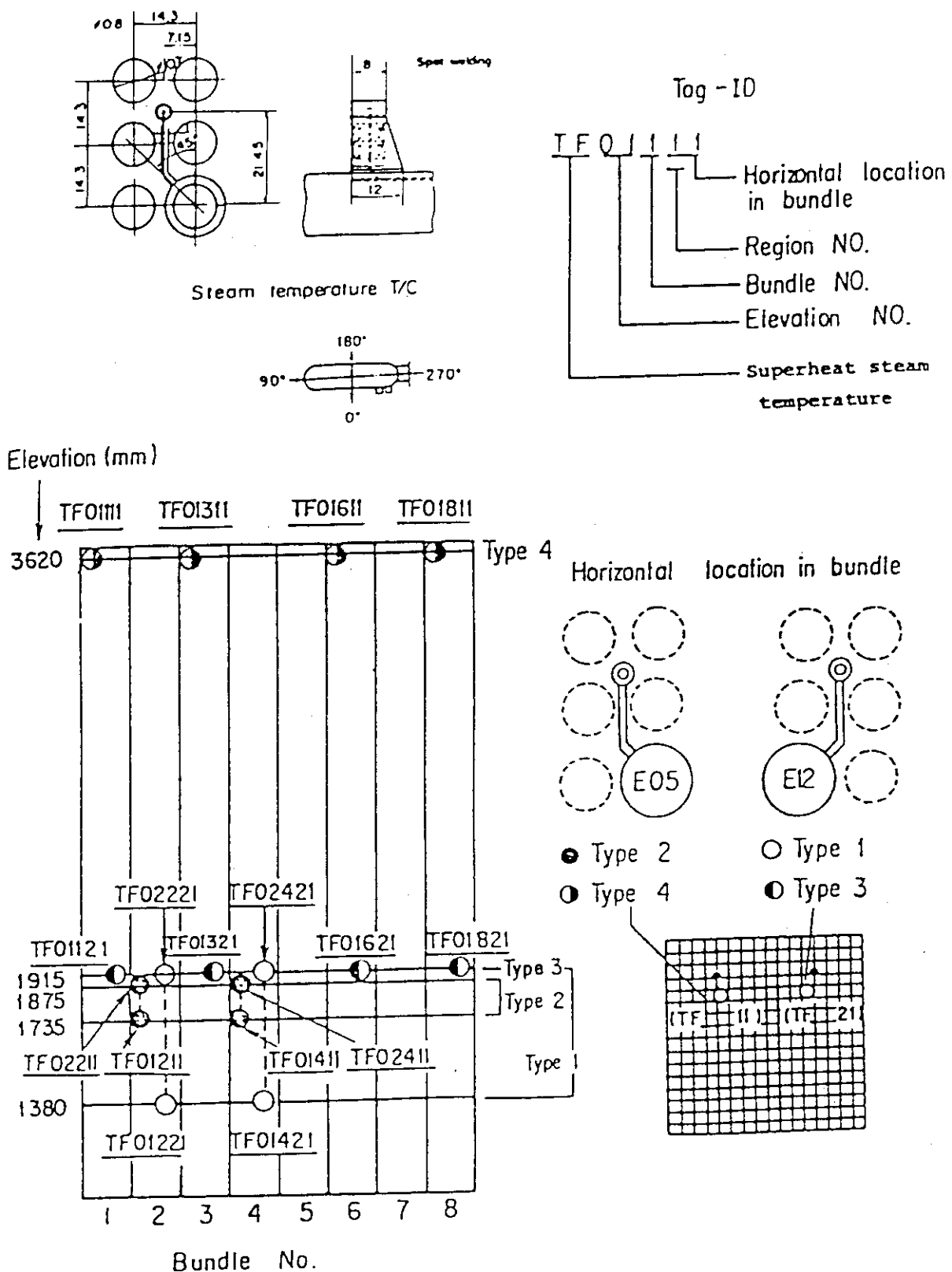


Fig. A-19 Thermocouple Locations of Steam Temperature Measurements in Core

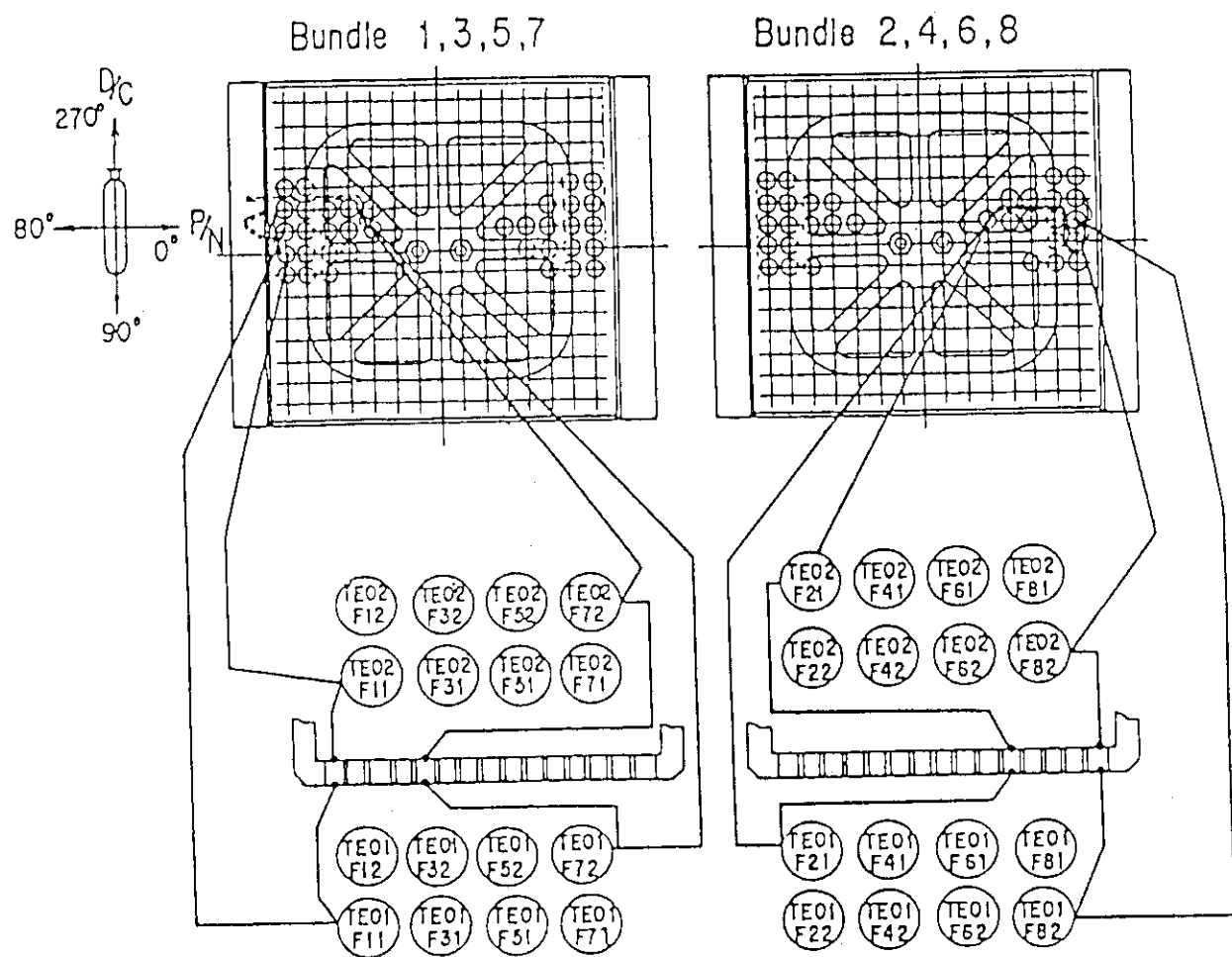


Fig. A-20 Thermocouple Locations of Fluid Temperature Measurements
just above and below End Box Tie Plate

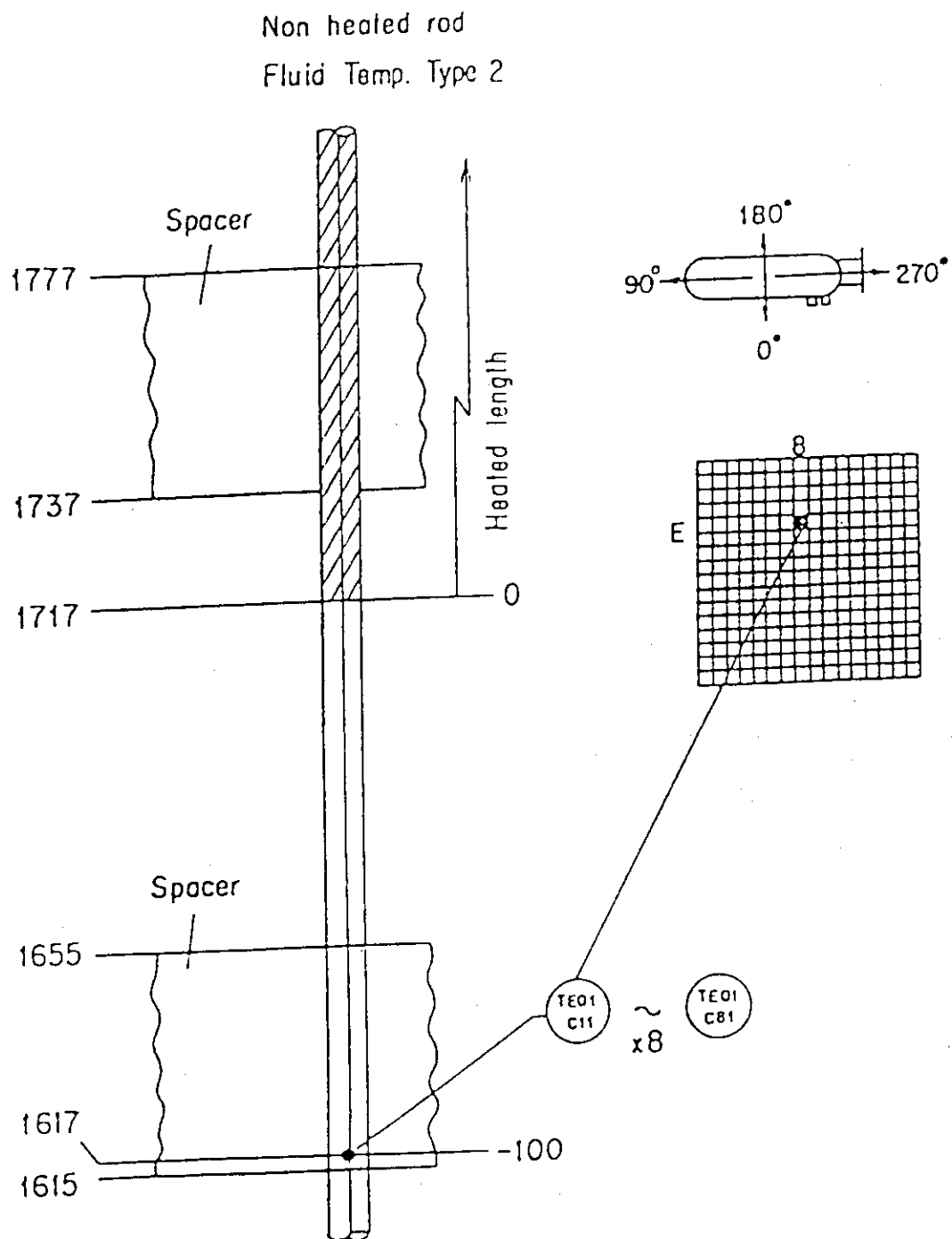


Fig. A-21 Thermocouple Locations of Fluid Temperature Measurements
at Core Inlet

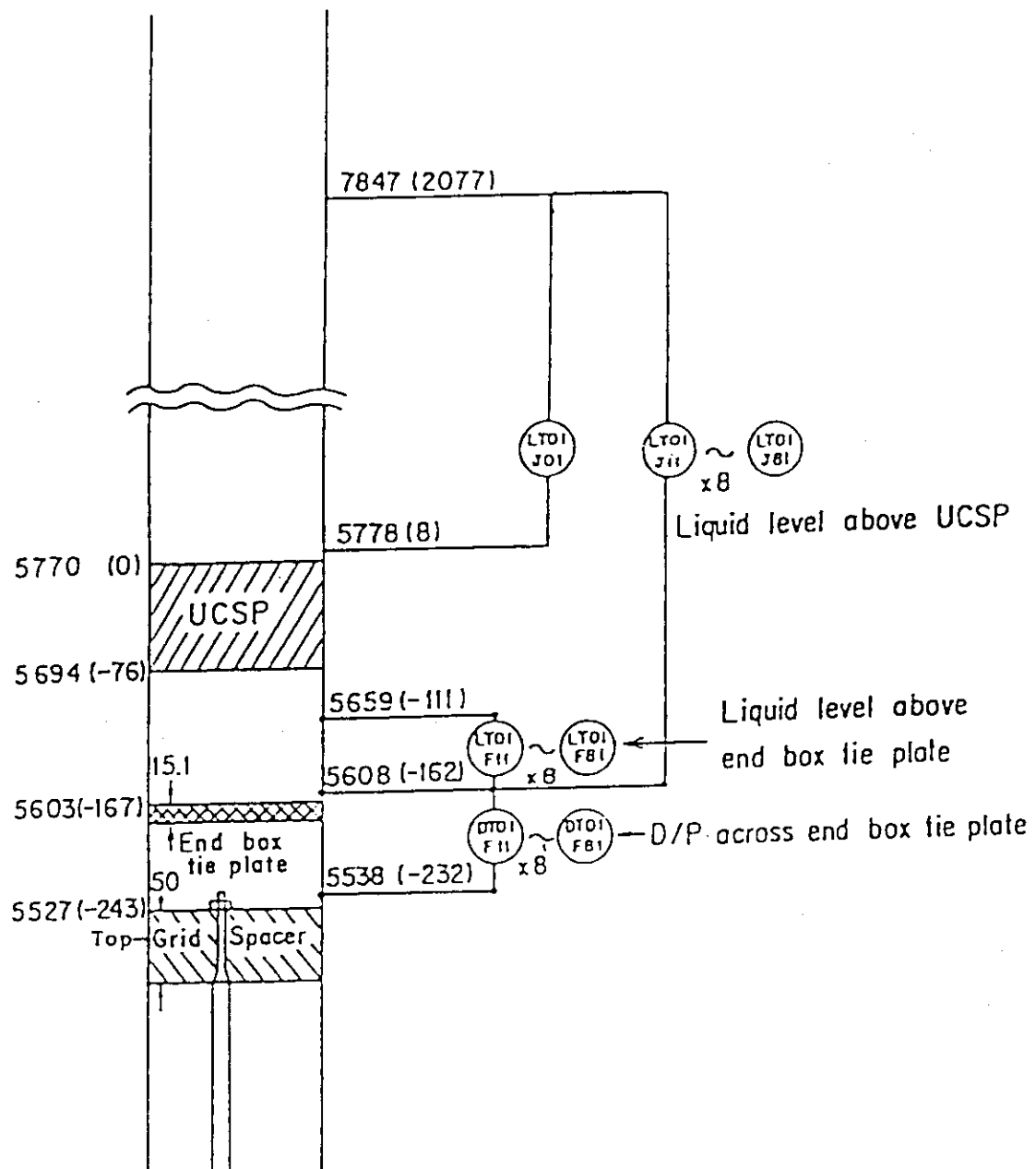


Fig. A-22 Locations of Differential Pressure Measurements across End Box Tie Plate and Liquid Level Measurements above UCSP and End Box Tie Plate

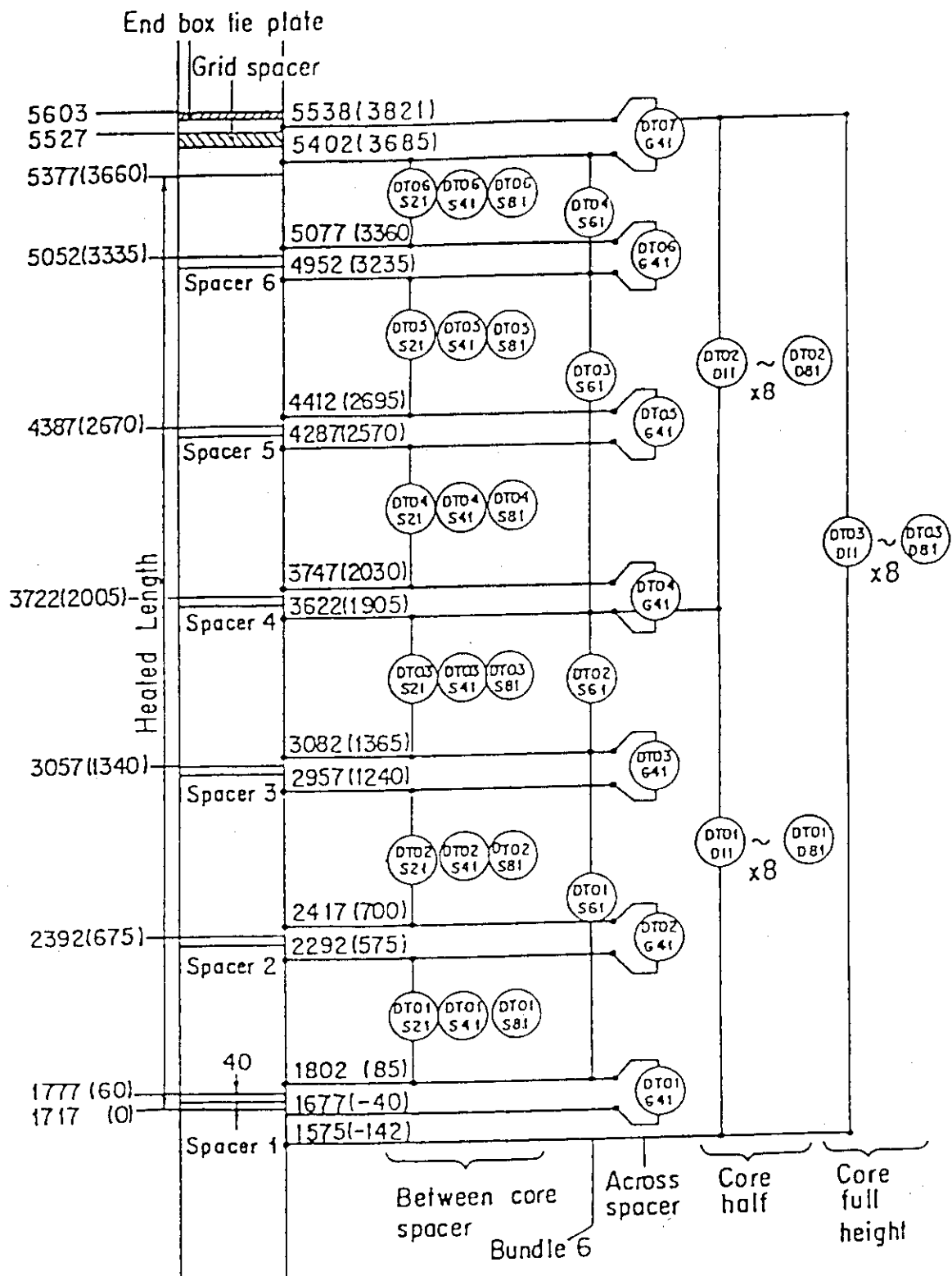


Fig. A-23 Locations of Vertical Differential Pressure Measurements in Core

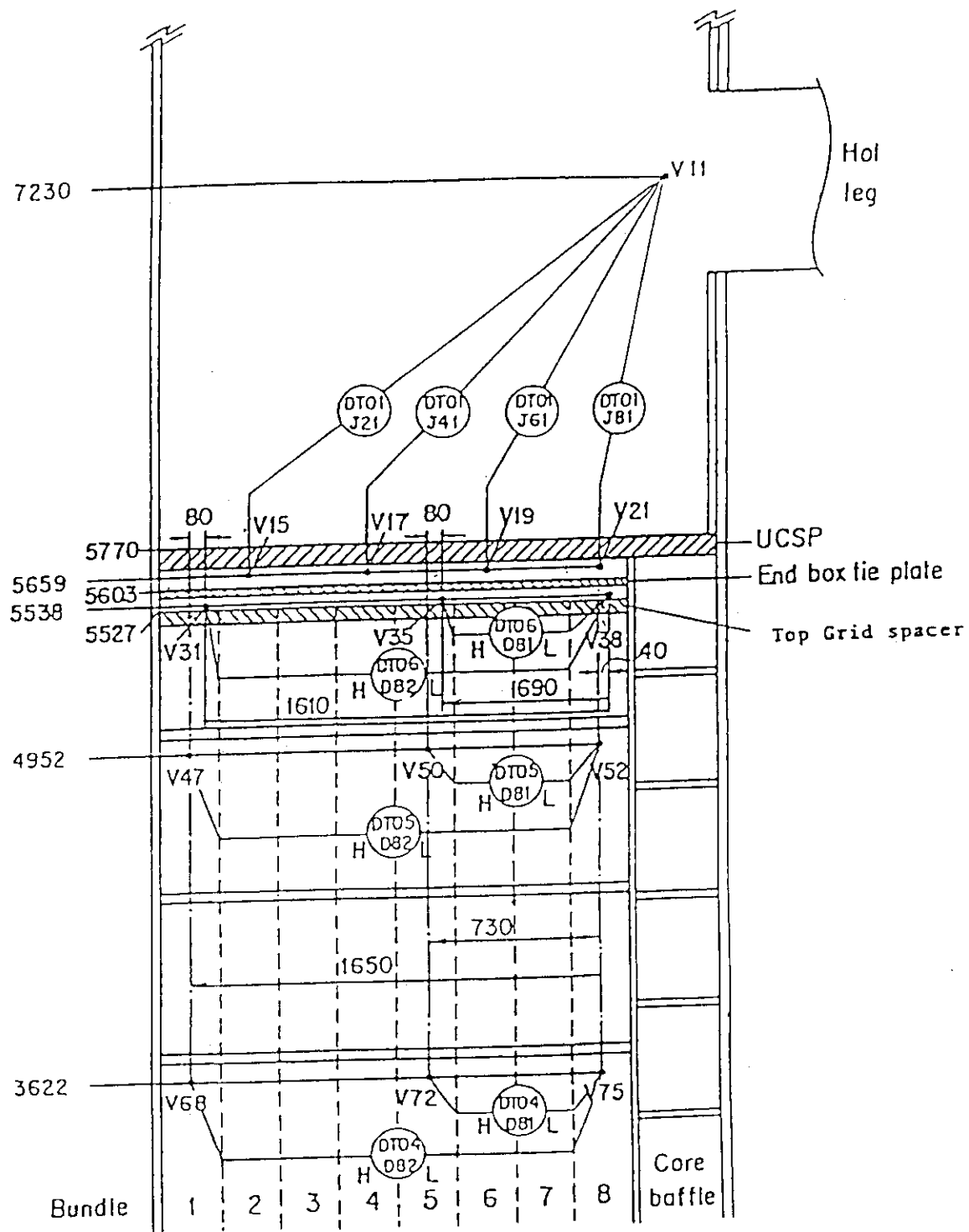


Fig. A-24 Locations of Horizontal Differential Pressure Measurements in Core and Differential Pressure Measurements between End Box and Inlet of Hot Leg

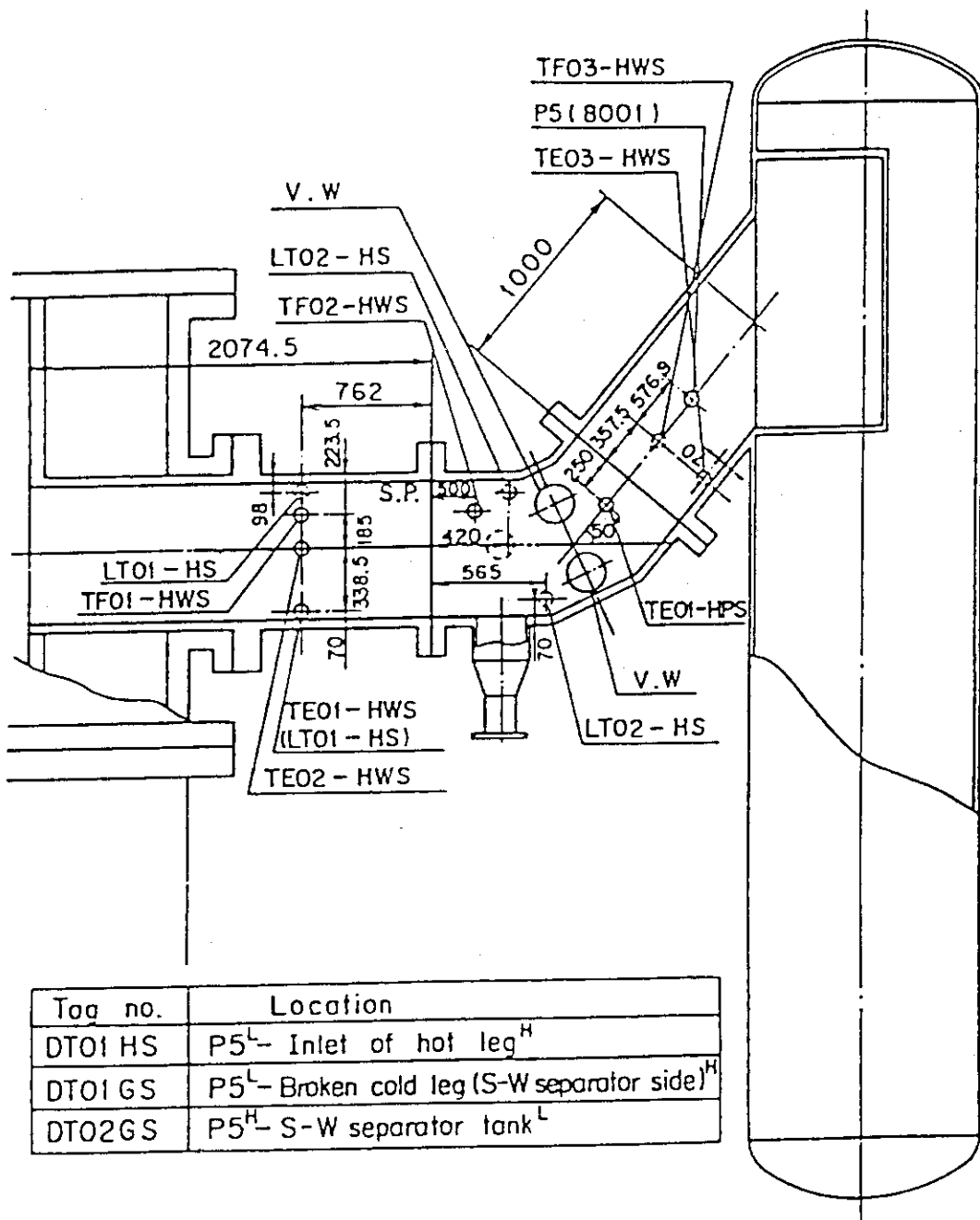


Fig. A-25 Locations of Hot Leg Instrumentation

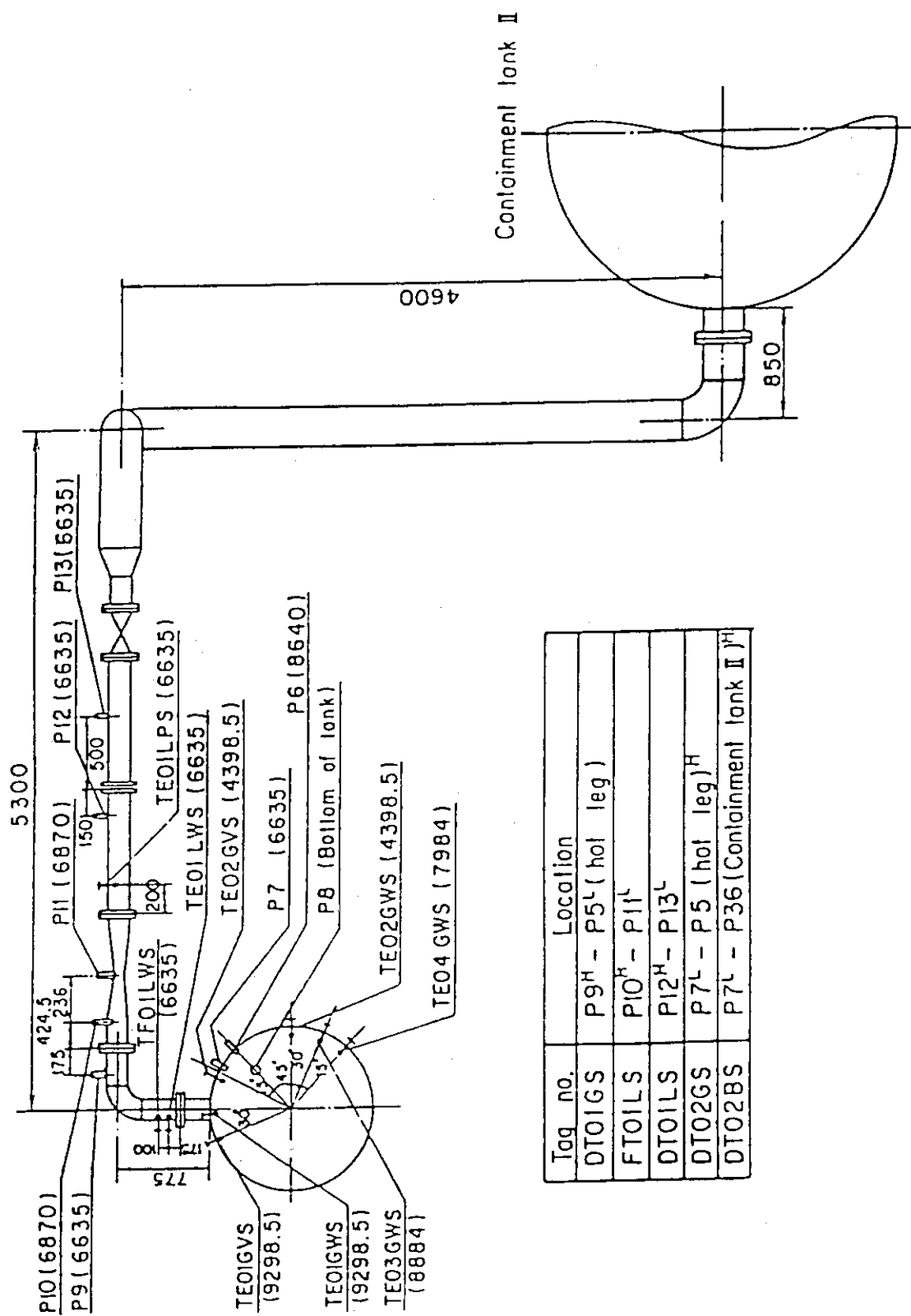


Fig. A-26 Locations of Steam-Water Separator Side Broken Cold Leg
Instrumentation

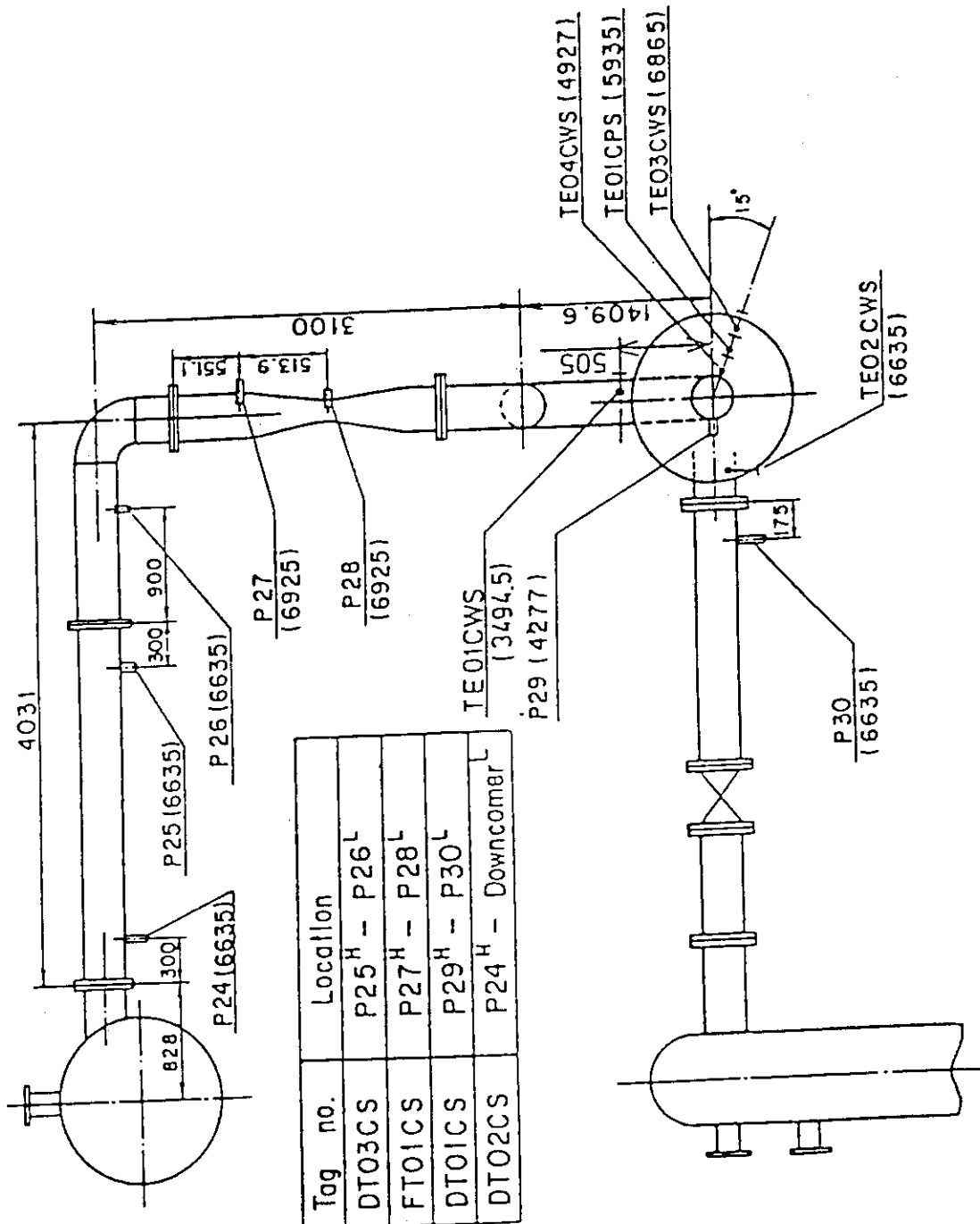


Fig. A-27 Locations of Intact Cold Leg Instrumentation

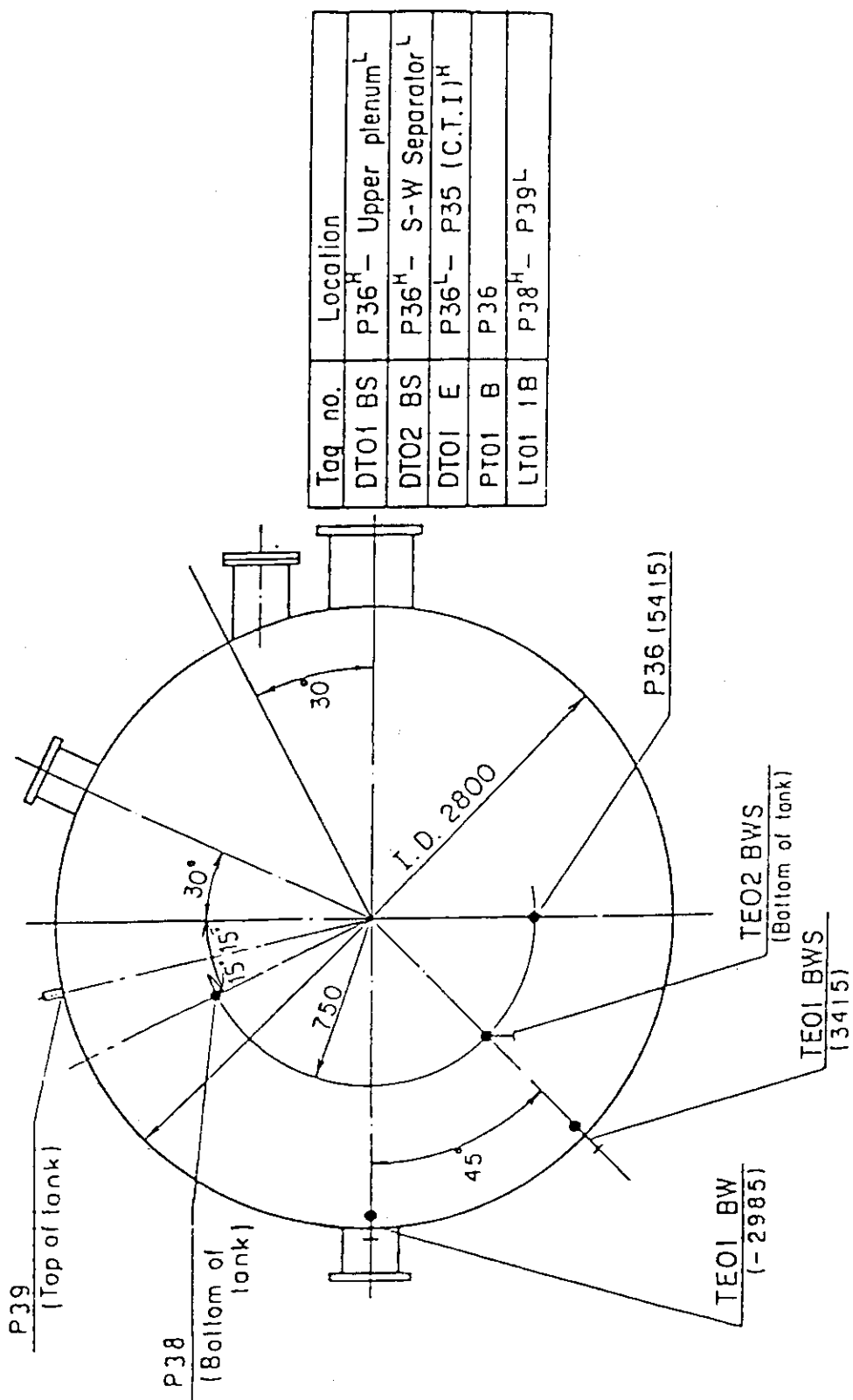


Fig. A-28 Locations of Containment Tank-II Instrumentation

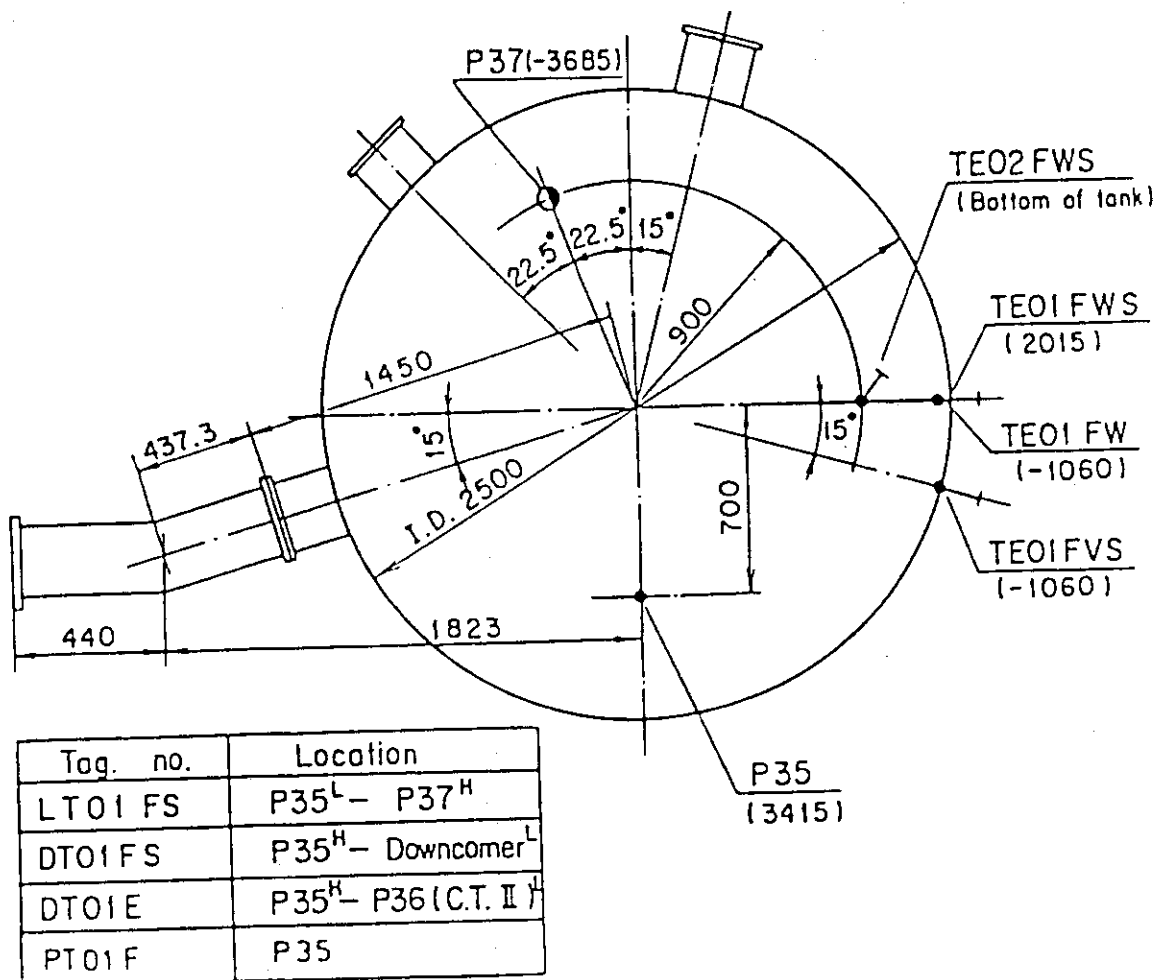
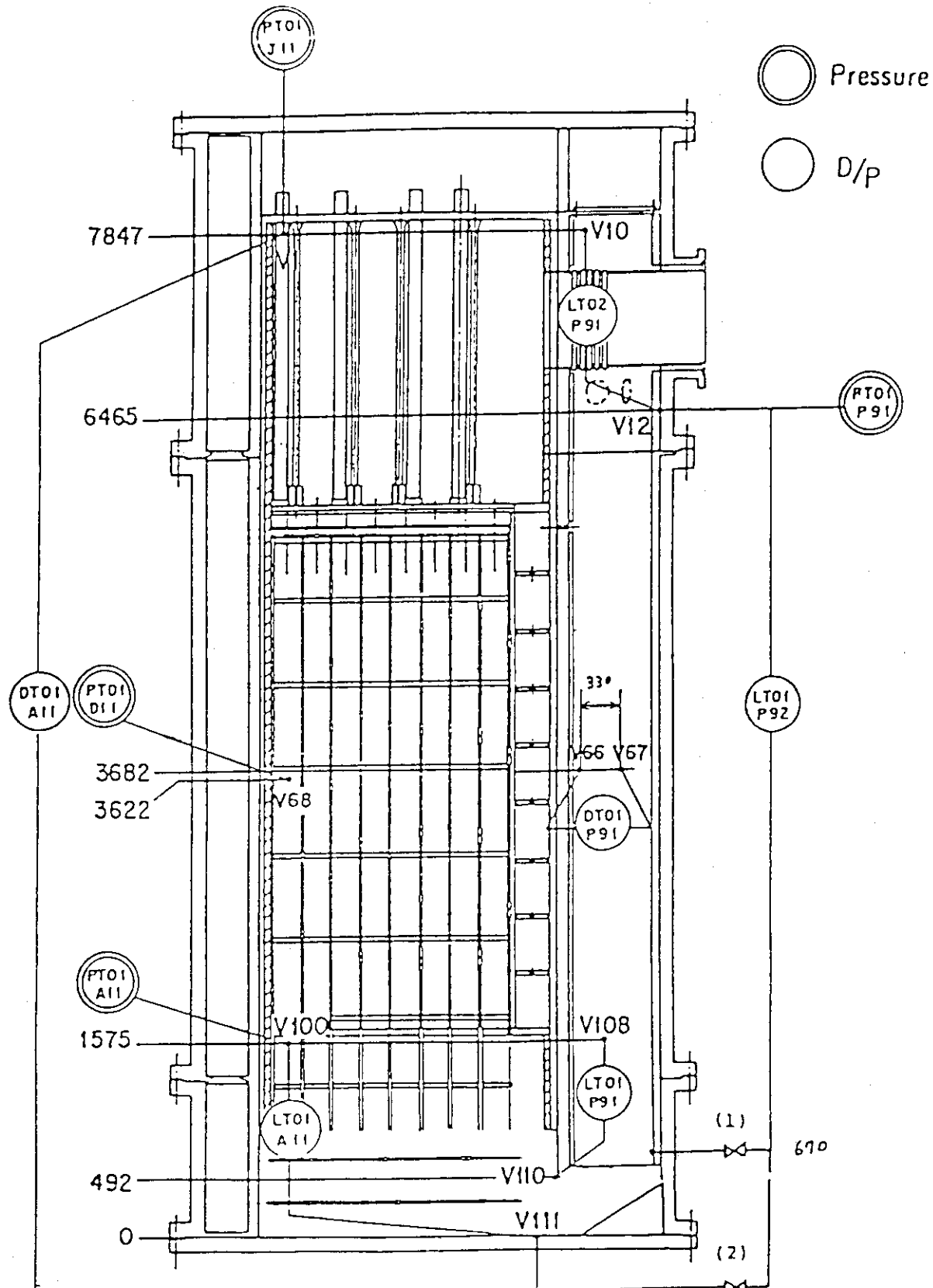


Fig. A-29 Locations of Containment Tank-I Instrumentation



- (1) used for lower plenum injection test
 (the bottom of downcomer is blocked)
 (2) used for the other tests

Fig. A-30 Location of Pressure Measurements in Pressure Vessel, Differential Pressure Measurements between Upper and Lower Plenums and Liquid Level Measurements in Downcomer and Lower Plenum

Appendix B

Selected Data for Test S1-14 (Run 520)

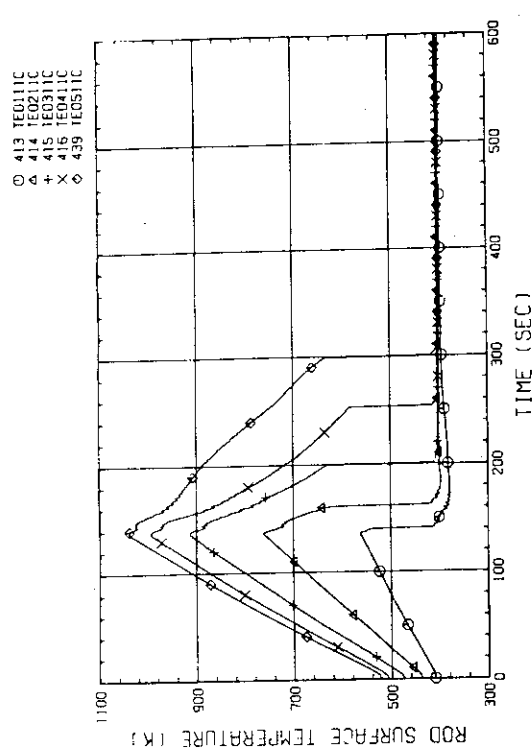


Fig. B-1(a) HEATER ROD TEMPERATURE
(BUNDLE 1-1C, LOWER HALF)

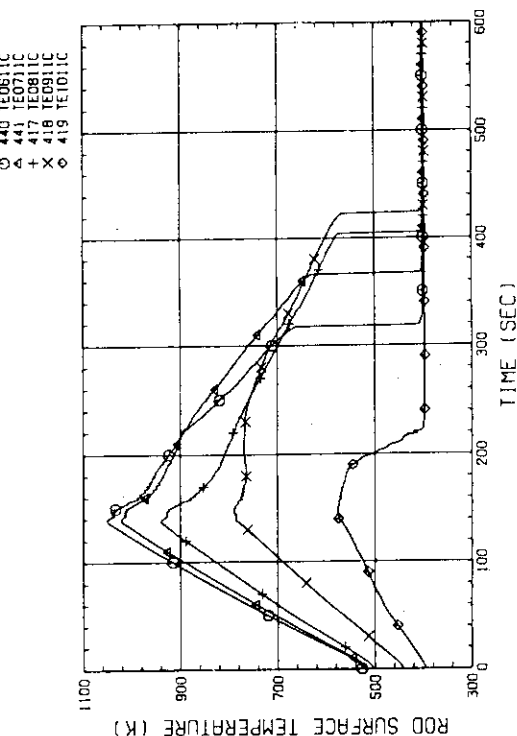


Fig. B-1(b) HEATER ROD TEMPERATURE
(BUNDLE 1-1C, UPPER HALF)

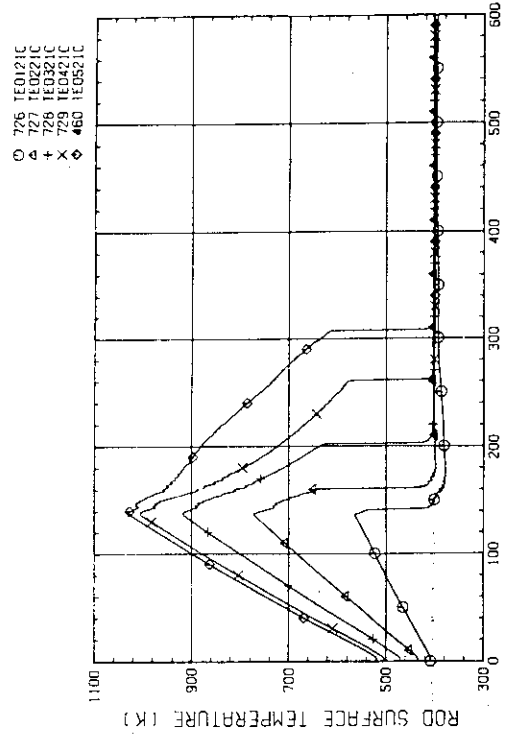


Fig. B-2(a) HEATER ROD TEMPERATURE
(BUNDLE 2-1C, LOWER HALF)

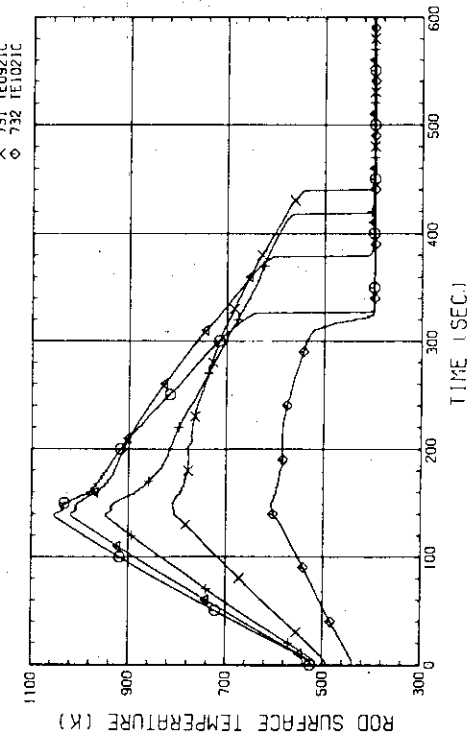
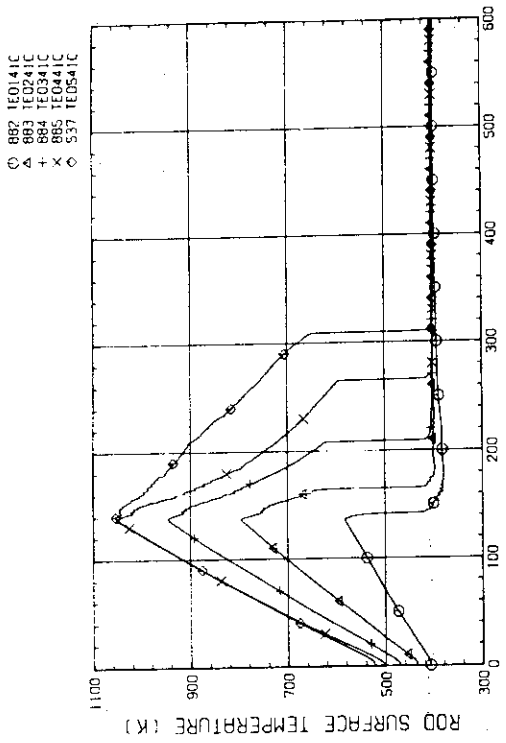
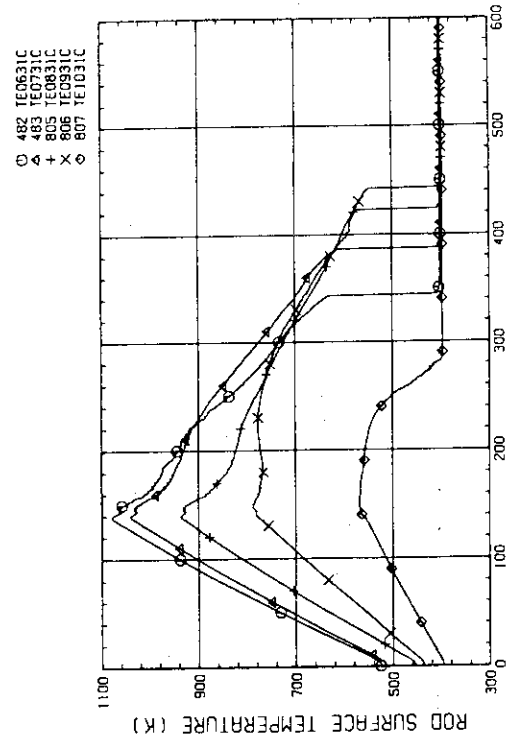
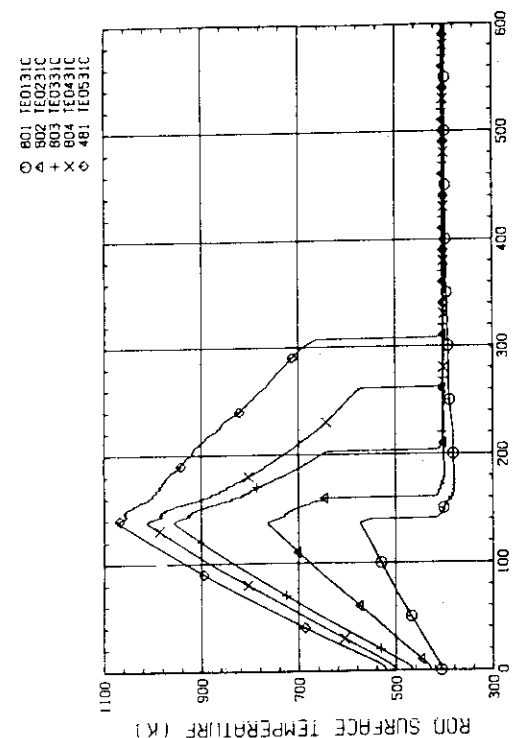
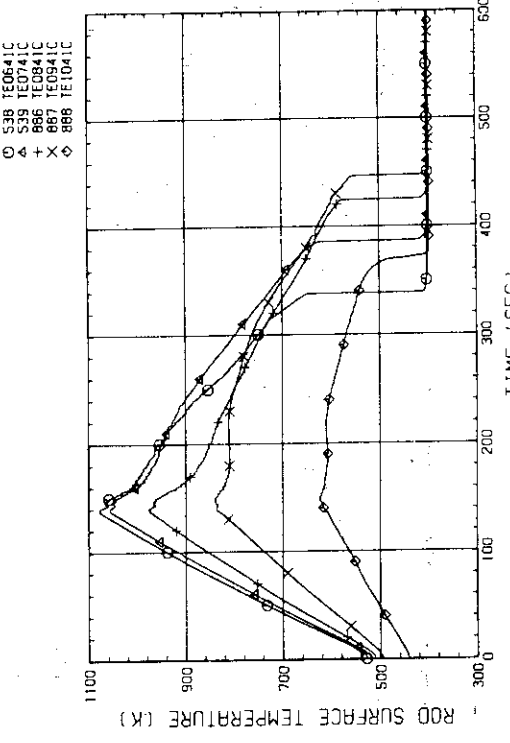
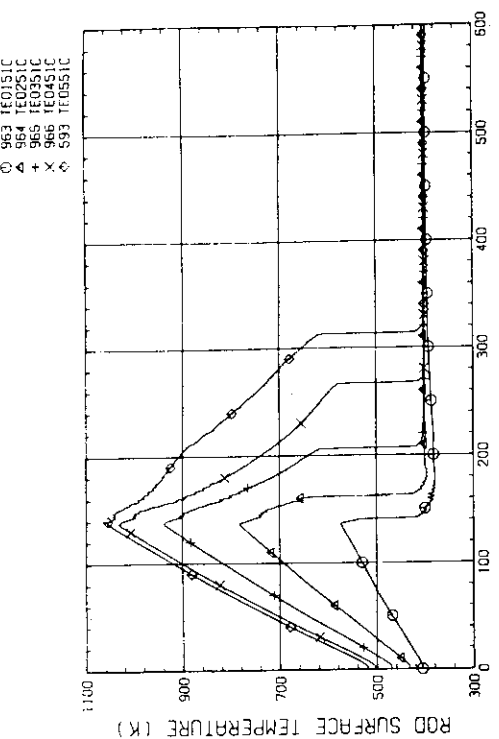
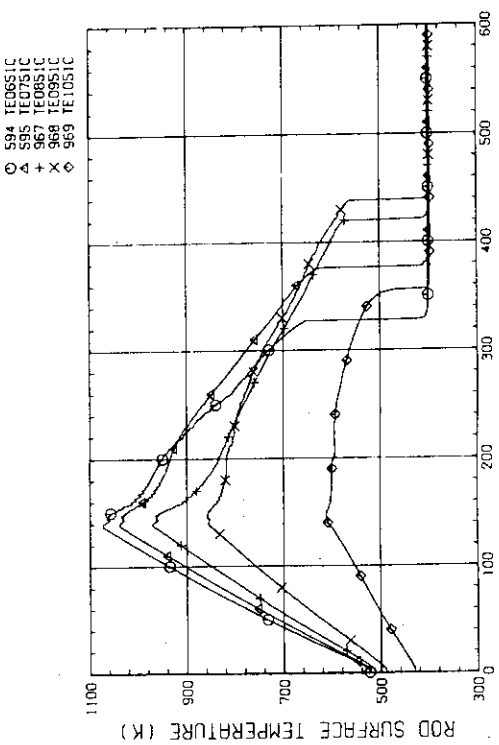
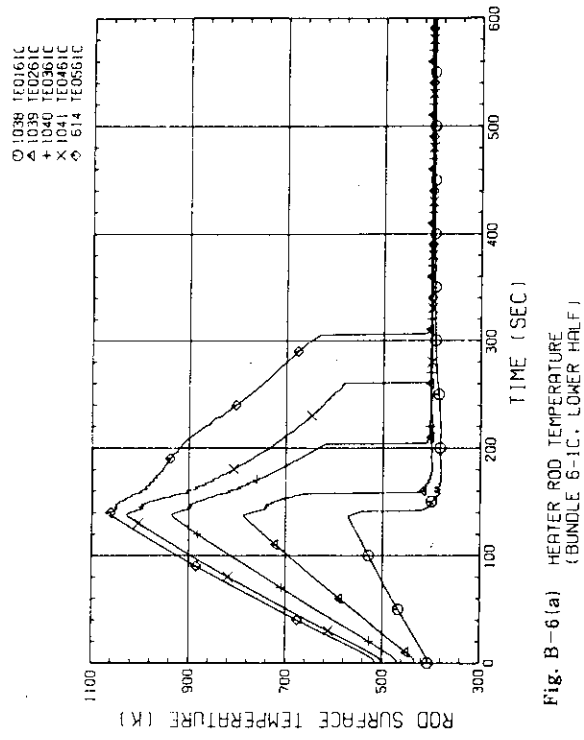
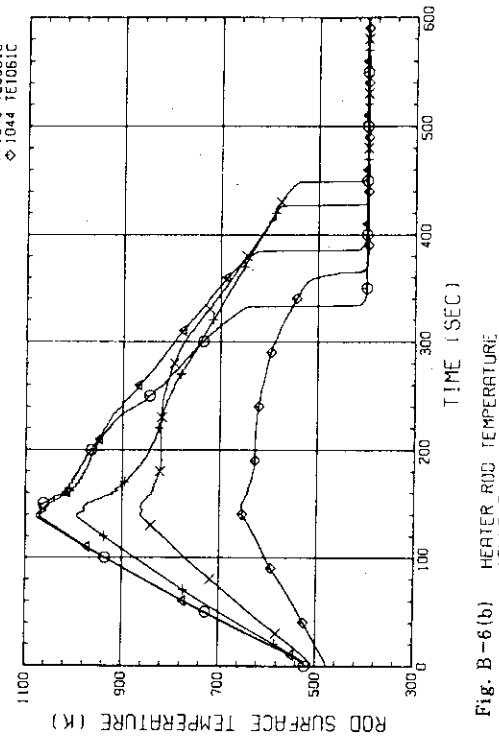


Fig. B-2(b) HEATER ROD TEMPERATURE
(BUNDLE 2-1C, UPPER HALF)

Fig. B-3(a) HEATER ROD TEMPERATURE
(BUNDLE 3-1C, LOWER HALF)Fig. B-3(b) HEATER ROD TEMPERATURE
(BUNDLE 3-1C, UPPER HALF)Fig. B-4(a) HEATER ROD TEMPERATURE
(BUNDLE 4-1C, LOWER HALF)Fig. B-4(b) HEATER ROD TEMPERATURE
(BUNDLE 4-1C, UPPER HALF)

Fig. B-5(a) HEATER ROD TEMPERATURE
(BUNDLE 5-1C, LOWER HALF)Fig. B-5(b) HEATER ROD TEMPERATURE
(BUNDLE 5-1C, UPPER HALF)Fig. B-6(a) HEATER ROD TEMPERATURE
(BUNDLE 6-1C, LOWER HALF)Fig. B-6(b) HEATER ROD TEMPERATURE
(BUNDLE 6-1C, UPPER HALF)

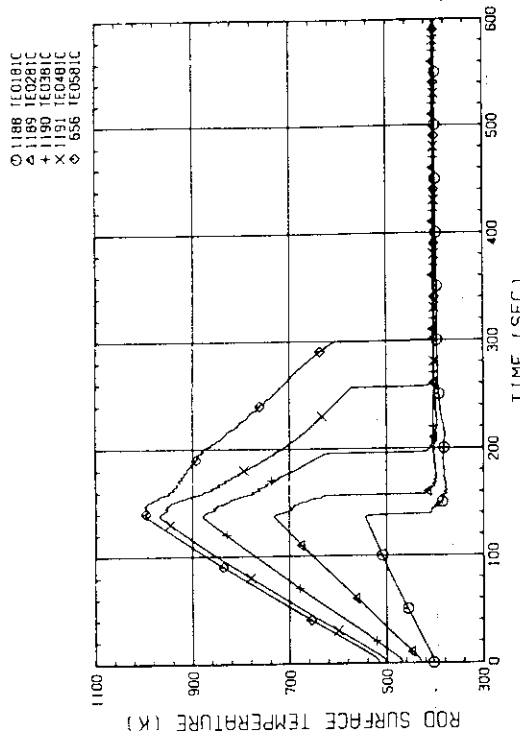


Fig. B-7(a) HEATER ROD TEMPERATURE
(BUNDLE 7-1C, LOWER HALF)

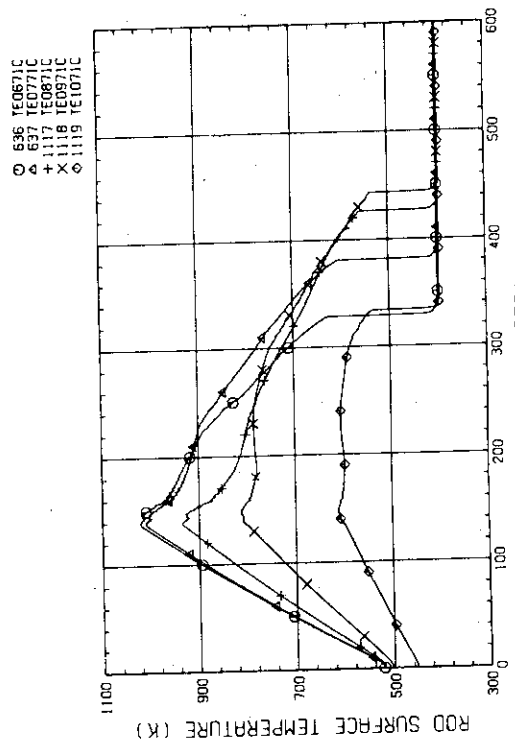


Fig. B-7(b) HEATER ROD TEMPERATURE
(BUNDLE 7-1C, UPPER HALF)

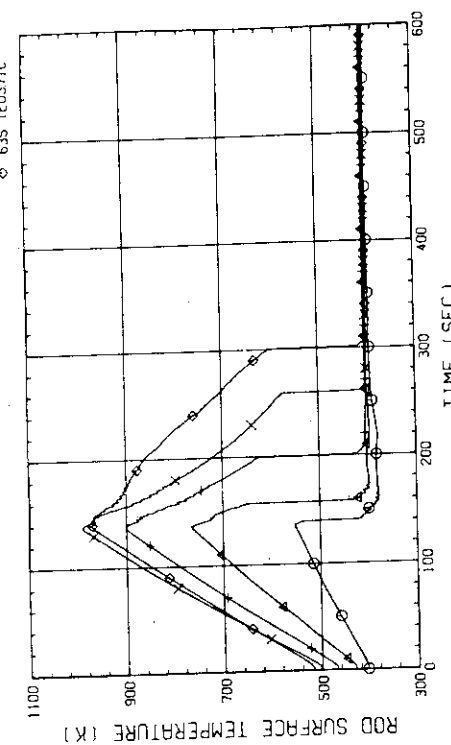


Fig. B-8(a) HEATER ROD TEMPERATURE
(BUNDLE 8-1C, LOWER HALF)

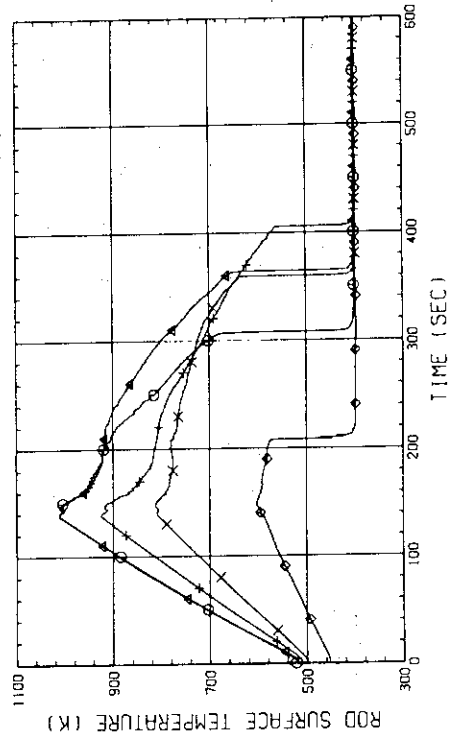


Fig. B-8(b) HEATER ROD TEMPERATURE
(BUNDLE 8-1C, UPPER HALF)

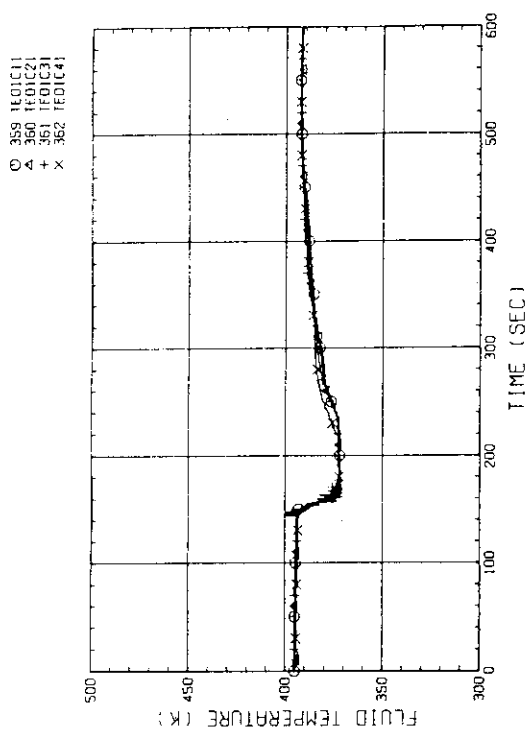


Fig. B-9(a) FLUID TEMPERATURE AT CORE INLET
(BUNDLE 1.2.3.4, 100MM BELOW HEATED PART)

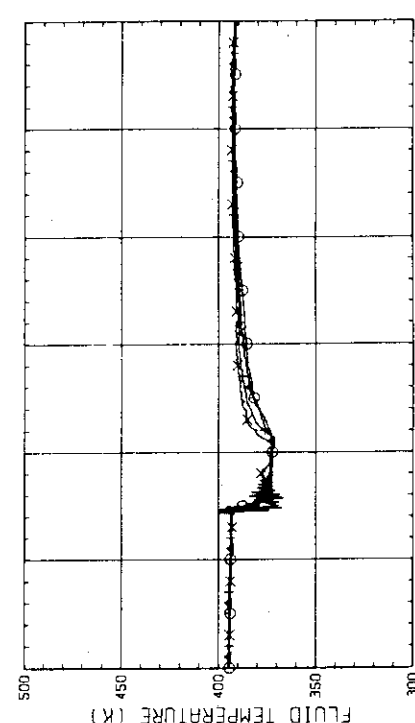


Fig. B-9(b) FLUID TEMPERATURE AT CORE INLET
(BUNDLE 5, 6, 7, 8, 100MM BELOW HEATED PART)

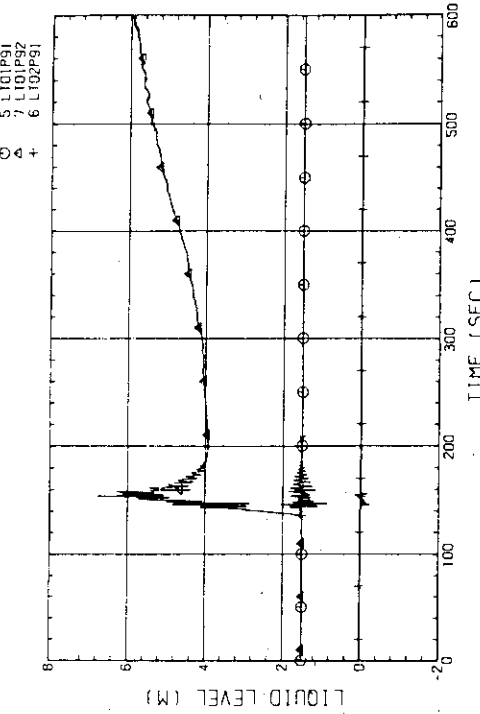
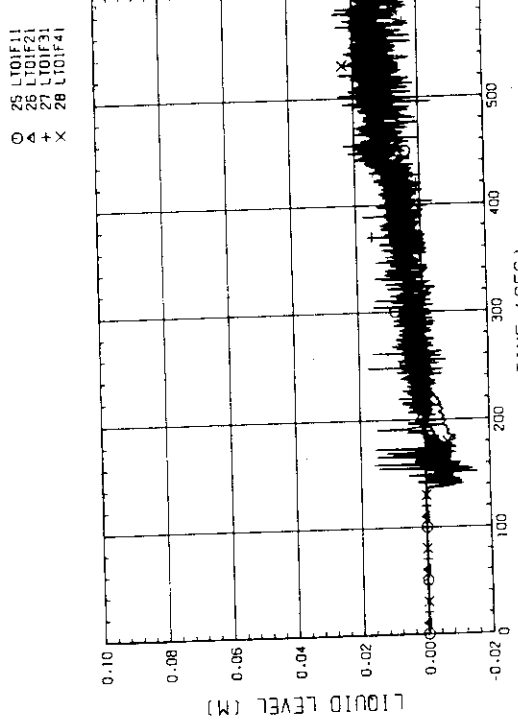
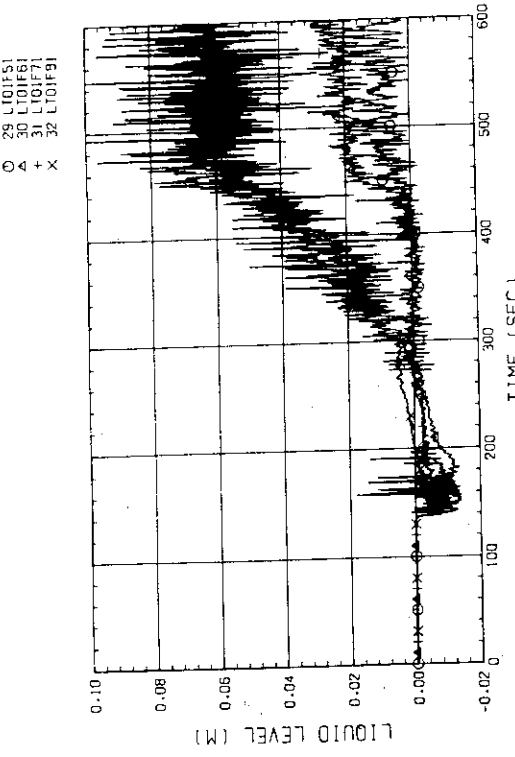
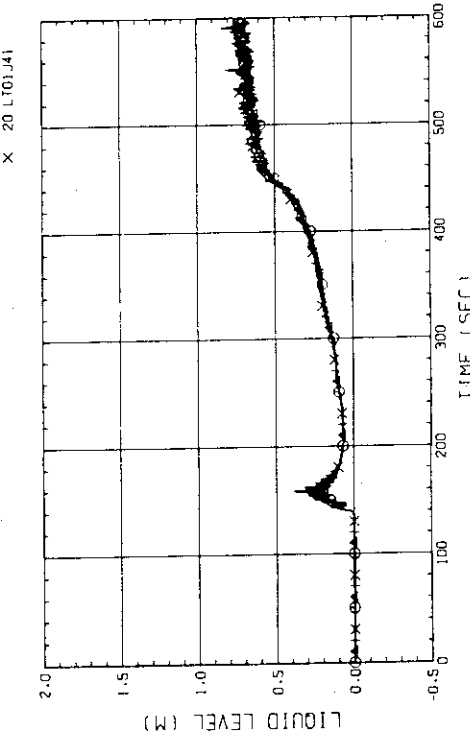
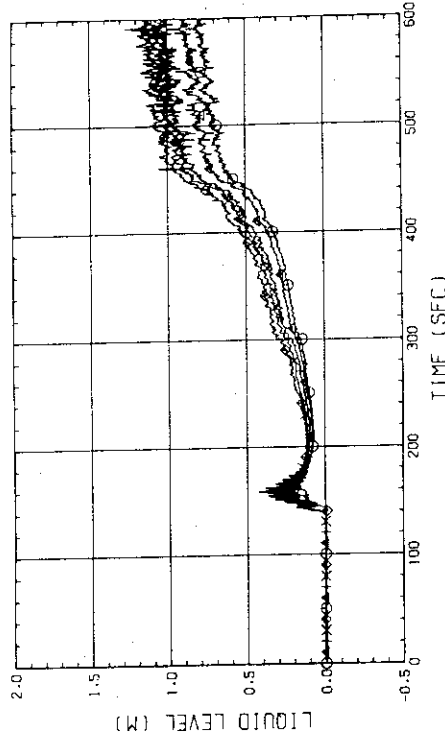


Fig. B-10 LIQUID LEVEL IN DOWNCOMER (01P91-BELOW CORE INLET,
01P92-BOTTOM TO COLD LEG, 02P91-COLD LEG TO TOP OF PV)

Fig. B-11(a) LIQUID LEVEL ABOVE END BOX TIE PLATE
(BUNDLE 1,2,3,4)Fig. B-11(b) LIQUID LEVEL ABOVE END BOX TIE PLATE
(BUNDLE 5,6,7,8)Fig. B-12(a) LIQUID LEVEL ABOVE UCSP
(BUNDLE 1,2,3,4)Fig. B-12(b) LIQUID LEVEL ABOVE UCSP
(BUNDLE 5,6,7,8)

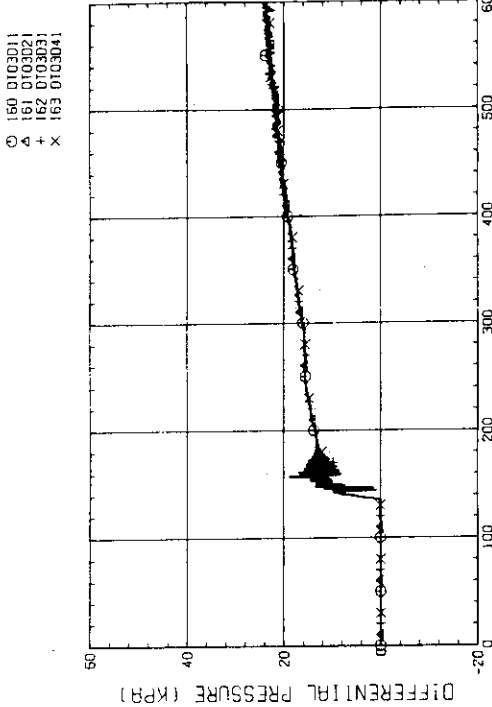


Fig. B-13(a) DIFFERENTIAL PRESSURE OF CORE FULL HEIGHT
(BUNDLE 1,2,3,4)

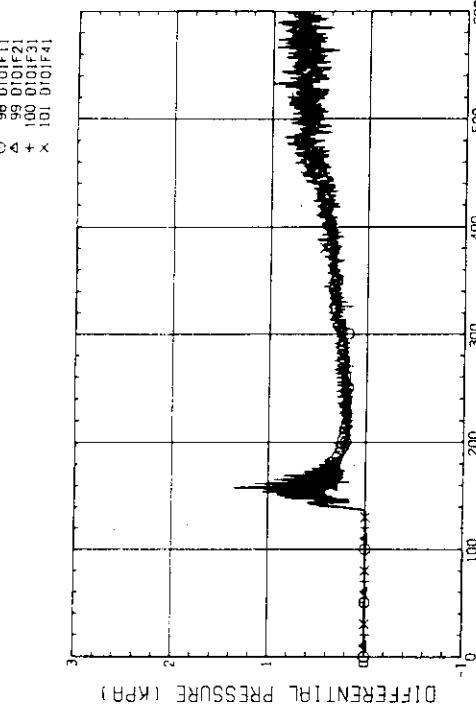


Fig. B-14(a) DIFFERENTIAL PRESSURE ACROSS END BOX TIE PLATE
(BUNDLE 1,2,3,4)

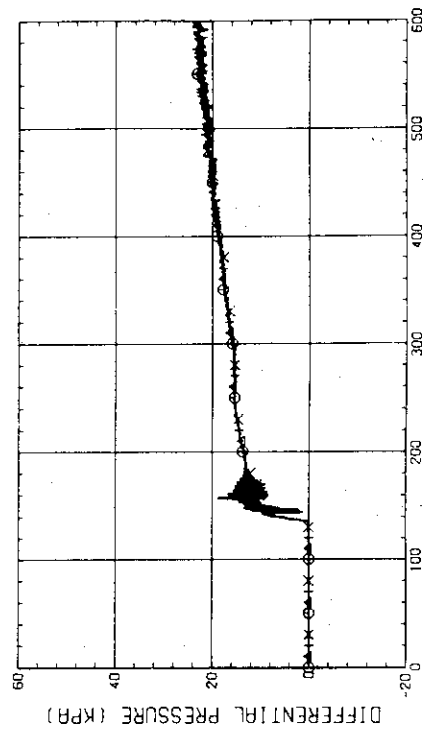


Fig. B-13(b) DIFFERENTIAL PRESSURE OF CORE FULL HEIGHT
(BUNDLE 5,6,7,8)

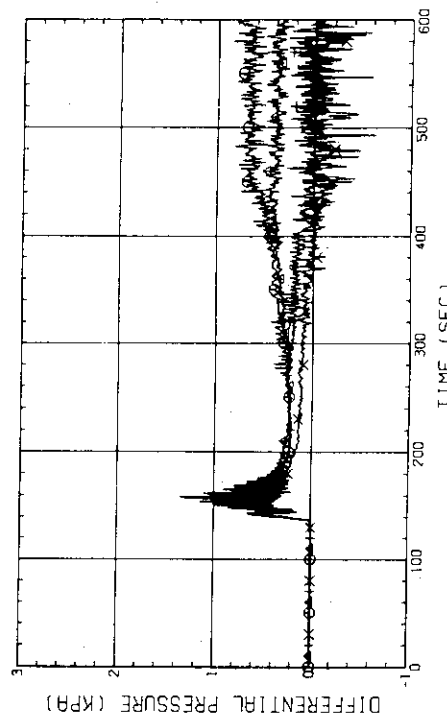


Fig. B-14(b) DIFFERENTIAL PRESSURE ACROSS END BOX TIE PLATE
(BUNDLE 5,6,7,8)

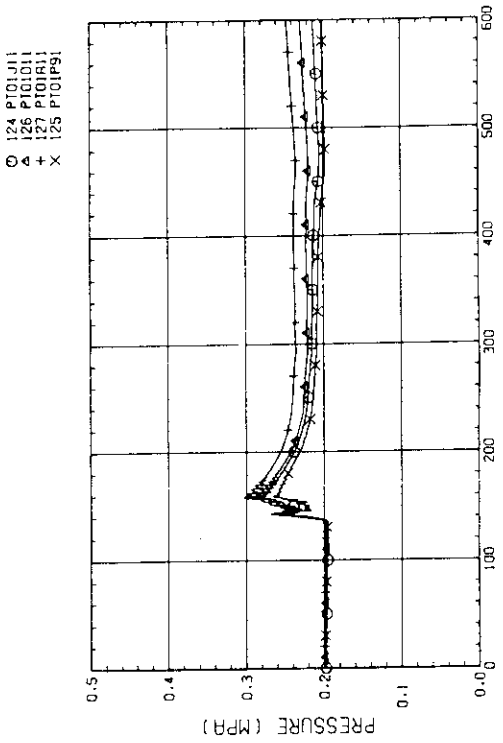


Fig. B-16. PRESSURE IN PV (J - TOP OF PV, D - CORE CENTER, A - CORE INLET, P - BELOW COLD LEG NOZZLE IN DOWNCOMER)

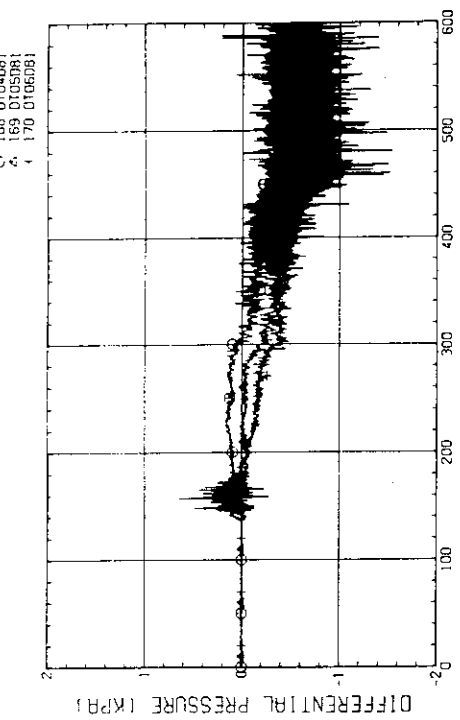


Fig. B-15(a) DIFFERENTIAL PRESSURE, HORIZONTAL BUNDLE 5-8 (04-BELOW SPACER 4, 05-BELOW SPACER 6, 06-BELOW END BOX)

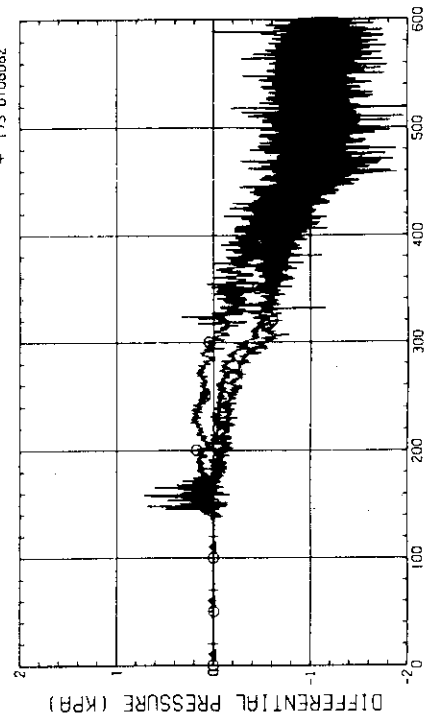


Fig. B-15(b) DIFFERENTIAL PRESSURE, HORIZONTAL BUNDLE 1-8 (04-BELOW SPACER 4, 05-BELOW SPACER 6, 06-BELOW END BOX)

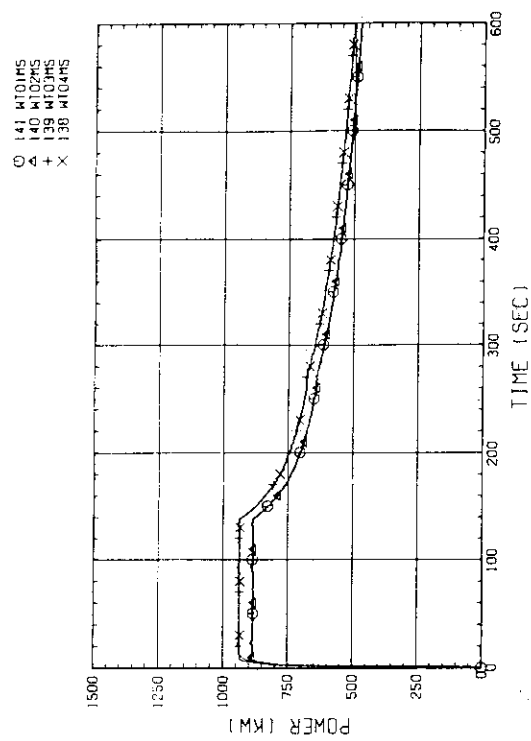


Fig. B-17-(a) BUNDLE POWER
(BUNDLE 1,2,3,4)

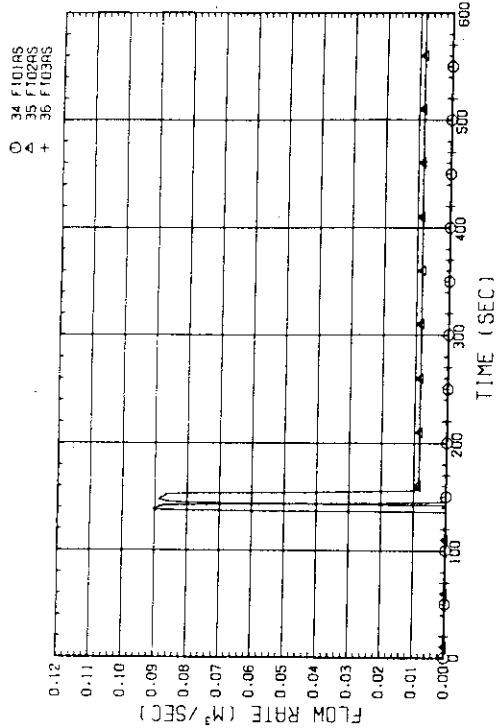
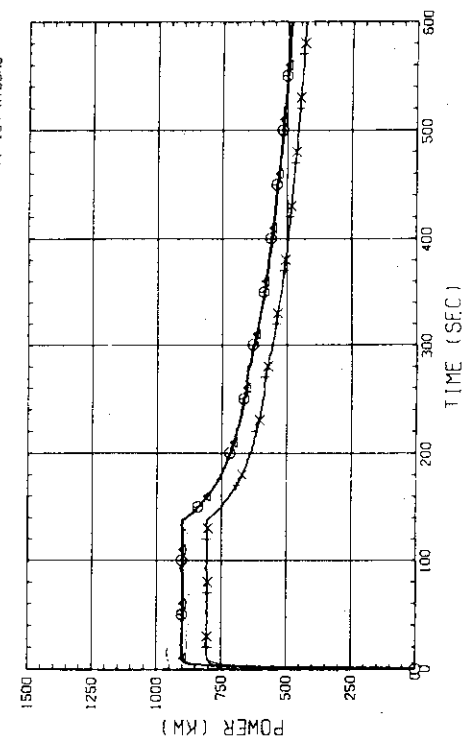


Fig. B-18 FLOW RATE OF ECC WATER (01-DOWNCOMER/LOWER PLENUM/
HOT LEG, 02-INTEGRAL COLD LEG, 03-BROKEN COLD LEG)

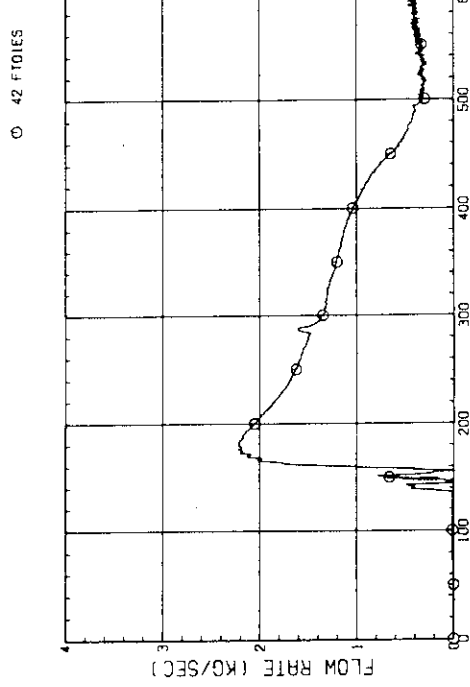


Fig. B-19(c) MASS FLOW RATE FROM CONTAINMENT TANK-1 TO CONTAINMENT TANK-11

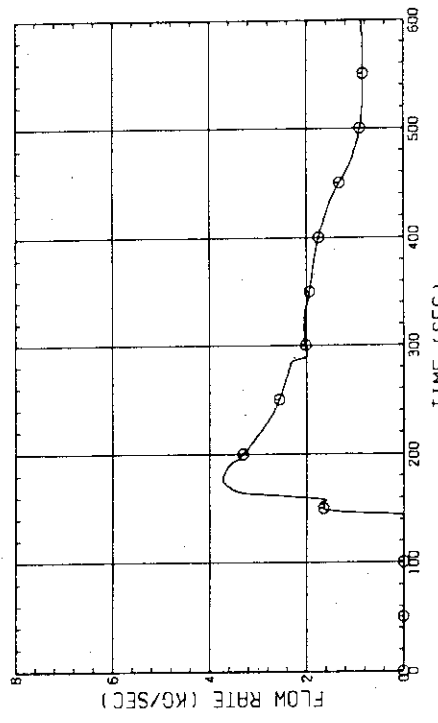


Fig. B-19(e) MASS FLOW RATE FROM CONTAINMENT TANK-1 TO CONTAINMENT TANK-11

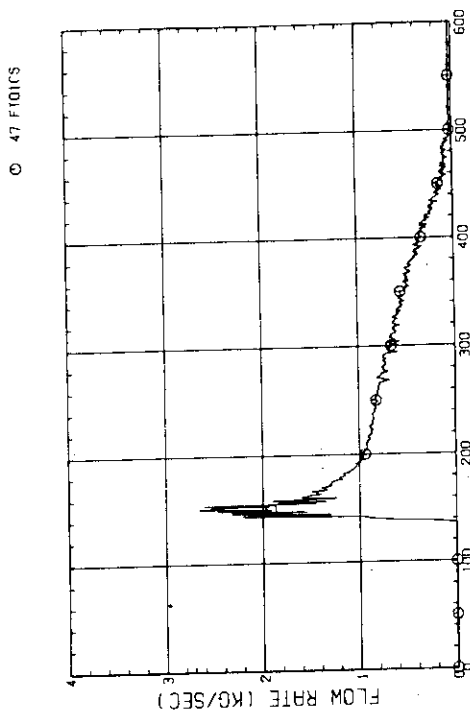


Fig. B-19(a) MASS FLOW RATE OF INTACT COLD LEG

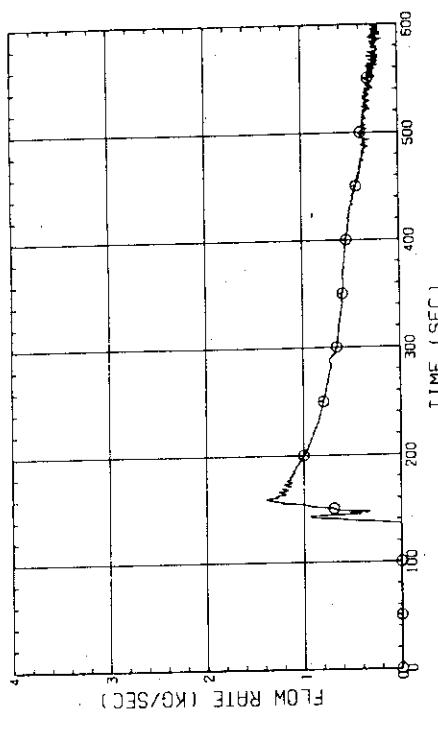


Fig. B-19(b) MASS FLOW RATE OF BROKEN COLD LEG - STEAM/WATER SEPARATOR SIDE

Appendix C

Selected Data for Test S1-15 (Run 521)

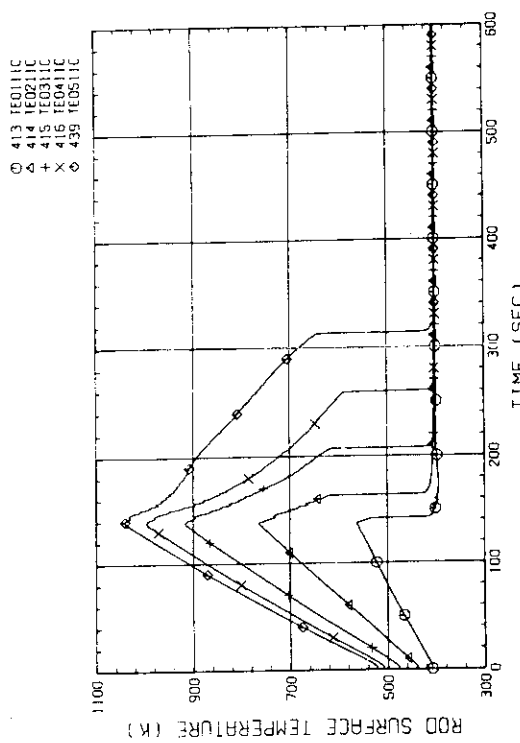


Fig. C-1(a) HEATER ROD TEMPERATURE
(BUNDLE 1-1C, LOWER HALF)

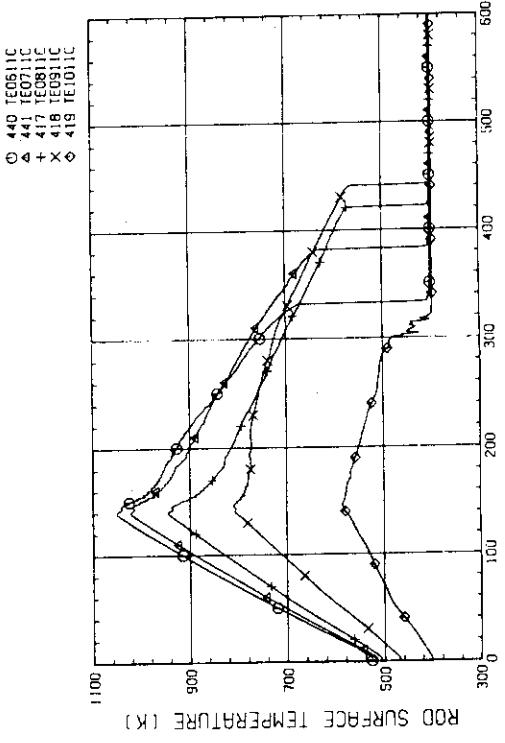


Fig. C-1(b) HEATER ROD TEMPERATURE
(BUNDLE 1-1C, UPPER HALF)

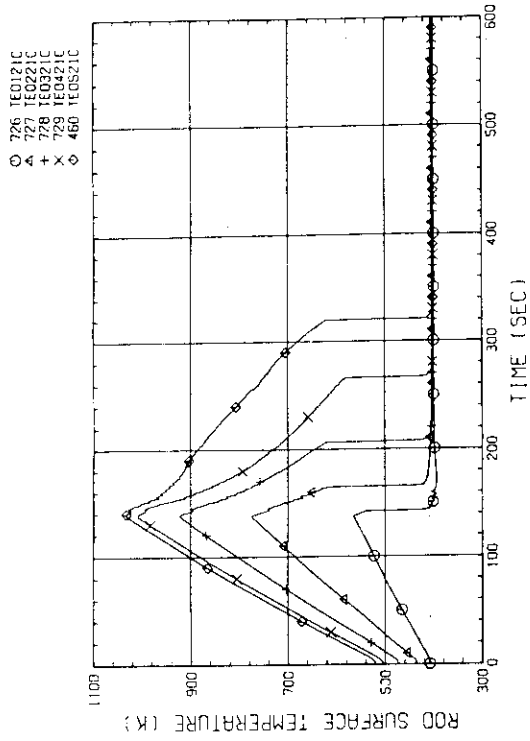


Fig. C-2(a) HEATER ROD TEMPERATURE
(BUNDLE 2-1C, LOWER HALF)

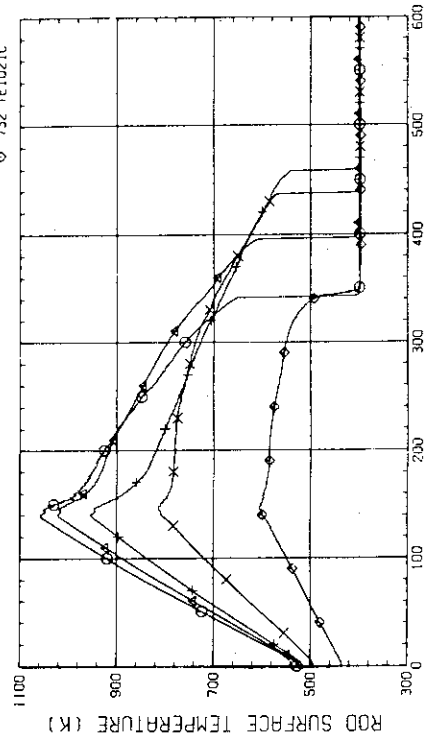


Fig. C-2(b) HEATER ROD TEMPERATURE
(BUNDLE 2-1C, UPPER HALF)

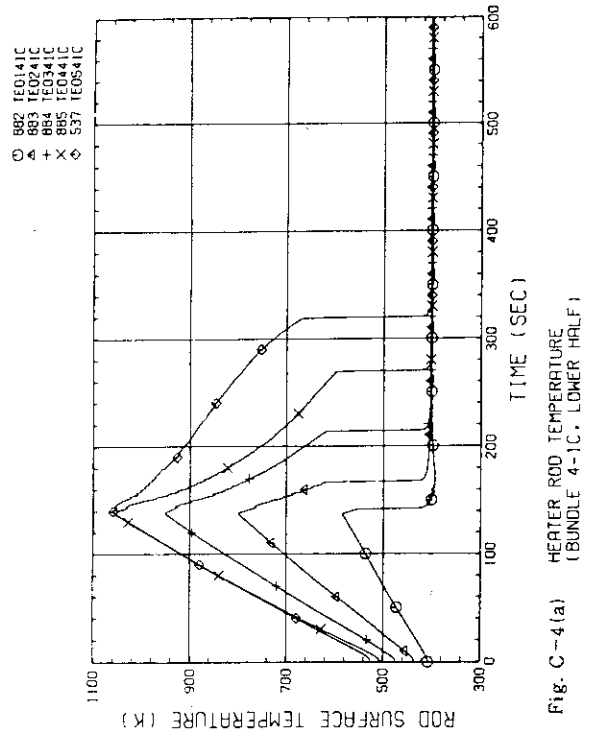


Fig. C-4(a) HEATER ROO TEMPERATURE
(BUNDLE 4-1C, LOWER HALF)

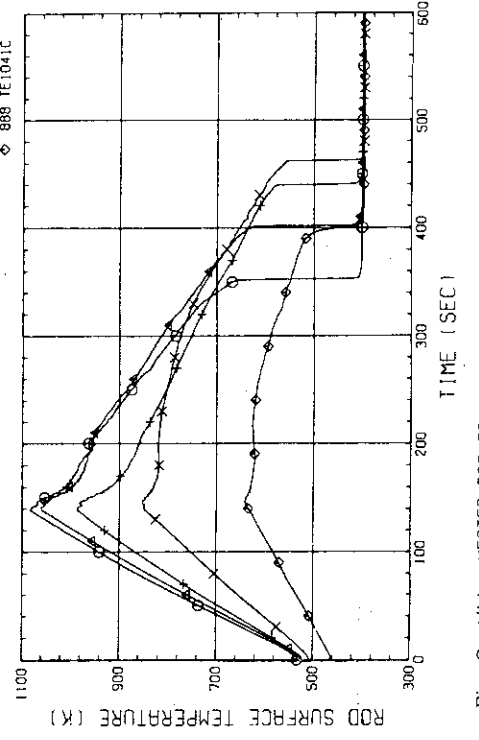


Fig. C-4 (b) HEATER ROD TEMPERATURE
1 BUNDLE 4-1C, UPPER HALF 1

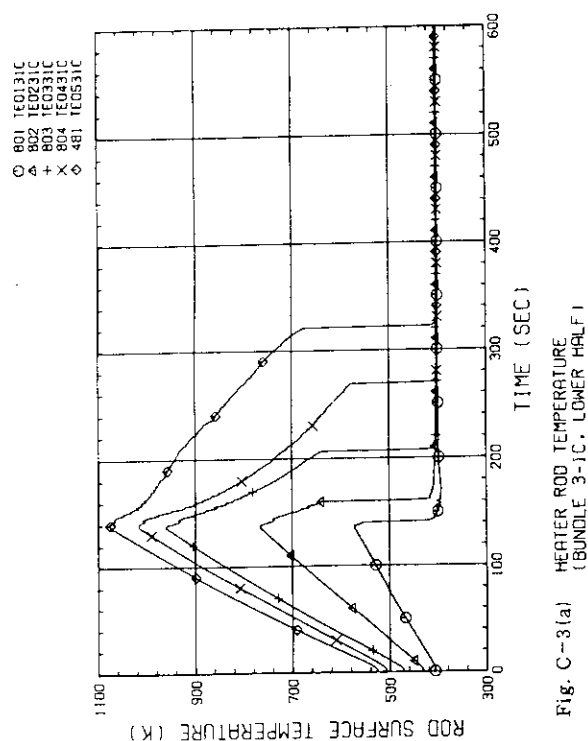


Fig. C-3(a) HEATER ROD TEMPERATURE
(BUNDLE 3-1C, LOWER HALF)

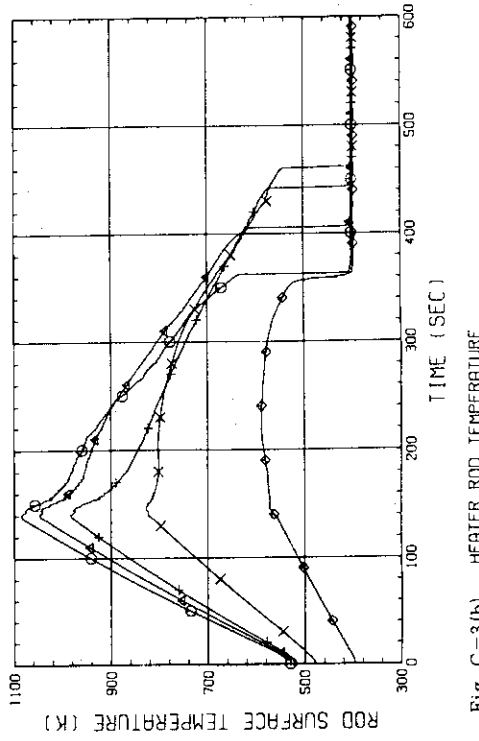


Fig. C-3(b) HEATER ROD TEMPERATURE
(BUNDLE 3-1C, UPPER HALF)

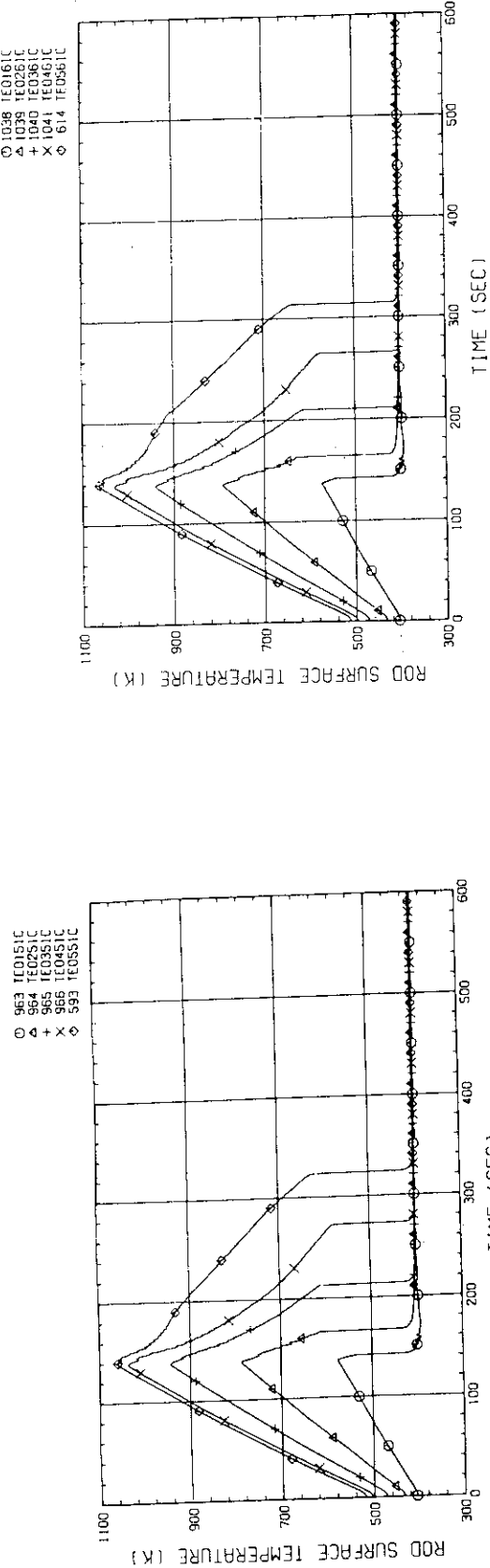


Fig. C-5(a) HEATER ROD TEMPERATURE
(BUNDLE S-1C, LOWER HALF)

- 106 -

Fig. C-6(a) HEATER ROD TEMPERATURE
(BUNDLE 6-1C, LOWER HALF)

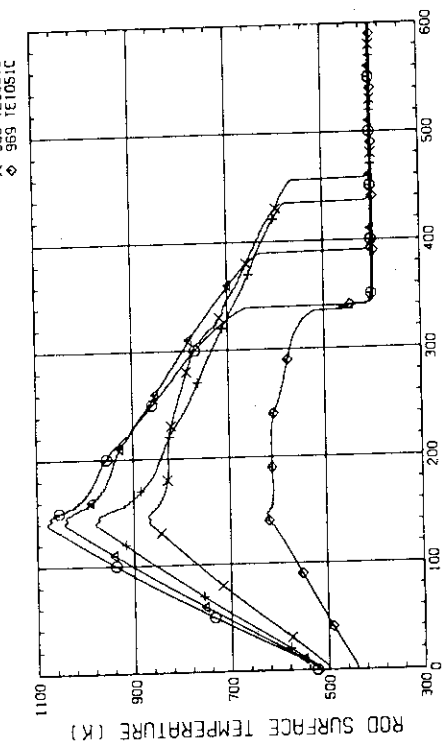


Fig. C-6(b) HEATER ROD TEMPERATURE
(BUNDLE 6-1C, LOWER HALF)

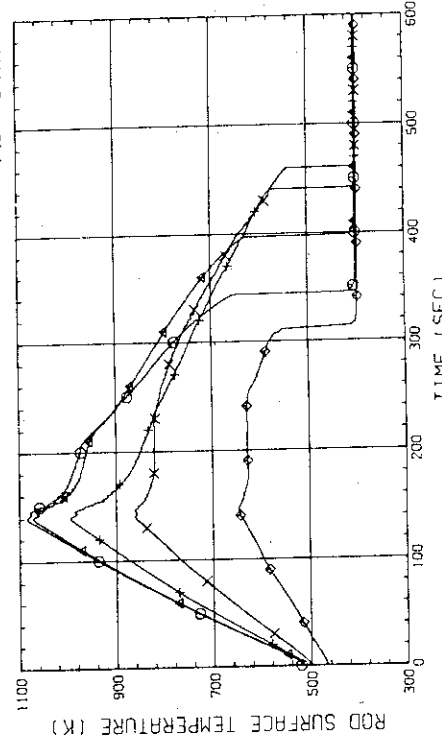
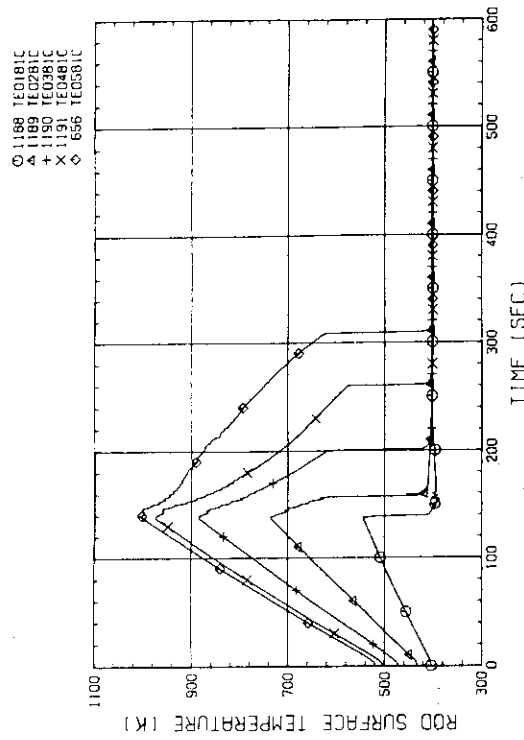
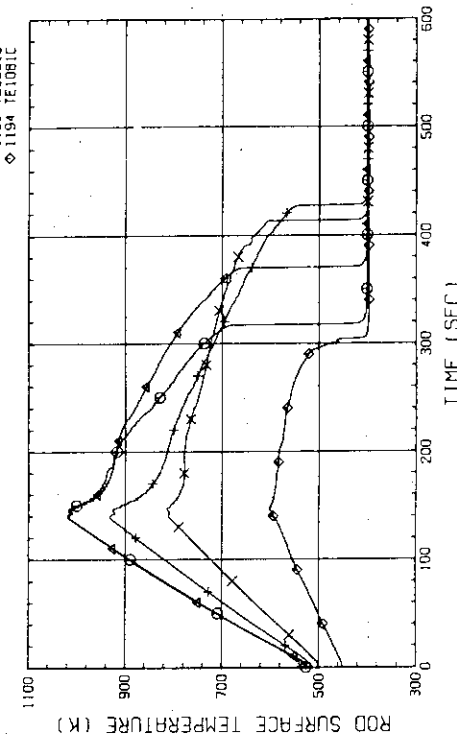
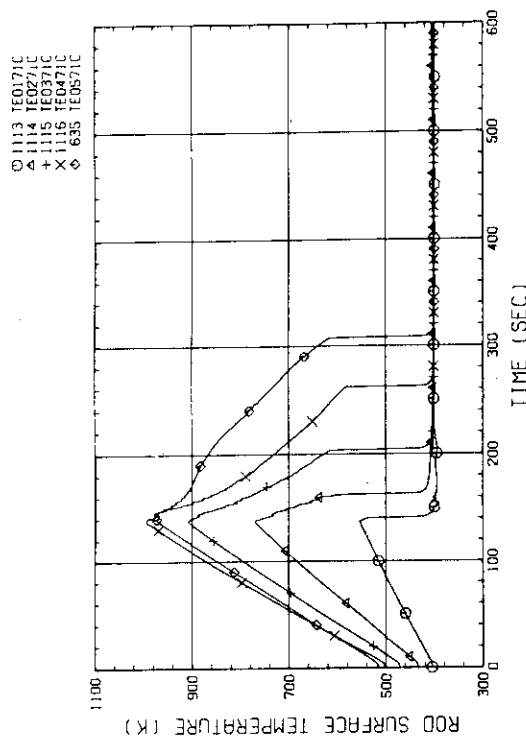
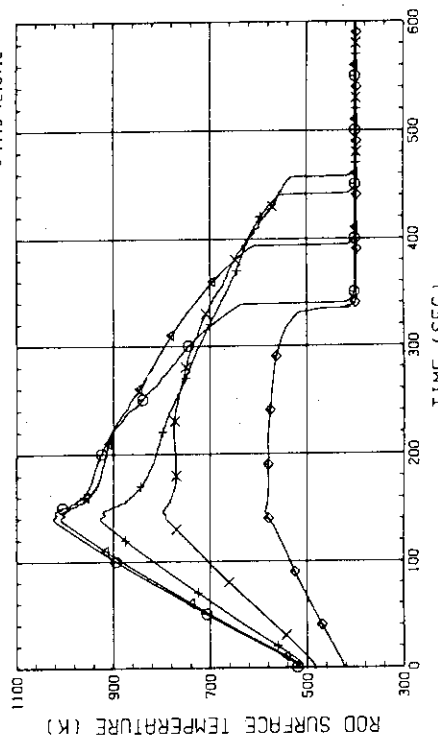


Fig. C-6(b) HEATER ROD TEMPERATURE
(BUNDLE 6-1C, UPPER HALF)

Fig. C-8 (a) HEATER ROD TEMPERATURE
(BUNDLE 8-IC, LOWER HALF)Fig. C-8 (b) HEATER ROD TEMPERATURE
(BUNDLE 8-IC, UPPER HALF)Fig. C-7 (a) HEATER ROD TEMPERATURE
(BUNDLE 7-IC, LOWER HALF)Fig. C-7 (b) HEATER ROD TEMPERATURE
(BUNDLE 7-IC, UPPER HALF)

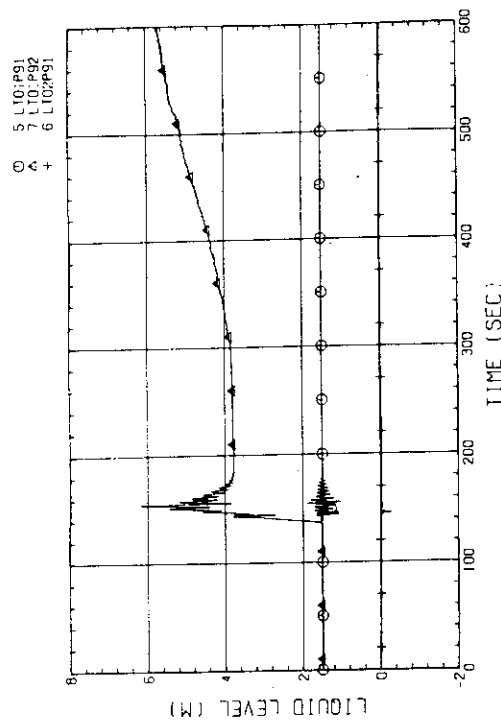


Fig. C-10 LIQUID LEVEL IN DOWNCOMER (10P91) BELOW CORE INLET.
01P92-BOTTOM TO COLD LEG. 02P91-COLD LEG TO TOP OF PV

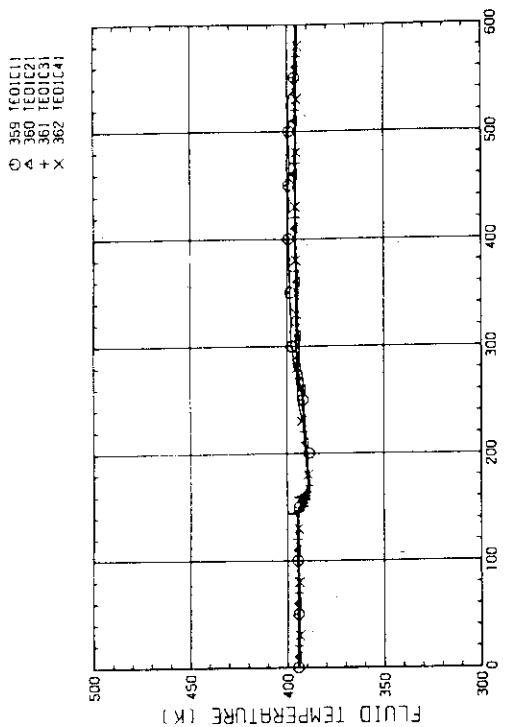


Fig. C-9(a) FLUID TEMPERATURE AT CORE INLET
(BUNDLE 1,2,3,4, 100MM BELOW HEATED PART)

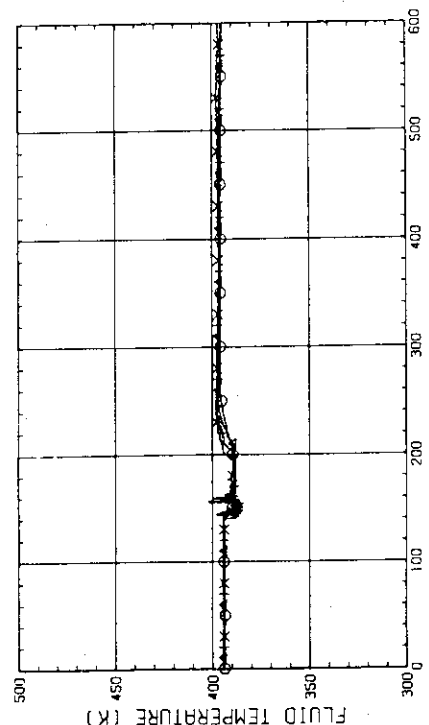


Fig. C-9(b) FLUID TEMPERATURE AT CORE INLET
(BUNDLE 5,6,7,8, 100MM BELOW HEATED PART)

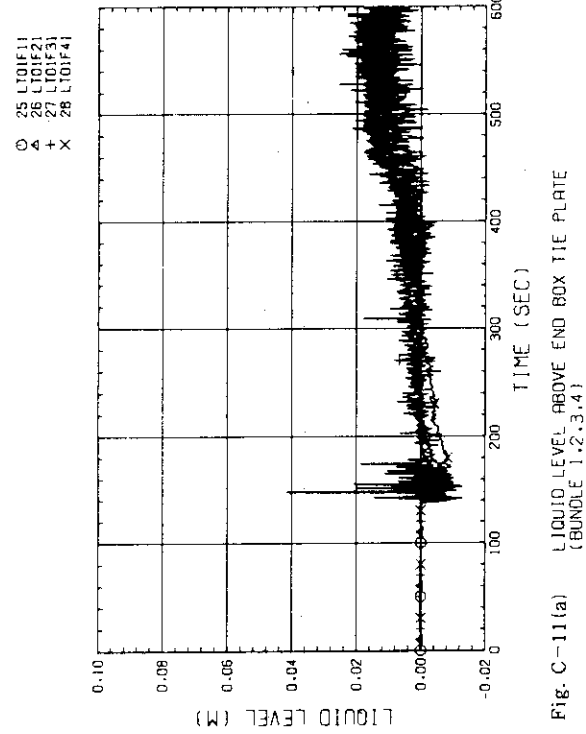


Fig. C-11(a) LIQUID LEVEL ABOVE END BOX TIE PLATE
(BUNDLE 1.2.3.4)

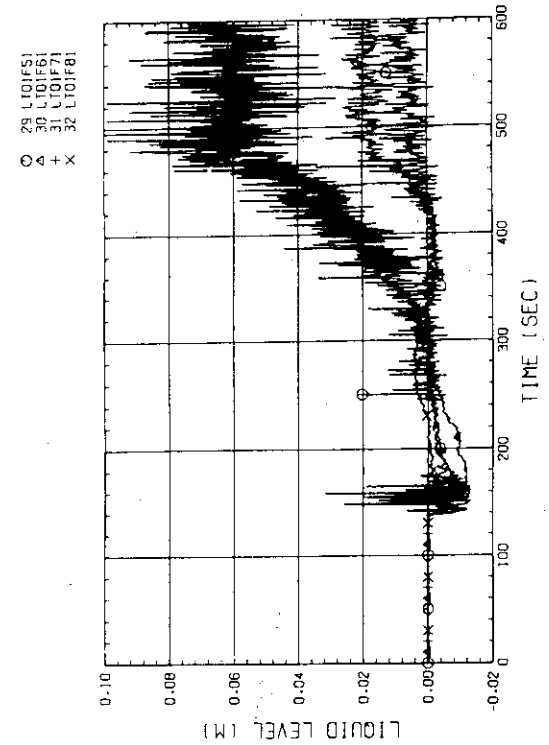


Fig. C-11(b) LIQUID LEVEL ABOVE END BOX TIE PLATE
(BUNDLE 5.6.7.8)

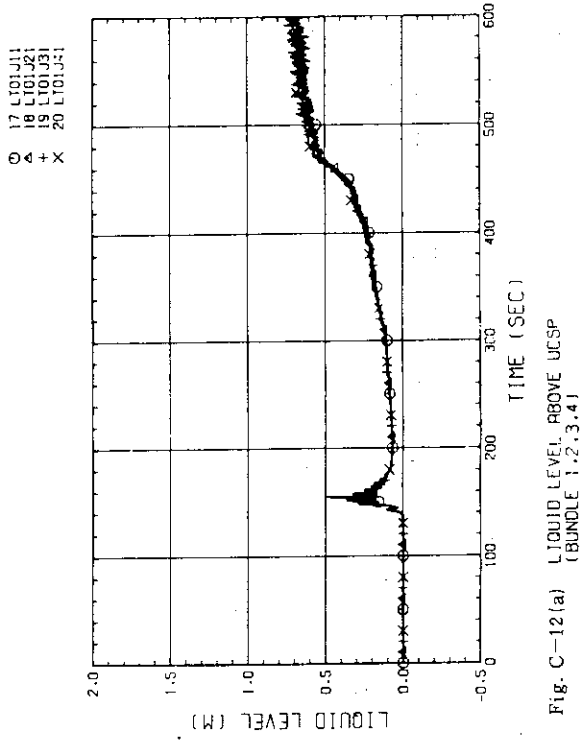


Fig. C-12(a) LIQUID LEVEL ABOVE UCSP
(BUNDLE 1.2.3.4)

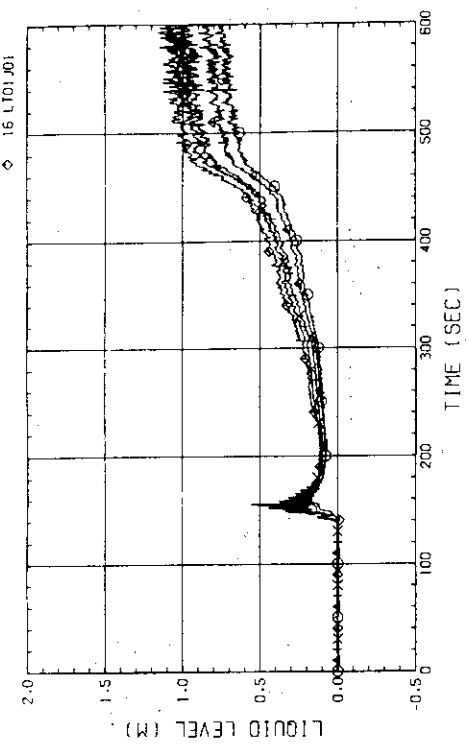


Fig. C-12(b) LIQUID LEVEL ABOVE UCSP
(BUNDLE 5.6.7.8 AND CORE BAFFLE)

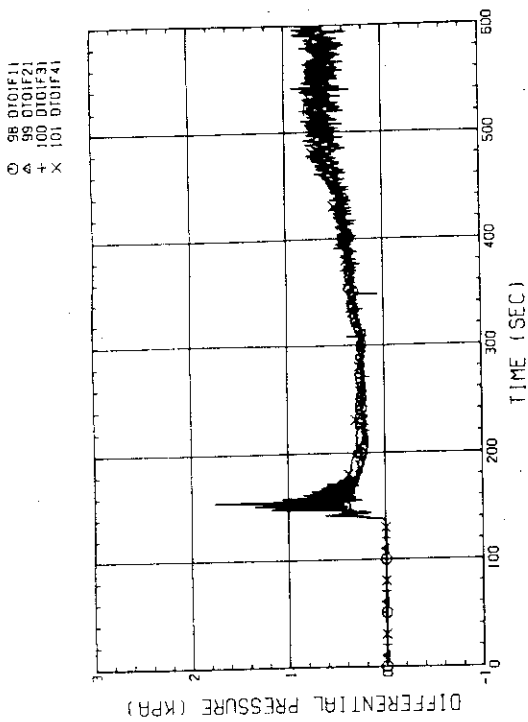


Fig. C-13(a) DIFFERENTIAL PRESSURE OF CORE FULL HEIGHT
(BUNDLE 1,2,3,4)

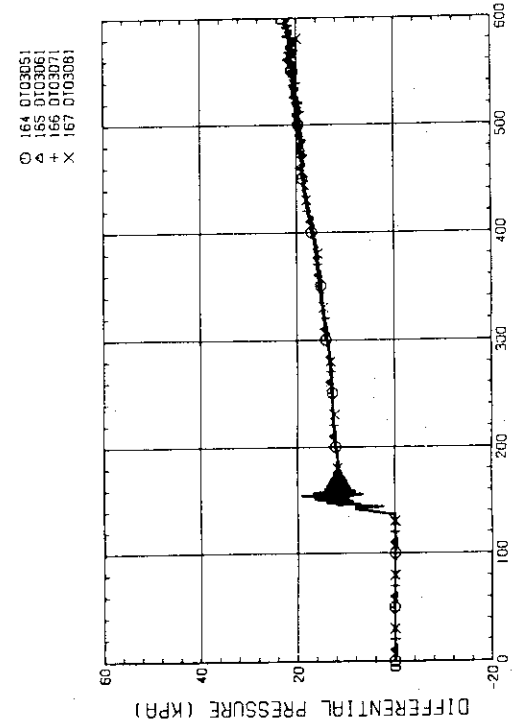


Fig. C-13(b) DIFFERENTIAL PRESSURE OF CORE FULL HEIGHT
(BUNDLE 5,6,7,8)

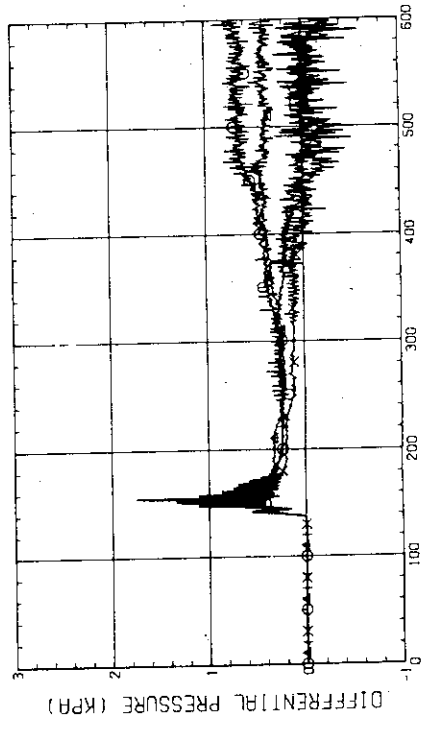


Fig. C-14(a) DIFFERENTIAL PRESSURE ACROSS END BOX TIE PLATE
(BUNDLE 1,2,3,4)



Fig. C-14(b) DIFFERENTIAL PRESSURE ACROSS END BOX TIE PLATE
(BUNDLE 5,6,7,8)

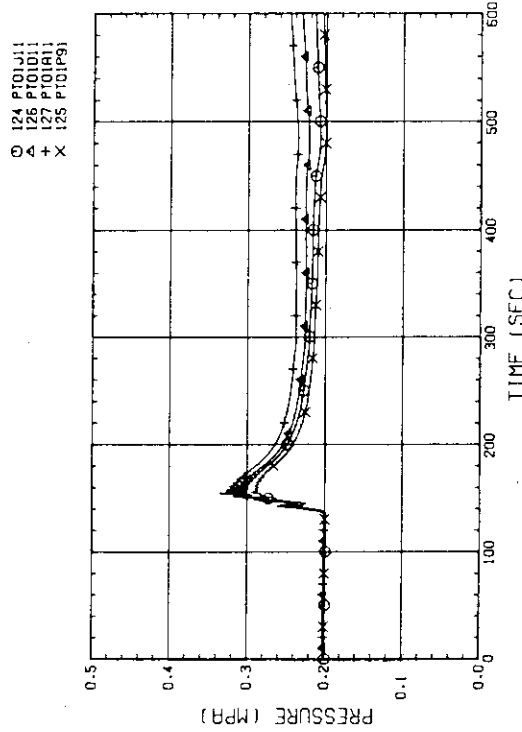


Fig. C-16 PRESSURE IN PV (J - TOP OF PV, O - CORE CENTER, A - CORE INLET, P - BELOW COLD LEG NOZZLE IN DOWNCOMER)

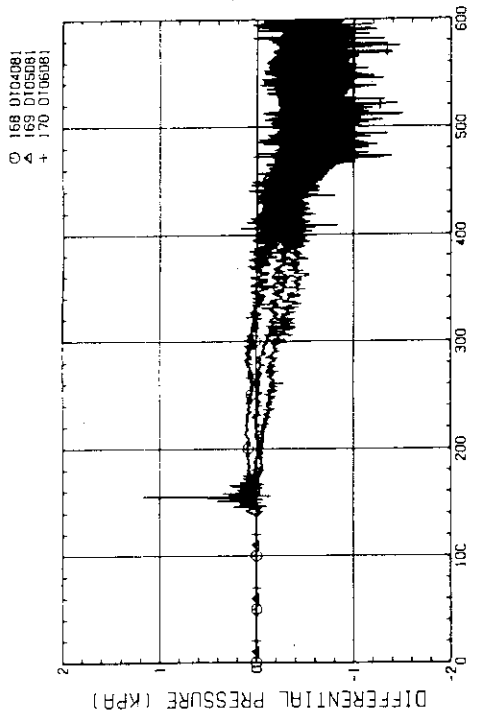


Fig. C-15(a) DIFFERENTIAL PRESSURE, HORIZONTAL BUNDLE 5-8 (04-BELOW SPACER 4, 05-BELOW SPACER 6, 06-BELOW END BOX)

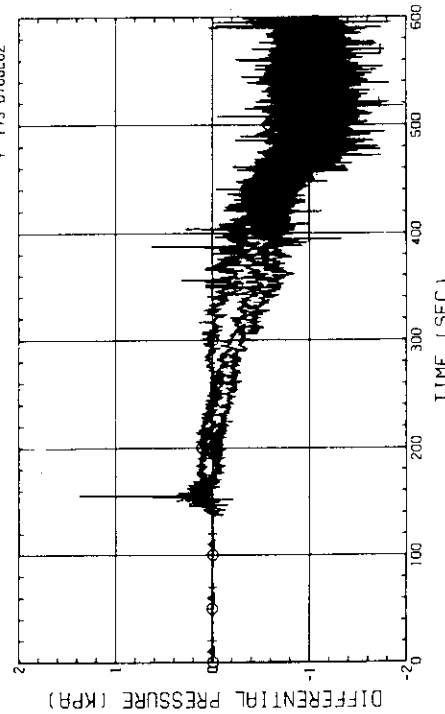


Fig. C-15(b) DIFFERENTIAL PRESSURE, HORIZONTAL BUNDLE 1-8 (04-BELOW SPACER 4, 05-BELOW SPACER 6, 06-BELOW END BOX)

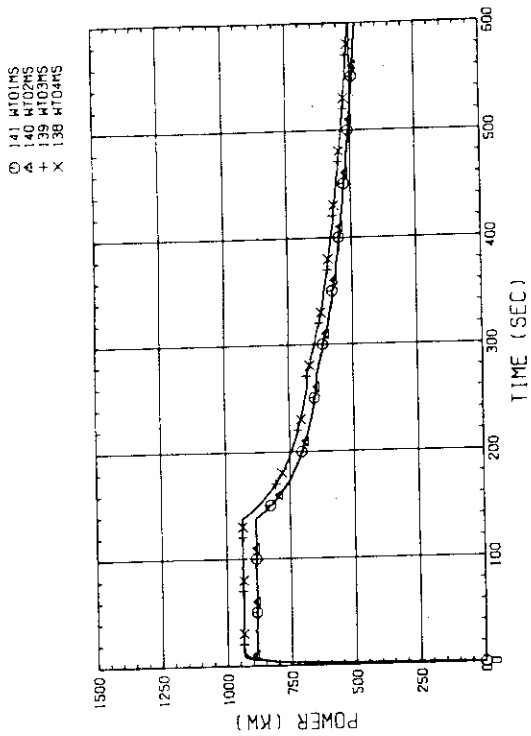


Fig. C-17(a) BUNDLE POWER
(BUNDLE 1.2, 3, 4)

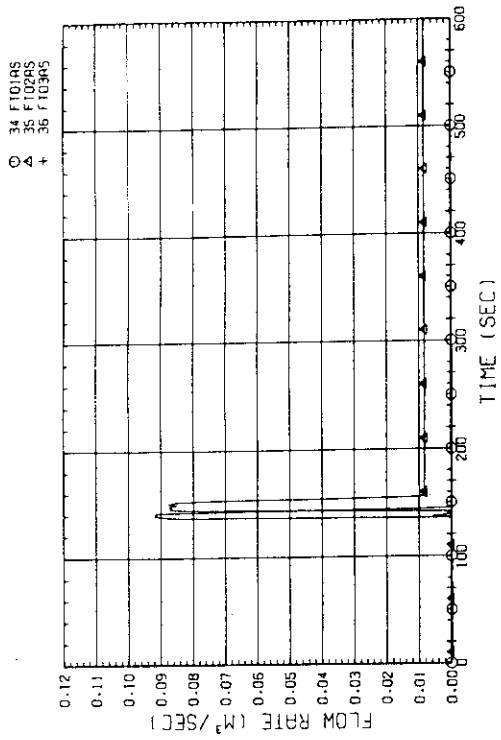
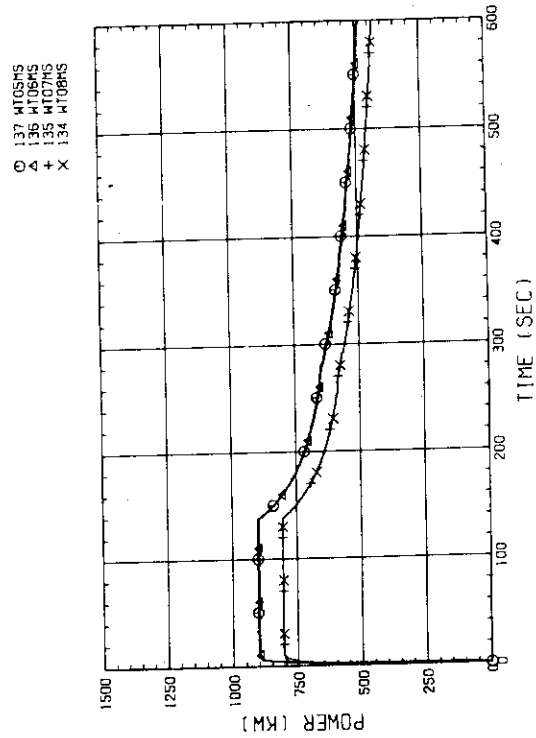


Fig. C-18 FLOW RATE OF ECC WATER 101-DOWNCOMER/LOWER PLENUM/
HOT LEG. 02-INTEGRAL COLD LEG. 03-BROKEN COLD LEG!

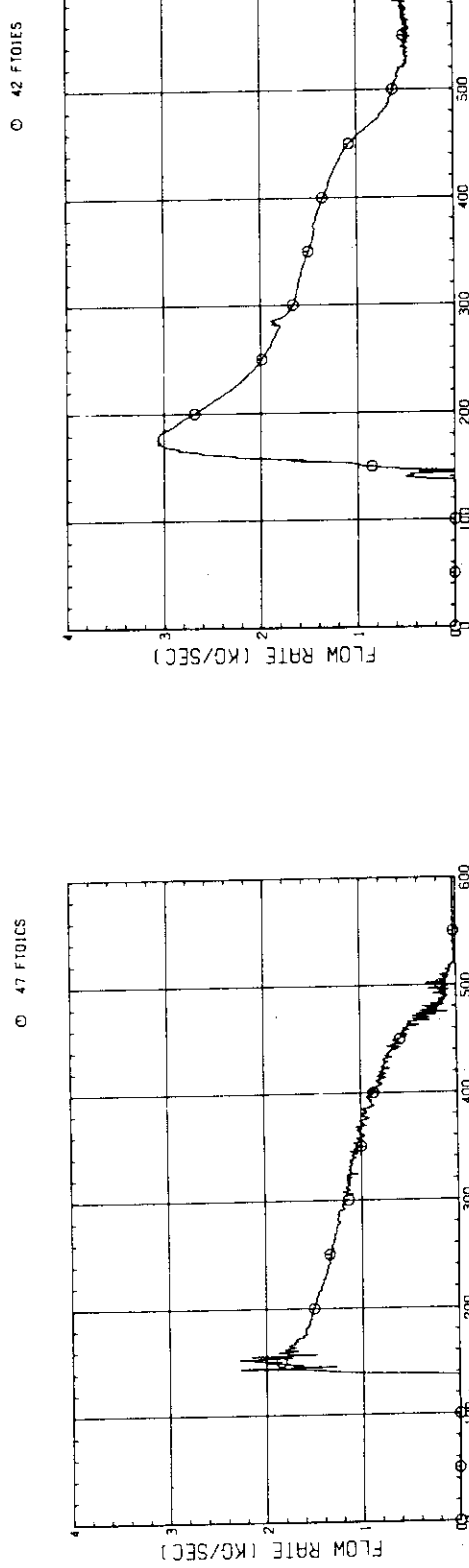


Fig. C-19(a) MASS FLOW RATE OF INTACT COLD LEG

Fig. C-19(c) MASS FLOW RATE FROM CONTAINMENT TANK-1 TO CONTAINMENT TANK-11

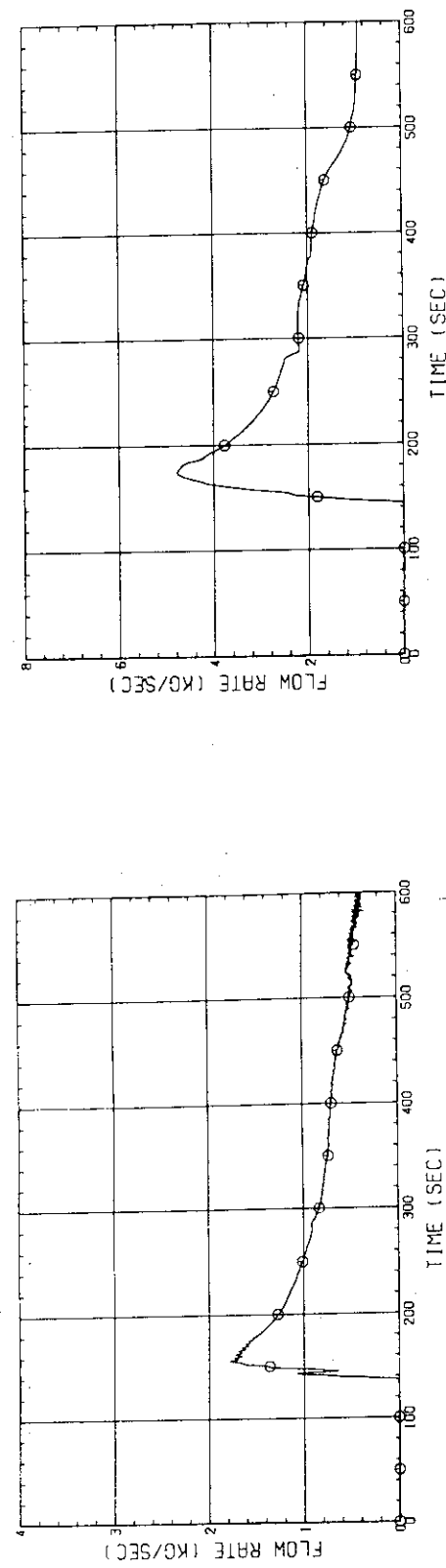


Fig. C-19(b) MASS FLOW RATE OF BROKEN COLD LEG - STEAM/WATER SEPARATOR SIDE

Fig. C-20 STEAM FLOW RATE OF DISCHARGE FROM CONTAINMENT TANK-11

Appendix D

Selected Data for Test S1-16 (Run 522)

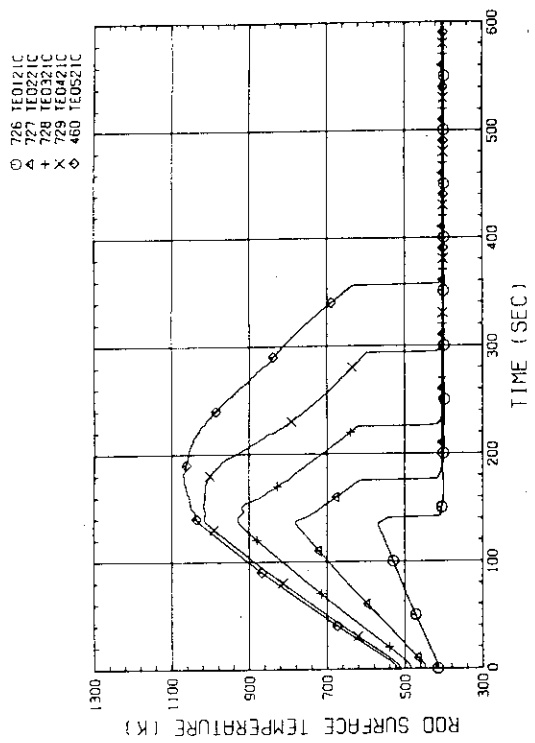


Fig. D-1(a) HEATER ROD TEMPERATURE
(BUNDLE 1-1C, LOWER HALF)

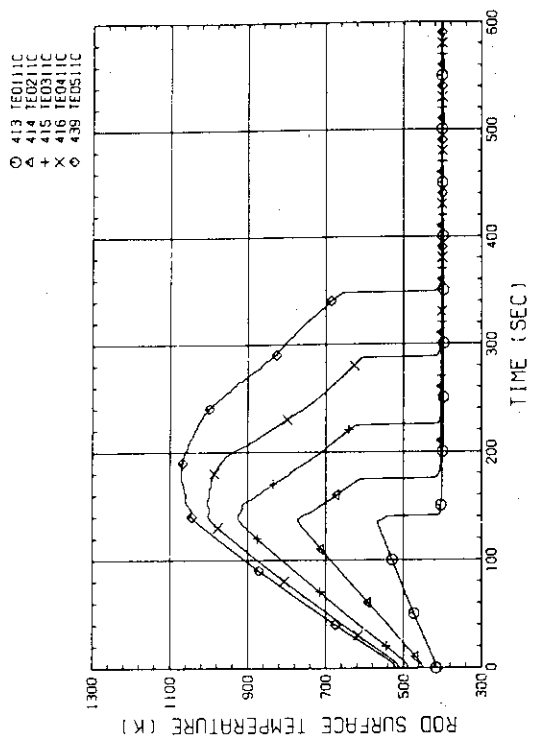


Fig. D-1(b) HEATER ROD TEMPERATURE
(BUNDLE 1-1C, UPPER HALF)

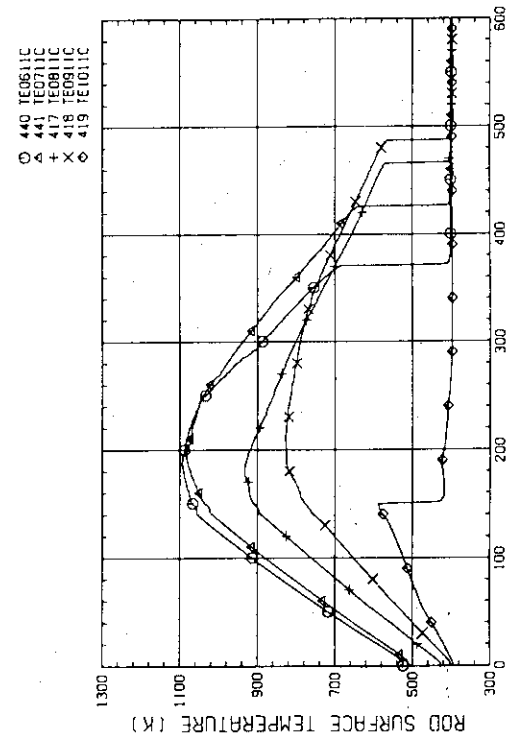


Fig. D-2(a) HEATER ROD TEMPERATURE
(BUNDLE 2-1C, LOWER HALF)

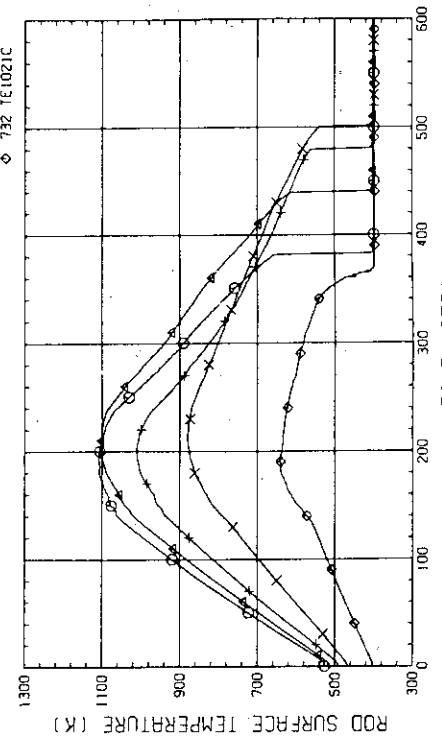


Fig. D-2(b) HEATER ROD TEMPERATURE
(BUNDLE 2-1C, UPPER HALF)

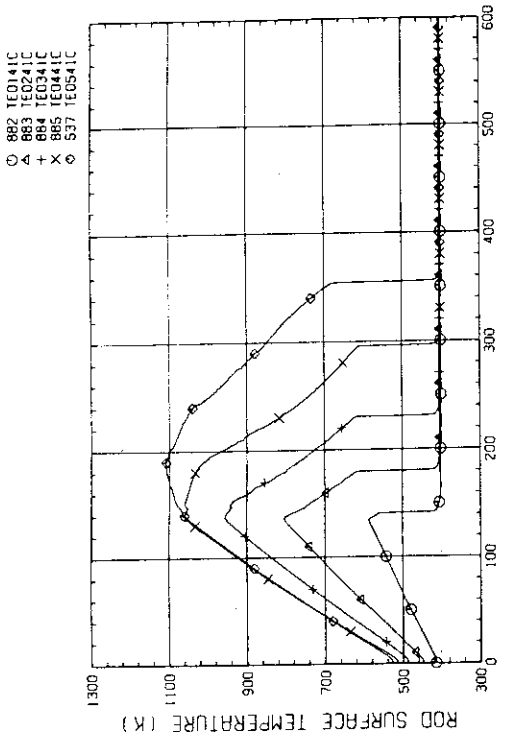


Fig. D-3(a) HEATER ROD TEMPERATURE
(BUNDLE 3-1C, LOWER HALF)

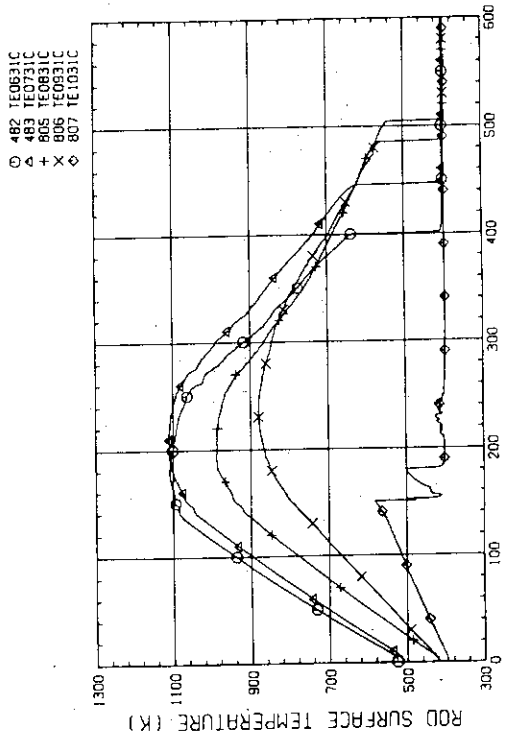


Fig. D-3(b) HEATER ROD TEMPERATURE
(BUNDLE 3-1C, UPPER HALF)

Fig. D-4(a) HEATER ROD TEMPERATURE
(BUNDLE 4-1C, LOWER HALF)

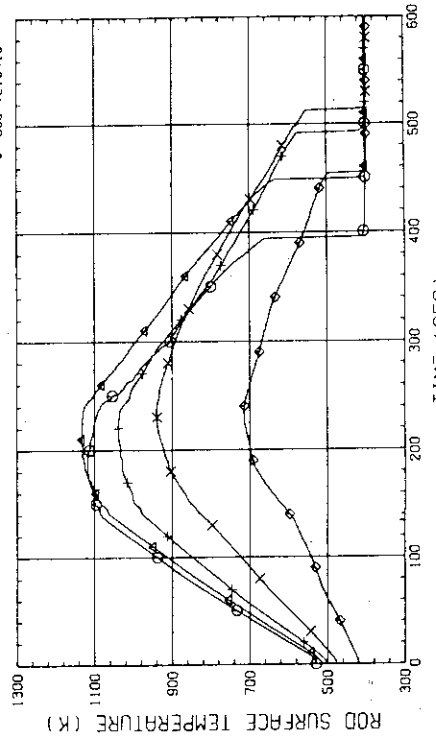


Fig. D-4(b) HEATER ROD TEMPERATURE
(BUNDLE 4-1C, UPPER HALF)

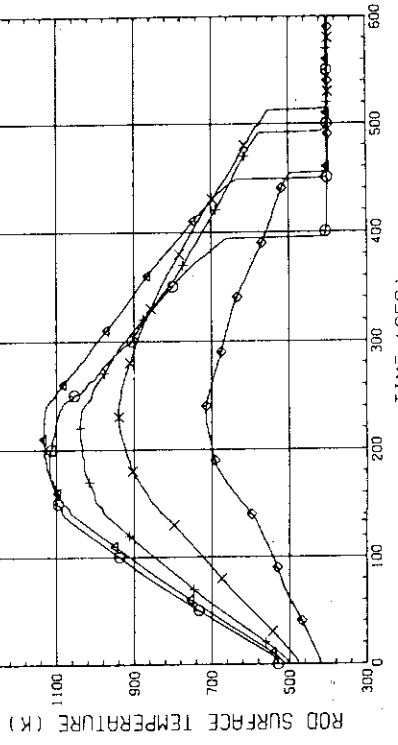


Fig. D-4(b) HEATER ROD TEMPERATURE
(BUNDLE 4-1C, UPPER HALF)

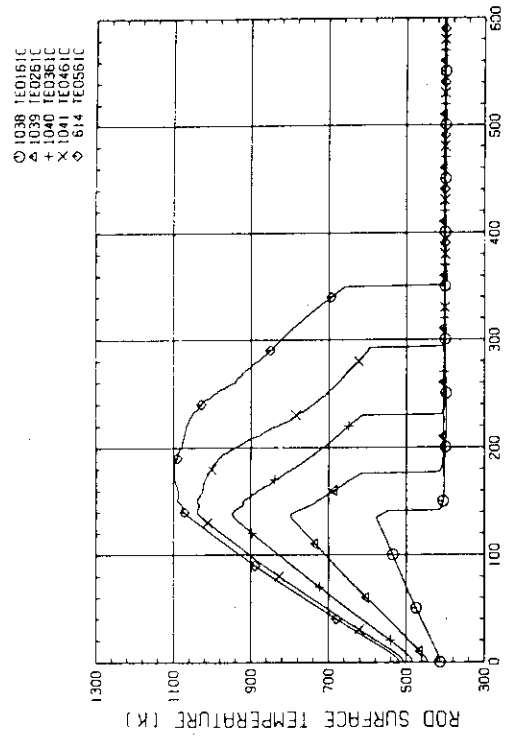


Fig. D-5(a) HEATER ROD TEMPERATURE
(BUNDLE S-1C, LOWER HALF)

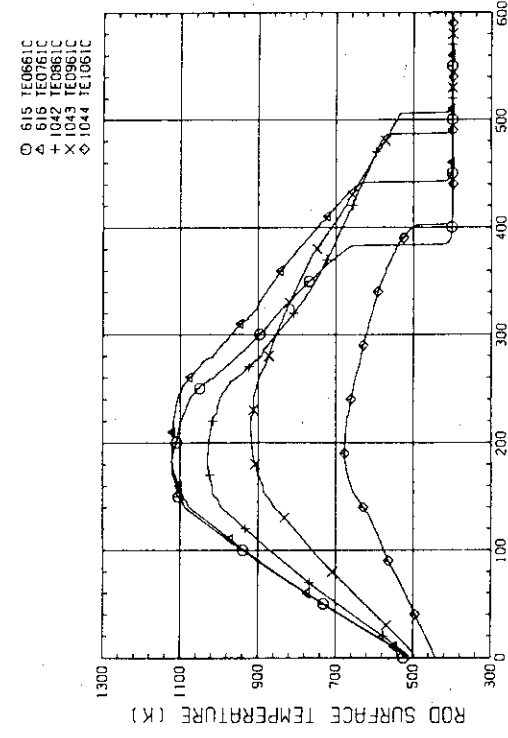


Fig. D-6(a) HEATER ROD TEMPERATURE
(BUNDLE 6-1C, LOWER HALF)

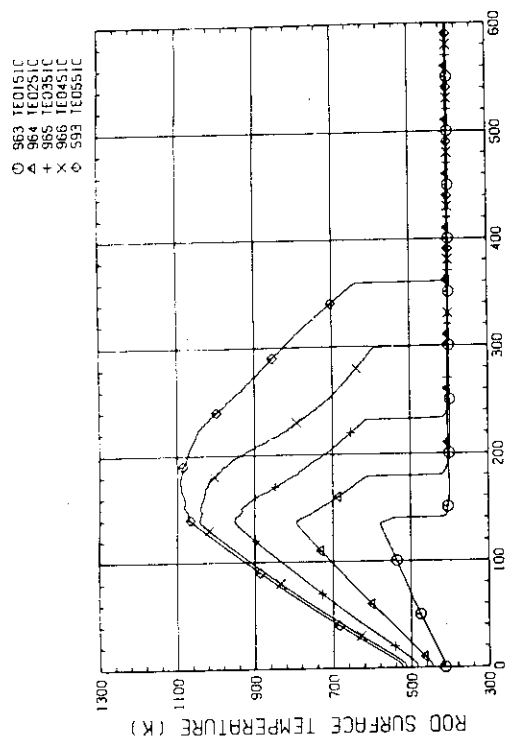


Fig. D-5(b) HEATER ROD TEMPERATURE
(BUNDLE S-1C, UPPER HALF)

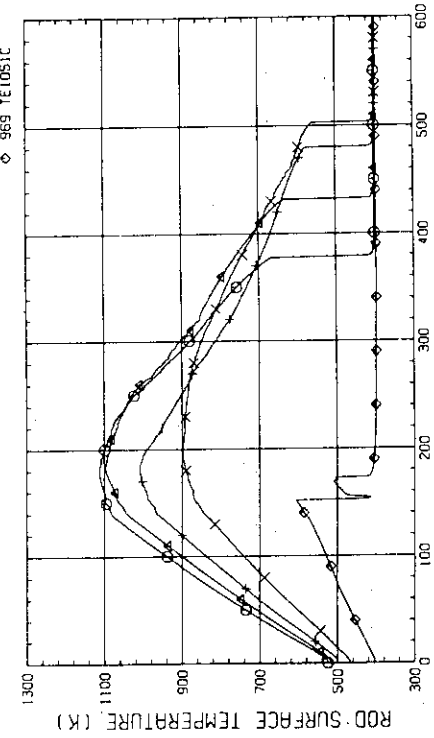


Fig. D-6(b) HEATER ROD TEMPERATURE
(BUNDLE 6-1C, UPPER HALF)

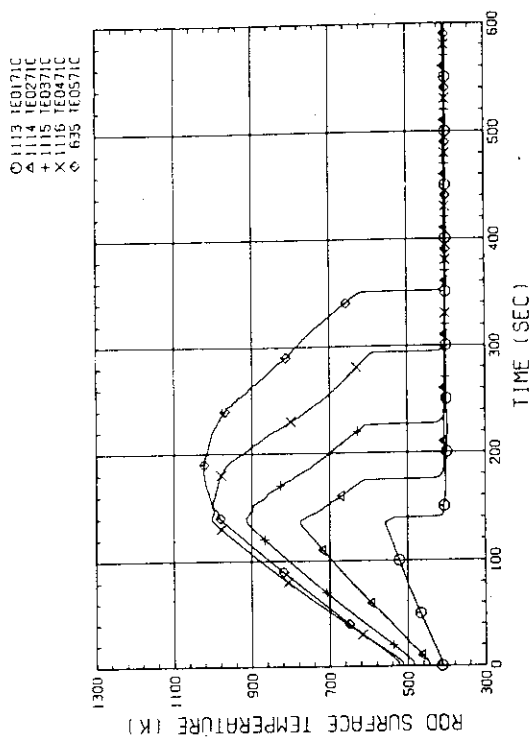


Fig. D-7(a) HEATER ROD TEMPERATURE
(BUNDLE 7-IC, LOWER HALF)

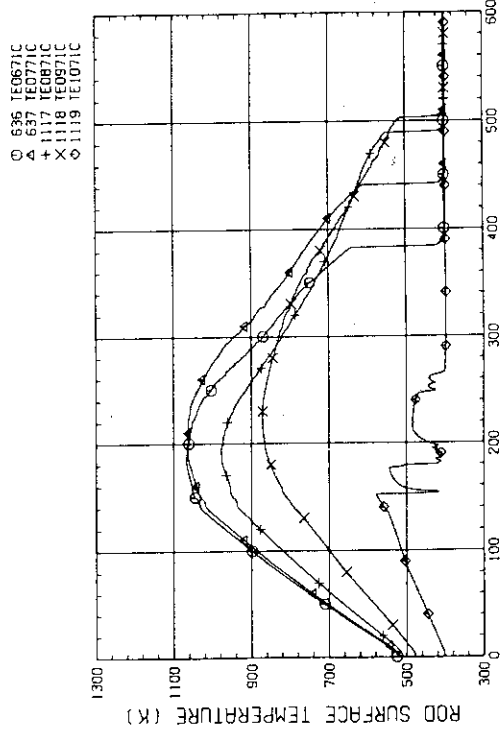


Fig. D-7(b) HEATER ROD TEMPERATURE
(BUNDLE 7-IC, UPPER HALF)

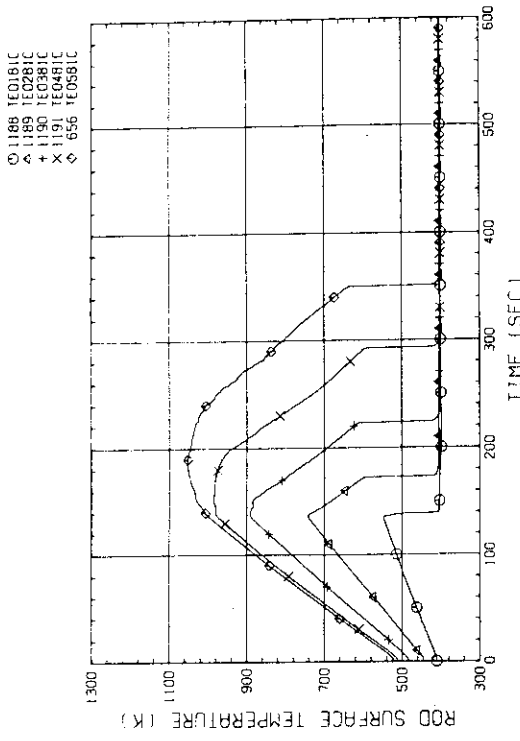


Fig. D-8(a) HEATER ROD TEMPERATURE
(BUNDLE 8-IC, LOWER HALF)

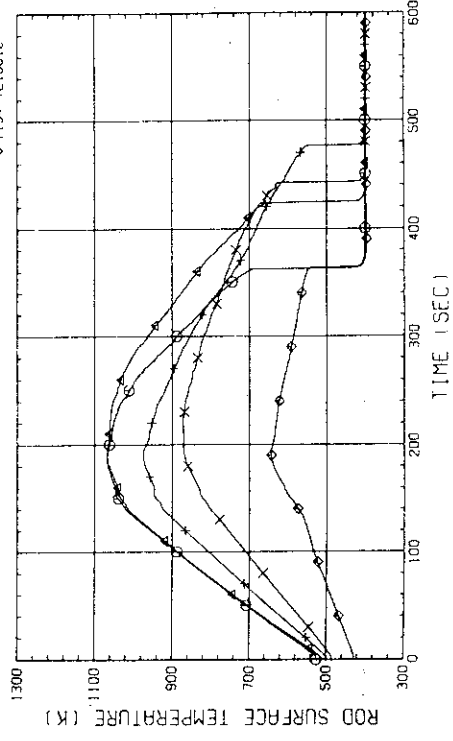


Fig. D-8(b) HEATER ROD TEMPERATURE
(BUNDLE 8-IC, UPPER HALF)

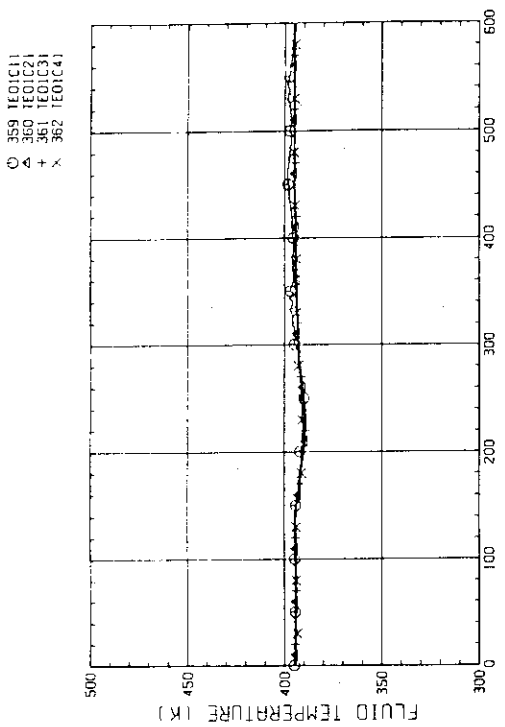


Fig. D-9(a) FLUID TEMPERATURE AT CORE INLET
(BUNDLE 1,2,3,4, 100MM BELOW HEATED PART)

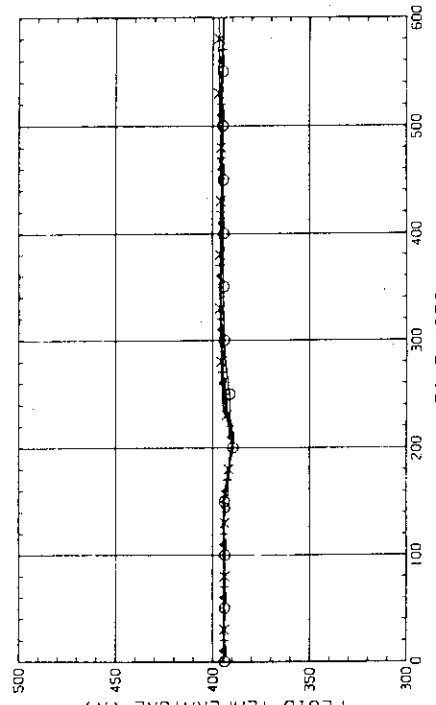
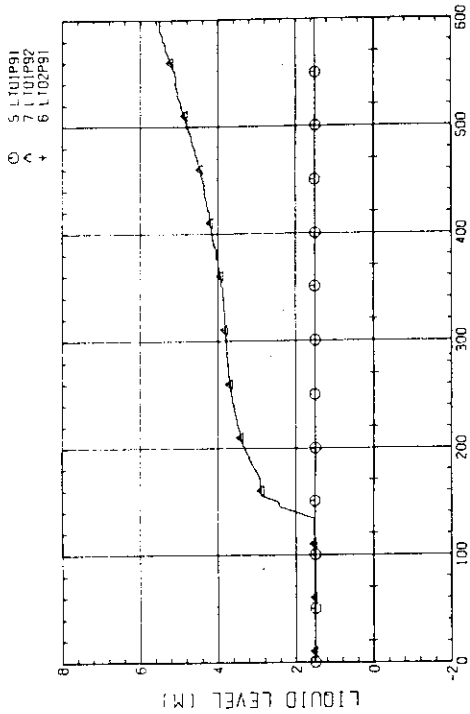


Fig. D-10 LIQUID LEVEL IN DOWNCOMER (01P91-BELOW CORE INLET
01P92-BOTTOM TO COLD LEG, 02P91-COLD LEG TO TOP OF PV)



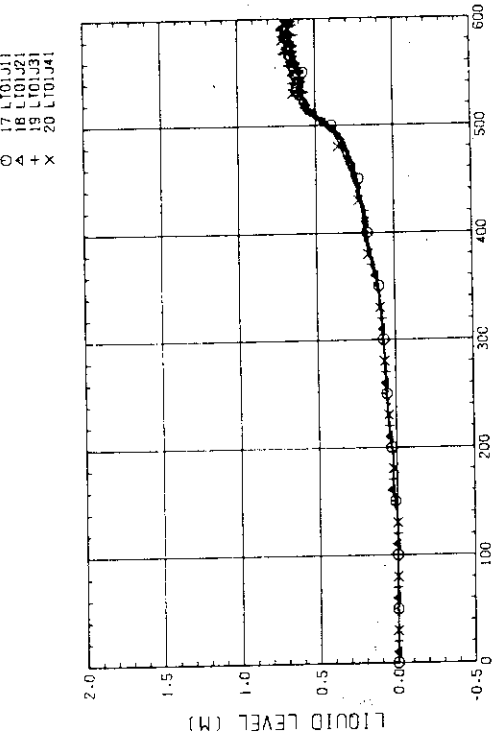


Fig. D-11(a) LIQUID LEVEL ABOVE END BOX 11 PLATE
(BUNDLE 1,2,3,4)

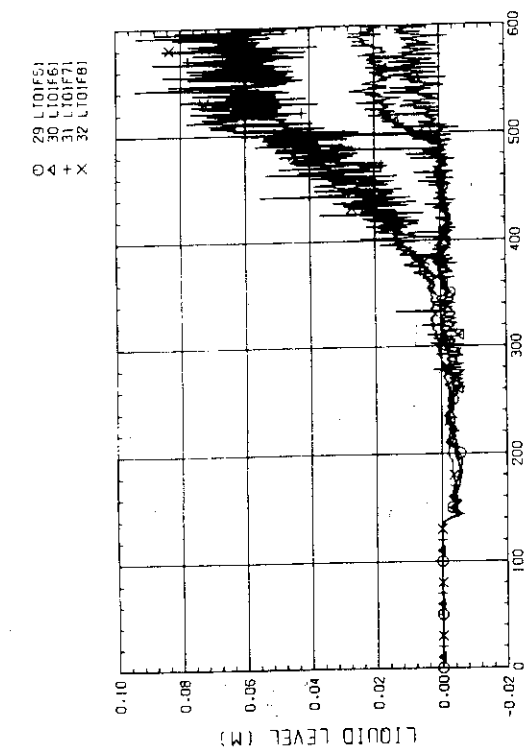


Fig. D-11(b) LIQUID LEVEL ABOVE END BOX 11 PLATE
(BUNDLE 5,6,7,8)

Fig. D-12(a) LIQUID LEVEL ABOVE UCSP
(BUNDLE 1,2,3,4)

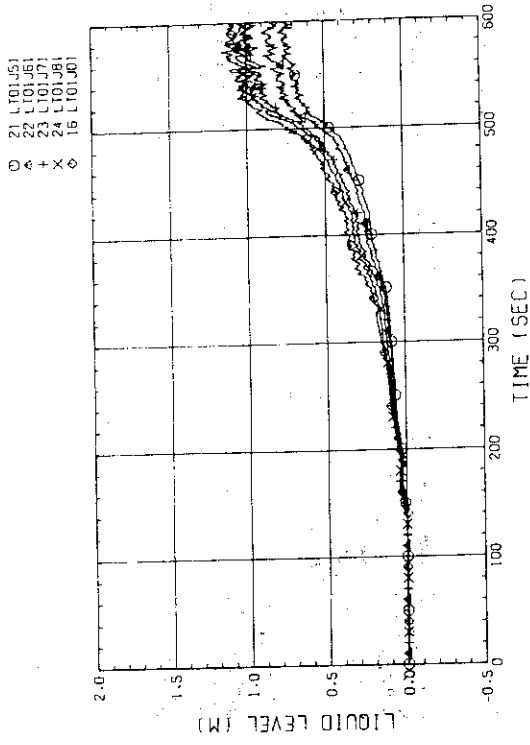


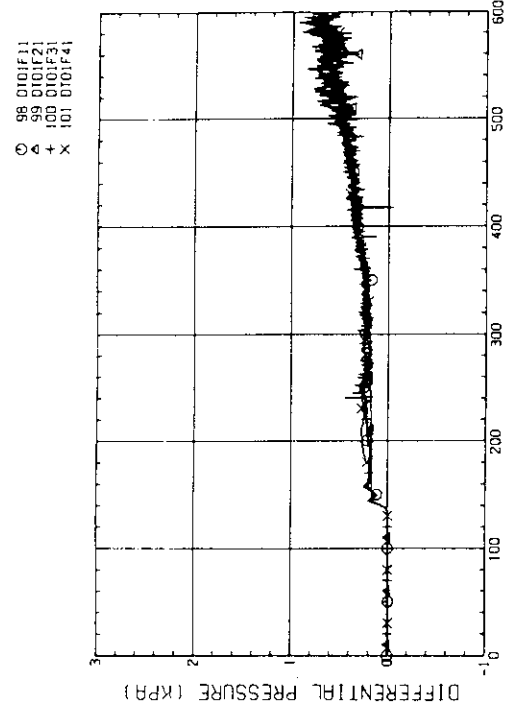
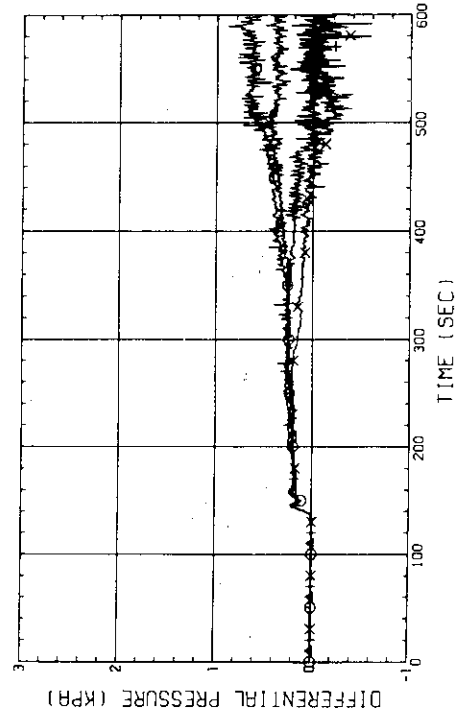
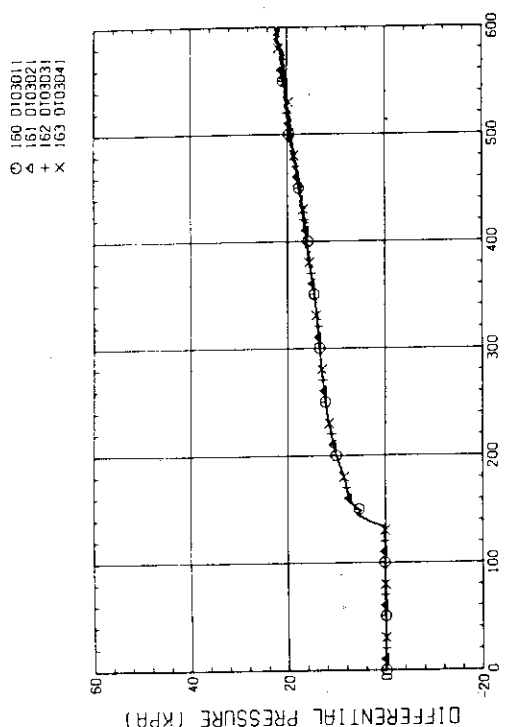
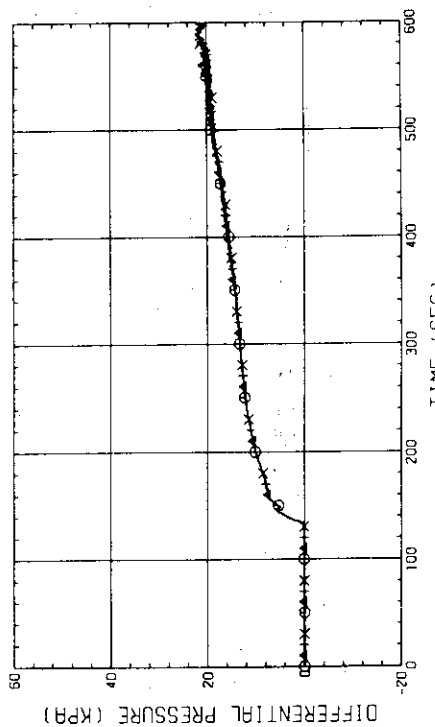
Fig. D-12(b) LIQUID LEVEL ABOVE UCSP
(BUNDLE 5,6,7,8 AND CORE BAFFLE)

17 LTO1J1
18 LTO1J2
19 LTO1J3
20 LTO1J4

21 LTO1J5
22 LTO1J6
23 LTO1J7
24 LTO1J8
16 LTO1J0

Fig. D-12(a) LIQUID LEVEL ABOVE UCSP
(BUNDLE 1,2,3,4)

Fig. D-12(b) LIQUID LEVEL ABOVE UCSP
(BUNDLE 5,6,7,8 AND CORE BAFFLE)

Fig. D-14(a) DIFFERENTIAL PRESSURE ACROSS END BOX TIE PLATE
(BUNDLE 1,2,3,4)Fig. D-14(b) DIFFERENTIAL PRESSURE ACROSS END BOX TIE PLATE
(BUNDLE 5,6,7,8)Fig. D-13(a) DIFFERENTIAL PRESSURE OF CORE FULL HEIGHT
(BUNDLE 1,2,3,4)Fig. D-13(b) DIFFERENTIAL PRESSURE OF CORE FULL HEIGHT
(BUNDLE 5,6,7,8)

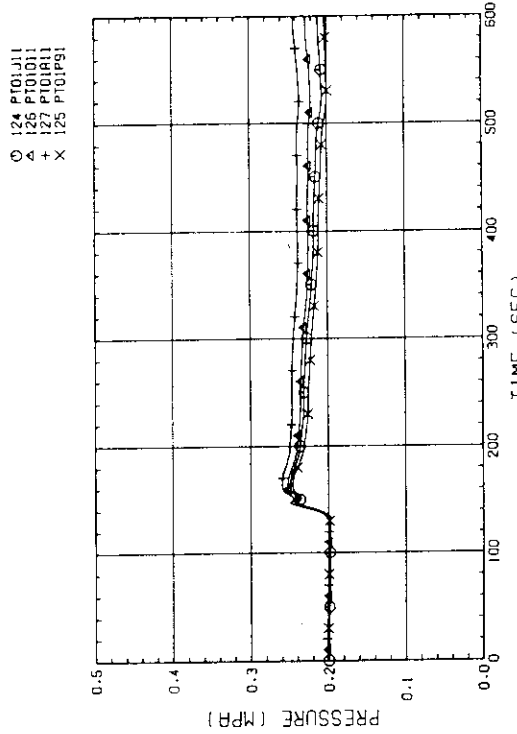


Fig. D-16 PRESSURE IN PV (J - TOP OF PV, O - CORE CENTER, A - CORE INLET, P - BELOW COLD LEG NOZZLE IN DOWNCOMER)

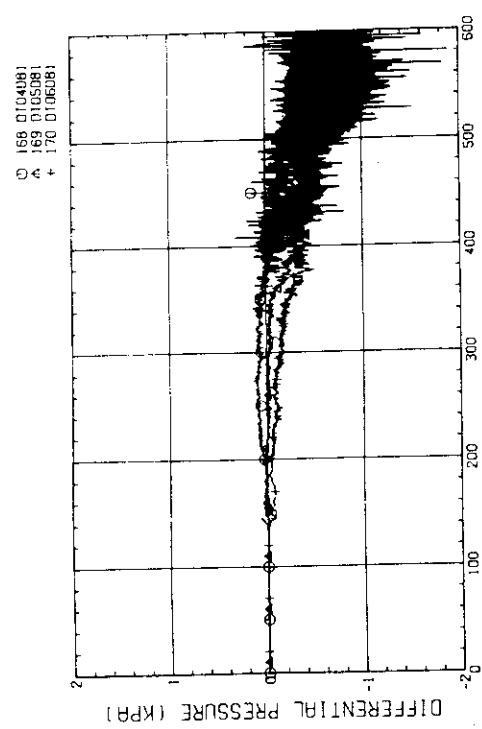


Fig. D-15(a) DIFFERENTIAL PRESSURE, HORIZONTAL BUNDLE S-8 (04-BELOW SPACER 4, 05-BELOW SPACER 6, 06-BELOW END BOX)

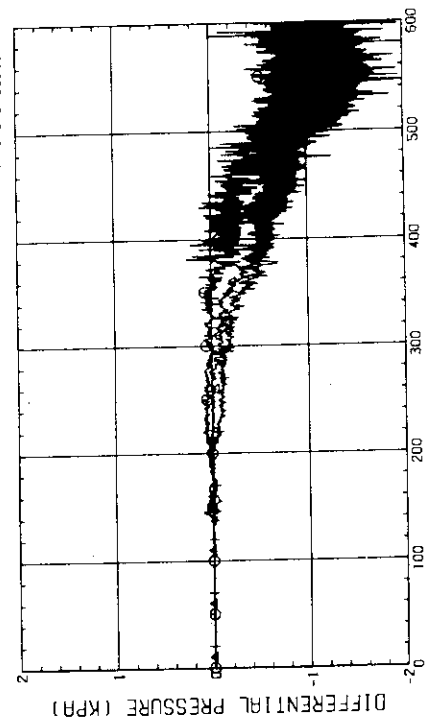


Fig. D-15(b) DIFFERENTIAL PRESSURE, HORIZONTAL BUNDLE 1-8 (04-BELOW SPACER 4, 05-BELOW SPACER 6, 06-BELOW END BOX)

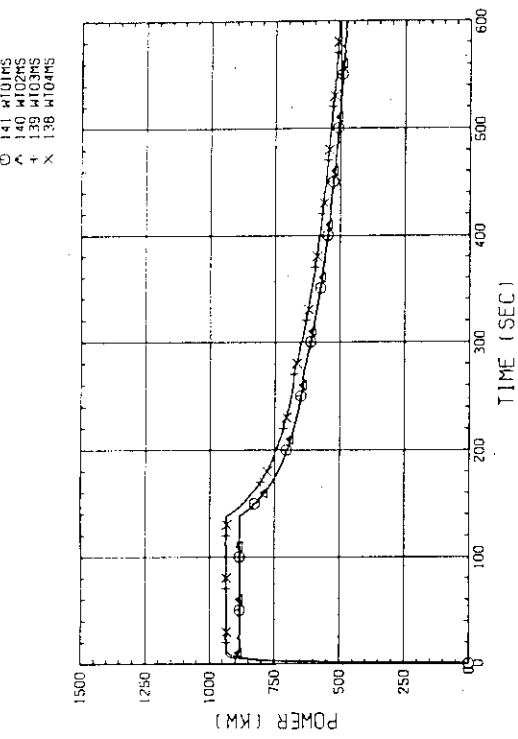


Fig. D-17(a) BUNDLE POWER
(BUNDLE 1,2,3,4)

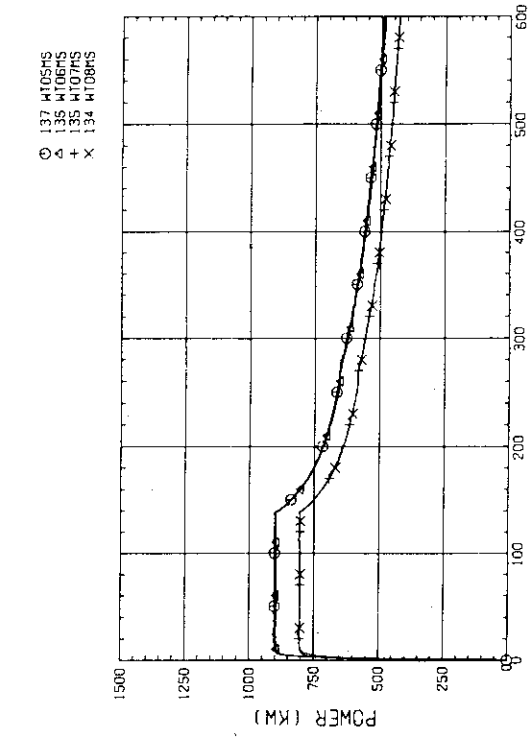


Fig. D-17(b) BUNDLE POWER
(BUNDLE 5,6,7,8)

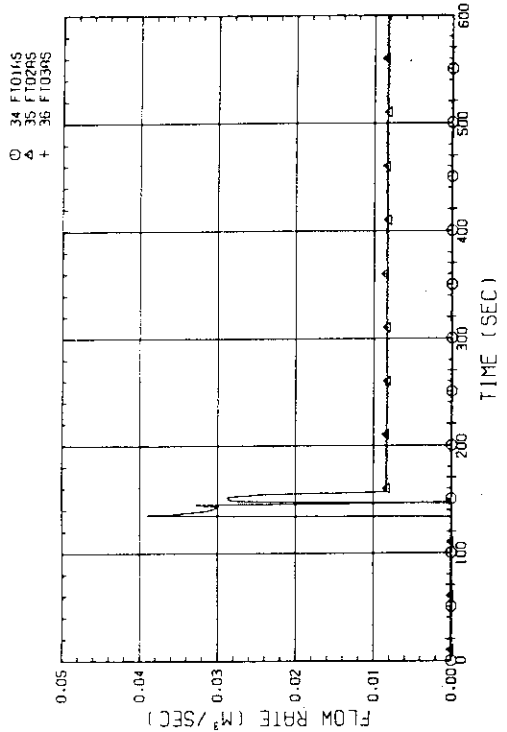


Fig. D-18 FLOW RATE OF ECC WATER (01-DONNCOMER/LOWER PLENUM/
HOT LEG. 02-INTACT COLD LEG, 03-BROKEN COLD LEG)

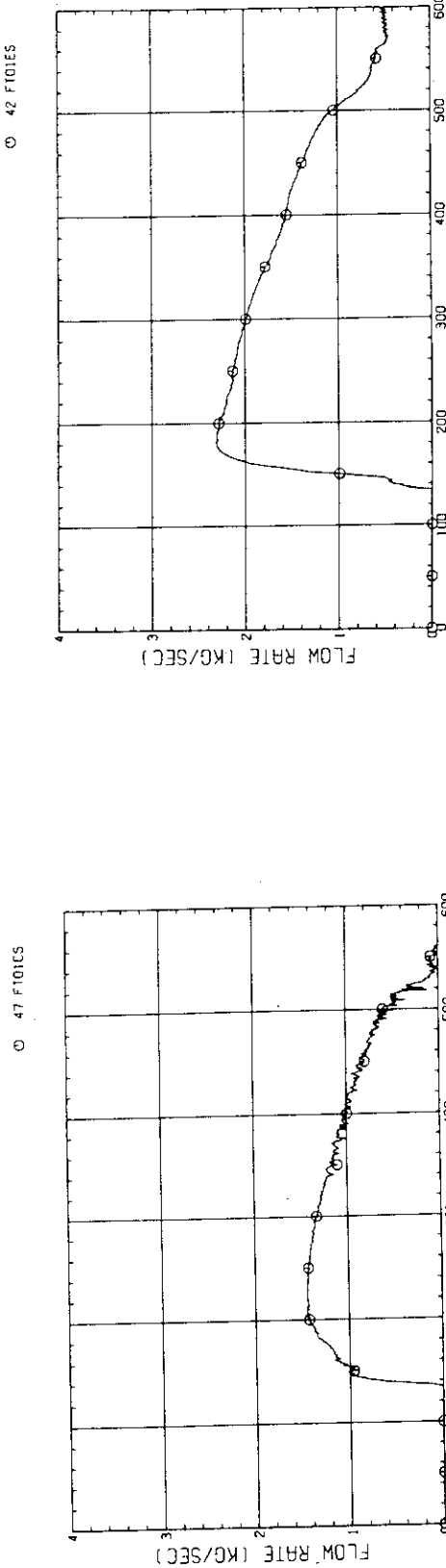


Fig. D-19(a) MASS FLOW RATE OF INTACT COLD LEG

Fig. D-19(c) MASS FLOW RATE FROM CONTAINMENT TANK-1 TO CONTAINMENT TANK-1;

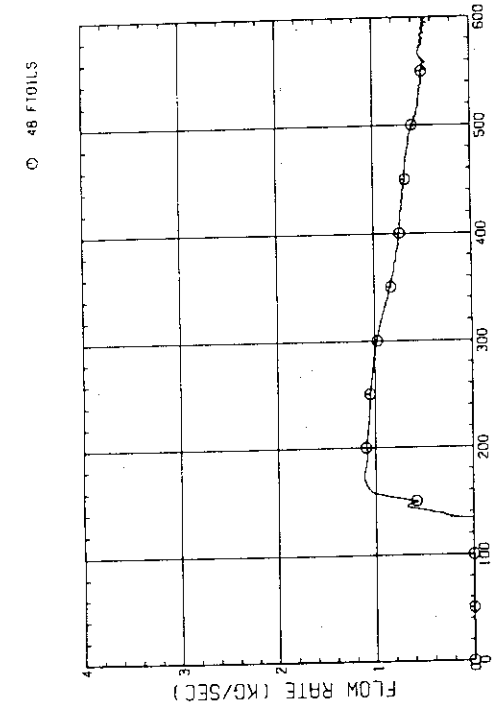


Fig. D-19(b) MASS FLOW RATE OF BROKEN COLD LEG - STEAM/WATER SEPARATOR SIDE

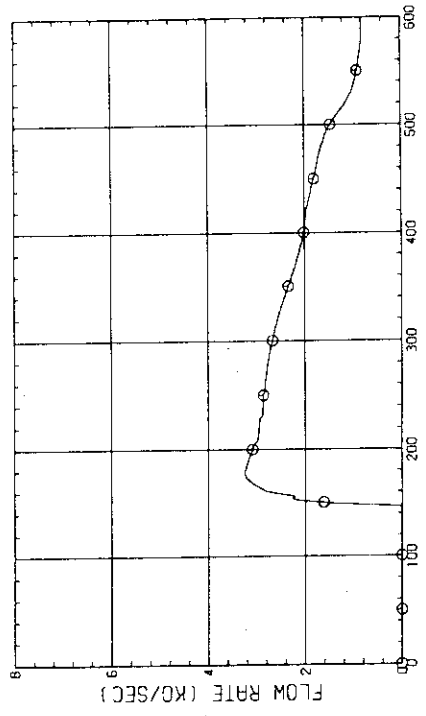


Fig. D-20 STEAM FLOW RATE OF DISCHARGE FROM CONTAINMENT TANK-11

Appendix E

Selected Data for Test S1-17 (Run 523)

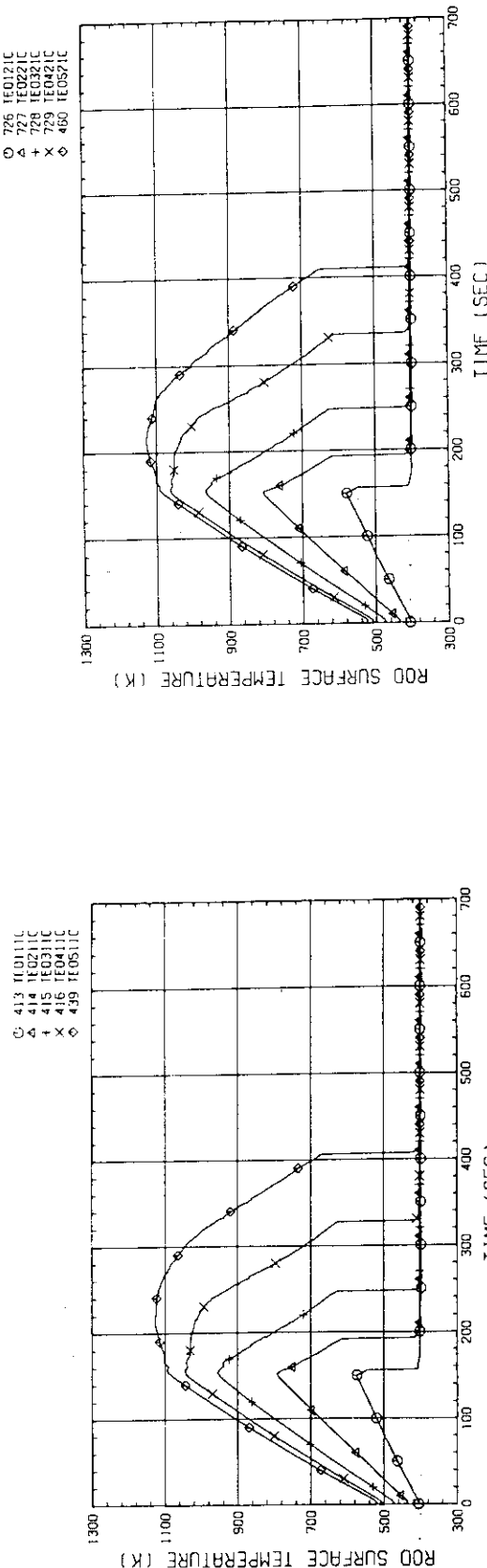


Fig. E-1(a) HEATER ROD TEMPERATURE
(BUNDLE 1-1C, LOWER HALF)

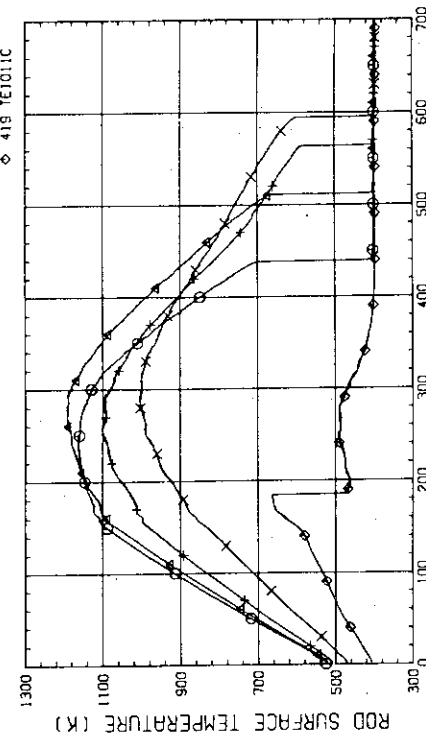


Fig. E-1(b) HEATER ROD TEMPERATURE
(BUNDLE 1-1C, UPPER HALF)

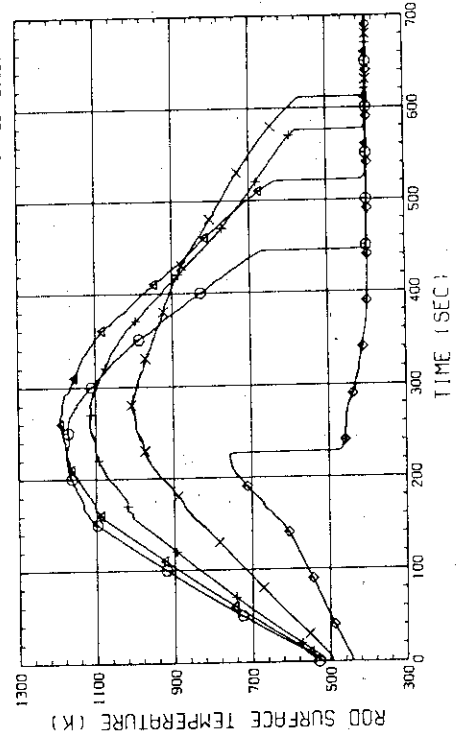


Fig. E-2(a) HEATER ROD TEMPERATURE
(BUNDLE 2-1C, LOWER HALF)

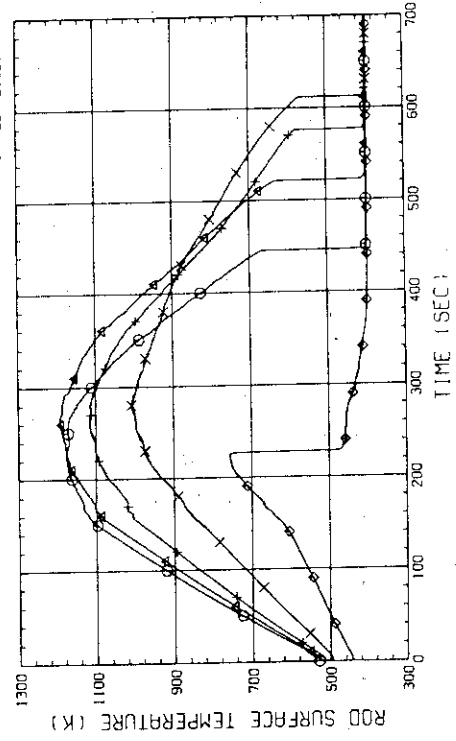


Fig. E-2(b) HEATER ROD TEMPERATURE
(BUNDLE 2-1C, UPPER HALF)

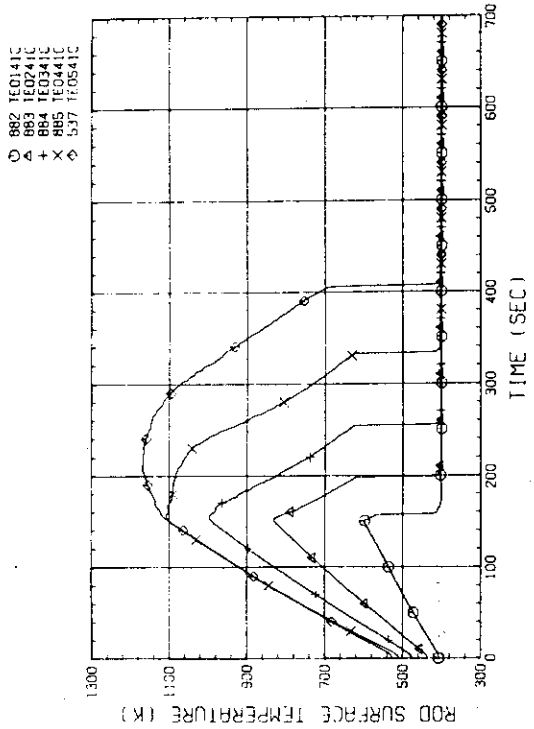


Fig. E-3(a) HEATER ROD TEMPERATURE
(BUNDLE 3-1C, LOWER HALF)

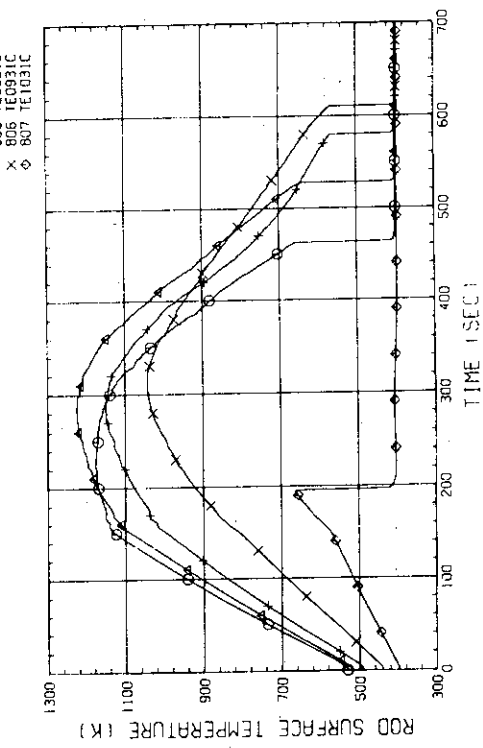


Fig. E-3(b) HEATER ROD TEMPERATURE
(BUNDLE 3-1C, UPPER HALF)

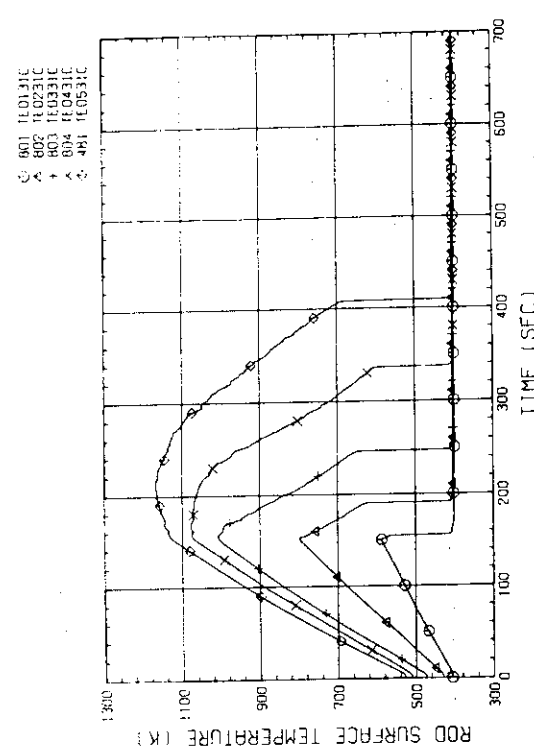


Fig. E-4(a) HEATER ROD TEMPERATURE
(BUNDLE 4-1C, LOWER HALF)

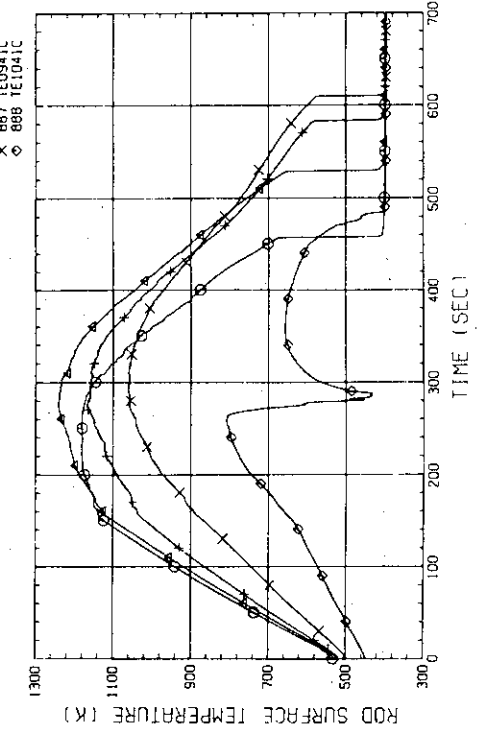


Fig. E-4(b) HEATER ROD TEMPERATURE
(BUNDLE 4-1C, UPPER HALF)

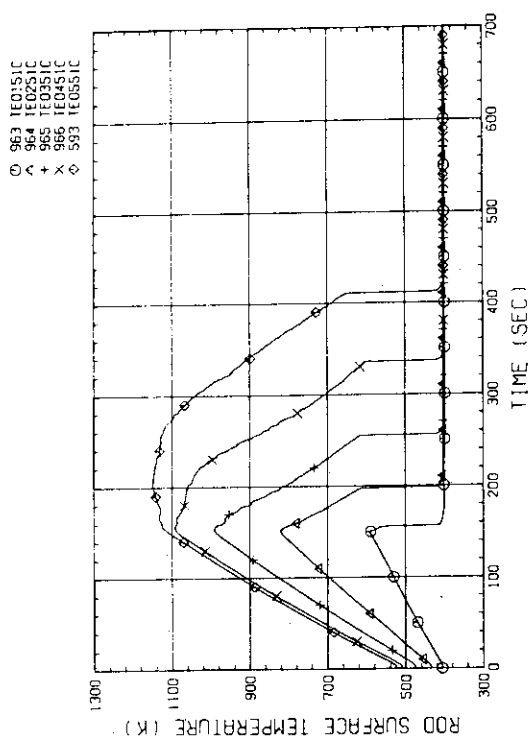


Fig. E-5(a) HEATER ROD TEMPERATURE
(BUNDLE S-1C, LOWER HALF)

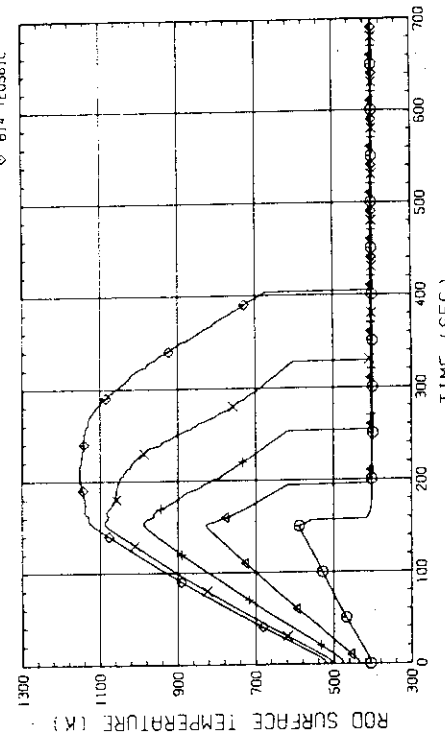


Fig. E-6(a) HEATER ROD TEMPERATURE
(BUNDLE 6-1C, LOWER HALF)

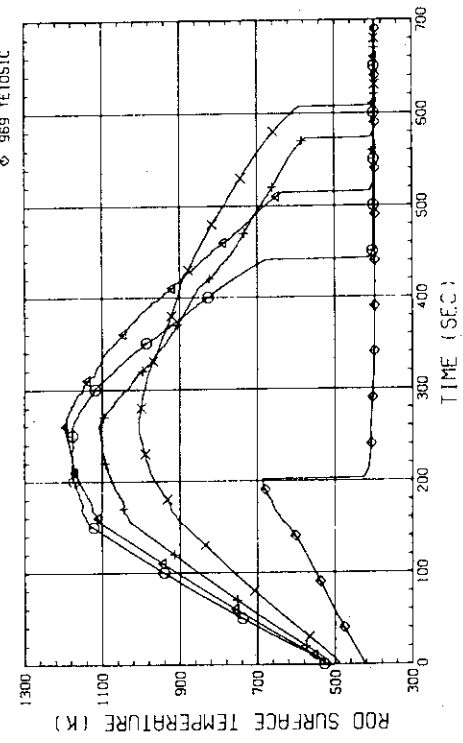


Fig. E-6(b) HEATER ROD TEMPERATURE
(BUNDLE 6-1C, UPPER HALF)

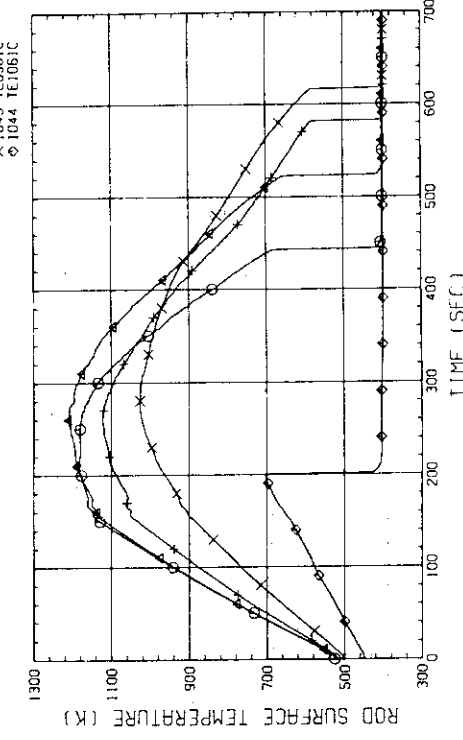
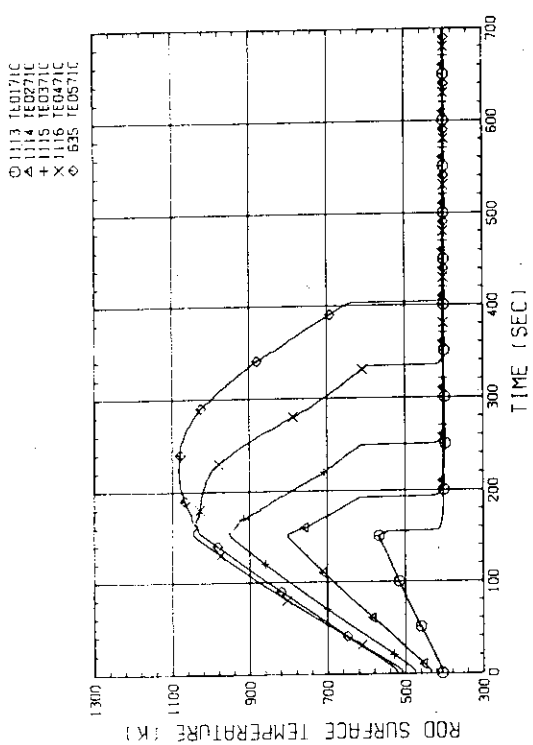
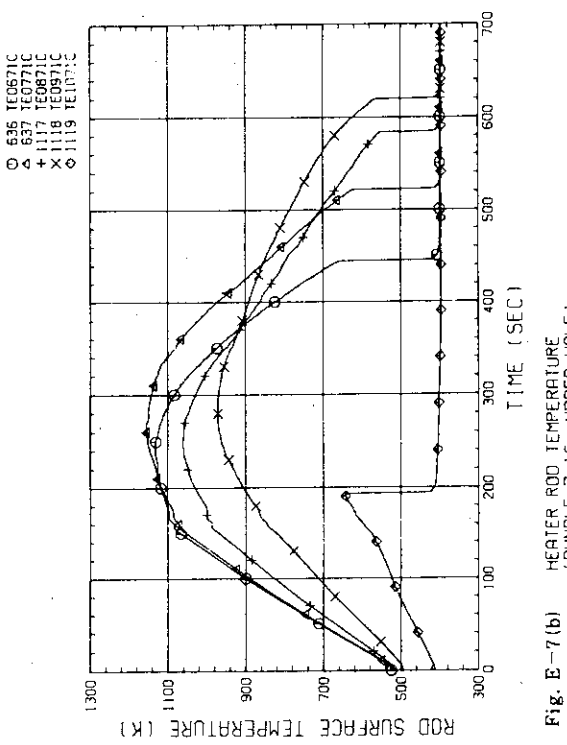
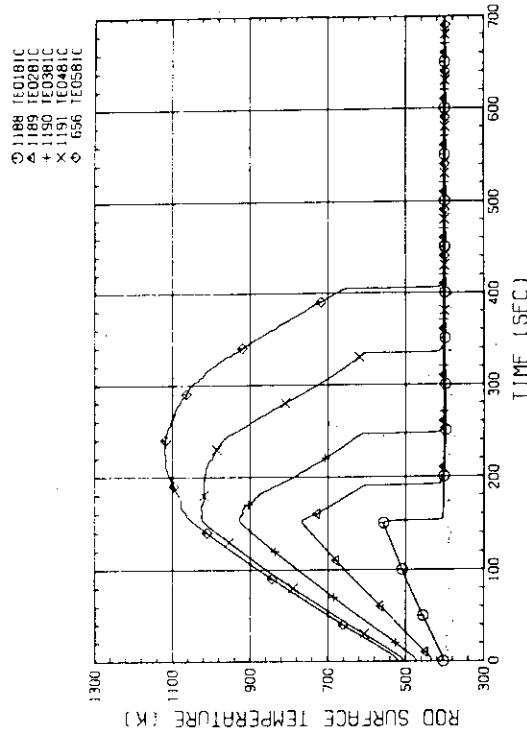
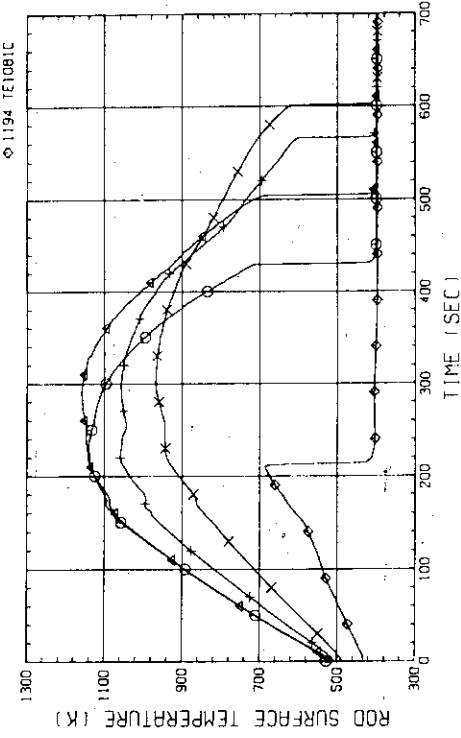


Fig. E-6(b) HEATER ROD TEMPERATURE
(BUNDLE 6-1C, LOWER HALF)

Fig. E-7(a) HEATER ROD TEMPERATURE
(BUNDLE 7-1C, LOWER HALF)Fig. E-7(b) HEATER ROD TEMPERATURE
(BUNDLE 7-1C, UPPER HALF)Fig. E-8(a) HEATER ROD TEMPERATURE
(BUNDLE 8-1C, LOWER HALF)Fig. E-8(b) HEATER ROD TEMPERATURE
(BUNDLE 8-1C, UPPER HALF)

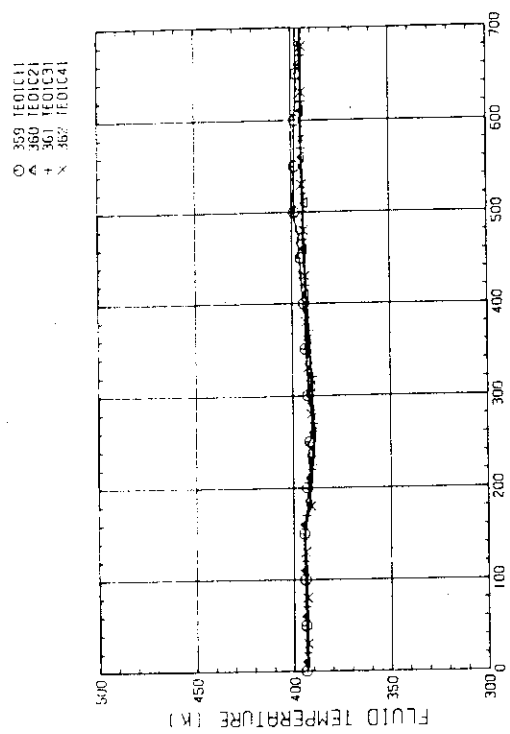


Fig. E-9(a) FLUID TEMPERATURE AT CORE INLET
(BUNDLE 1,2,3,4. 100MM BELOW HEATED PART)

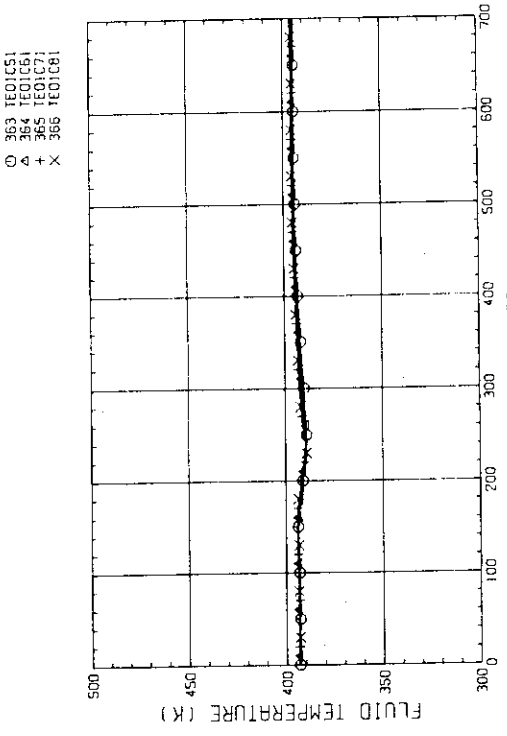


Fig. E-9(b) FLUID TEMPERATURE AT CORE INLET
(BUNDLE 5,6,7,8. 100MM BELOW HEATED PART)

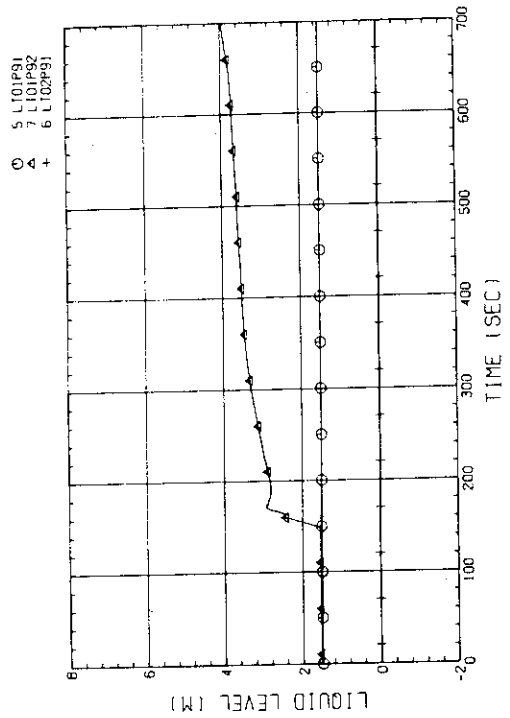


Fig. E-10 LIQUID LEVEL IN CONDENSER (LIOP91-BELOW CORE INLET
01P91-BOTTOM TO COLD LEG. 02P91-COLD LEG TO TOP OF PV1)

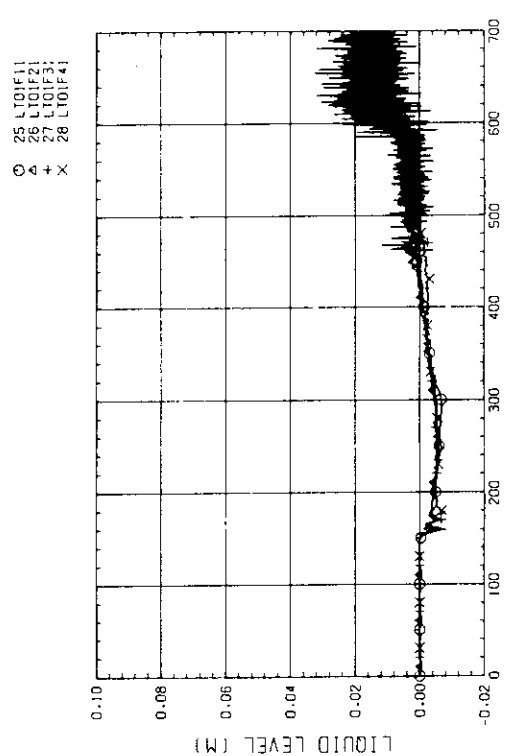


Fig. E-11(a) LIQUID LEVEL ABOVE END BOX TIE PLATE
(BUNDLE 1.2, 3, 4)

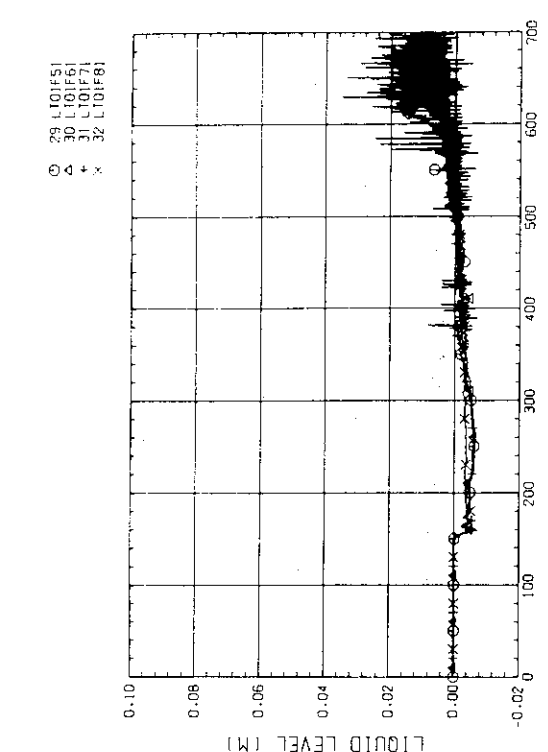


Fig. E-11(b) LIQUID LEVEL ABOVE END BOX TIE PLATE
(BUNDLE 5, 6, 7, 8)

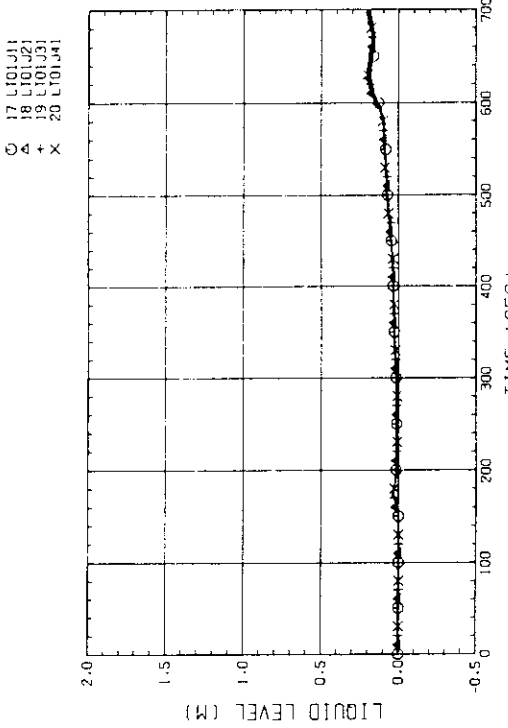


Fig. E-12(a) LIQUID LEVEL ABOVE UESP
(BUNDLE 1, 2, 3, 4)

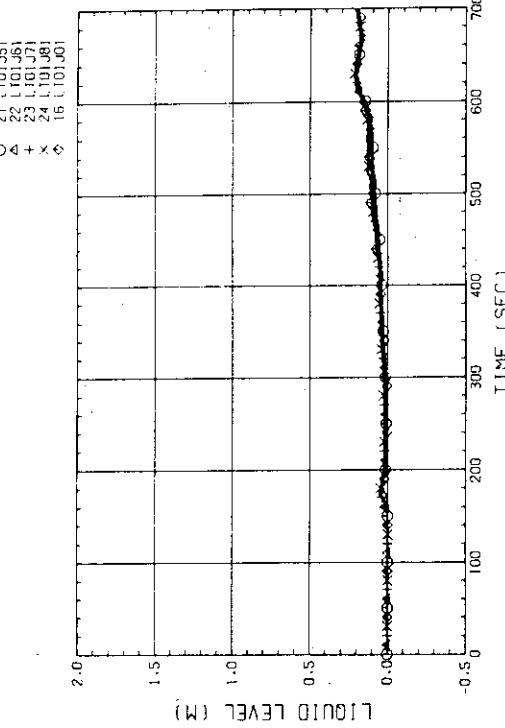
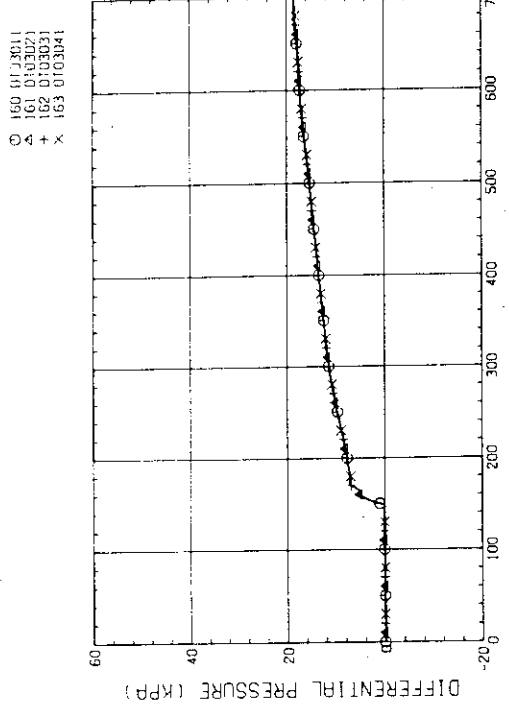
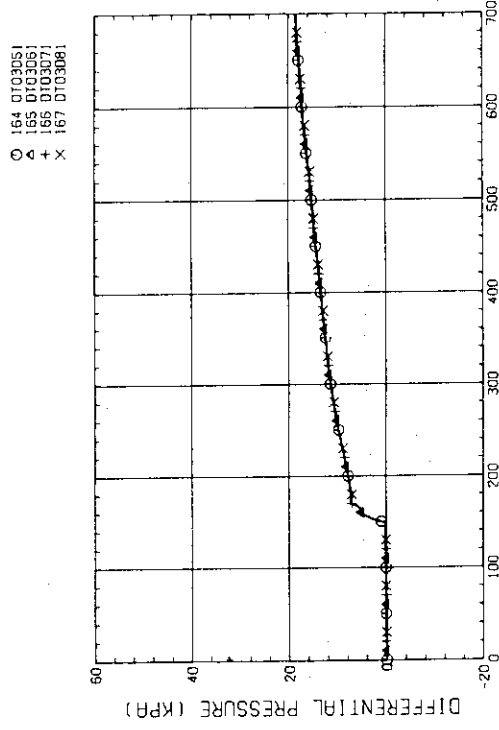
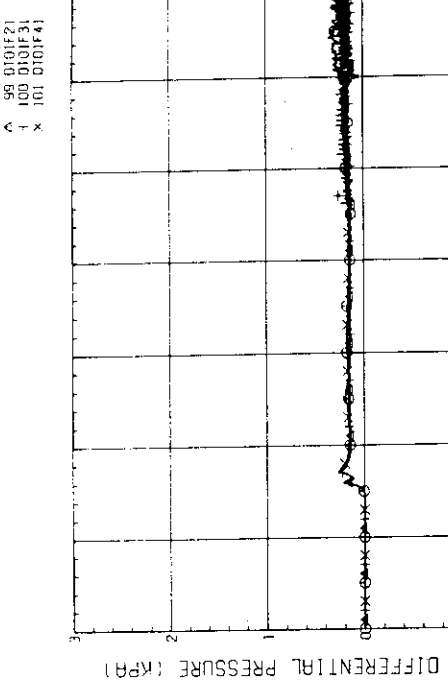
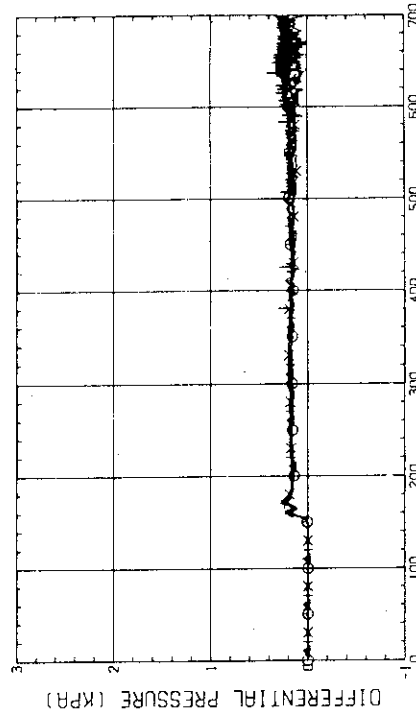


Fig. E-12(b) LIQUID LEVEL ABOVE UESP
(BUNDLE 5, 6, 7, 8)

Fig. E-13(a) DIFFERENTIAL PRESSURE OF CORE FULL HEIGHT
(BUNDLE 1,2,3,4)Fig. E-13(b) DIFFERENTIAL PRESSURE OF CORE FULL HEIGHT
(BUNDLE 5,6,7,8)Fig. E-14(a) DIFFERENTIAL PRESSURE ACROSS END BOX TIE PLATE
(BUNDLE 1,2,3,4)Fig. E-14(b) DIFFERENTIAL PRESSURE ACROSS END BOX TIE PLATE
(BUNDLE 5,6,7,8)

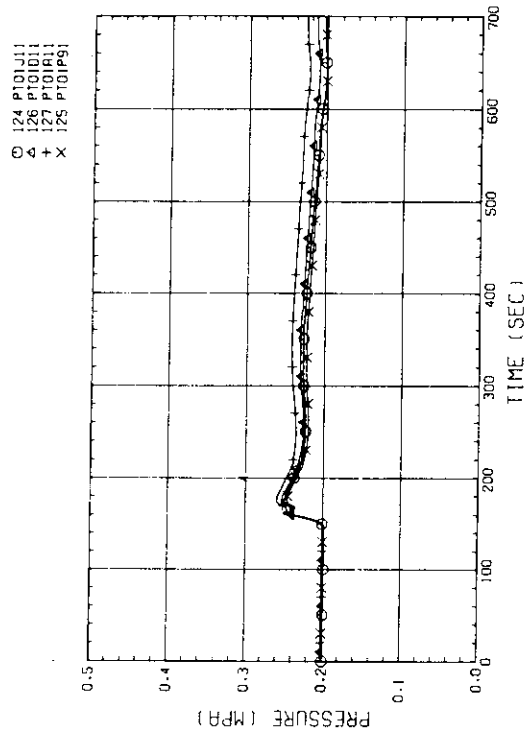


Fig. E-16 PRESSURE IN PV (TOP OF PV) - CORE CENTER, A
CORE INIT. P - BELOW COLD LEG NOZZLE IN DOWNCOMER

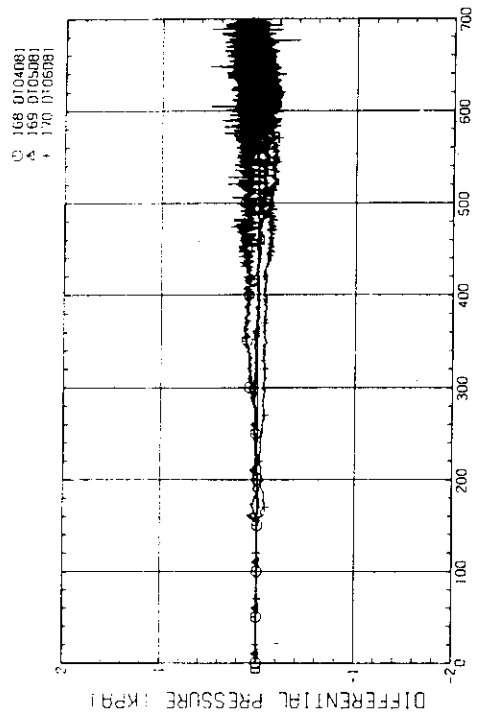


Fig. E-15(a) DIFFERENTIAL PRESSURE, HORIZONTAL BUNDLE S-8 (04-BELOW SPACER 4, 05-BELOW SPACER 6, 06-BELOW END BOX)

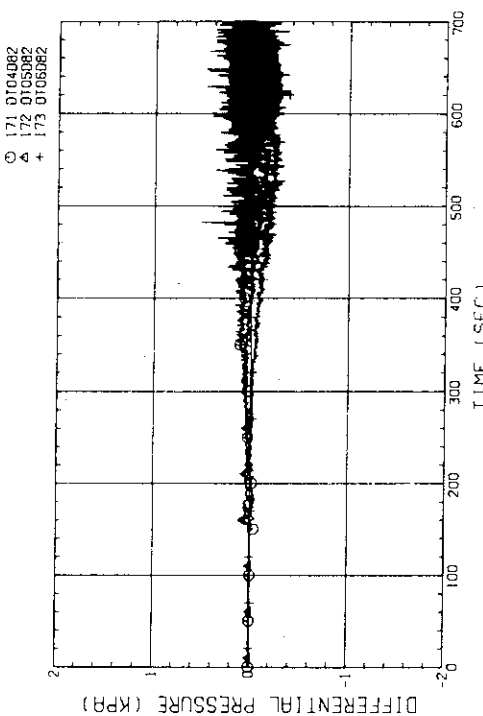


Fig. E-15(b) DIFFERENTIAL PRESSURE, HORIZONTAL BUNDLE 1-8 (04-BELOW SPACER 4, 05-BELOW SPACER 6, 06-BELOW END BOX)

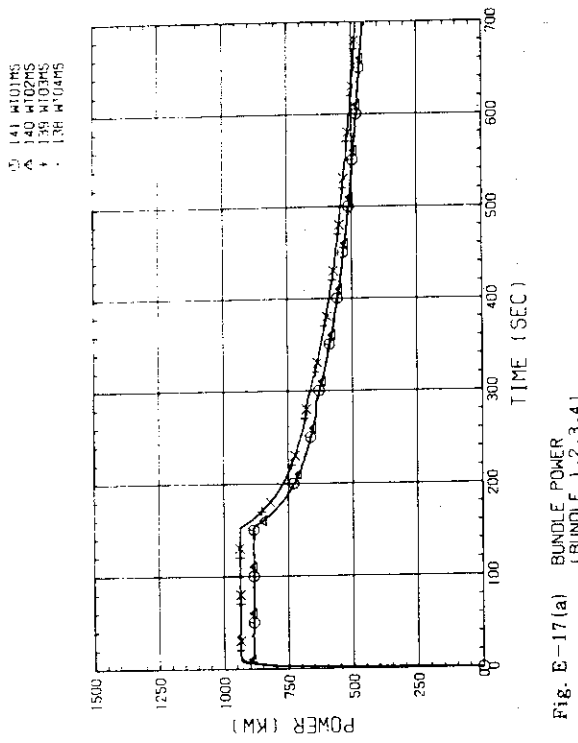


Fig. E-17(a)

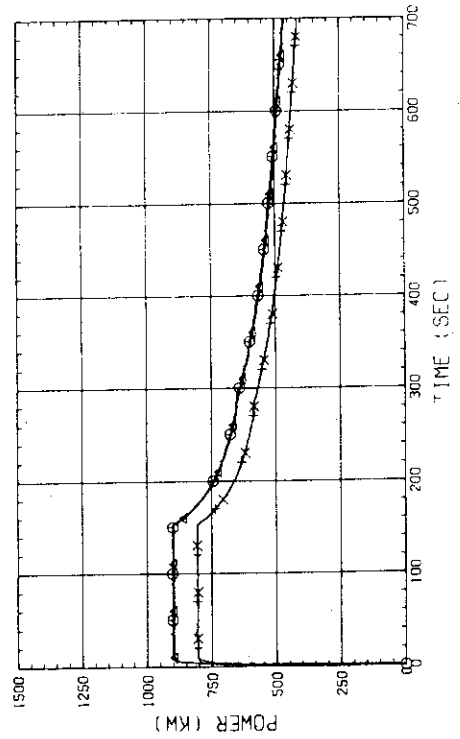


Fig. E-18
FLOW RATE OF ECC WATER (01-DOWNCOMER/LOWER PLUNGE/
HOT LEG, 02-JACKET COLD LEG, 03-BROKEN COLD LEG)

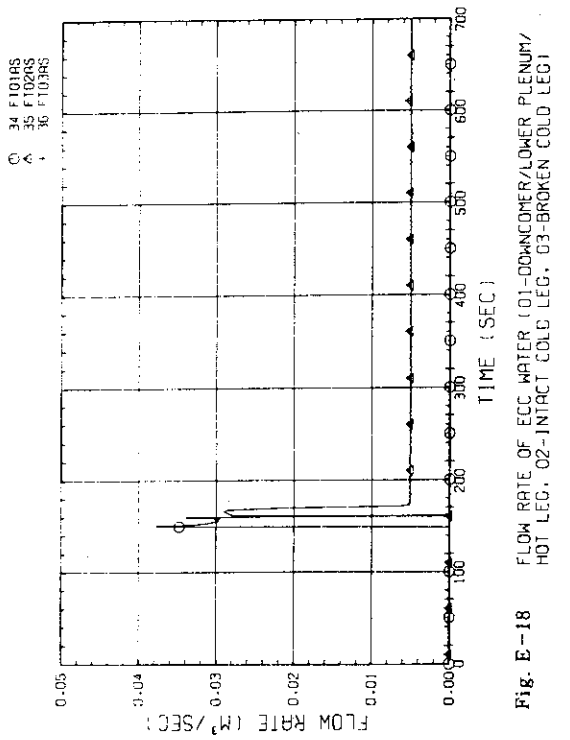


Fig. E-18
FLOW RATE OF ECC WATER (01-DOWNCOMER/LOWER PLUNGE/
HOT LEG, 02-JACKET COLD LEG, 03-BROKEN COLD LEG)

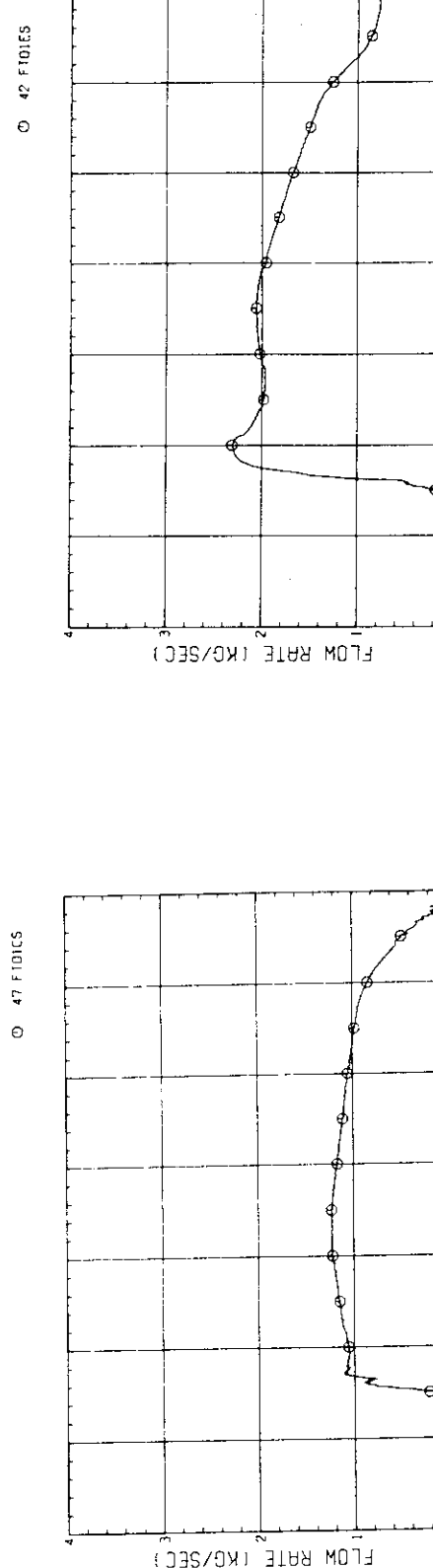


Fig. E-19(a) MASS FLOW RATE OF INTACT COLD LEG

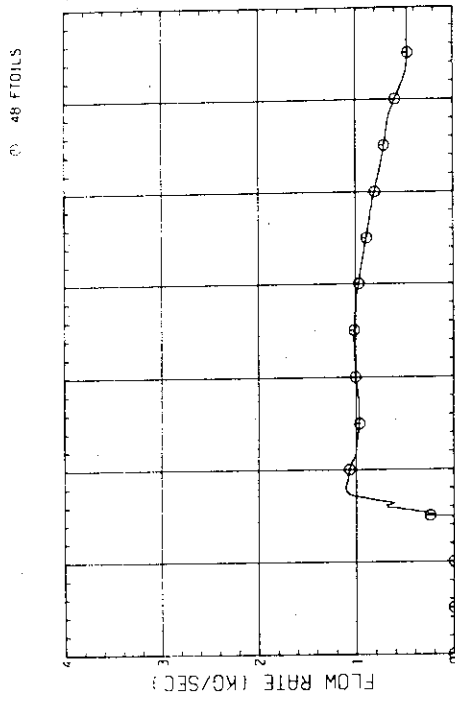


Fig. E-19(b) MASS FLOW RATE OF BROKEN COLD LEG - STEAM/WATER
SEPARATOR SIDE

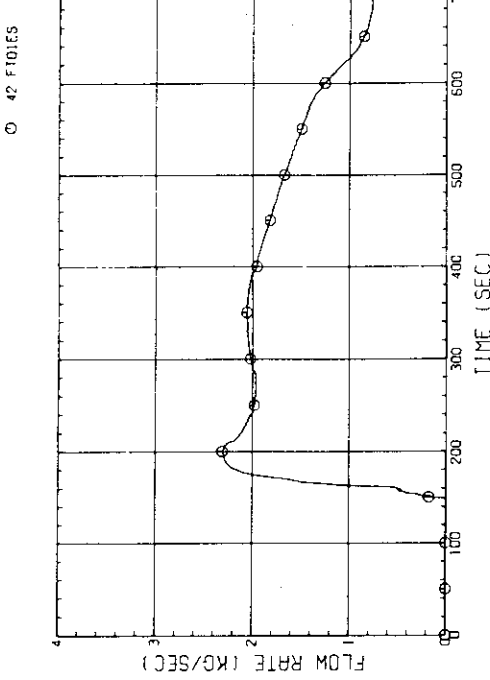


Fig. E-19(c) MASS FLOW RATE FROM CONTAINMENT TANK-1 TO CONTAINMENT
TANK-11

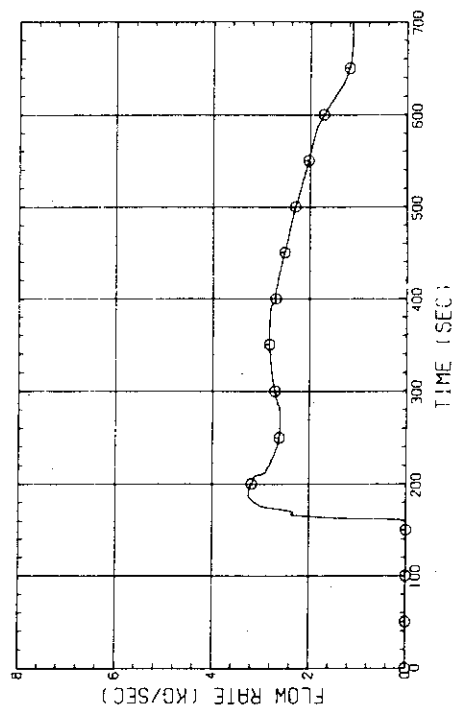


Fig. E-20 STEAM FLOW RATE OF DISCHARGE FROM CONTAINMENT TANK-11

Appendix F

Selected Data for Test S1-20 (Run 530)

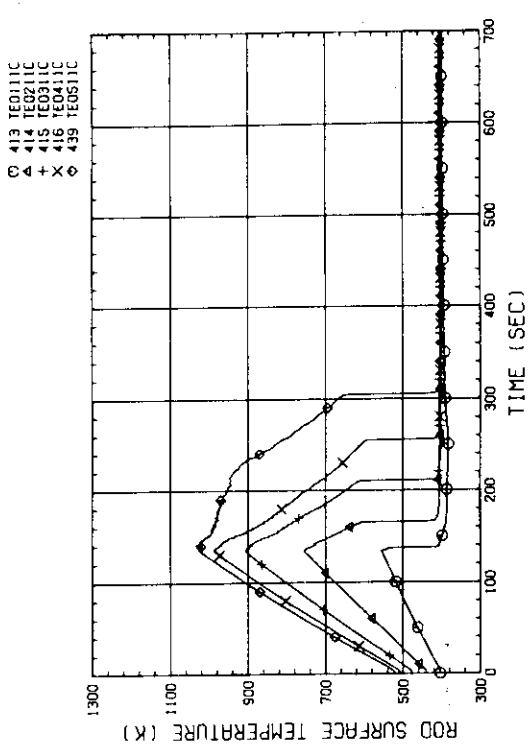


Fig. F-1(a) HEATER ROD TEMPERATURE
(BUNDLE 1-1C, LOWER HALF)

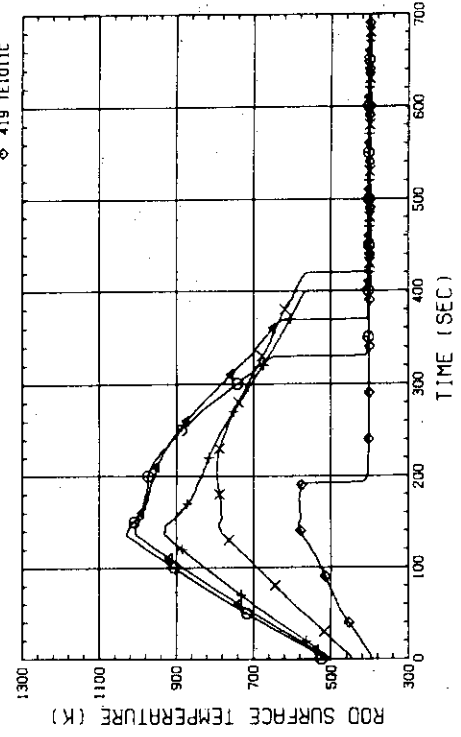


Fig. F-1(b) HEATER ROD TEMPERATURE
(BUNDLE 1-1C, UPPER HALF)

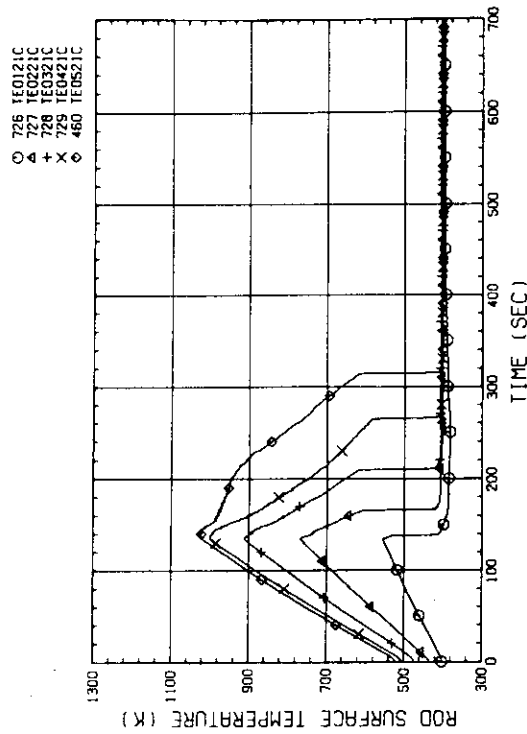


Fig. F-2(a) HEATER ROD TEMPERATURE
(BUNDLE 2-1C, LOWER HALF)

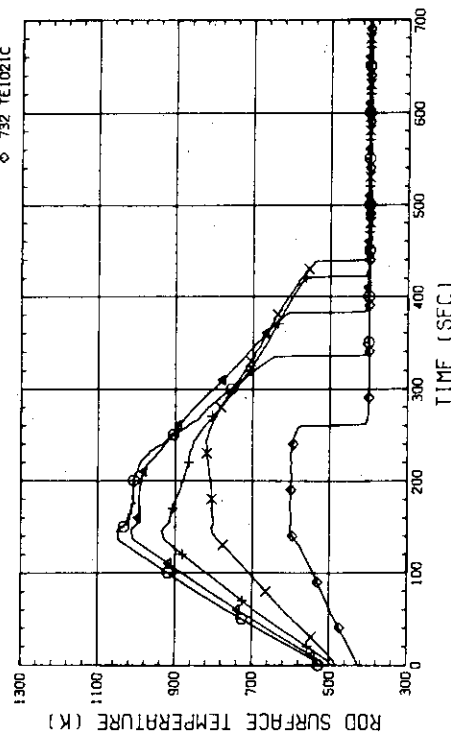


Fig. F-2(b) HEATER ROD TEMPERATURE
(BUNDLE 2-1C, UPPER HALF)

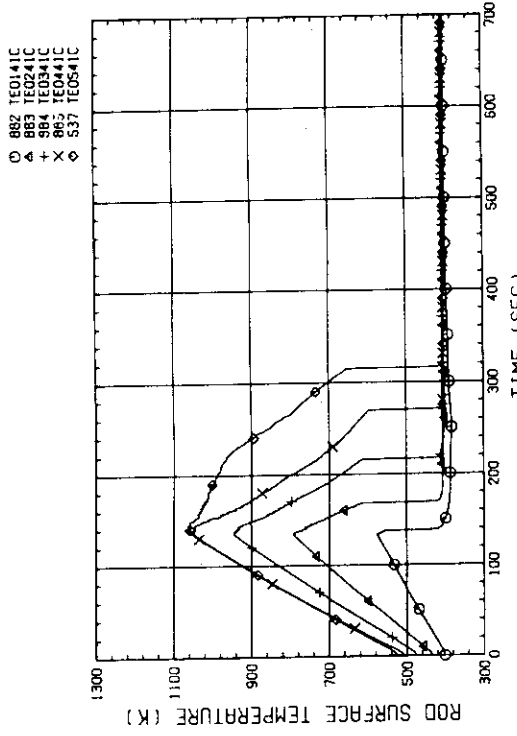


Fig. F-3(a) HEATER ROD TEMPERATURE
(BUNDLE 3-1C, LOWER HALF)

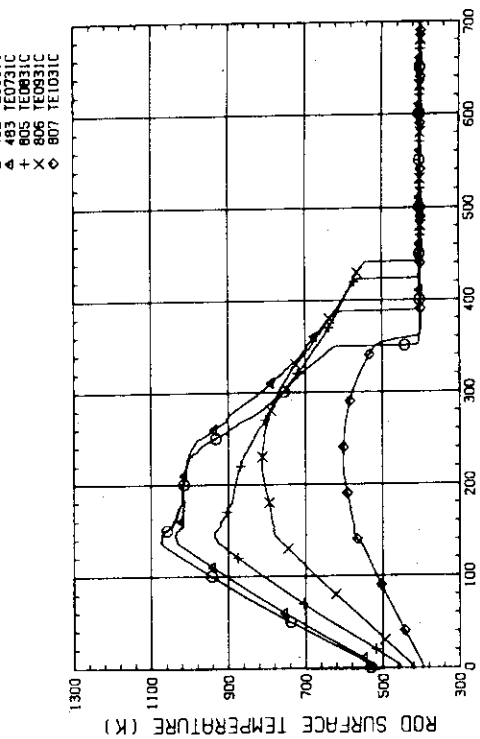


Fig. F-3(b) HEATER ROD TEMPERATURE
(BUNDLE 3-1C, UPPER HALF)

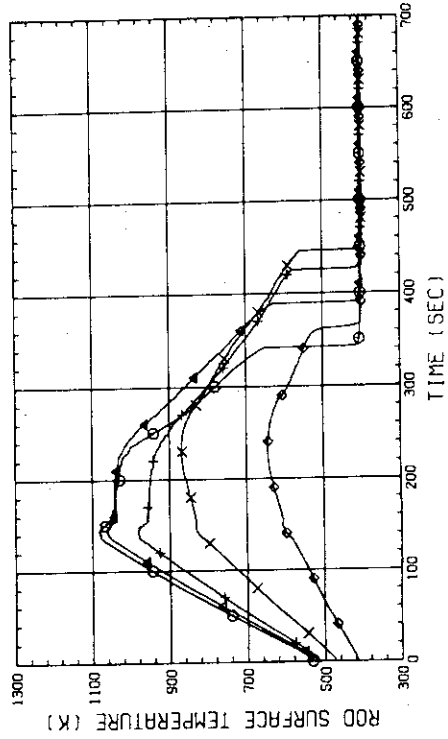
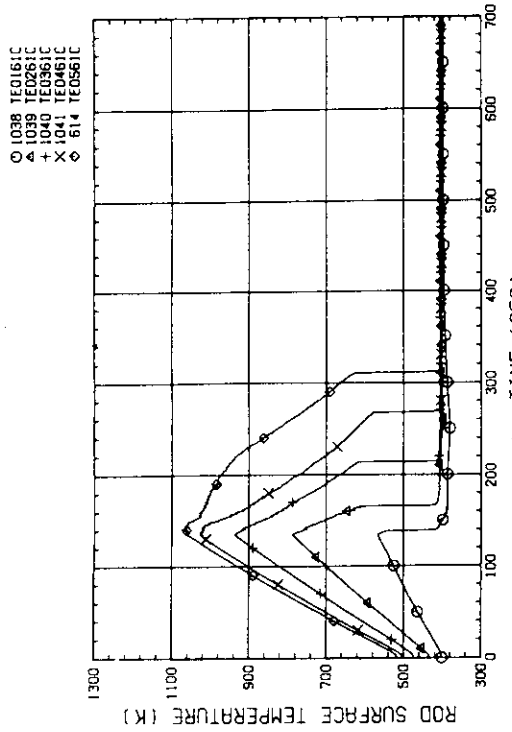
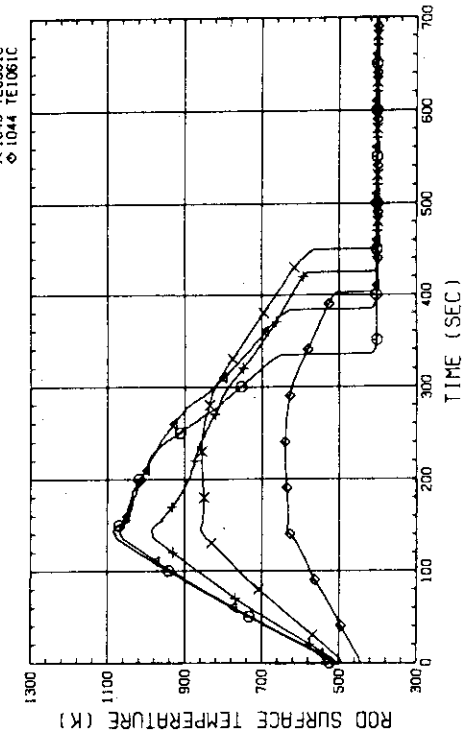
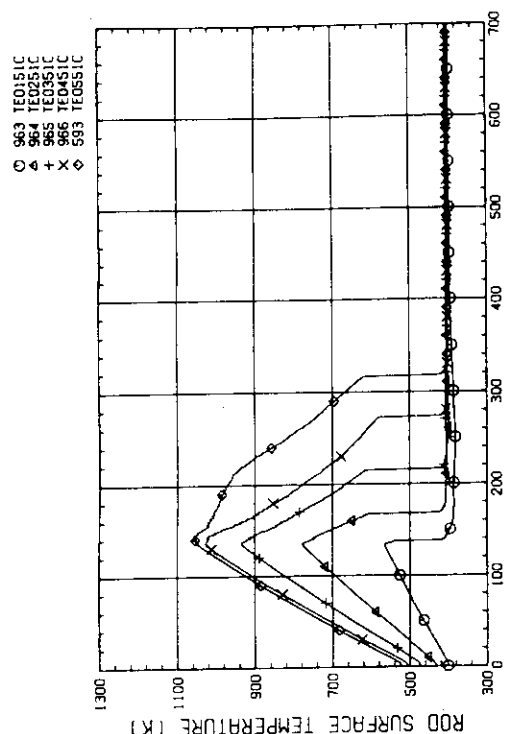
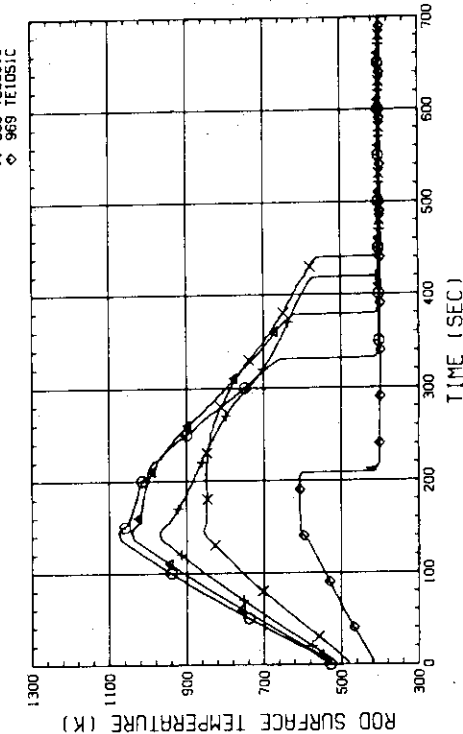


Fig. F-4(a) HEATER ROD TEMPERATURE
(BUNDLE 4-1C, LOWER HALF)

Fig. F-4(b) HEATER ROD TEMPERATURE
(BUNDLE 4-1C, UPPER HALF)

Fig. F-6(a) HEATER ROD TEMPERATURE
(BUNDLE 6-1C, LOWER HALF)Fig. F-6(b) HEATER ROD TEMPERATURE
(BUNDLE 6-1C, UPPER HALF)Fig. F-5(a) HEATER ROD TEMPERATURE
(BUNDLE 5-1C, LOWER HALF)Fig. F-5(b) HEATER ROD TEMPERATURE
(BUNDLE 5-1C, UPPER HALF)

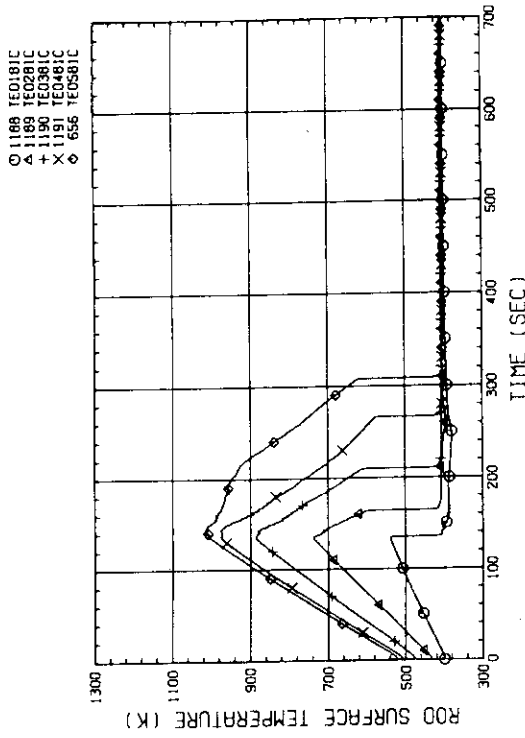


Fig. F-7(a) HEATER ROD TEMPERATURE
(BUNDLE 7-1C, LOWER HALF)

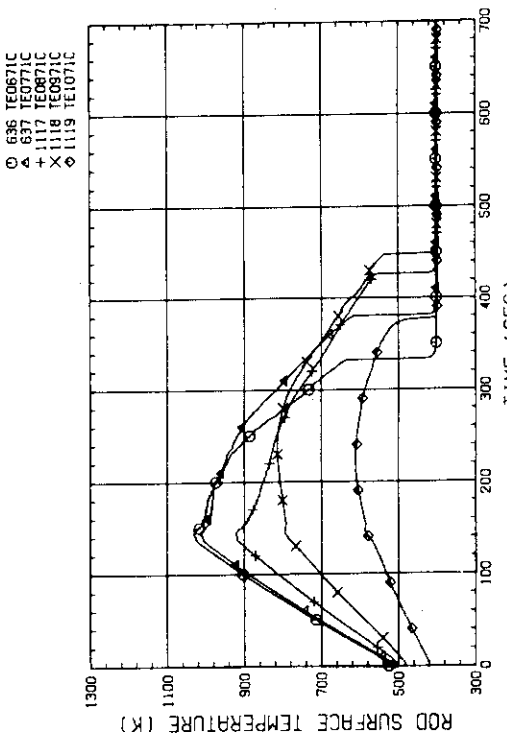


Fig. F-7(b) HEATER ROD TEMPERATURE
(BUNDLE 7-1C, UPPER HALF)

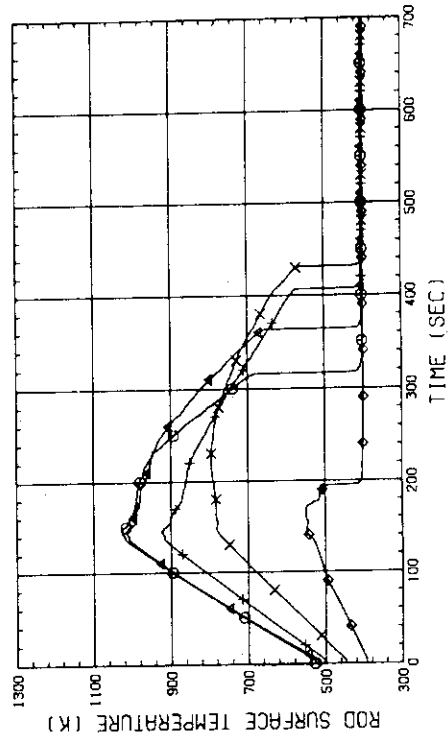


Fig. F-8(a) HEATER ROD TEMPERATURE
(BUNDLE 8-1C, LOWER HALF)

Fig. F-8(b) HEATER ROD TEMPERATURE
(BUNDLE 8-1C, UPPER HALF)

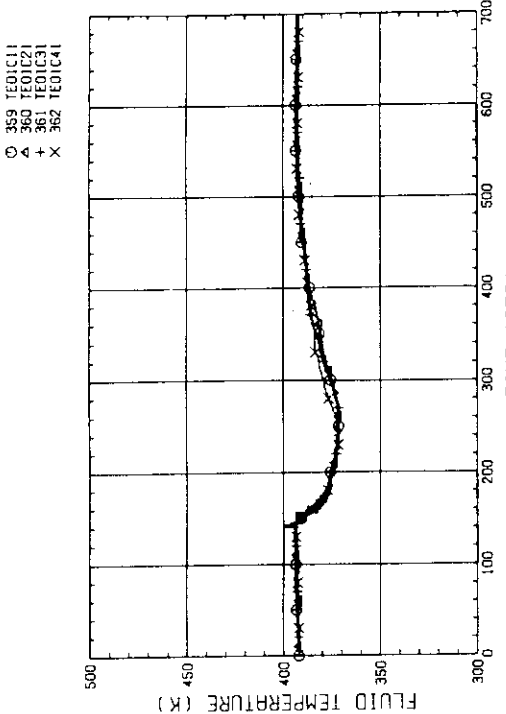


Fig. F-9(a) FLUID TEMPERATURE AT CORE INLET
(BUNDLE 1,2,3,4, 100MM BELOW HEATED PART)

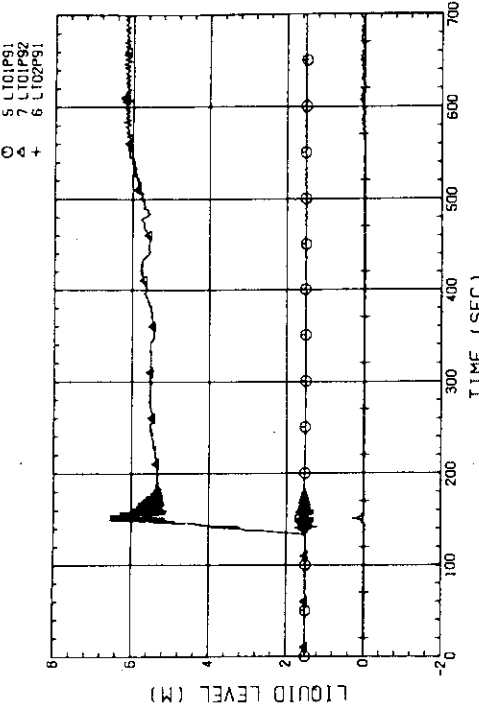


Fig. F-10 LIQUID LEVEL IN DOWNCOMER [01PP91-BELOW CORE INLET,
01P92-BOTTOM TO COLD LEG, 02PP91-COLD LEG TO TOP OF PV1]

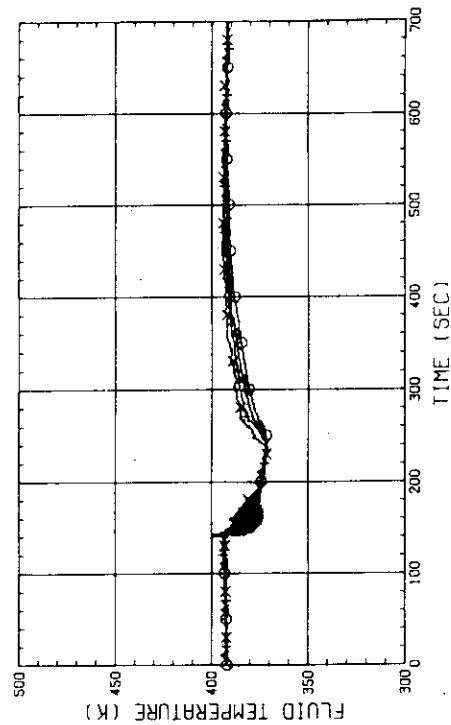


Fig. F-9(b) FLUID TEMPERATURE AT CORE INLET
(BUNDLE 5,6,7,8, 100MM BELOW HEATED PART)

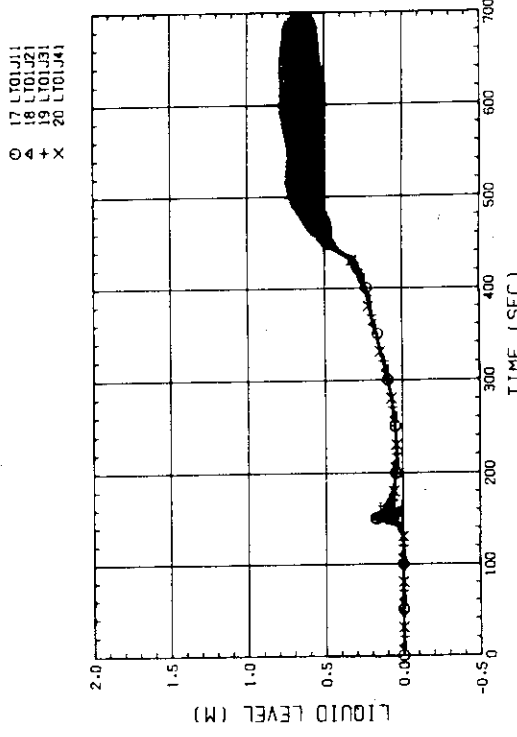


Fig. F-11(a) LIQUID LEVEL ABOVE UCSP
(BUNDLE 1,2,3,4)

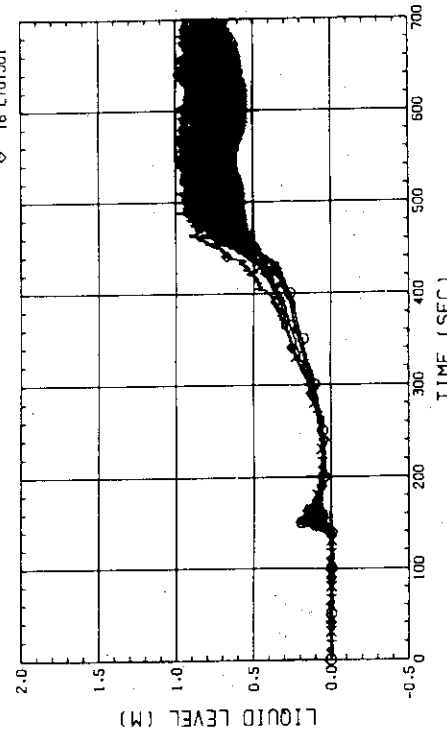


Fig. F-12(a) LIQUID LEVEL ABOVE UCSP
(BUNDLE 1,2,3,4)

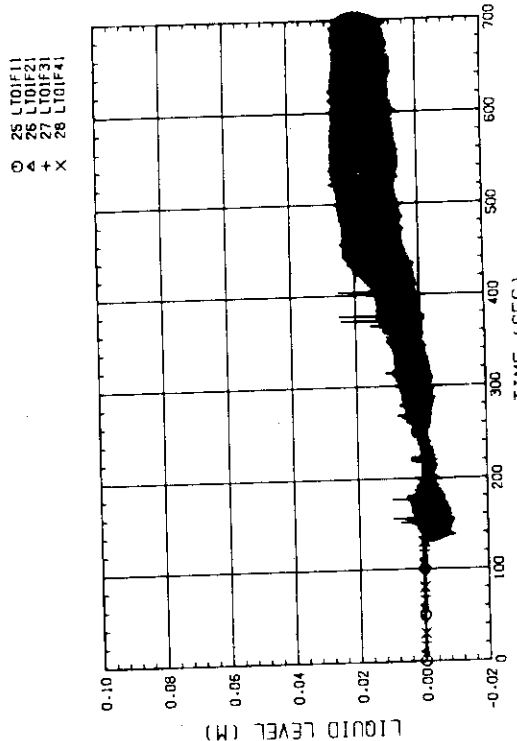


Fig. F-11(b) LIQUID LEVEL ABOVE END BOX TIE PLATE
(BUNDLE 5,6,7,8)

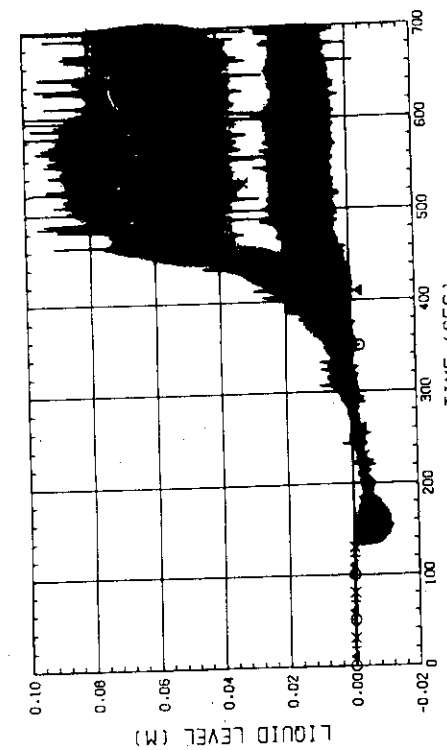
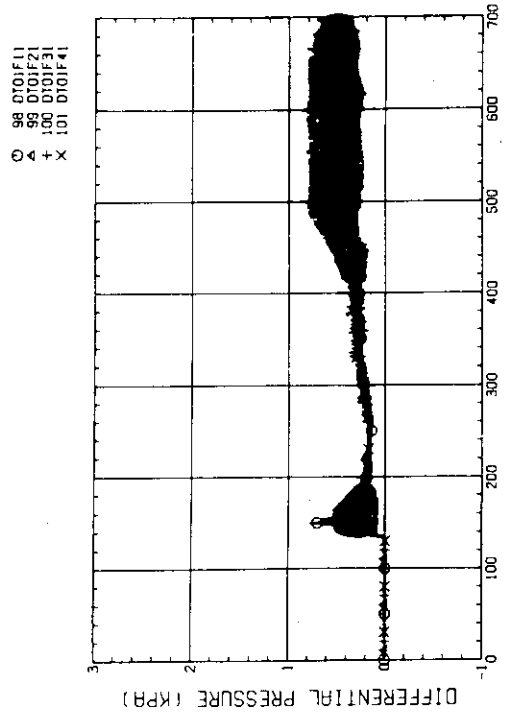
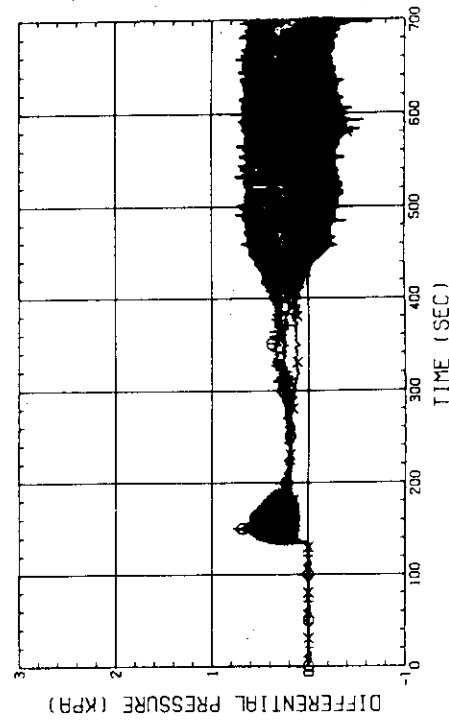
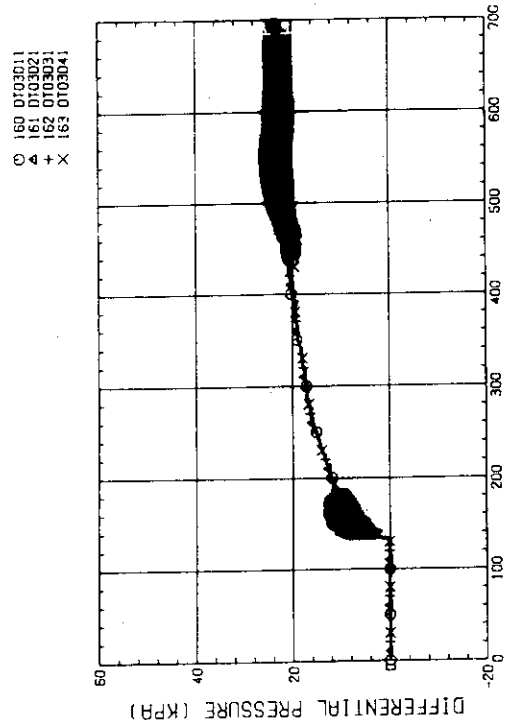
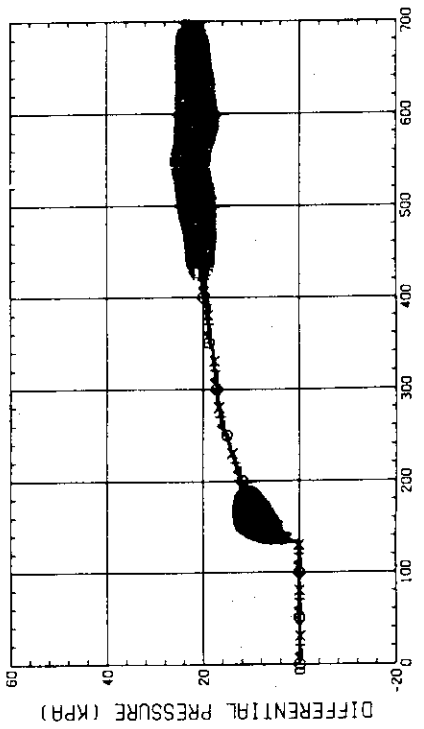


Fig. F-12(b) LIQUID LEVEL ABOVE END BOX TIE PLATE
(BUNDLE 5,6,7,8)

Fig. F-14(a) DIFFERENTIAL PRESSURE ACROSS END BOX TIE PLATE
(BUNDLE 1, 2, 3, 4)Fig. F-14(b) DIFFERENTIAL PRESSURE ACROSS END BOX TIE PLATE
(BUNDLE 5, 6, 7, 8)Fig. F-13(a) DIFFERENTIAL PRESSURE OF CORE FULL HEIGHT
(BUNDLE 1, 2, 3, 4)Fig. F-13(b) DIFFERENTIAL PRESSURE OF CORE FULL HEIGHT
(BUNDLE 5, 6, 7, 8)

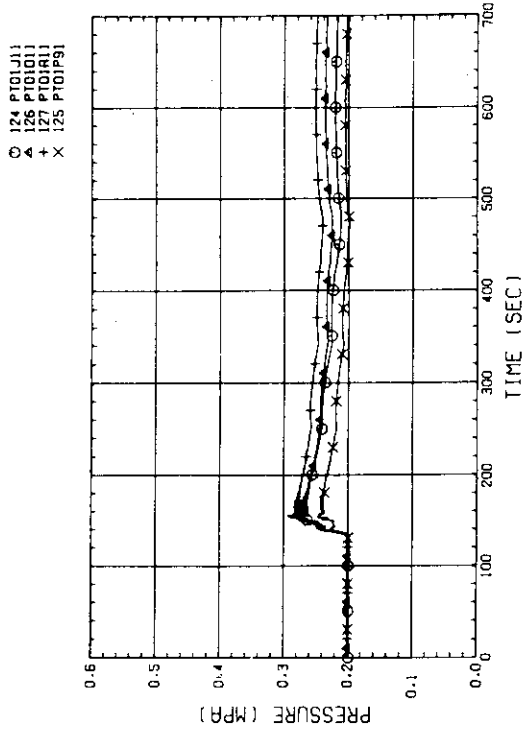


Fig. F-16 PRESSURE IN PV (U - TOP OF PV, D - CORE CENTER, R - CORE INLET, P - BELOW COLD LEG NOZZLE IN DOWNCOMER)

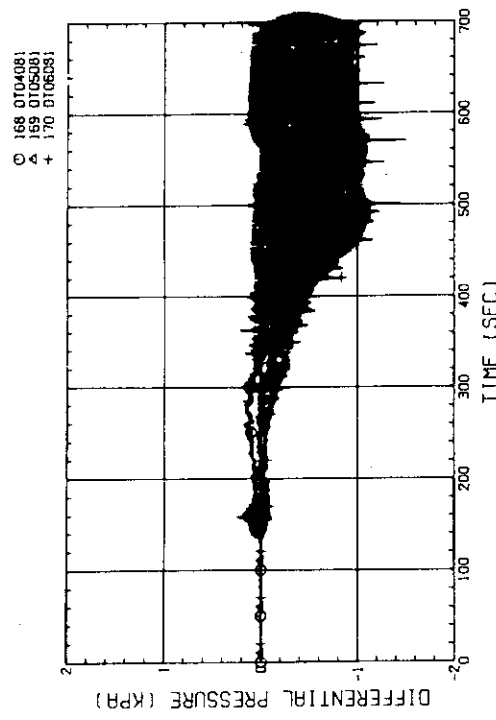


Fig. F-15 (a) DIFFERENTIAL PRESSURE, HORIZONTAL BUNDLE 5-8 (04-BELOW SPACER 4, 05-BELOW SPACER 6, 06-BELOW END BOX)

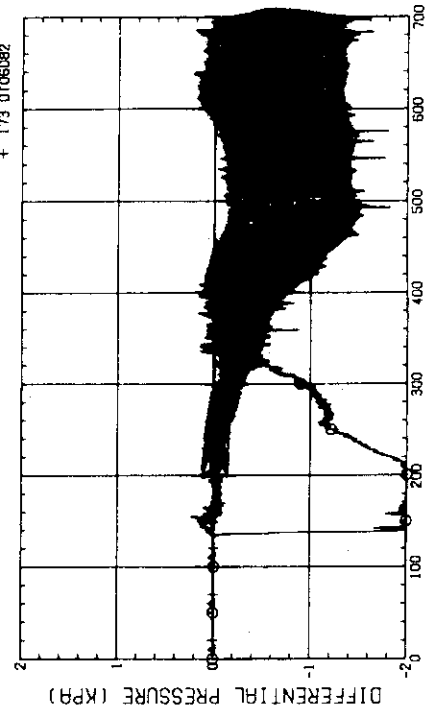


Fig. F-15 (b) DIFFERENTIAL PRESSURE, HORIZONTAL BUNDLE 1-8 (04-BELOW SPACER 4, 05-BELOW SPACER 6, 06-BELOW END BOX)

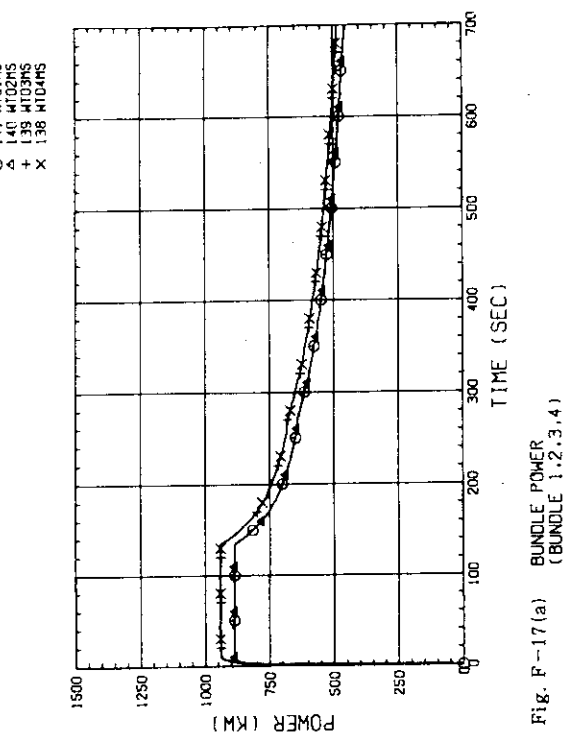


Fig. F-17(a) BUNDLE POWER
(BUNDLE 1,2,3,4)

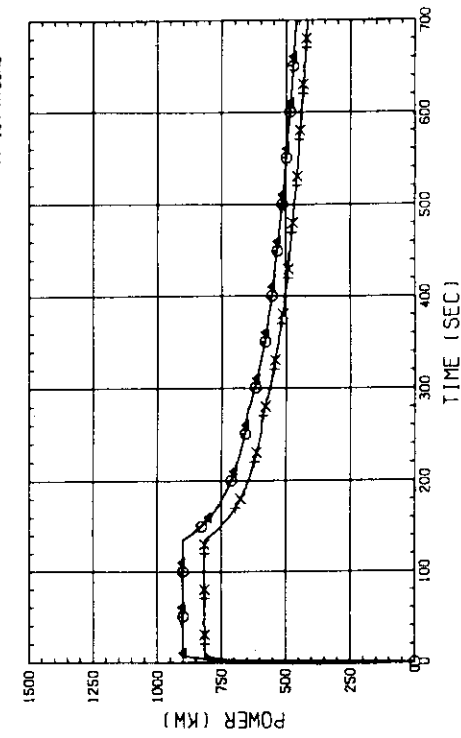


Fig. F-17(b) BUNDLE POWER
(BUNDLE 5,6,7,8)

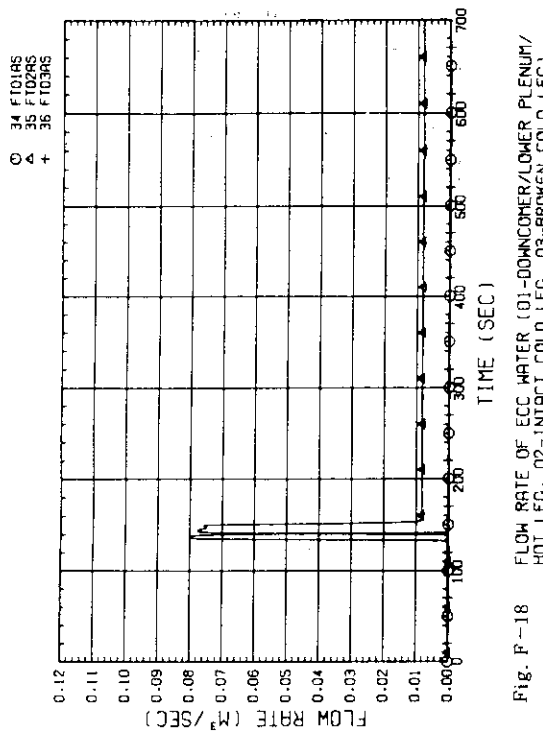


Fig. F-18 FLOW RATE OF ECC WATER (01-DOWNCOMER/LOWER PLENUM/
HOT LEG, 02-INTEGRAL COLD LEG, 03-BROKEN COLD LEG)

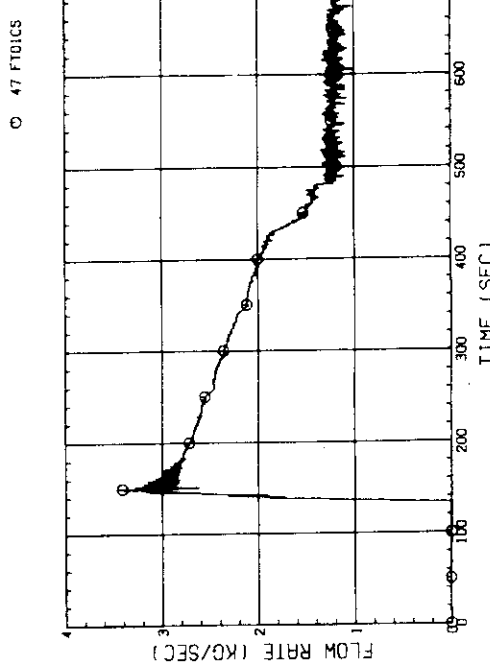


Fig. F-19(a) MASS FLOW RATE OF INTACT COLD LEG

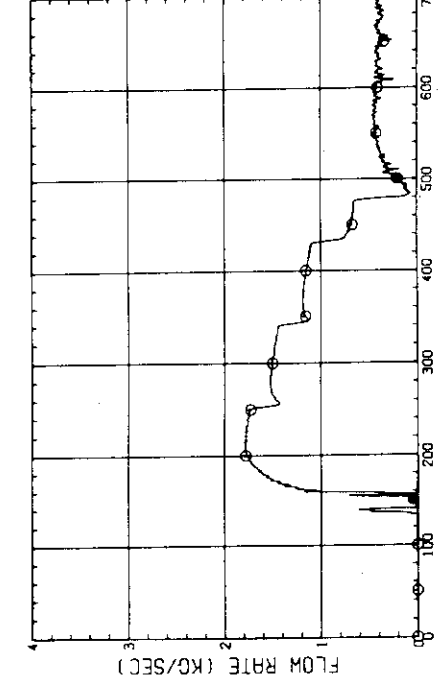


Fig. F-19(c) MASS FLOW RATE FROM CONTAINMENT TANK-1 TO CONTAINMENT TANK-11

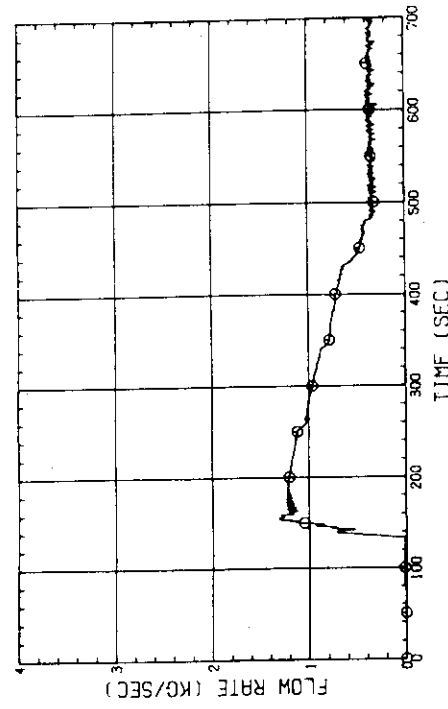


Fig. F-19(b) MASS FLOW RATE OF BROKEN COLD LEG - STEAM/WATER
SEPARATOR SIDE

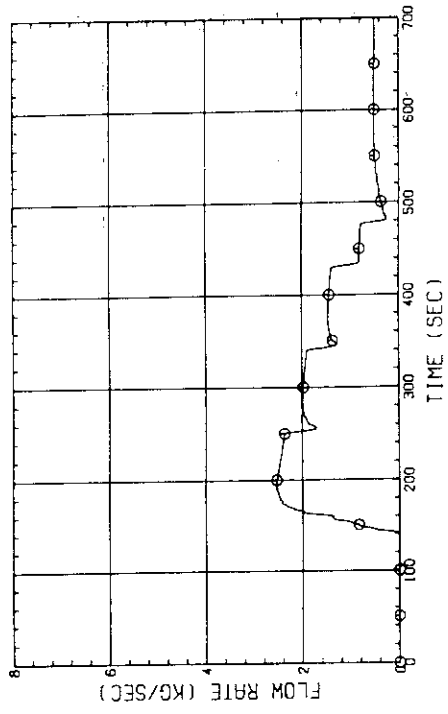


Fig. F-20 STEAM FLOW RATE OF DISCHARGE FROM CONTAINMENT TANK-11

Appendix G

Selected Data for Test S1-21 (Run 531)

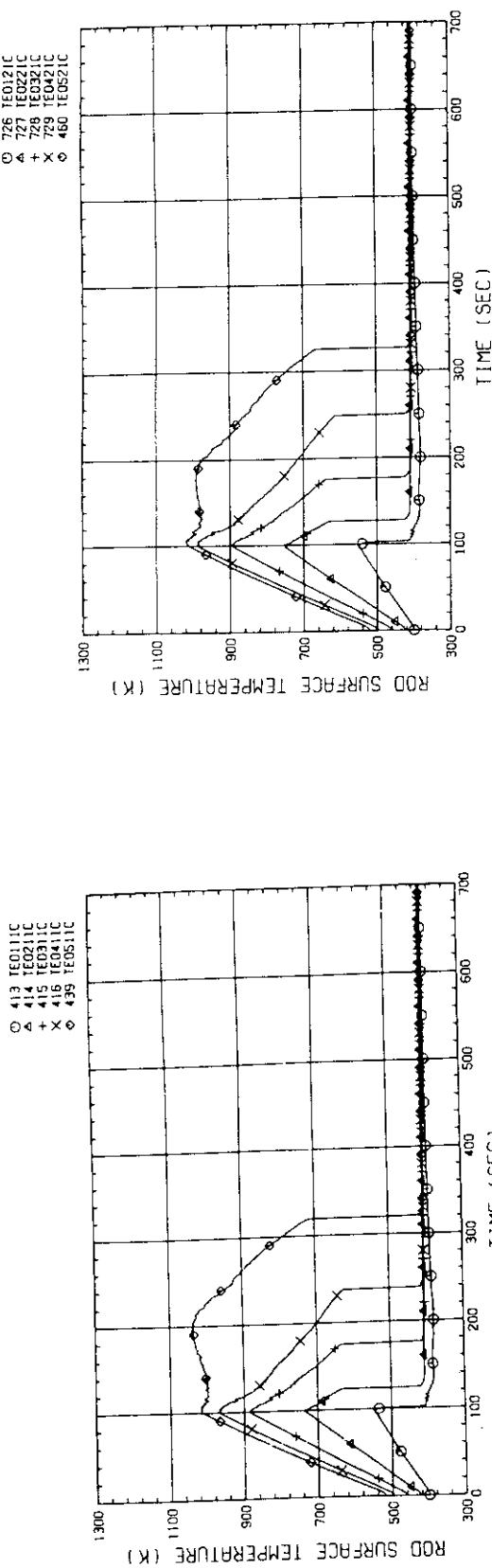


Fig. G-1(a) HEATER ROD TEMPERATURE
(BUNDLE 1-1C, LOWER HALF)

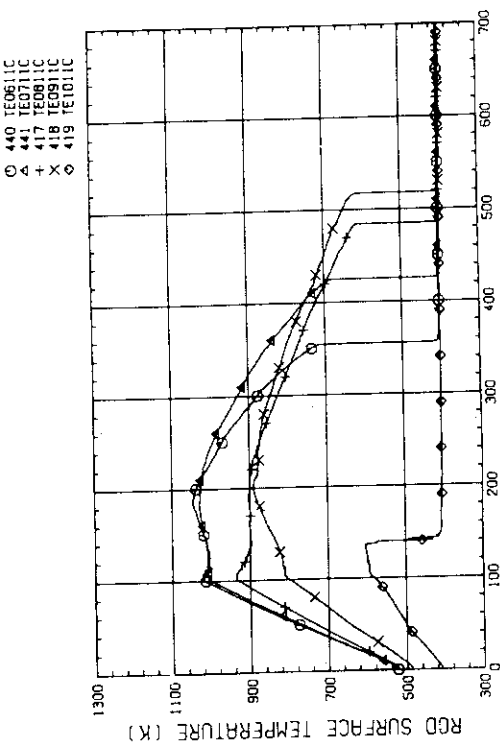


Fig. G-1(b) HEATER ROD TEMPERATURE
(BUNDLE 1-1C, UPPER HALF)

Fig. G-2 (a) HEATER ROD TEMPERATURE
(BUNDLE 2-1C, LOWER HALF)

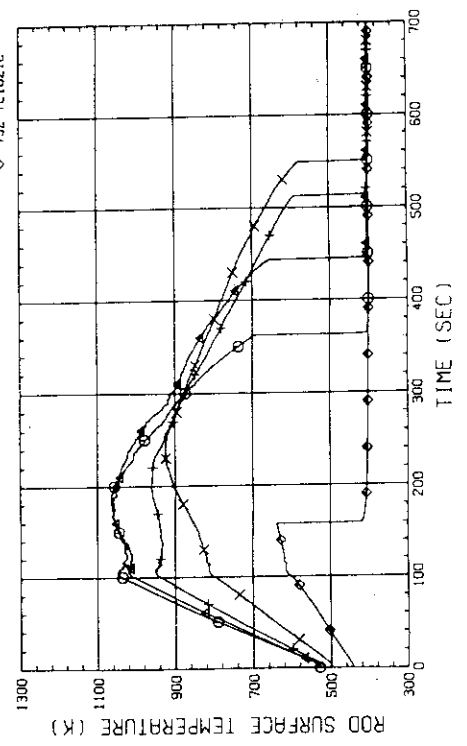
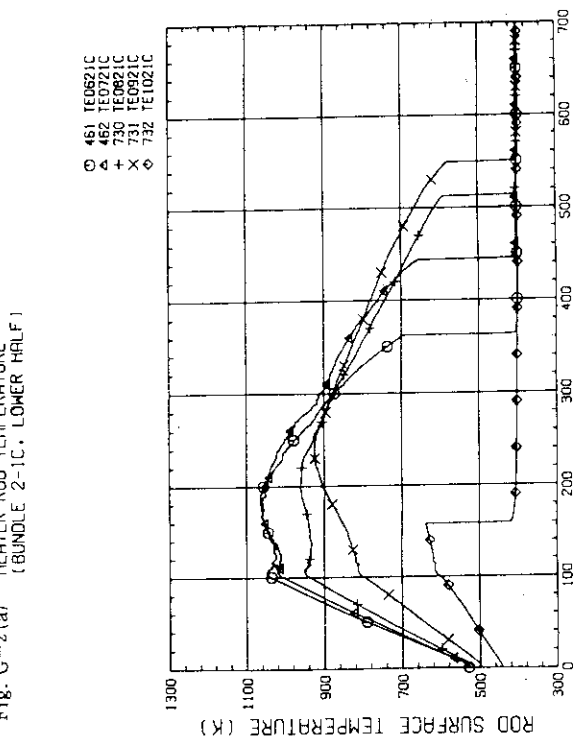


Fig. G-2 (b) HEATER ROD TEMPERATURE
(BUNDLE 2-1C, UPPER HALF)



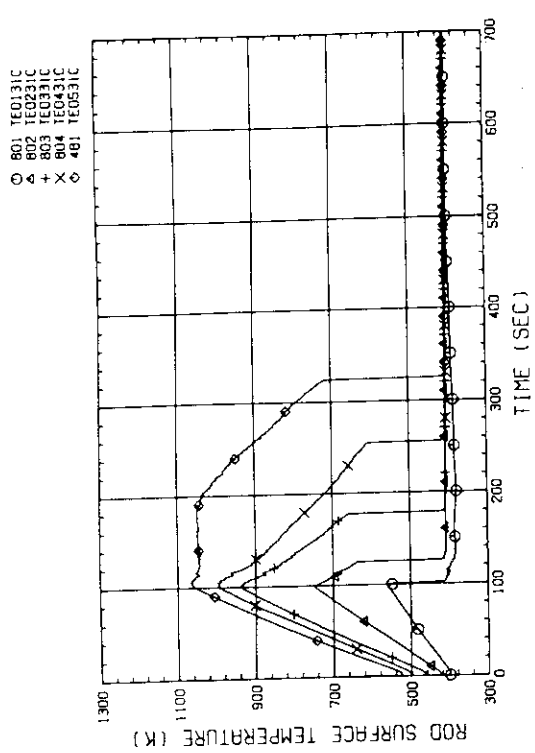


Fig. G-3(a) HEATER ROD TEMPERATURE
(BUNDLE 3-1C, LOWER HALF)

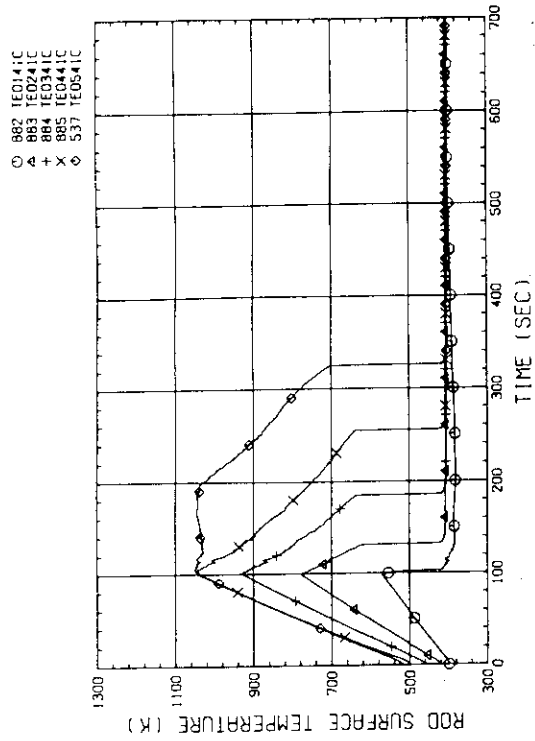


Fig. G-4(a) HEATER ROD TEMPERATURE
(BUNDLE 4-1C, LOWER HALF)

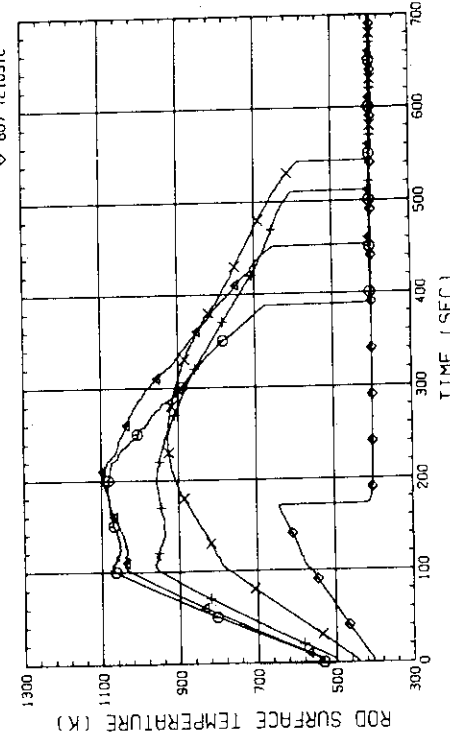


Fig. G-3(b) HEATER ROD TEMPERATURE
(BUNDLE 3-1C, UPPER HALF)

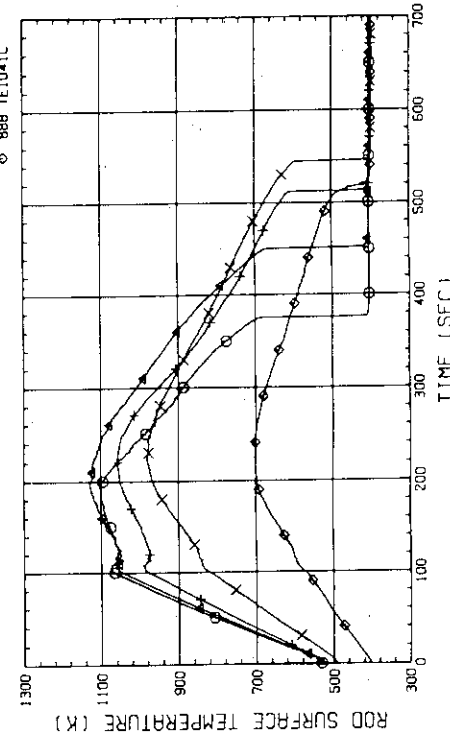


Fig. G-4(b) HEATER ROD TEMPERATURE
(BUNDLE 4-1C, UPPER HALF)

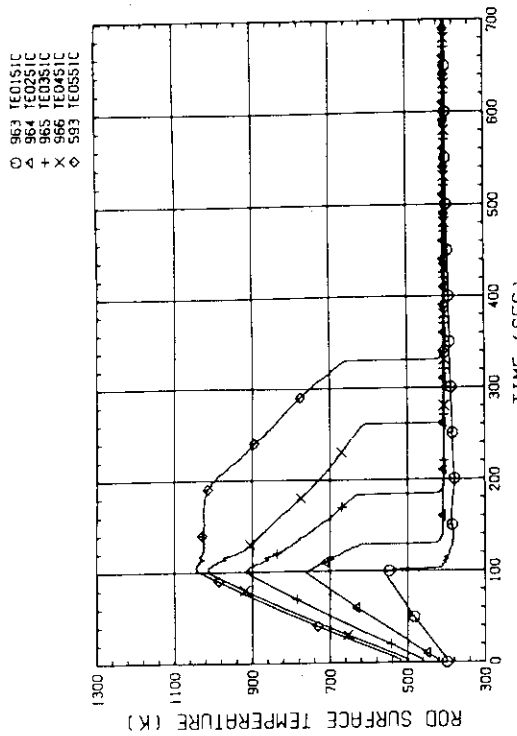


Fig. G-5(a) HEATER ROD TEMPERATURE
(BUNDLE 5-1C, LOWER HALF)

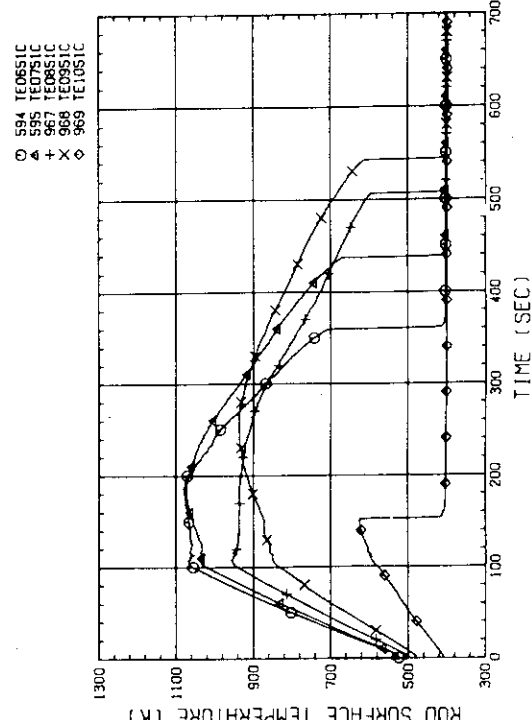


Fig. G-5(b) HEATER ROD TEMPERATURE
(BUNDLE 5-1C, UPPER HALF)

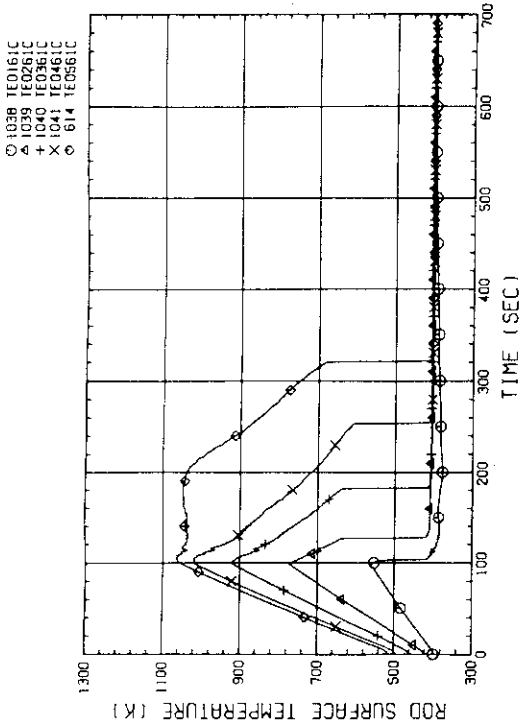


Fig. G-6(a) HEATER ROD TEMPERATURE
(BUNDLE 6-1C, LOWER HALF)

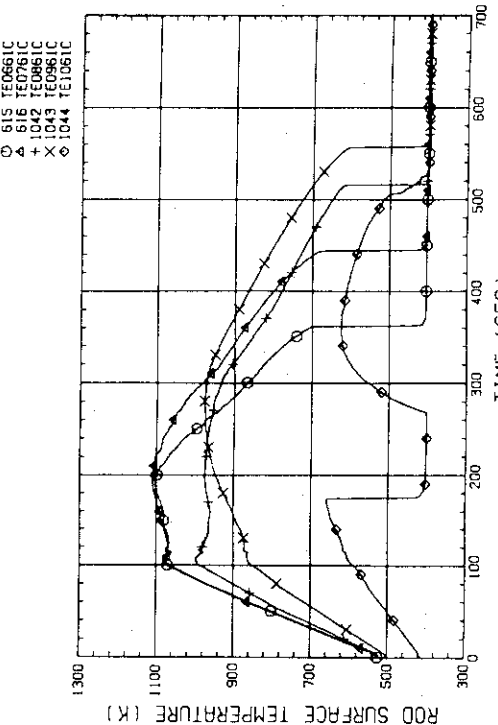


Fig. G-6(b) HEATER ROD TEMPERATURE
(BUNDLE 6-1C, UPPER HALF)

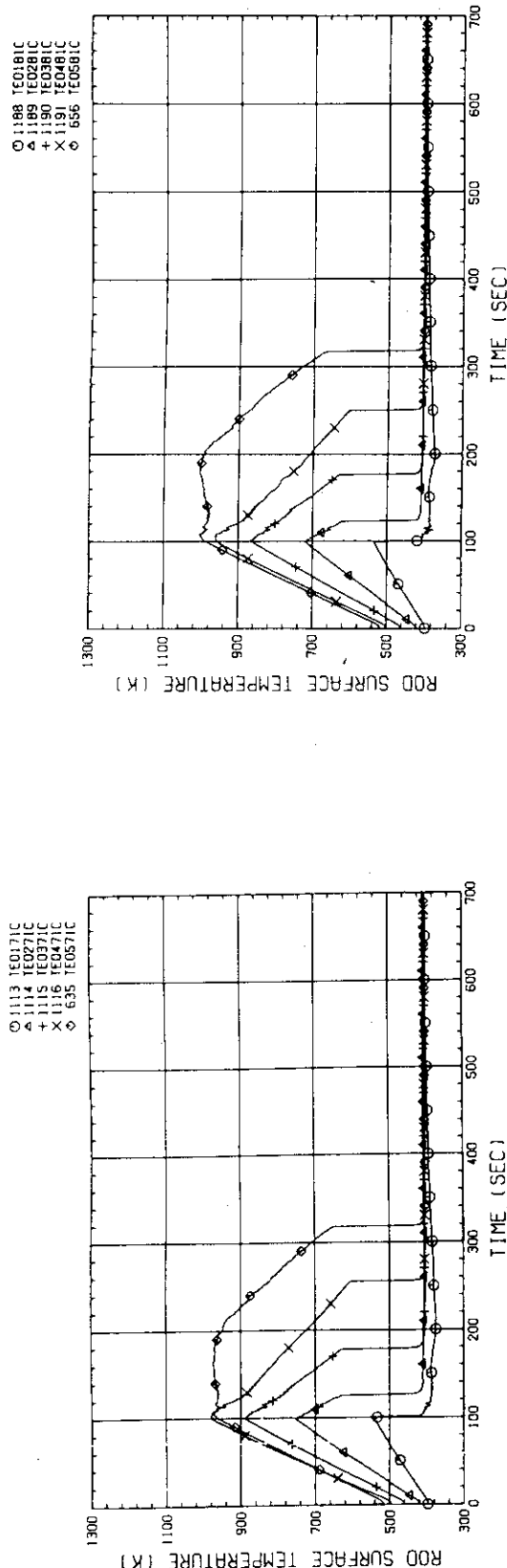


Fig. G-7(a) HEATER ROD TEMPERATURE (K)
(BUNDLE 7-1C, LOWER HALF)

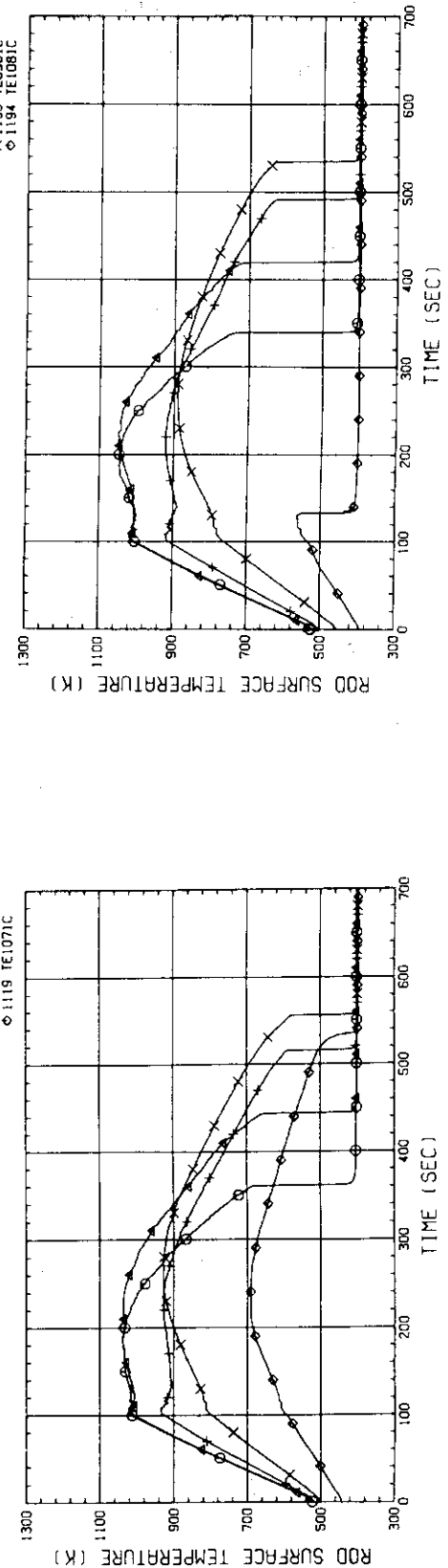


Fig. G-7(b) HEATER ROD TEMPERATURE (K)
(BUNDLE 7-1C, UPPER HALF)

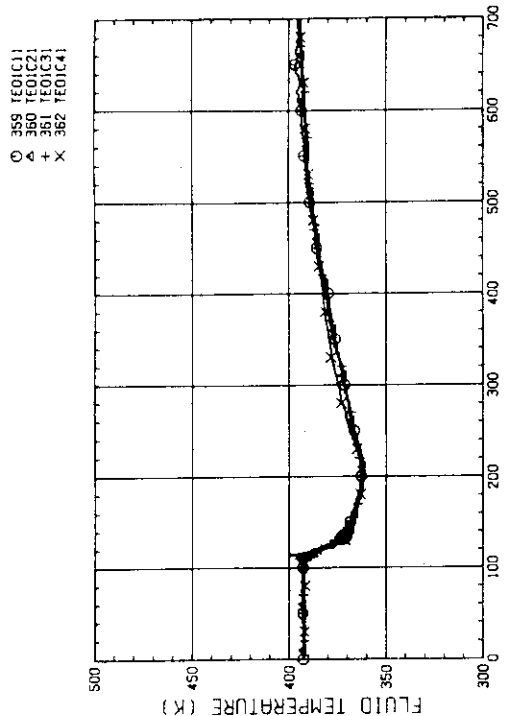


Fig. G-9(a) FLUID TEMPERATURE AT CORE INLET
(BUNDLE 1.2.3.4. 100MM BELOW HEATED PART)

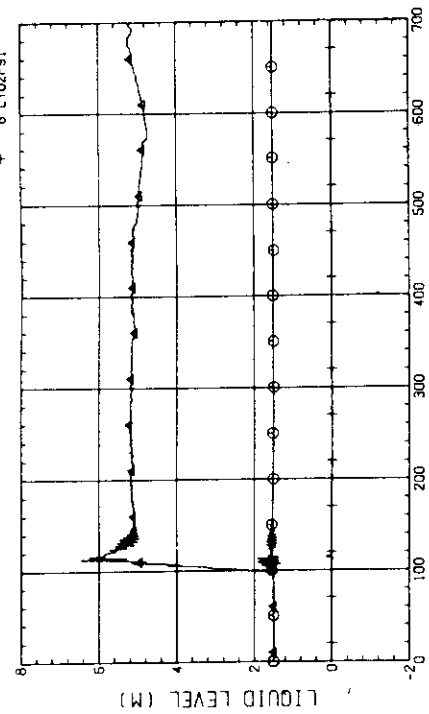


Fig. G-10 LIQUID LEVEL IN DOWNCOMER (L101P91)-BELOW CORE INLET
01P92-BOTTOM TO COLD LEG. 02P91-COLD LEG TO TOP OF PV1

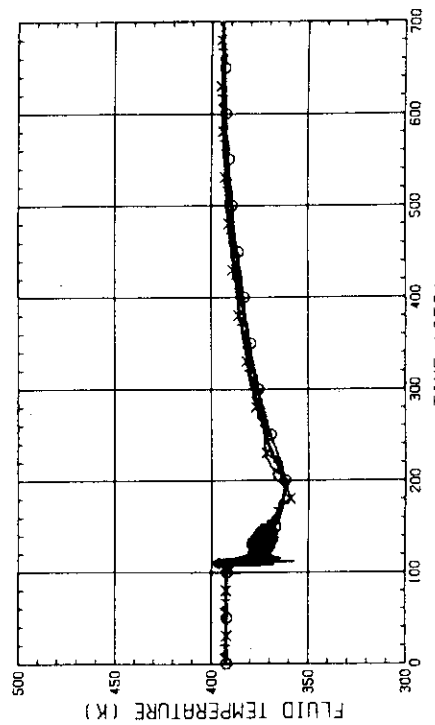


Fig. G-9(b) FLUID TEMPERATURE AT CORE INLET
(BUNDLE 5.6.7.8. 100MM BELOW HEATED PART)

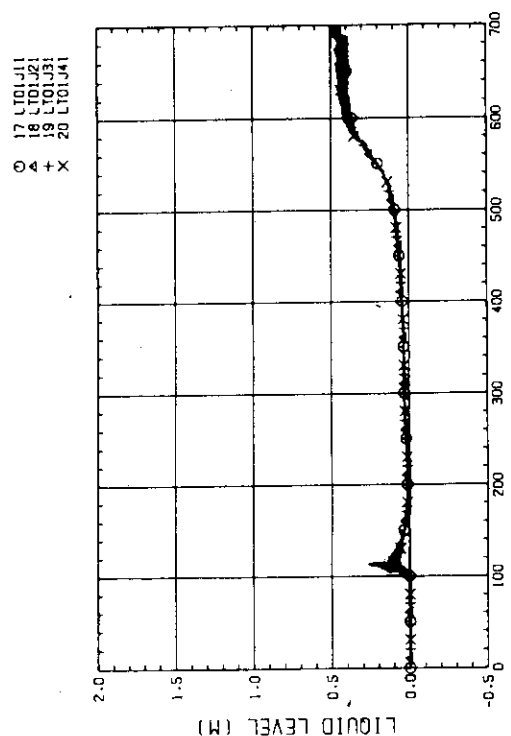


Fig. G-12(a) LIQUID LEVEL ABOVE UCSP
(BUNDLE 1,2,3,4)

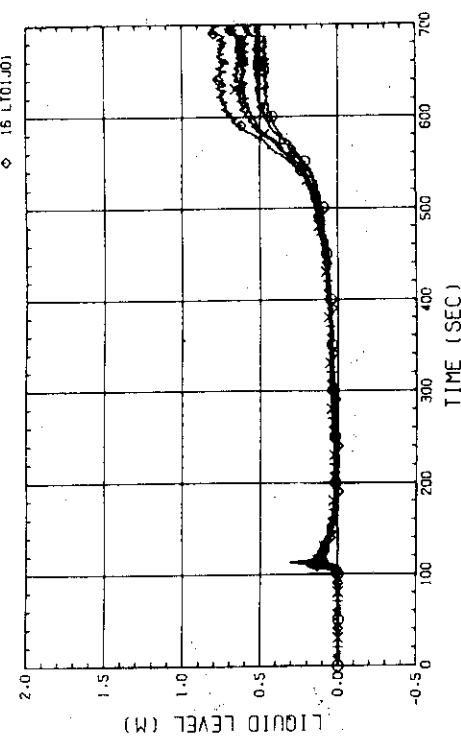


Fig. G-12(b) LIQUID LEVEL ABOVE UCSP
(BUNDLE 5,6,7,8 AND CORE BAFFLE)

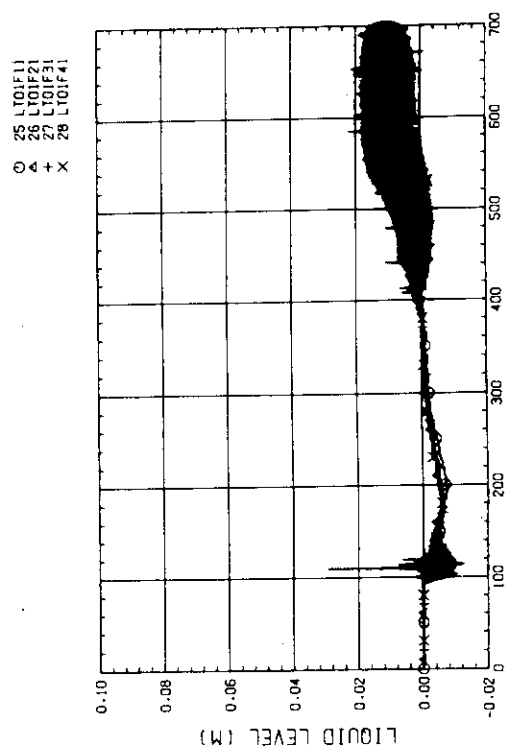


Fig. G-11(a) LIQUID LEVEL ABOVE END BOX TIE PLATE
(BUNDLE 1,2,3,4)

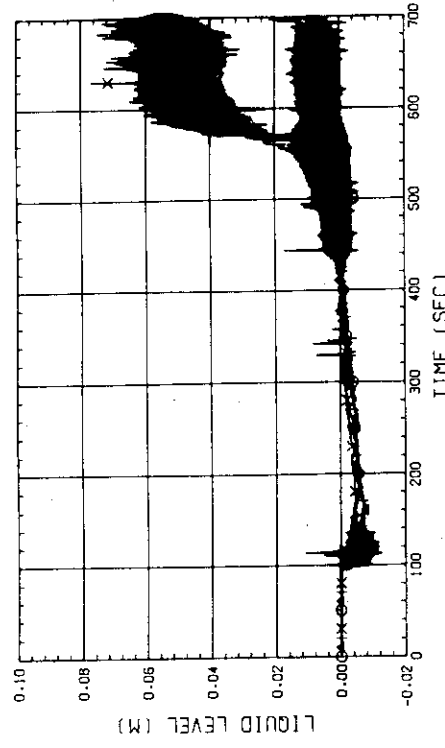


Fig. G-11(b) LIQUID LEVEL ABOVE END BOX TIE PLATE
(BUNDLE 5,6,7,8)

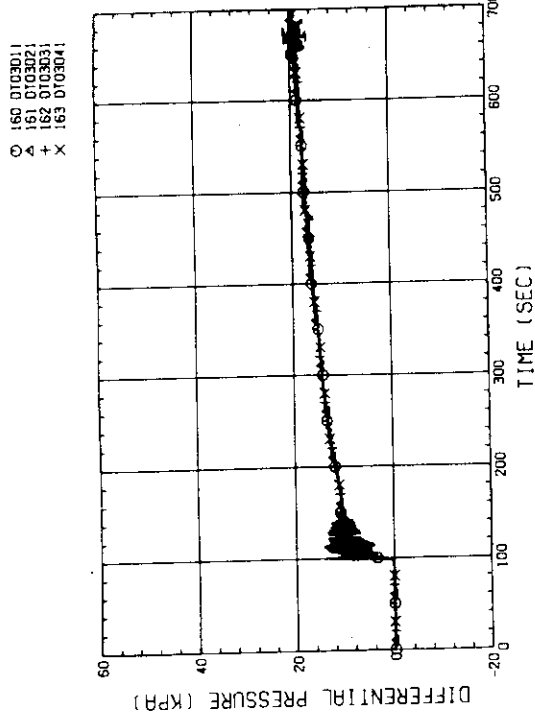


Fig. G-13(a) DIFFERENTIAL PRESSURE OF CORE FULL HEIGHT
(BUNDLE 1,2,3,4)

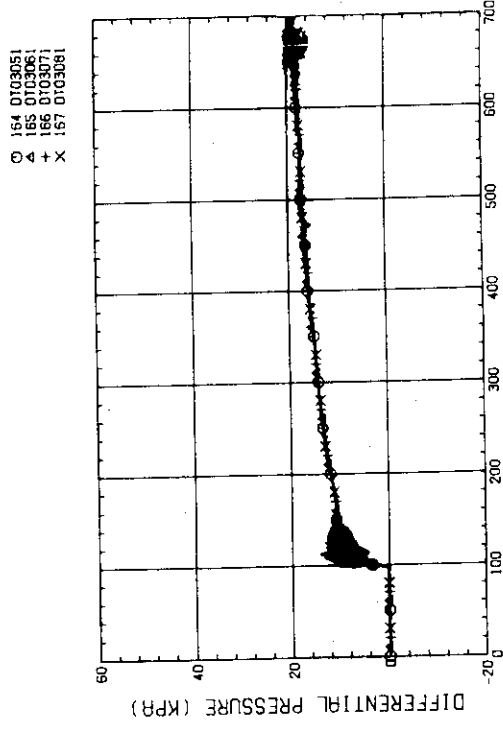


Fig. G-13(b) DIFFERENTIAL PRESSURE OF CORE FULL HEIGHT
(BUNDLE 5,6,7,8)

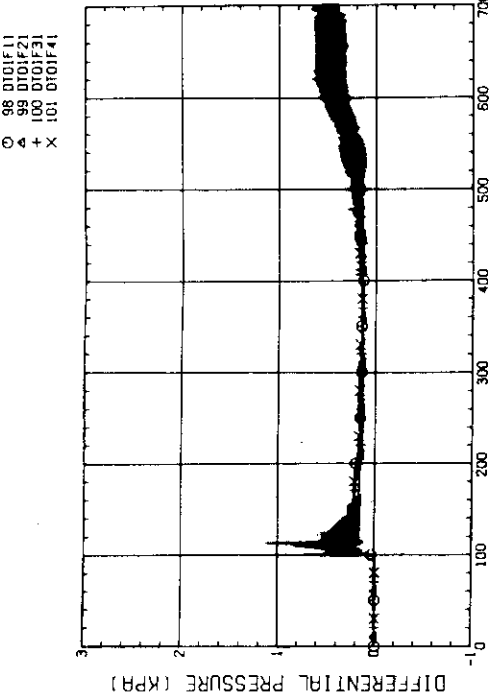


Fig. G-14 (a) DIFFERENTIAL PRESSURE ACROSS END BOX TIE PLATE
(BUNDLE 1,2,3,4)

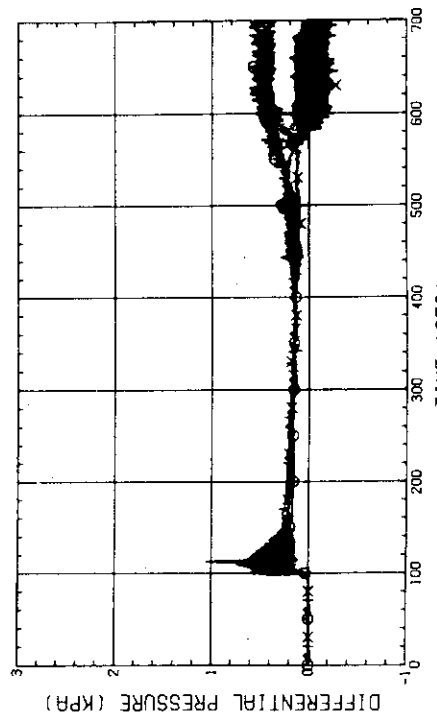


Fig. G-14 (b) DIFFERENTIAL PRESSURE ACROSS END BOX TIE PLATE
(BUNDLE 5,6,7,8)

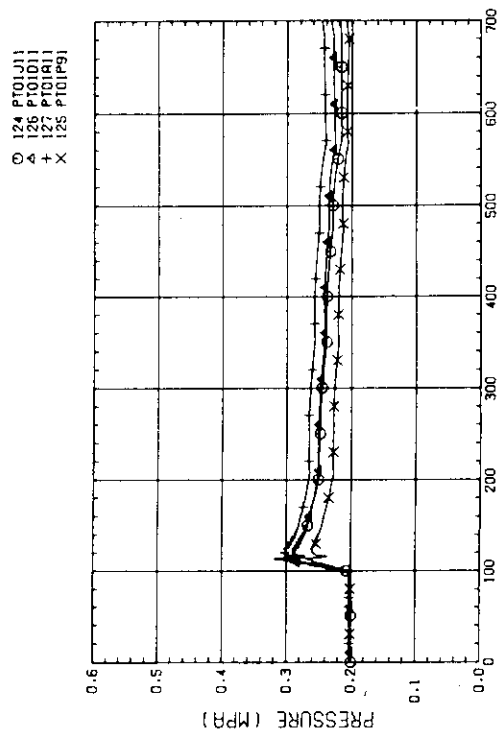


Fig. G-16 PRESSURE IN PV () - TOP OF PV, D - CORE CENTER, A - CORE INLET, P - BELOW COLD LEG NOZZLE IN DOWNCOMER

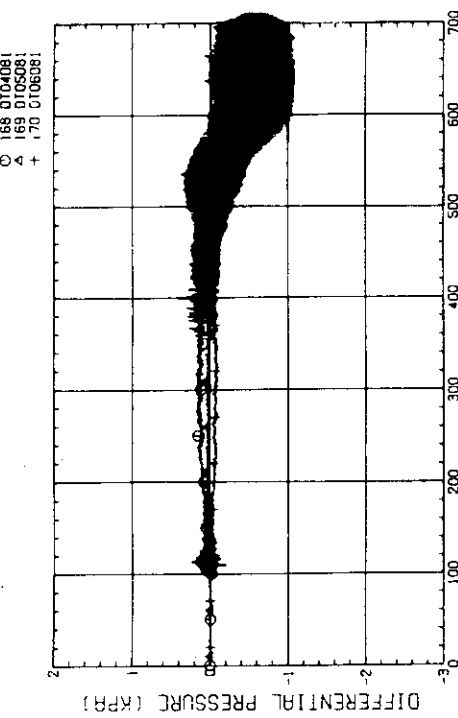


Fig. G-15(a) DIFFERENTIAL PRESSURE, HORIZONTAL BUNDLE 5-8 (04-BELOW SPACER 4, 05-BELOW SPACER 6, 06-BELOW END BOX)

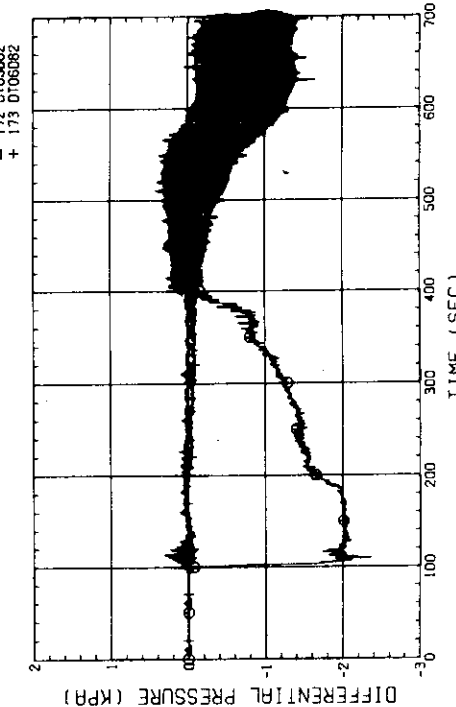


Fig. G-15(b) DIFFERENTIAL PRESSURE, HORIZONTAL BUNDLE 1-8 (04-BELOW SPACER 4, 05-BELOW SPACER 6, 06-BELOW END BOX)

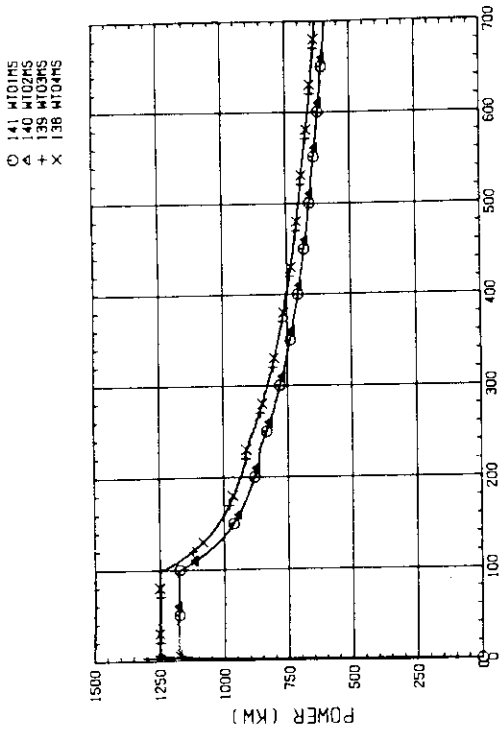


Fig. G-17 (a) BUNDLE POWER (BUNDLE 1,2,3,4)

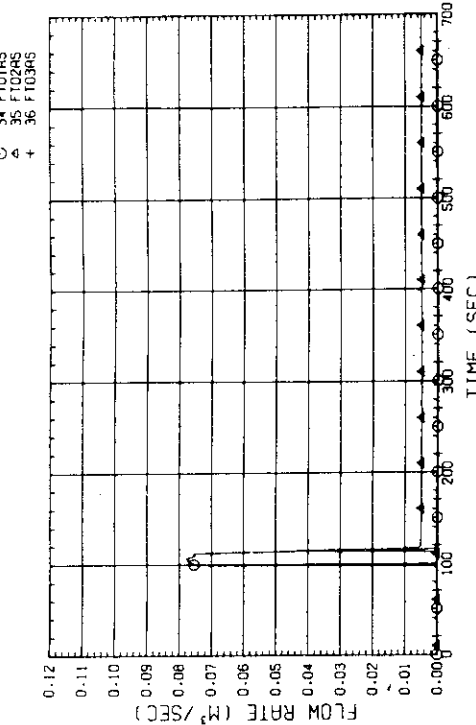


Fig. G-18 FLOW RATE OF ECC WATER (01-DOWNCOMER/LOWER PLenum/HOT LEG, 02-INTACT COLD LEG, 03-BROKEN COLD LEG)

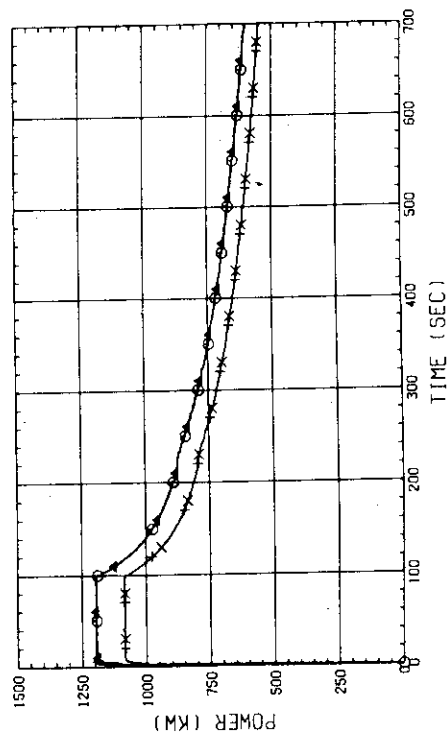


Fig. G-17 (b) BUNDLE POWER (BUNDLE 5,6,7,8)

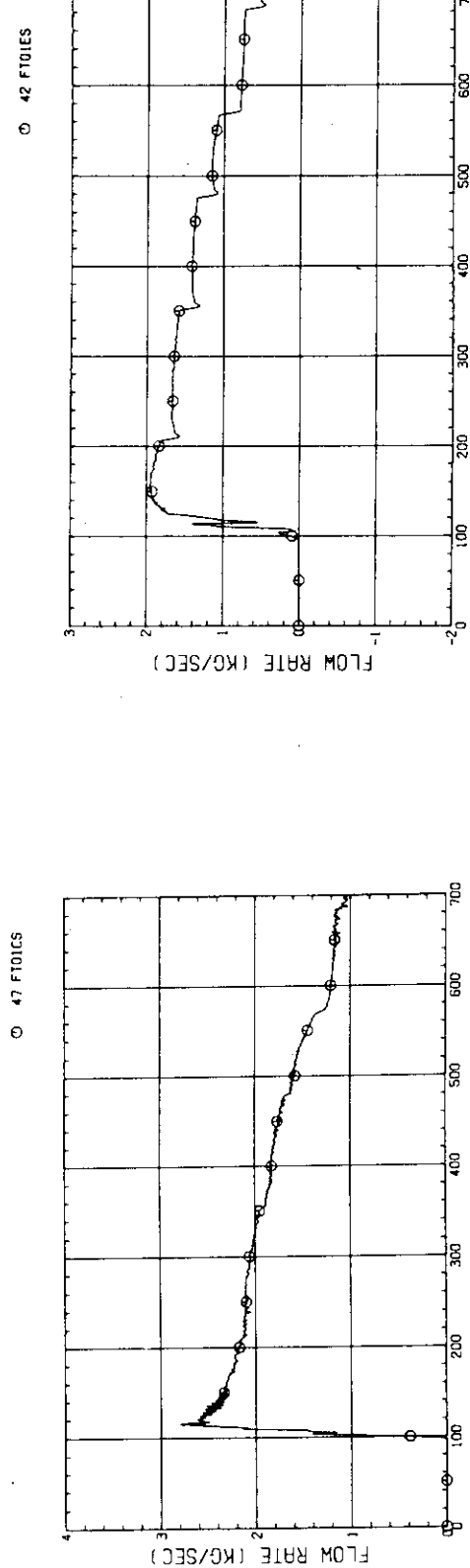


Fig. G-19(a) MASS FLOW RATE OF INTACT COLD LEG

Fig. G-19(c) MASS FLOW RATE FROM CONTAINMENT TANK-1 TO CONTAINMENT TANK-11

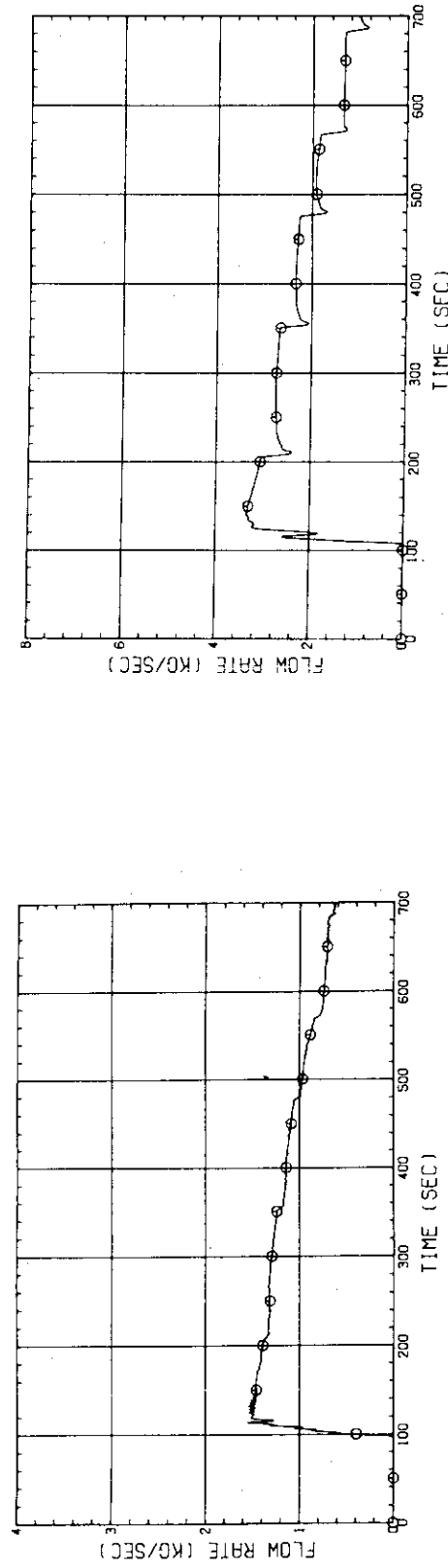
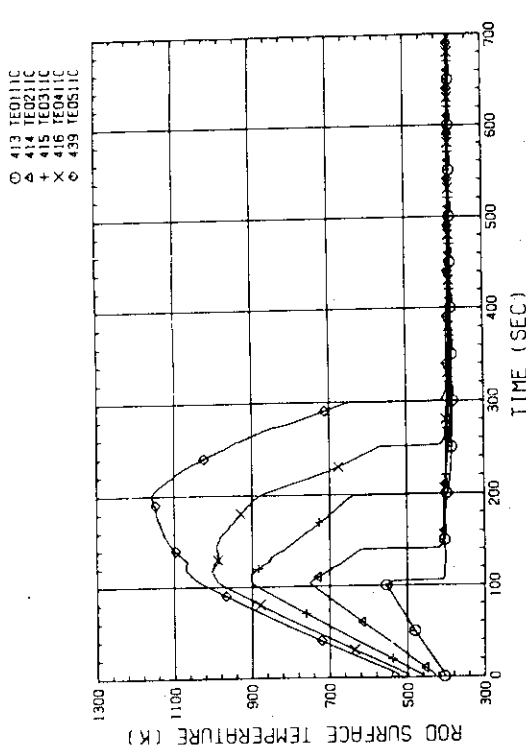
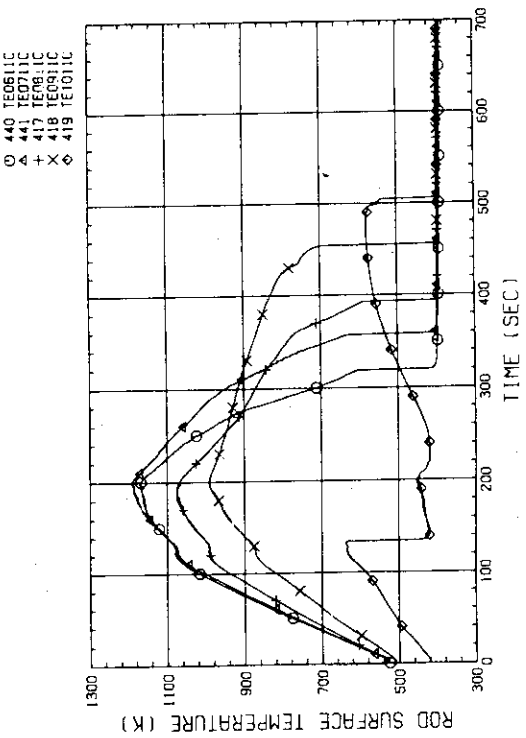
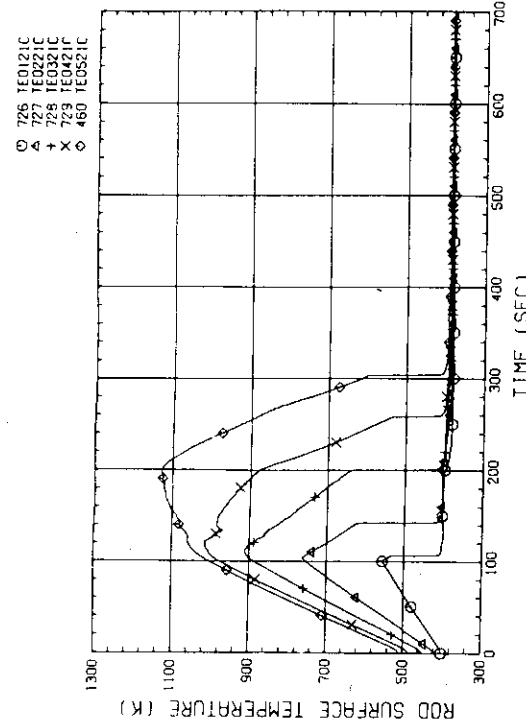
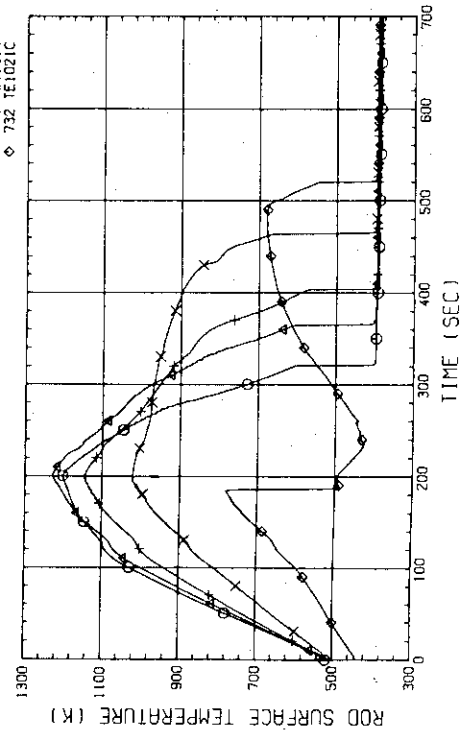


Fig. G-19(b) MASS FLOW RATE OF BROKEN COLD LEG - SEPARATOR SIDE

Fig. G-20 STEAM FLOW RATE OF DISCHARGE FROM CONTAINMENT TANK-11

Appendix H

Selected Data for Test S1-23 (Run 536)

Fig. H-1(a) HEATER ROD TEMPERATURE
(BUNDLE 1-1C, LOWER HALF)Fig. H-1(b) HEATER ROD TEMPERATURE
(BUNDLE 1-1C, UPPER HALF)Fig. H-2(a) HEATER ROD TEMPERATURE
(BUNDLE 2-1C, LOWER HALF)Fig. H-2(b) HEATER ROD TEMPERATURE
(BUNDLE 2-1C, UPPER HALF)

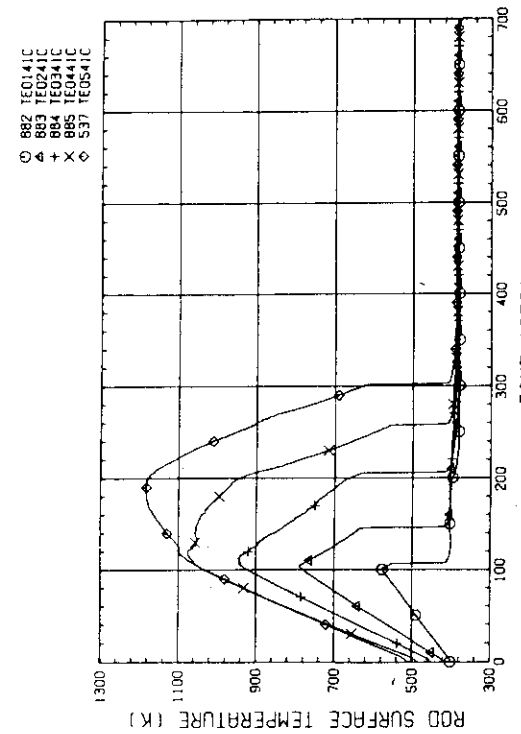


Fig. H-3(a) HEATER ROD TEMPERATURE
(BUNDLE 3-iC, LOWER HALF)

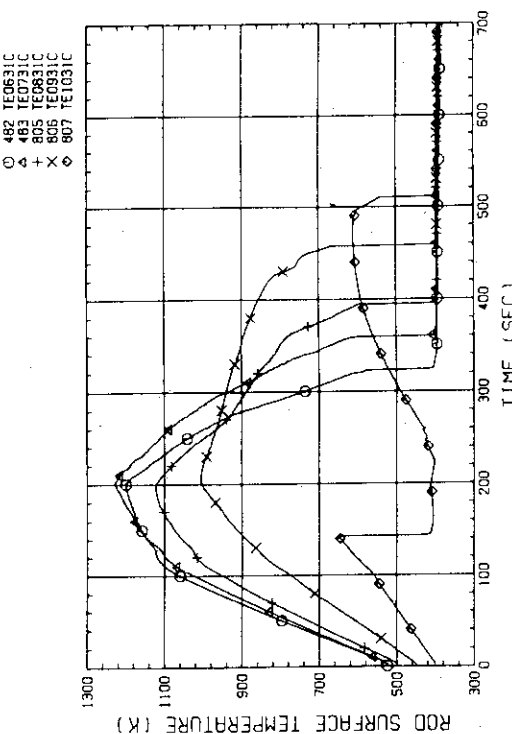


Fig. H-3(b) HEATER ROD TEMPERATURE
(BUNDLE 3-iC, UPPER HALF)

Fig. H-4(a) HEATER ROD TEMPERATURE
(BUNDLE 4-1C, LOWER HALF)

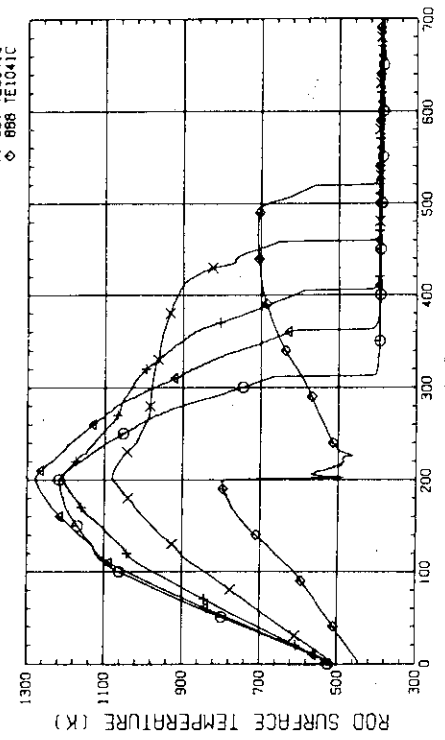
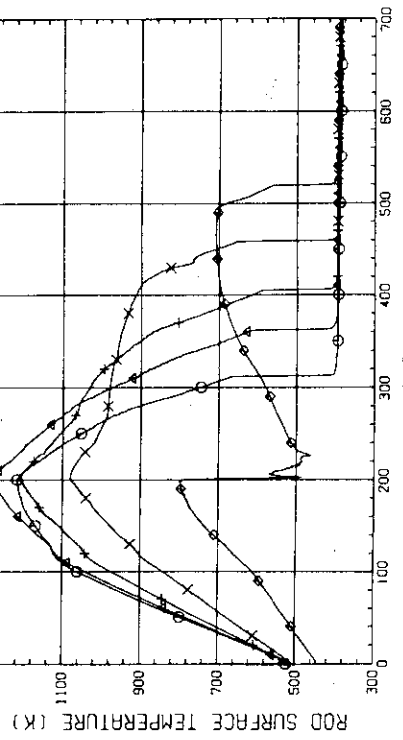
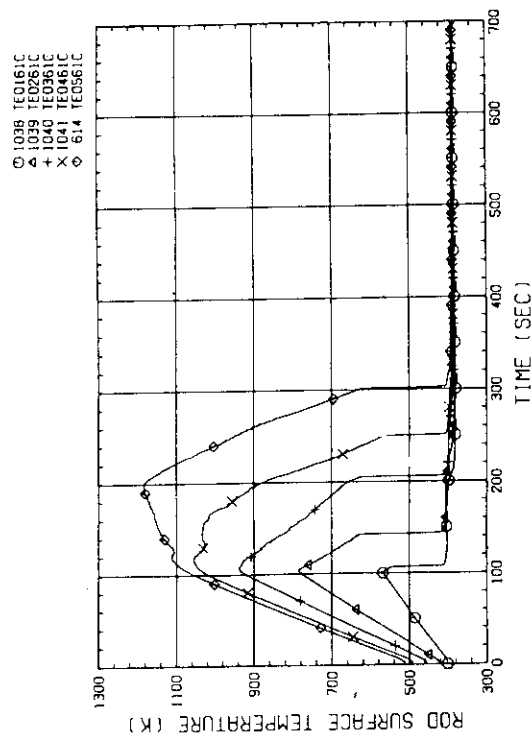
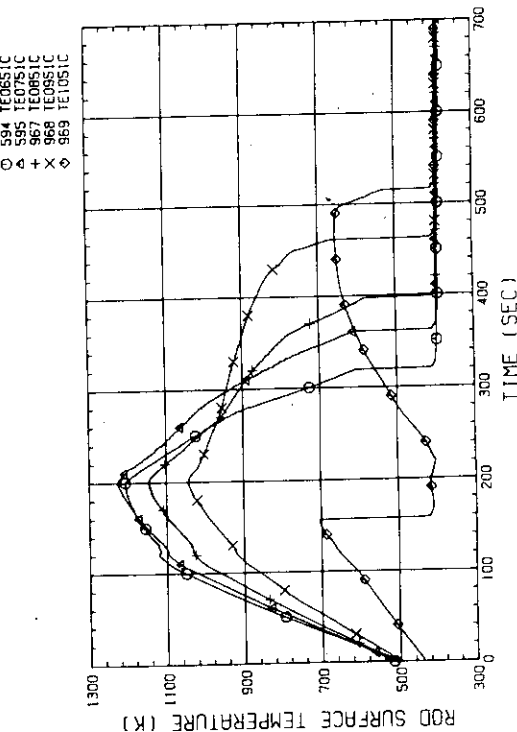
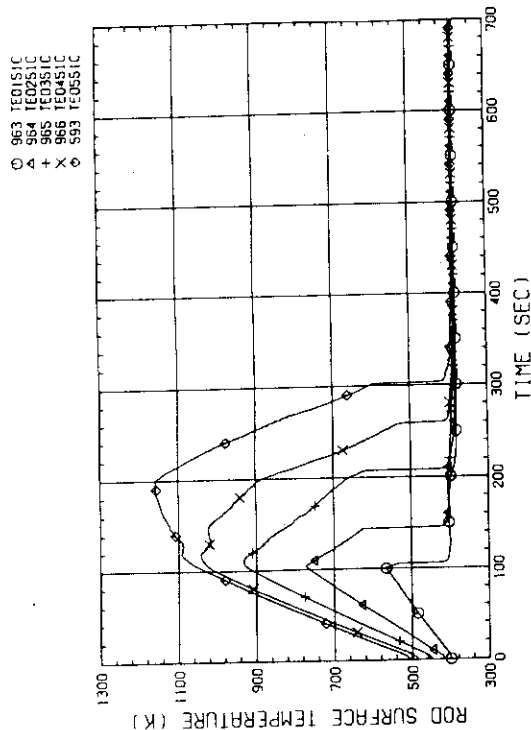
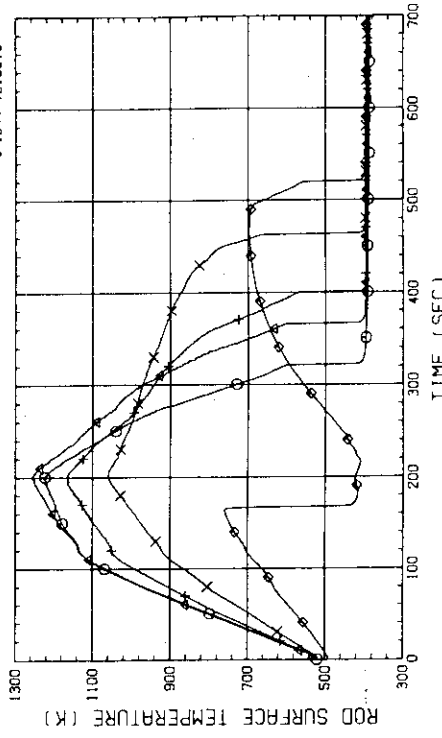


Fig. H-4(b) HEATER ROD TEMPERATURE
(BUNDLE 4-1C, UPPER HALF)



Fig. H-5(a) HEATER ROD TEMPERATURE (K)
(BUNDLE S-1C, LOWER HALF)Fig. H-5(b) HEATER ROD TEMPERATURE (K)
(BUNDLE S-1C, UPPER HALF)Fig. H-6(a) HEATER ROD TEMPERATURE (K)
(BUNDLE 6-1C, LOWER HALF)Fig. H-6(b) HEATER ROD TEMPERATURE (K)
(BUNDLE 6-1C, UPPER HALF)

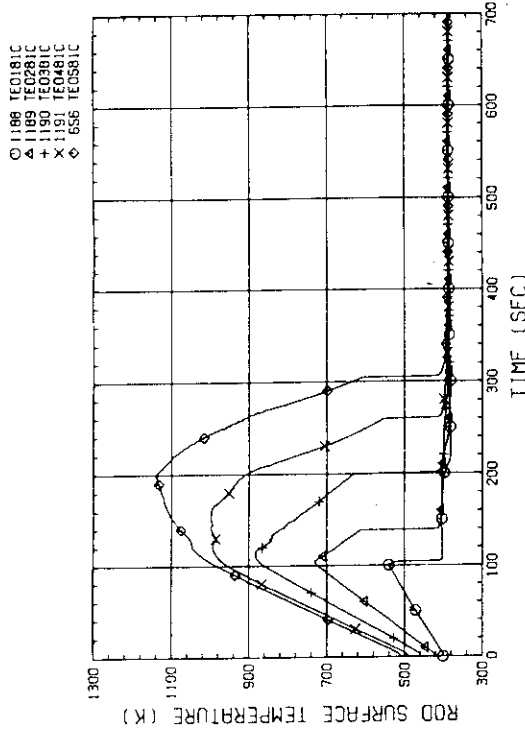


Fig. H-7 (a) HEATER ROD TEMPERATURE
(BUNDLE 7-1C, LOWER HALF)

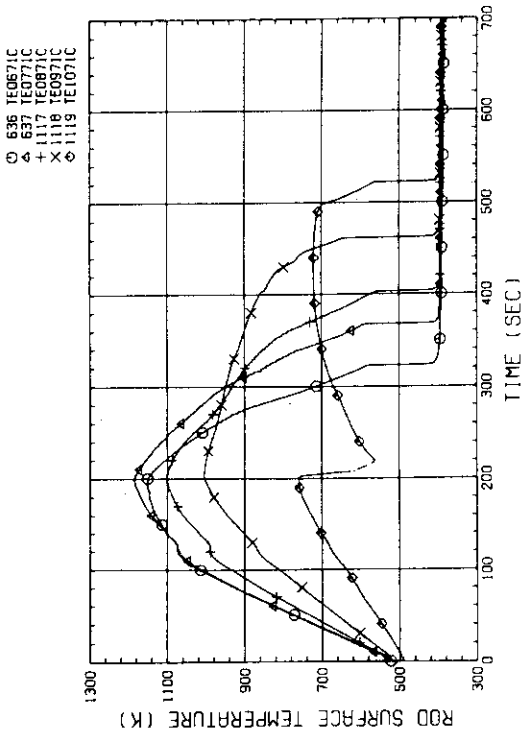


Fig. H-7 (b) HEATER ROD TEMPERATURE
(BUNDLE 7-1C, UPPER HALF)

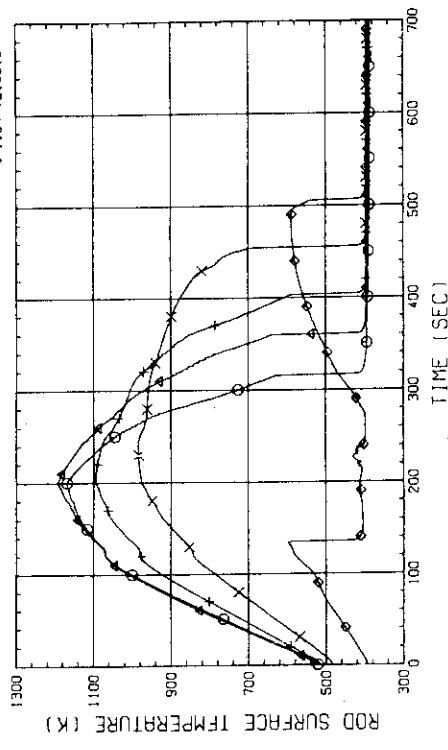


Fig. H-8 (a) HEATER ROD TEMPERATURE
(BUNDLE 8-1C, LOWER HALF)

-

-

-

-

-

-

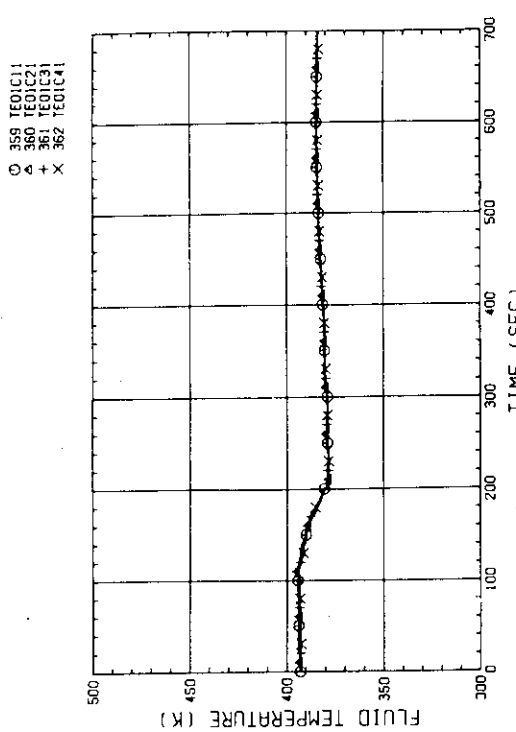


Fig. H-9(a) FLUID TEMPERATURE AT CORE INLET
(BUNDLE 1,2,3,4, 100MM BELOW HEATED PART)

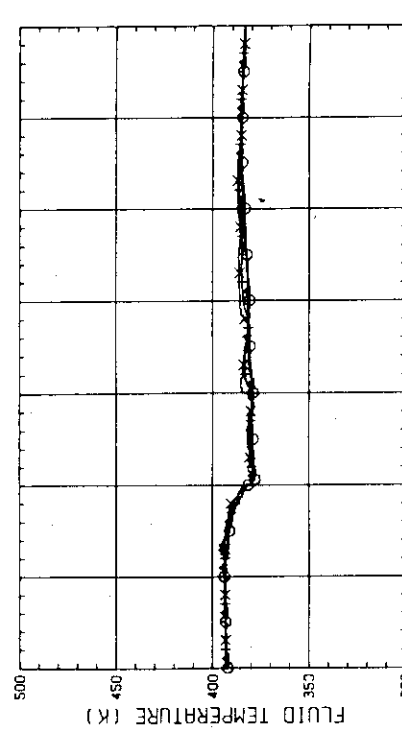


Fig. H-9(b) FLUID TEMPERATURE AT CORE INLET
(BUNDLE 5,6,7,8, 100MM BELOW HEATED PART)

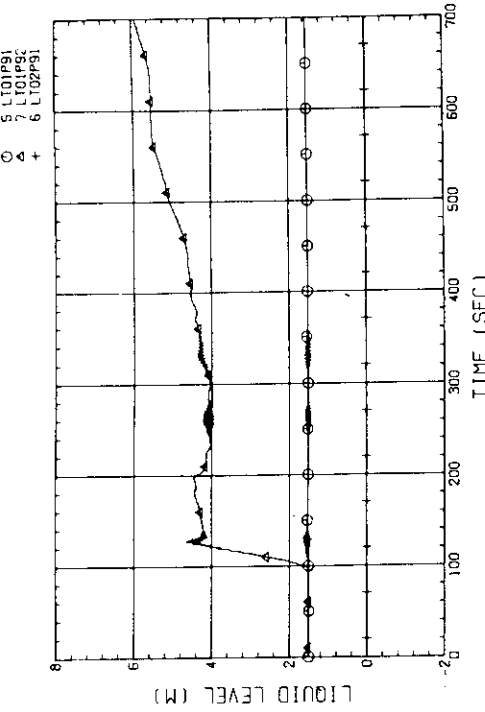


Fig. H-10 LIQUID LEVEL IN OMNIONER (Q1P91-BELOW CORE INLET,
Q1P92-BOTTOM TO COLD LEG, Q2P91-COLD LEG TO TOP OF PV)

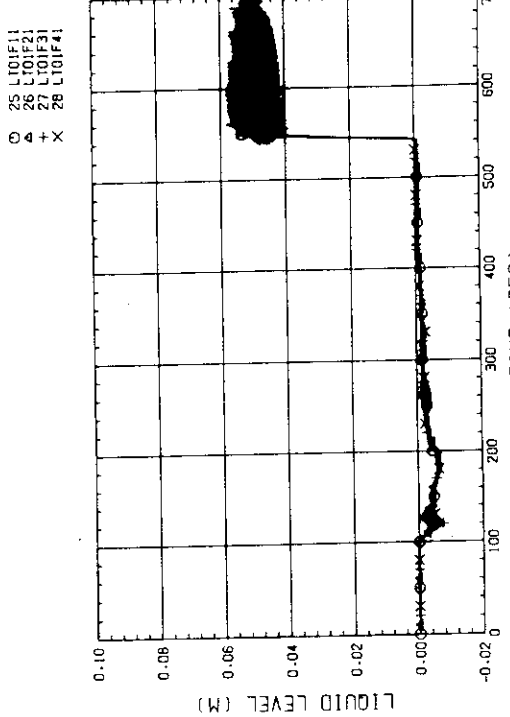


Fig. H-11(a) LIQUID LEVEL ABOVE END BOX TIE PLATE
(BUNDLE 1,2,3,4)

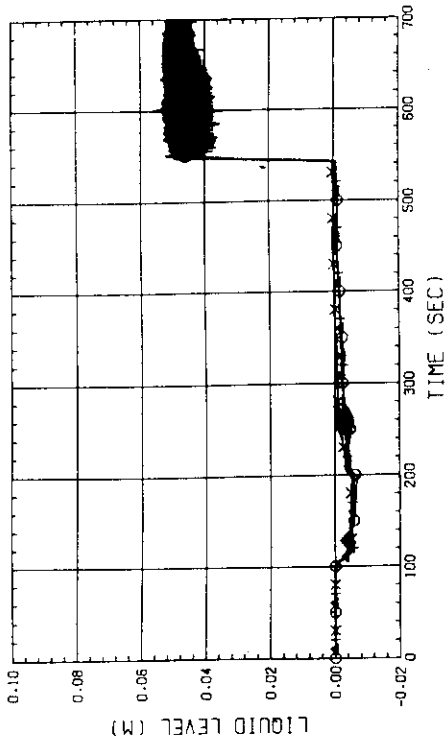


Fig. H-11(b) LIQUID LEVEL ABOVE END BOX TIE PLATE
(BUNDLE 5,6,7,8)

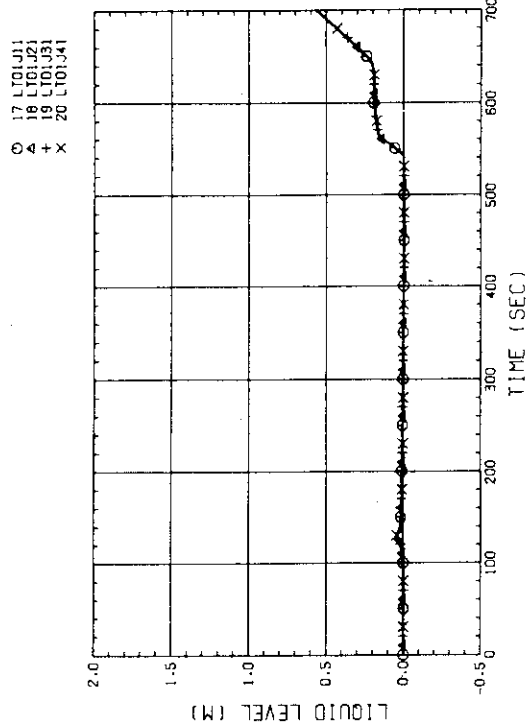


Fig. H-12(a) LIQUID LEVEL ABOVE UCSP
(BUNDLE 1,2,3,4)

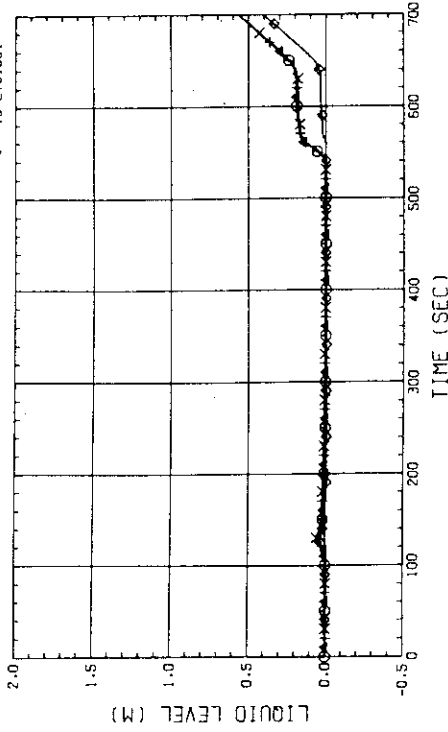


Fig. H-12(b) LIQUID LEVEL ABOVE UCSP
(BUNDLE 5,6,7,8 AND CORE BAFFLE)

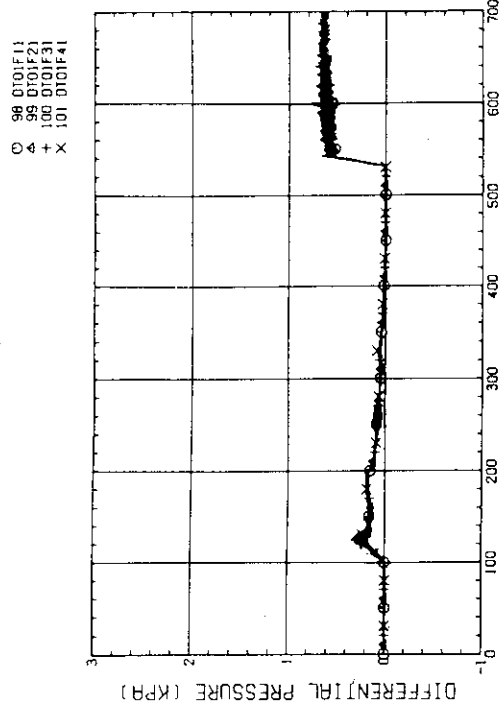


Fig. H-14(a) DIFFERENTIAL PRESSURE ACROSS END BOX TIE PLATE
(BUNDLE 1,2,3,4)

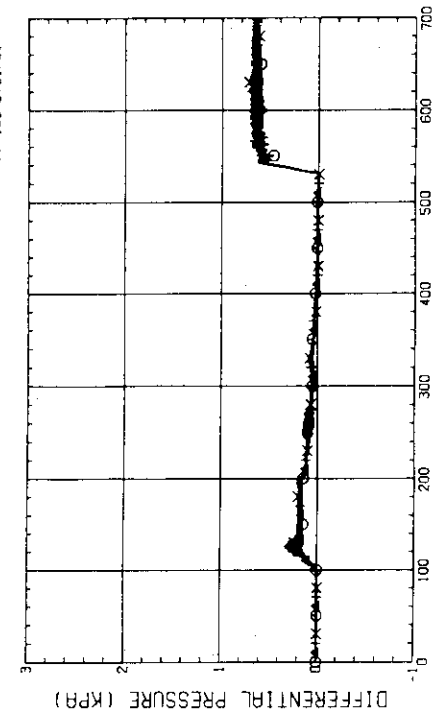


Fig. H-14(b) DIFFERENTIAL PRESSURE ACROSS END BOX TIE PLATE
(BUNDLE 5,6,7,8)

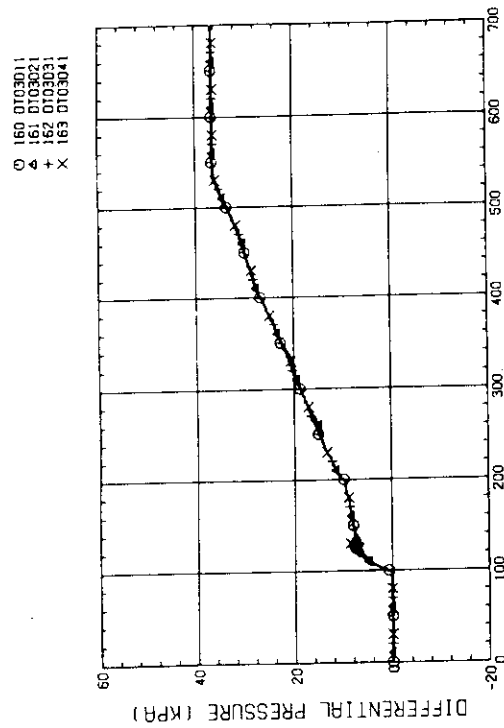


Fig. H-13(a) DIFFERENTIAL PRESSURE OF CORE FULL HEIGHT
(BUNDLE 1,2,3,4)

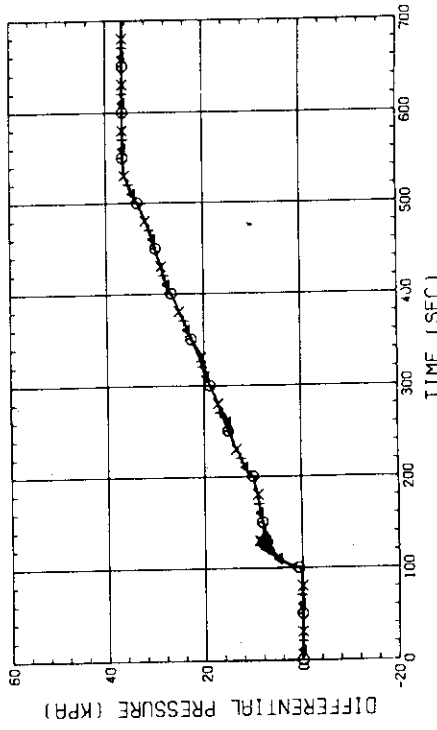


Fig. H-13(b) DIFFERENTIAL PRESSURE OF CORE FULL HEIGHT
(BUNDLE 5,6,7,8)

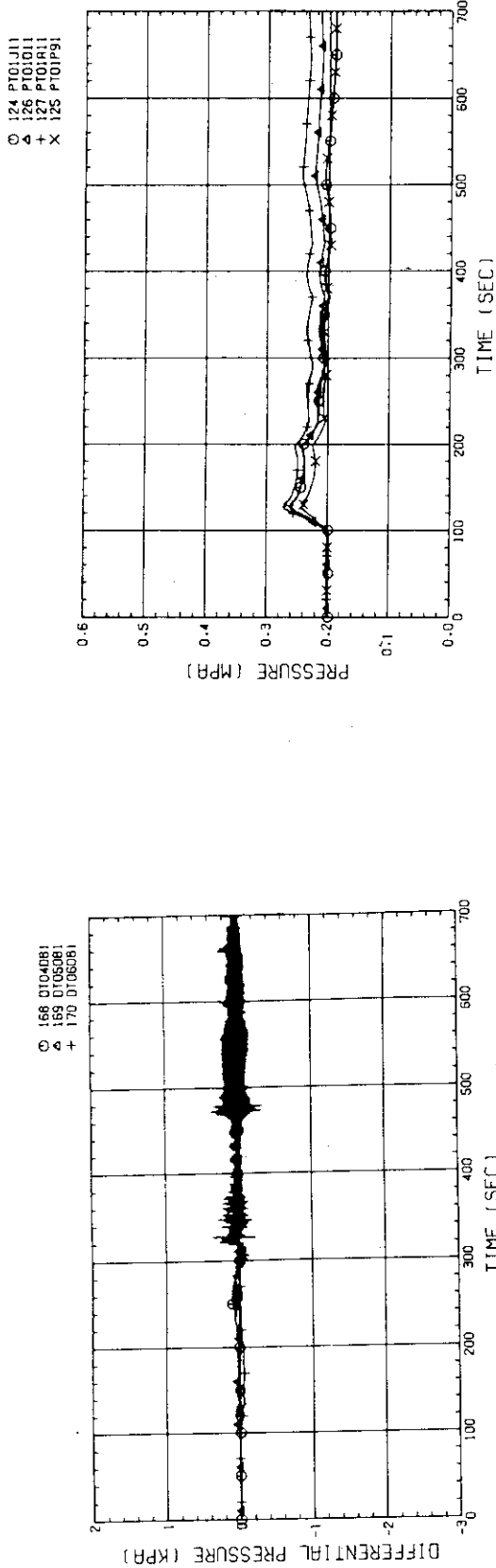


Fig. H-15(a) DIFFERENTIAL PRESSURE, HORIZONTAL BUNDLE S-8 (04-BELOW SPACER 4, 05-BELOW SPACER 6, 06-BELOW END BOX)

Fig. H-16 PRESSURE IN PV (□ - TOP OF PV, ○ - CORE CENTER, ▲ - CORE INLET, + - BELOW COLD LEG NOZZLE IN DOWNCOMER)

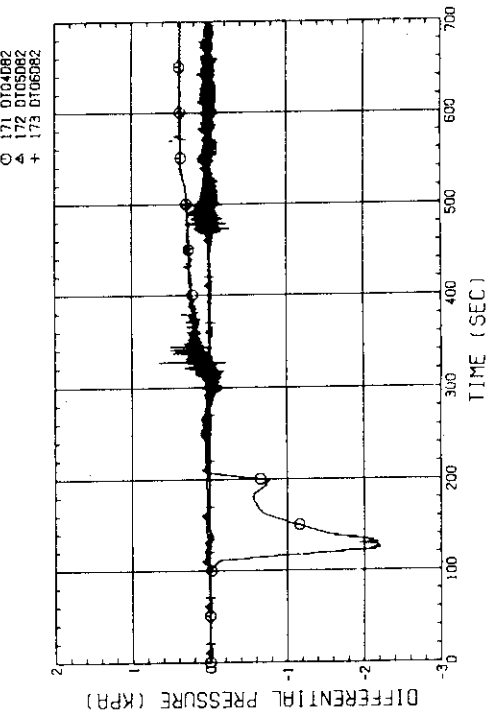


Fig. H-15(b) DIFFERENTIAL PRESSURE, HORIZONTAL BUNDLE 1-8 (04-BELOW SPACER 4, 05-BELOW SPACER 6, 06-BELOW END BOX)

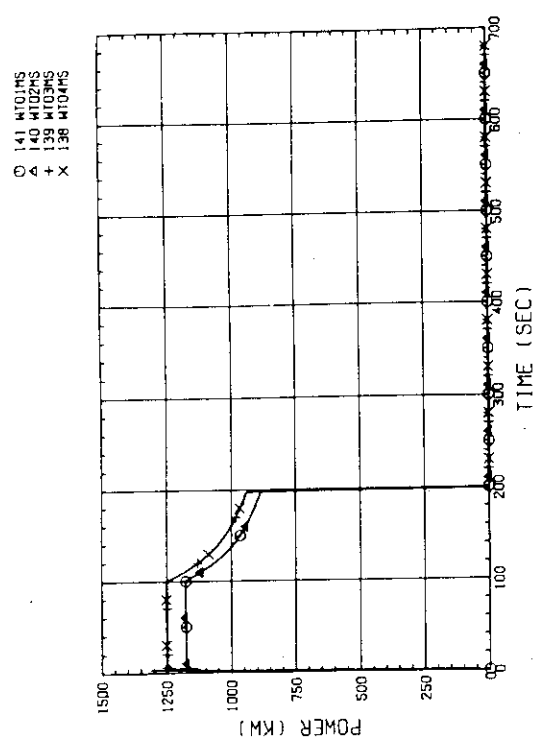


Fig. H-17(a) BUNDLE POWER
(BUNDLE 1,2,3,4)

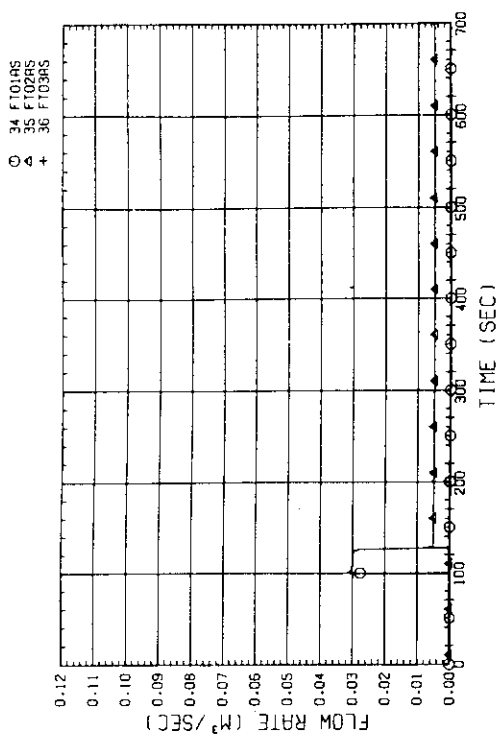
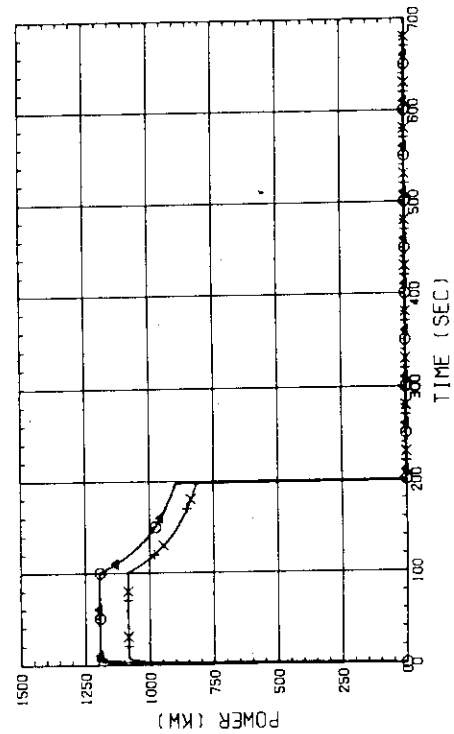


Fig. H-18 FLOW RATE OF ECC. WATER (01-DOWNCOMER/LOWER PLENUM/
HOT LEG, 02-INTACT COLD LEG, 03-BROKEN COLD LEG)



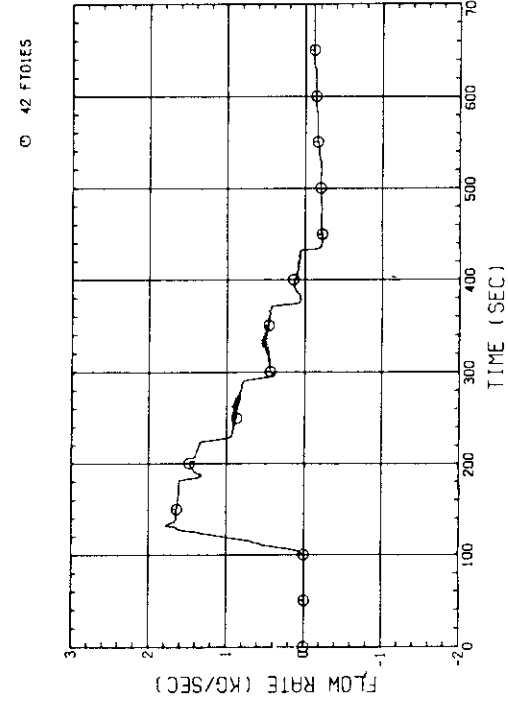


Fig. H-19(a) MASS FLOW RATE OF INTACT COLD LEG

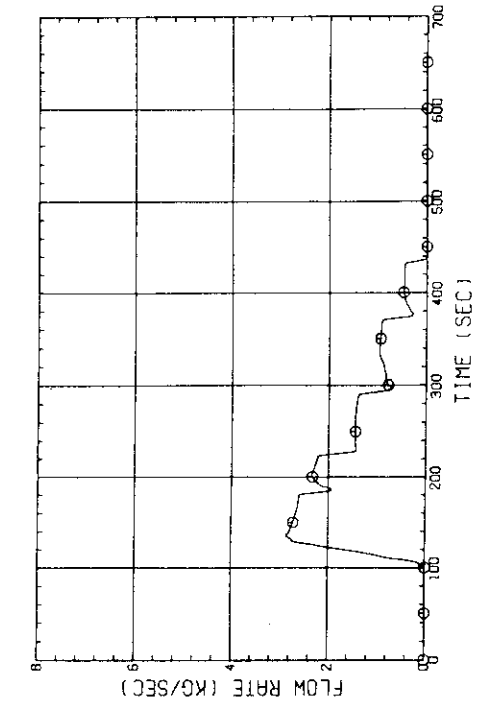


Fig. H-19(c) MASS FLOW RATE FROM CONTAINMENT TANK-I TO CONTAINMENT TANK-II

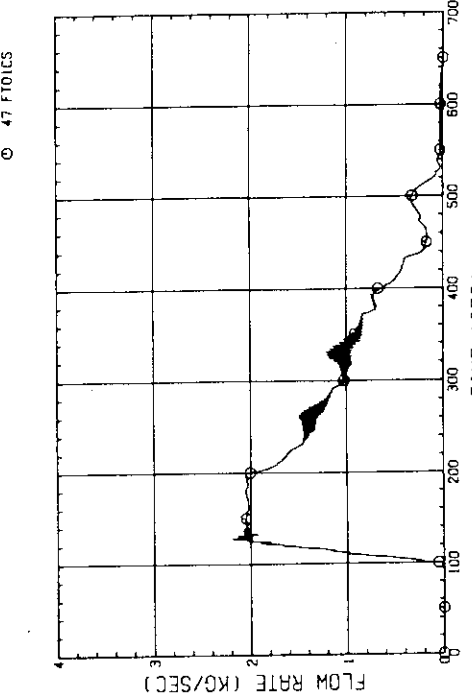


Fig. H-19(b) MASS FLOW RATE OF BROKEN COLD LEG - SEPARATOR SIDE

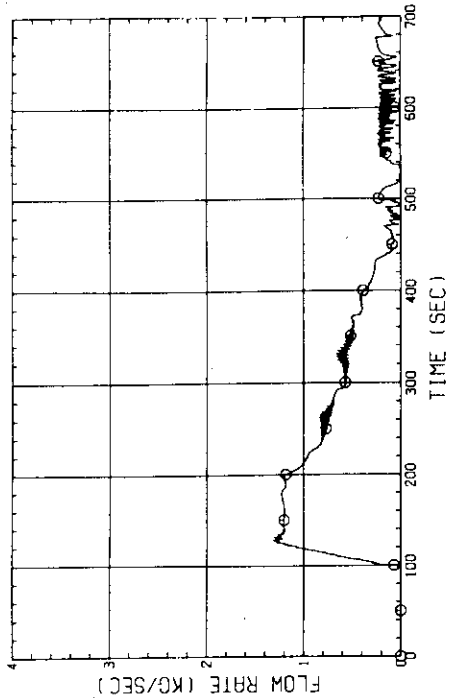
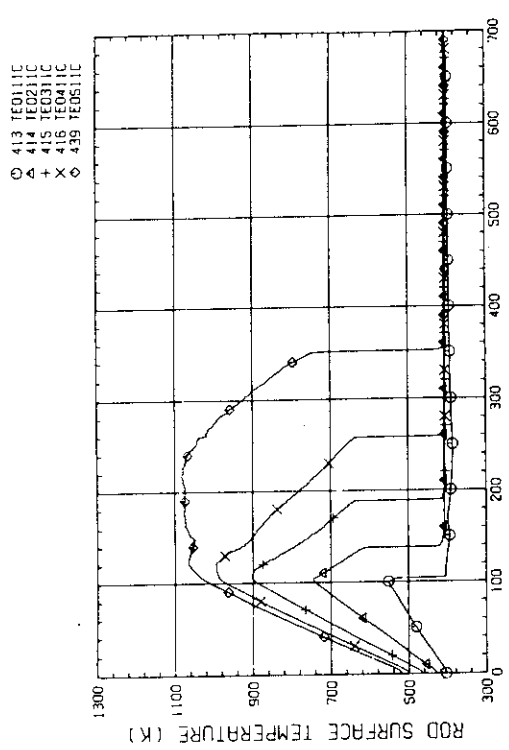
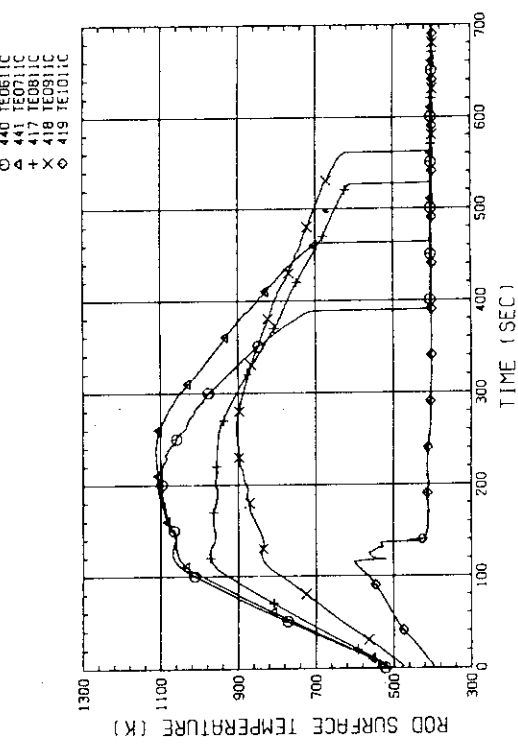
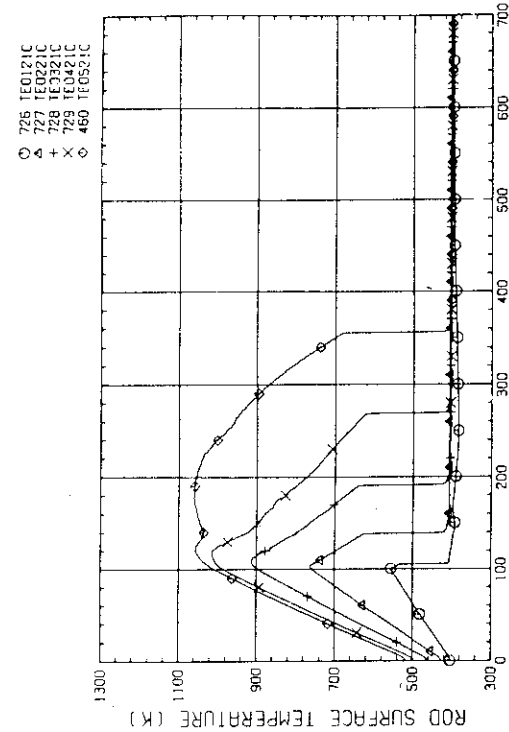
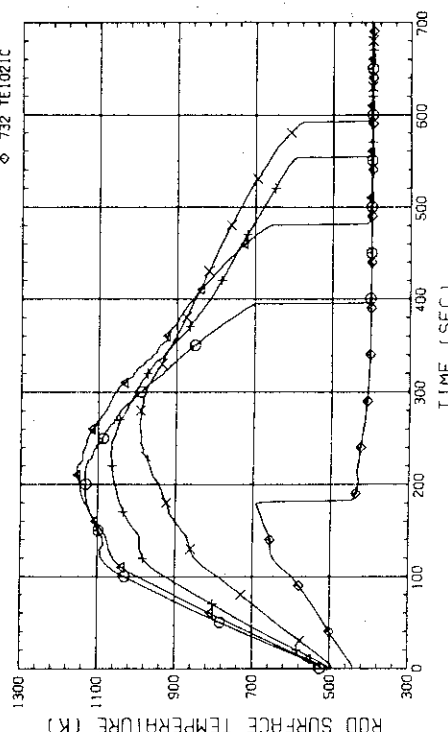


Fig. H-20 STEAM FLOW RATE OF DISCHARGE FROM CONTAINMENT TANK-II

Appendix I

Selected Data for Test S1-24 (Run 537)

Fig. I-1(a) HEATER ROD TEMPERATURE
(BUNDLE 1-1C, LOWER HALF)Fig. I-1(b) HEATER ROD TEMPERATURE
(BUNDLE 1-1C, UPPER HALF)Fig. I-2(a) HEATER ROD TEMPERATURE
(BUNDLE 2-1C, LOWER HALF)Fig. I-2(b) HEATER ROD TEMPERATURE
(BUNDLE 2-1C, UPPER HALF)

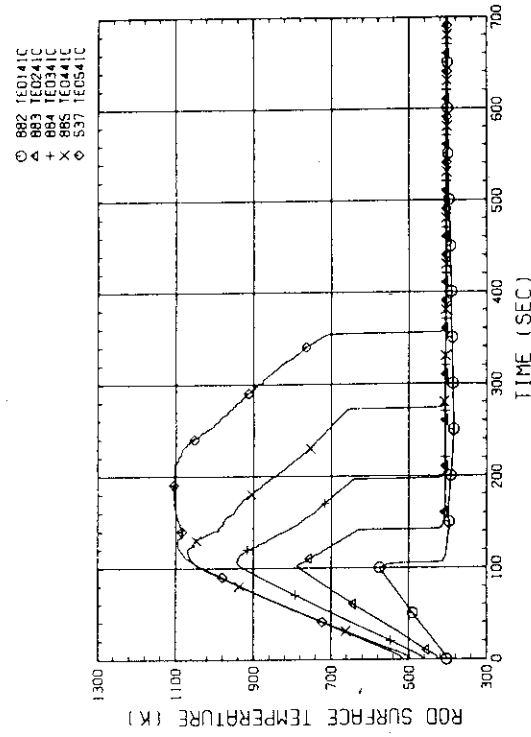


Fig. I-3(a) HEATER ROD TEMPERATURE
(BUNDLE 3-1C, LOWER HALF)

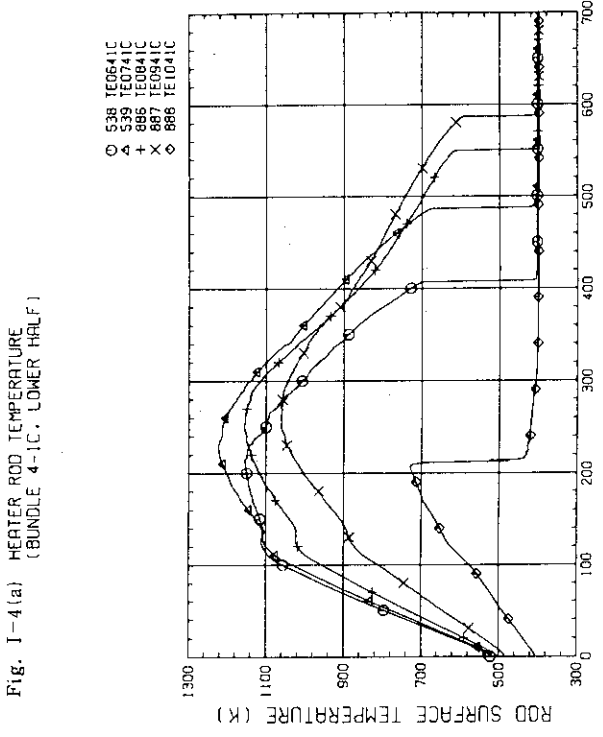


Fig. I-4(a) HEATER ROD TEMPERATURE
(BUNDLE 4-1C, LOWER HALF)

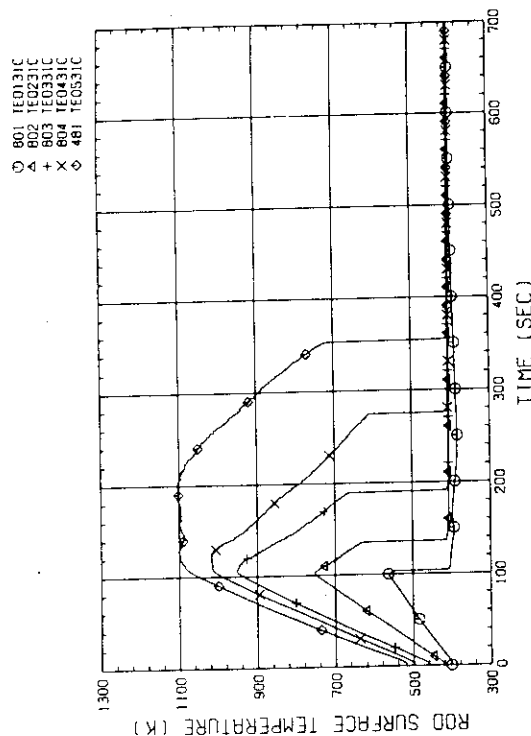


Fig. I-3(b) HEATER ROD TEMPERATURE
(BUNDLE 3-1C, UPPER HALF)

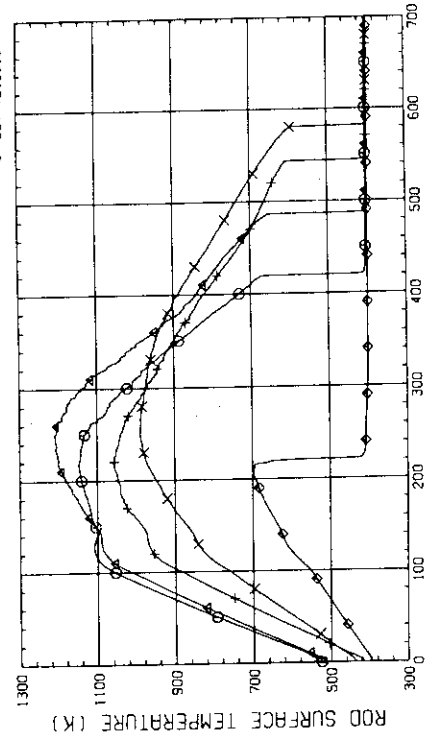


Fig. I-4(b) HEATER ROD TEMPERATURE
(BUNDLE 4-1C, UPPER HALF)

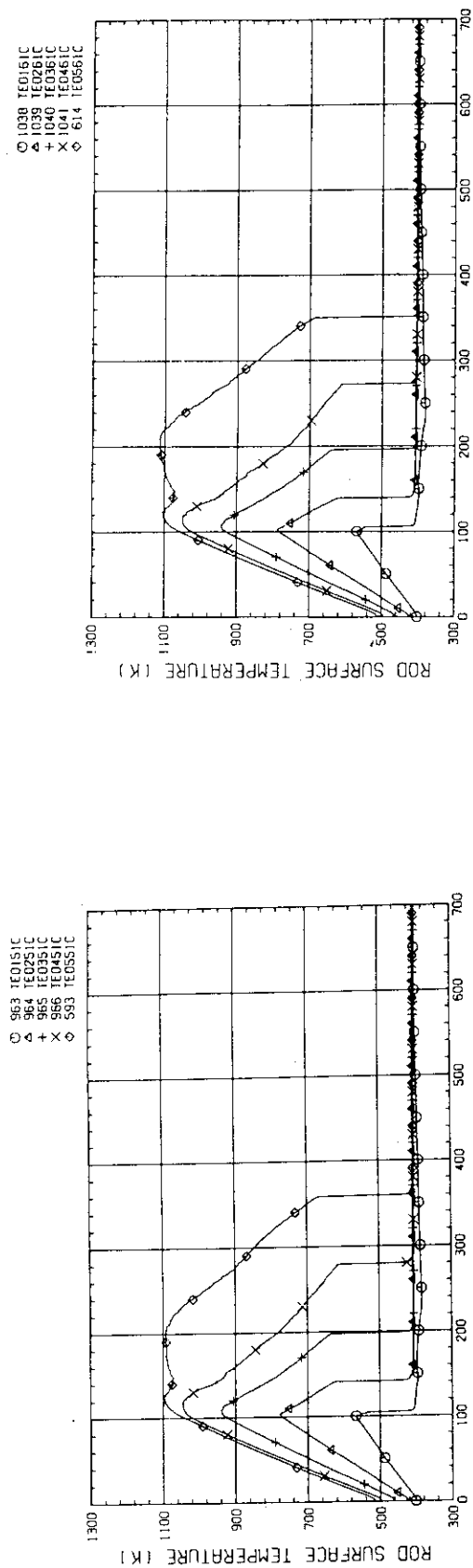


Fig. I-5(a) HEATER ROD TEMPERATURE (BUNDLE 5-1C, LOWER HALF)
Fig. I-5(b) ROD SURFACE TEMPERATURE (K)

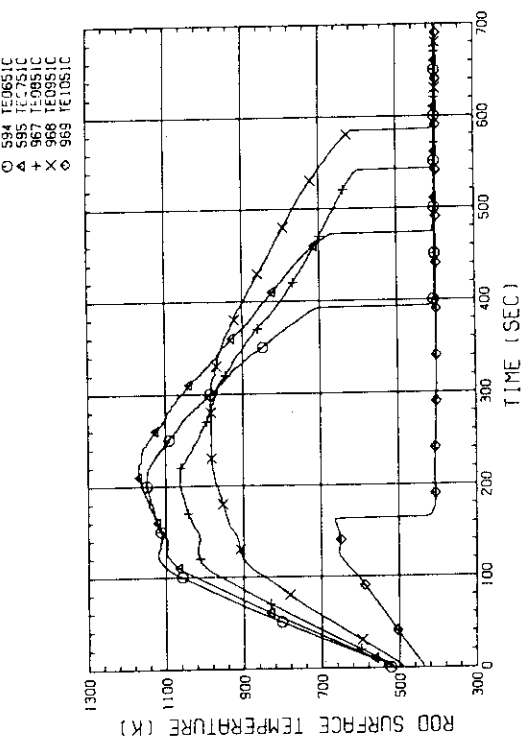


Fig. I-5(b) HEATER ROD TEMPERATURE (BUNDLE 5-1C, UPPER HALF)

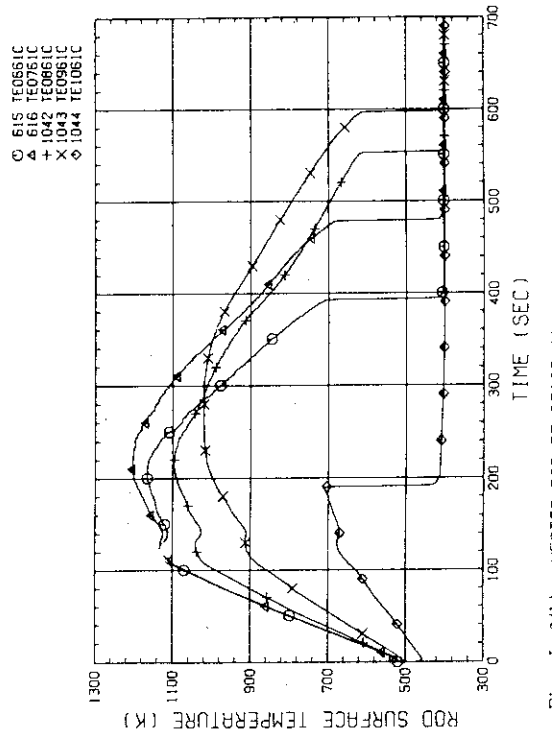
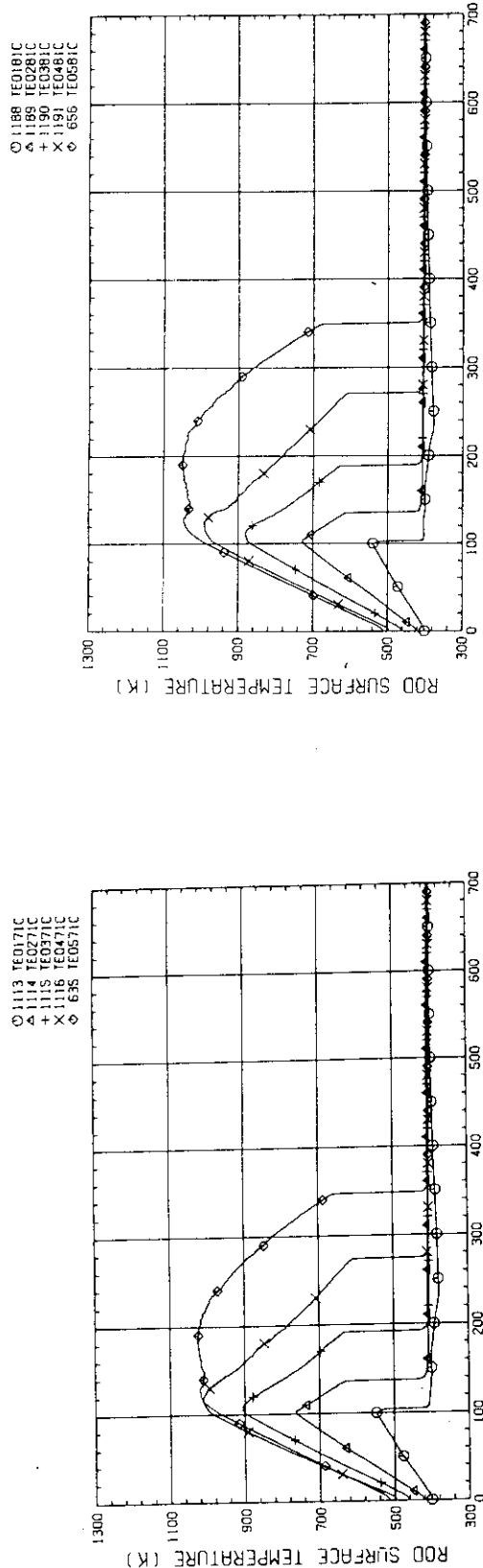
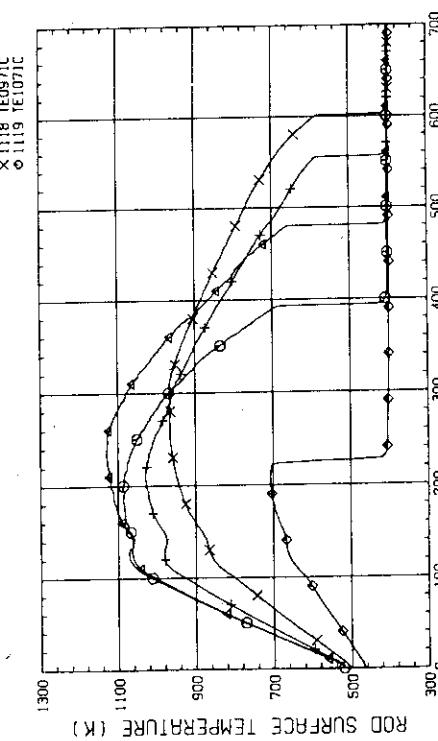
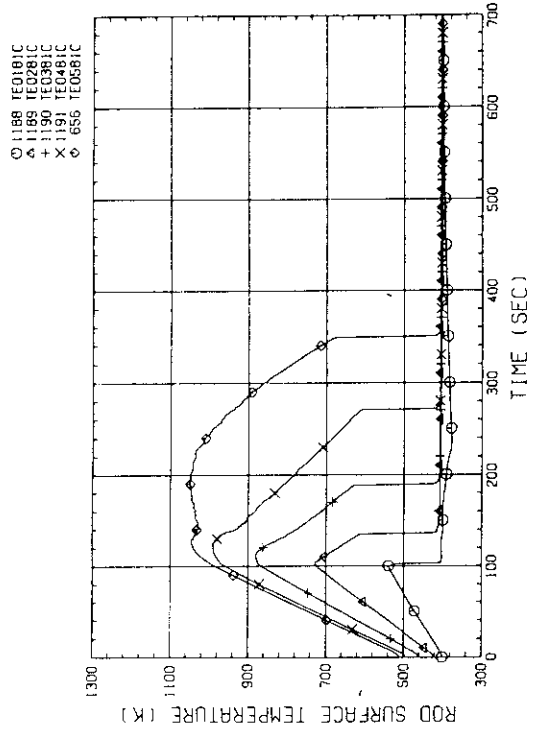
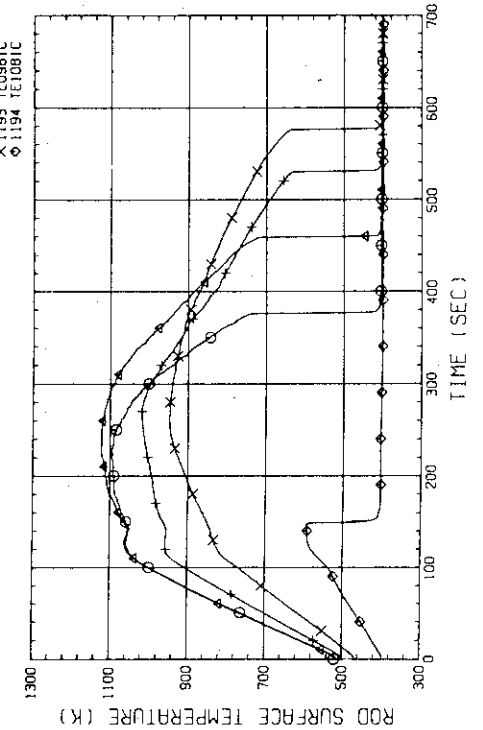


Fig. I-6(a) HEATER ROD TEMPERATURE (BUNDLE 6-1C, LOWER HALF)
Fig. I-6(b) ROD SURFACE TEMPERATURE (K)

Fig. I-7(a) HEATER ROD TEMPERATURE
(BUNDLE 7-1C, LOWER HALF)Fig. I-7(b) HEATER ROD TEMPERATURE
(BUNDLE 7-1C, UPPER HALF)Fig. I-8(a) HEATER ROD TEMPERATURE
(BUNDLE B-1C, LOWER HALF)Fig. I-8(b) HEATER ROD TEMPERATURE
(BUNDLE B-1C, UPPER HALF)

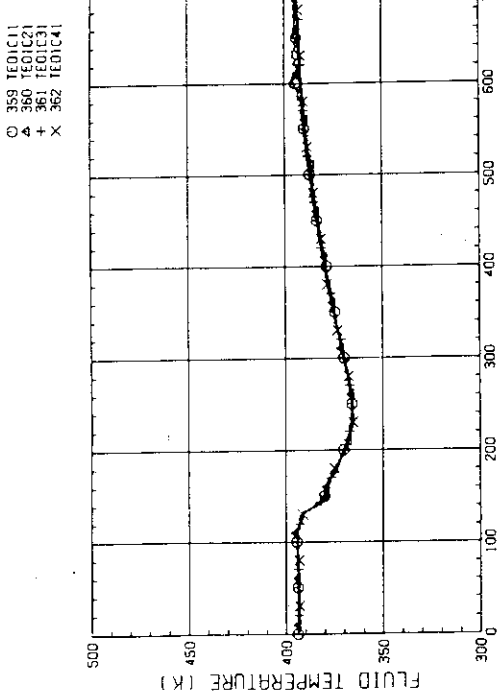


Fig. I-9(a) FLUID TEMPERATURE AT CORE INLET
(BUNDLE 1.2.3.4. 100MM BELOW HEATED PART)

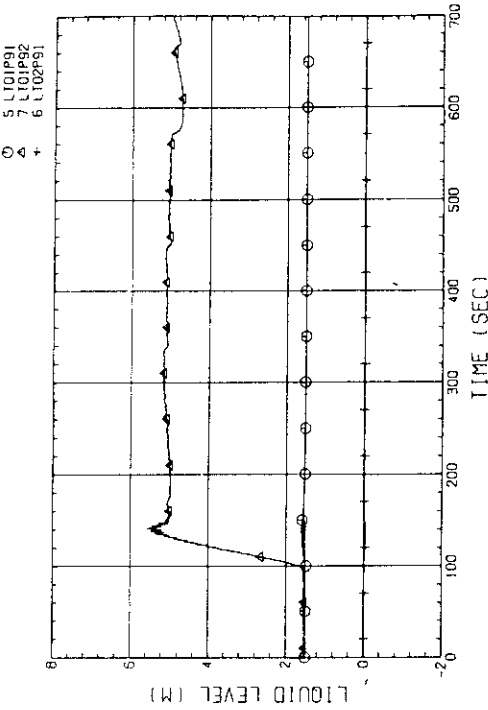


Fig. I-10 LIQUID LEVEL IN DOWNCOMER (01P91-BELOW CORE INLET,
01P92-BOTTOM TO COLD LEG, 02P91-COLD LEG TO TOP OF PV)

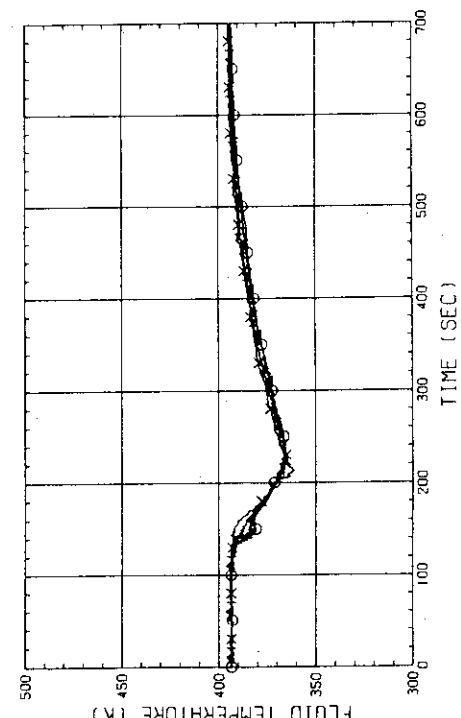


Fig. I-9(b) FLUID TEMPERATURE AT CORE INLET
(BUNDLE 5,6,7,8. 100MM BELOW HEATED PART)

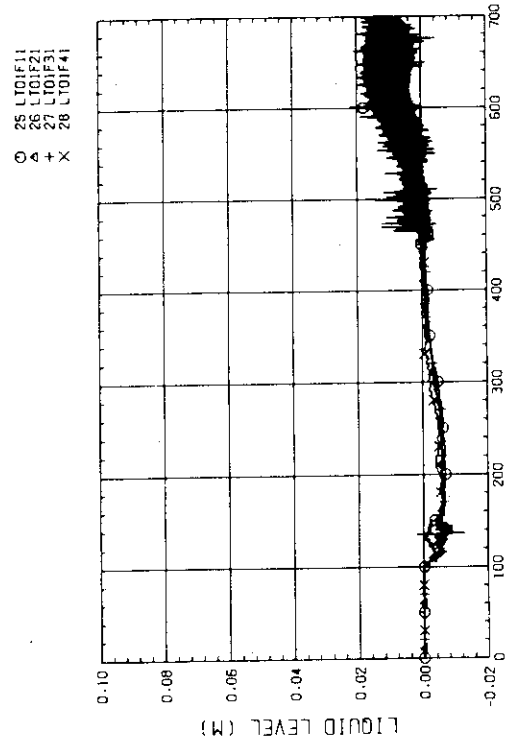


Fig. I-11(a) LIQUID LEVEL ABOVE END BOX TIE PLATE
(BUNDLE 1,2,3,4)

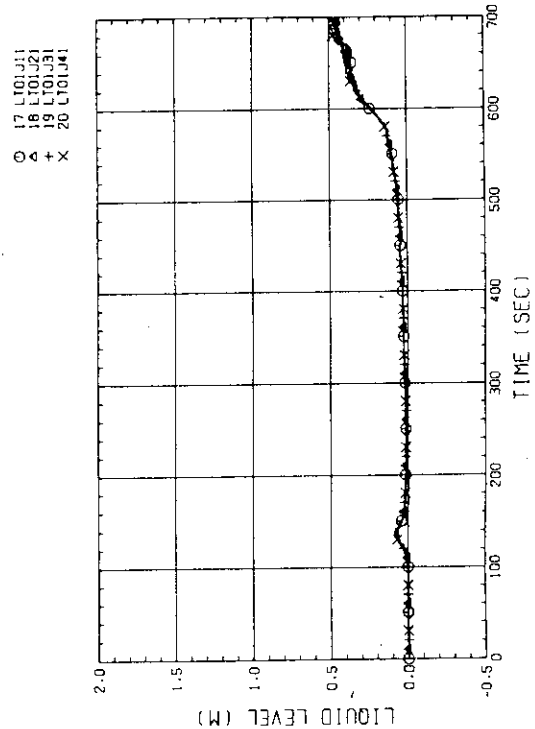


Fig. I-12(a) LIQUID LEVEL ABOVE UCSP
(BUNDLE 1,2,3,4)

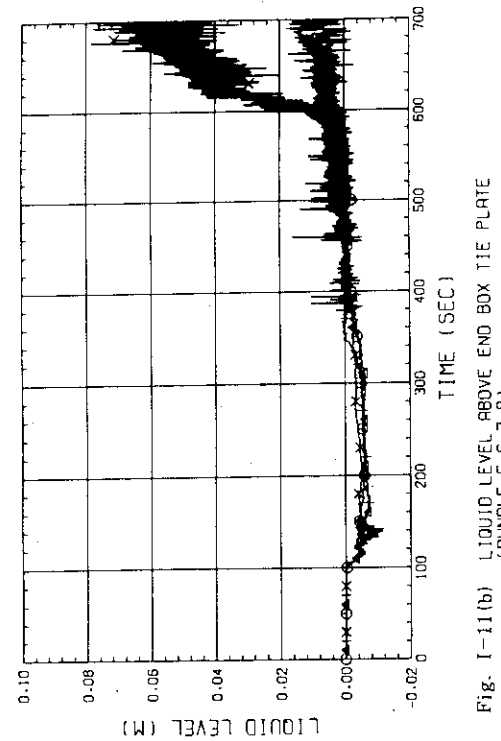


Fig. I-11(b) LIQUID LEVEL ABOVE END BOX TIE PLATE
(BUNDLE 5,6,7,8)

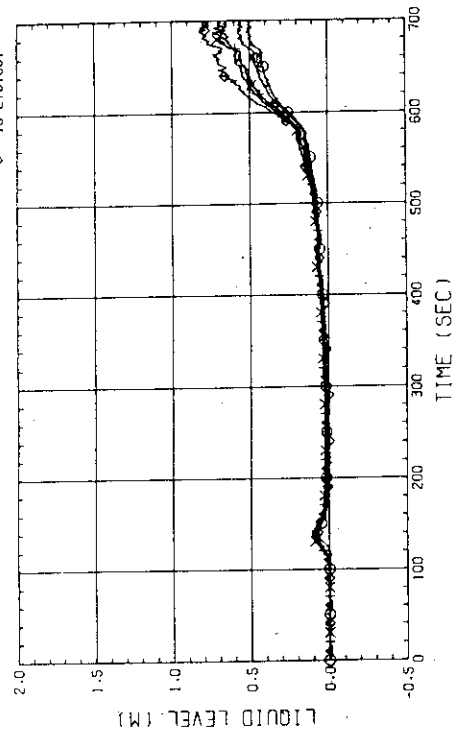
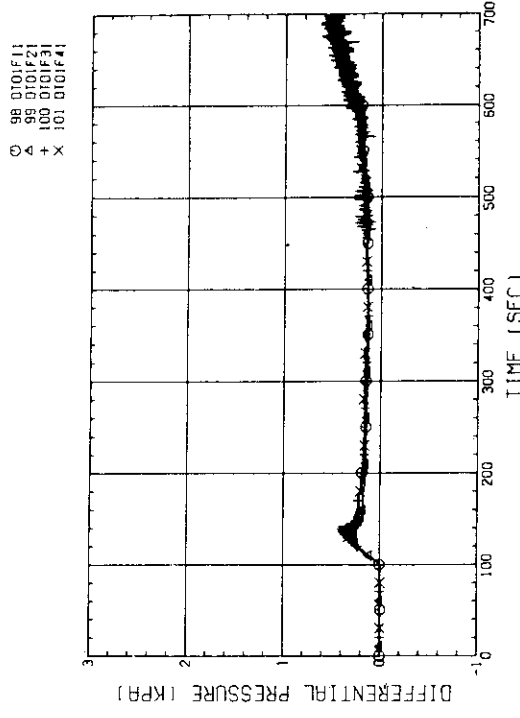
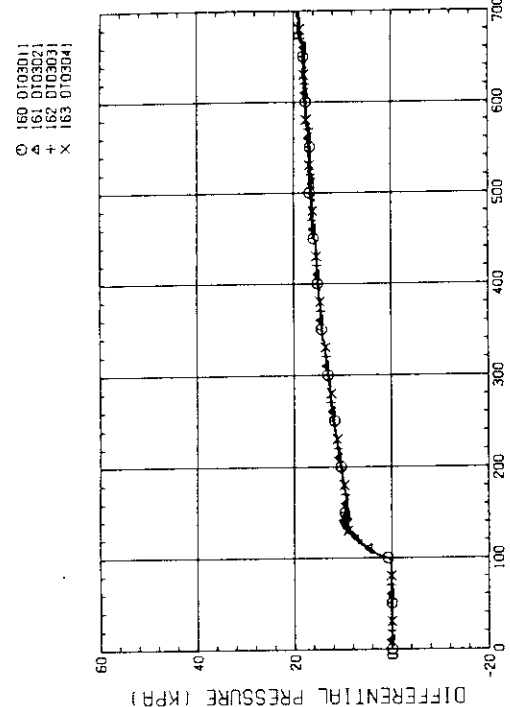
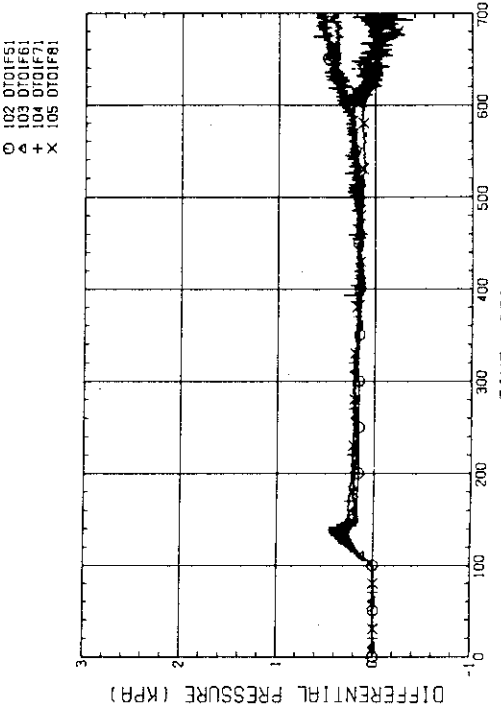
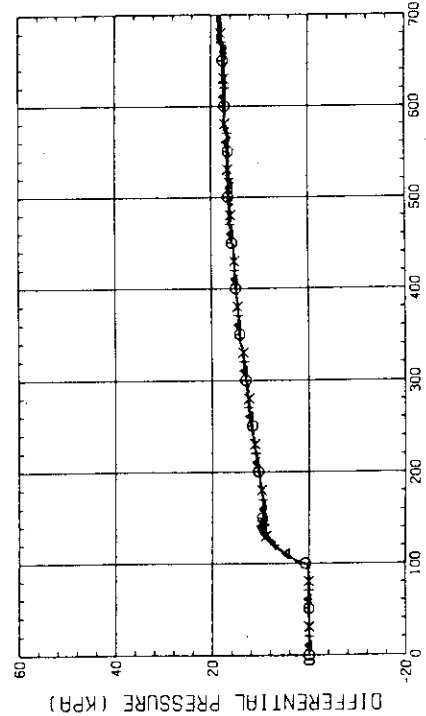


Fig. I-12(b) LIQUID LEVEL ABOVE UCSP
(BUNDLE 5,6,7,8 AND CORE BAFFLE)

Fig. I-13(a) DIFFERENTIAL PRESSURE OF CORE FULL HEIGHT
(BUNDLE 1,2,3,4)Fig. I-13(b) DIFFERENTIAL PRESSURE OF CORE FULL HEIGHT
(BUNDLE 5,6,7,8)Fig. I-14(a) DIFFERENTIAL PRESSURE ACROSS END BOX TIE PLATE
(BUNDLE 1,2,3,4)Fig. I-14(b) DIFFERENTIAL PRESSURE ACROSS END BOX TIE PLATE
(BUNDLE 5,6,7,8)

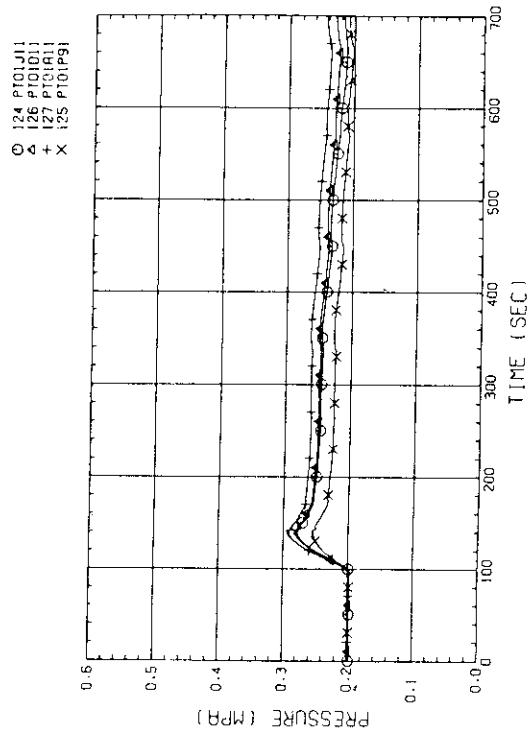


Fig. I-16 PRESSURE IN PV (J - TOP OF PV, D - CORE CENTER, A - CORE INLET, P - BELOW COLD LEG NOZZLE IN DOWNCOMER)

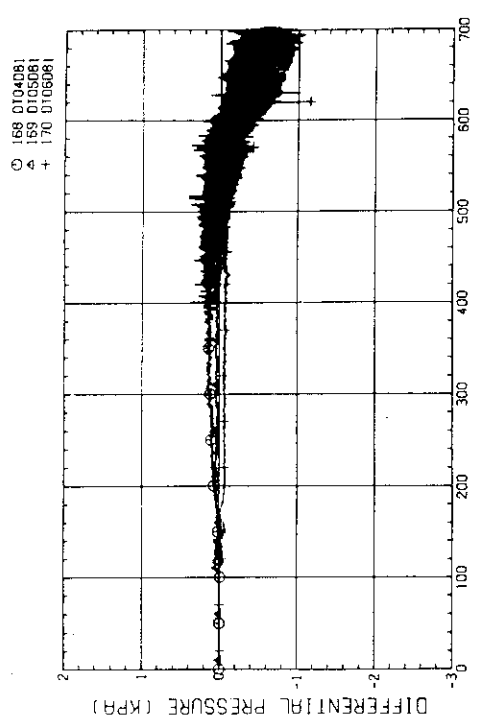


Fig. I-15(a) DIFFERENTIAL PRESSURE, HORIZONTAL BUNDLE 5-8 (04-BELOW SPACER 4, 05-BELOW END BOX)

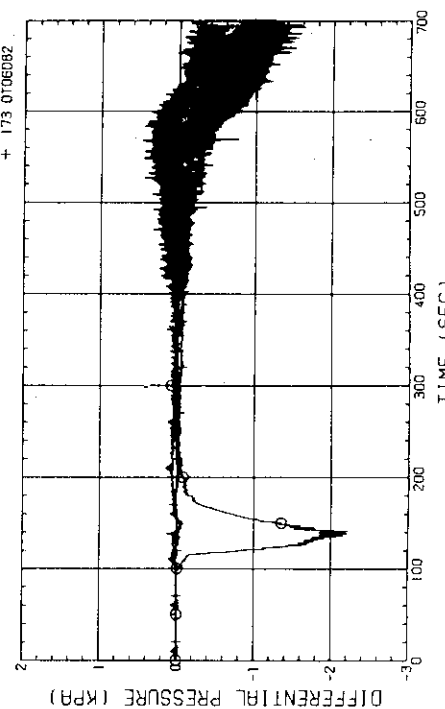


Fig. I-15(b) DIFFERENTIAL PRESSURE, HORIZONTAL BUNDLE 1-8 (04-BELOW SPACER 4, 05-BELOW END BOX)

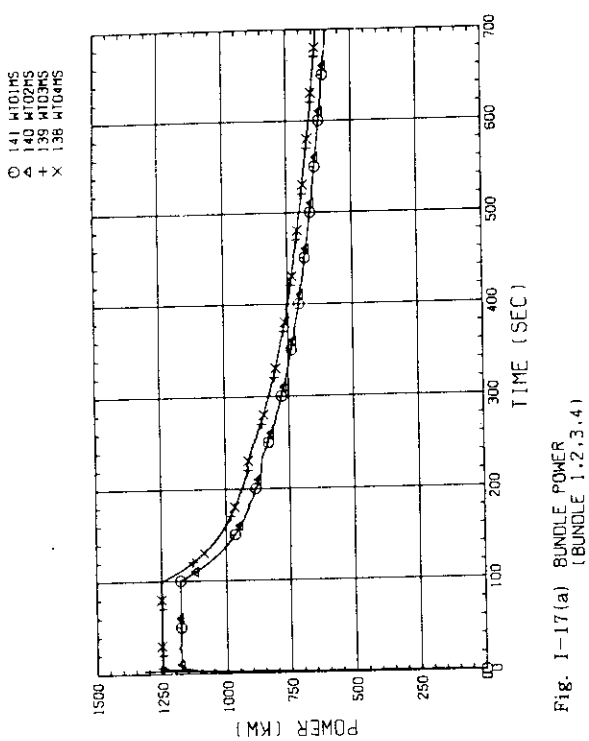


Fig. I-17(a) BUNDLE POWER (BUNDLE 1,2,3,4)

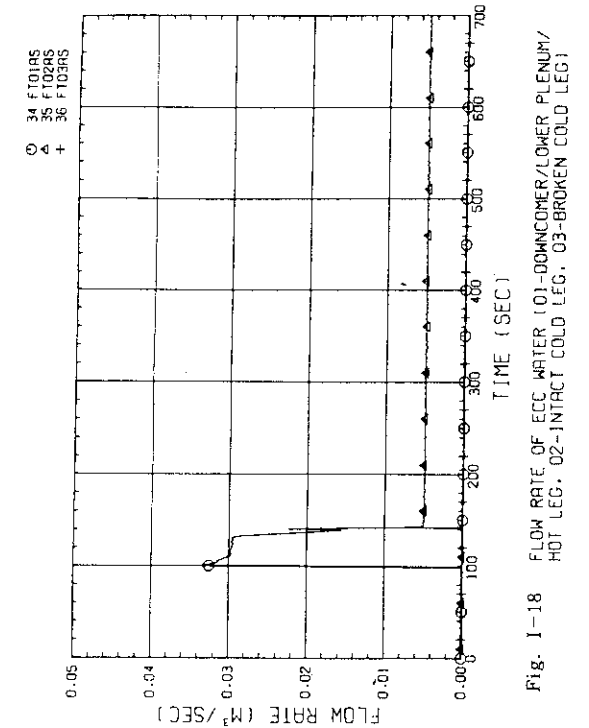


Fig. I-18 FLOW RATE OF ECC WATER (01-DOWNCOMER/LOWER PLUNER/HOT LEG, 02-INTEGRAL COLD LEG, 03-BROKEN COLD LEG)

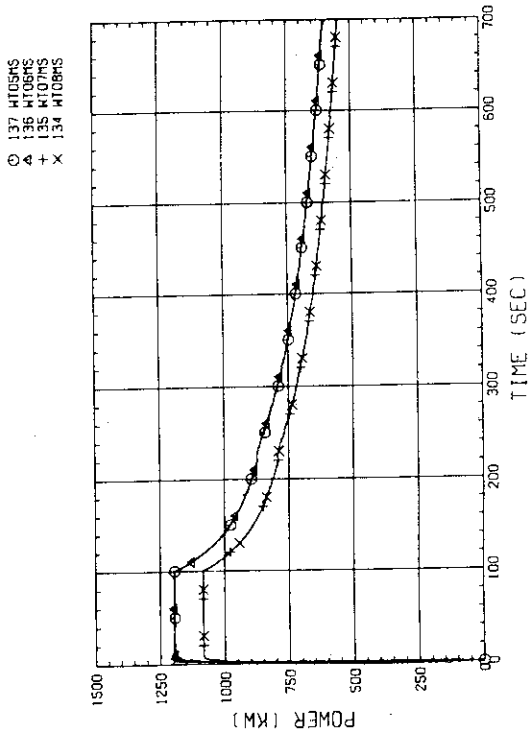


Fig. I-17(b) BUNDLE POWER (BUNDLE 5,6,7,8)

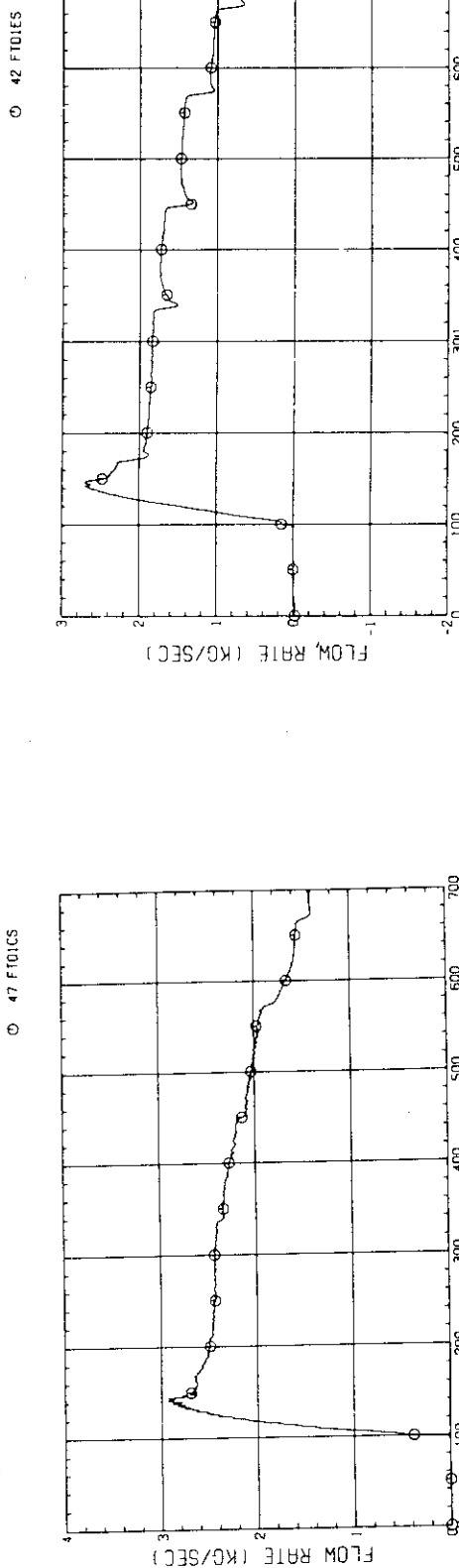


Fig. I-19(a) MASS FLOW RATE OF INTACT COLD LEG

Fig. I-19(c) MASS FLOW RATE FROM CONTAINMENT TANK-1 TO CONTAINMENT TANK-11

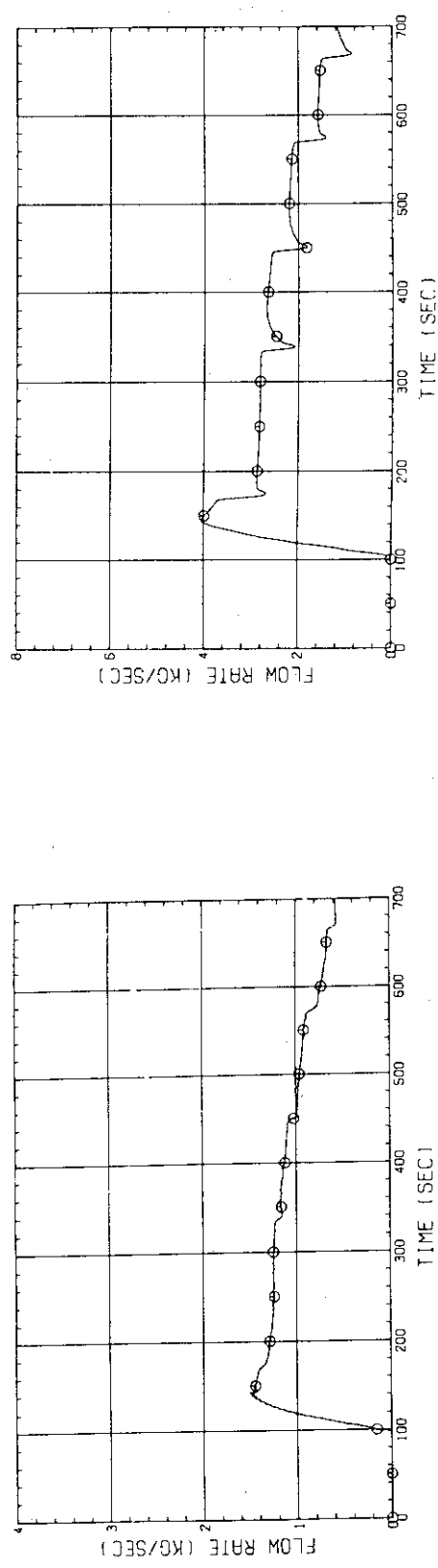


Fig. I-19(b) MASS FLOW RATE OF BROKEN COLD LEG - SEPARATOR SIDE

Fig. I-20 STEAM FLOW RATE OF DISCHARGE FROM CONTAINMENT TANK-11